

An investigation into the Anti-obesity properties of *Cyclopia*

By

Babalwa Unice Jack

*Dissertation presented for the degree of Doctor of Philosophy (Medical
Physiology) in the Faculty of Medicine and Health Sciences at
Stellenbosch University*



Supervisor: Dr Carmen Pheiffer

Co-supervisors: Dr Christiaan Malherbe and Prof Barbara Huisamen

December 2016

Declaration

By submitting this thesis electronically, I declare that the entirety of the work contained therein is my own, original work, that I am the sole author thereof (save to the extent explicitly otherwise stated), that reproduction and publication thereof by Stellenbosch University will not infringe any third party rights and that I have not previously in its entirety or in part submitted it for obtaining any qualification.

Babalwa Unice Jack

Date: December 2016

Copyright © 2016 Stellenbosch University

All rights reserved

ABSTRACT

Polyphenols have a range of health promoting effects against chronic diseases such as obesity and type 2 diabetes mellitus. Previous research in our group showed that *Cyclopia* species (honeybush), endemic South African plants, display anti-obesity effects. The aim of this study was to investigate the anti-obesity potential of polyphenol-enriched extracts of three *Cyclopia* spp. (*C. subternata*, *C. intermedia* and *C. maculata*) using bioactivity guided fractionation to facilitate the identification of anti-obesity polyphenols.

Aqueous methanol extracts of *C. subternata*, *C. intermedia* and *C. maculata* were prepared and separated into their aqueous and organic fractions, which were tested for their anti-obesity effects in 3T3-L1 adipocytes using the Oil Red O, glycerol release (marker of lipolysis), and triglyceride assays. Cytotoxicity was evaluated using the 3-[4,5-Dimethylthiazol-2-yl]-2,5-diphenyltetrazolium bromide (MTT) and adenosine triphosphate (ATP) assays. The anti-obesity properties of the organic fraction of the aqueous methanol extract of *C. intermedia* were evaluated in obese *Lepr^{db/db}* mice. Thereafter, the organic fraction was separated into four fractions (CCC F1 to CCC F4) using high performance counter-current chromatography (HPCCC), which were tested for their anti-obesity and cytotoxic effects in 3T3-L1 pre-adipocytes and in mature adipocytes. Liquid chromatography tandem mass spectrometry (LC-MS/MS) and quantitative high performance liquid chromatography diode array detection (HPLC-DAD) were used for determination of phenolic composition. The molecular mechanisms of action of the organic fraction and its CCC fractions were assessed with quantitative real-time PCR and western blot analysis.

The polyphenol-enriched extracts of *C. subternata*, *C. intermedia* and *C. maculata*, and their aqueous and organic fractions exhibited differences in phenolic composition and bioactivity. The aqueous fractions of *C. maculata* and *C. subternata*, containing lower phenolic content than the organic fractions, decreased lipid content in 3T3-L1 adipocytes compared to their organic counterparts. However, the organic fraction of *C. intermedia*, with higher phenolic content than its aqueous fraction, decreased lipid content compared

to its aqueous fraction in 3T3-L1 adipocytes. In $Lepr^{db/db}$ mice, the organic fraction of *C. intermedia* decreased body weight gain, without affecting food or water consumption. Further fractionation of the organic fraction of *C. intermedia* by HPLC provided four fractions with differences in phenolic composition and anti-obesity effects. None of the extracts or fractions, except for the aqueous *C. intermedia* and organic *C. maculata* fractions which decreased ATP content, affected cell viability as measured with the MTT and ATP assays during acute treatment. The highest concentrations of CCC F1 and CCC F3 decreased ATP content during chronic treatment in pre-adipocytes. In 3T3-L1 adipocytes, the organic fraction of *C. intermedia* and CCC fractions modulated the expression of genes implicated in lipid and energy metabolism, whereas the organic fraction of *C. intermedia* had no effect on the expression of these genes in $Lepr^{db/db}$ mice.

In conclusion, the organic fraction of *C. intermedia* exhibited anti-obesity properties *in vitro* and *in vivo*. A flavanone with anti-obesity potential, neoponcirin, was identified in *C. intermedia*, the first discovery of this compound in *Cyclopia* spp. Bioactivity guided fractionation of the organic fraction of *C. intermedia* resulted in CCC fractions retaining different polyphenols with varying anti-obesity effects. These results demonstrate that the anti-obesity potential of *C. intermedia* is due to the presence of more than one compound, with different mechanisms of action, or the synergistic effects of more than one compound, may contribute to the bioactivity of *C. intermedia*.

OPSOMMING

Polifenole het 'n verskeidenheid van voordelige gesondheids-effekte teen chroniese siekte toestande wat obesiteit en diabetes mellitus tipe 2 insluit. Voorafgaande navorsing in ons groep het aangedui dat die uitsluitlik inheems Suid-Afrikaanse *Cyclopia*-spesies (heuningbos), obesiteits-teenwerkende effekte toon. Die mikpunt van die huidige studie was om die obesiteits-teenwerkende potensiaal van polifenol-verrykte ekstrakte van drie *Cyclopia*-spesies (*C. subternata*, *C. intermedia* en *C. maculata*) te ondersoek deur bio-aktiwiteitsgerigte fraksionering te gebruik om obesiteits-teenwerkende polifenole te identifiseer.

Waterige metanol ekstrakte van *C. subternata*, *C. intermedia* en *C. maculata* was voorberei en geskei in water-oplosbare en organiese fraksies wat dan getoets was vir moontlike obesiteits-teenwerkende eienskappe in 3T3-L1 vetselle deur gebruik te maak van "Oil Red O", gliserol-vrystelling ('n merker vir lipolise) en trigliseried toetse. Seldodende effekte is ondersoek deur die 3-[4,5-Di-metielthiazool-2-iel]-2,5-difenieltetrazolium bromied (MTT) and adenosien trifosfaat (ATP) toetse te gebruik. Die obesiteits-teenwerkende effekte van die organiese fraksie verkry vanuit die waterige metanol ekstrak van *C. intermedia* is verder ondersoek in $Lepr^{db/db}$ -muise. Hierna is die organiese fraksie opgedeel in vier fraksies (CCC F1 tot CCC F4) deur hoë-werkverrigting teen-vloei chromatografie (HPCCC) te gebruik en dan weer getoets vir obesiteits-teenwerkende en seldodende effekte in 3T3-L1 pre-vetselle en volwasse vetselle. Vloeistof-chromatografie gekoppelde massaspektrometrie (LC-MS/MS) en kwantitatiewe hoë-werkverrigting vloeistof-chromatografie met diode-reeks deteksie (HPLC-DAD) is gebruik vir die bepaling van die fenoliese samestelling. Die molekuleêre werkingsmeganismes van die organiese fraksie en die CCC-fraksies is ondersoek deur die kwantitatiewe "intyds" polimerase kettingreaksie en western-klad tegnieke te gebruik.

Die polifenol-verrykte ekstrakte van *C. subternata*, *C. intermedia* en *C. maculata* en hul wateroplosbare en organiese fraksies het verskille getoon in fenoliese samestelling asook bio-aktiwiteit. Die wateroplosbare fraksies van *C. maculata* en *C. subternata*, met laer fenoliese inhoud as die organiese fraksies, het vet-inhoud in 3T3-L1 vetselle verlaag

relatief tot hul ooreenstemmende organiese fraksies. Die organiese fraksie van *C. intermedia*, met hoër fenoliese inhoud as die wateroplosbare fraksie, het egter die vetinhoud van die 3T3-L1 vetselle verlaag in vergelyking met die ooreenstemmende wateroplosbare fraksie. In $\text{Lepr}^{\text{db/db}}$ -muise het die organiese fraksie van *C. intermedia* 'n verlaging in liggaamsgewigstoename tot gevolg gehad sonder om die voedsel- of waterinname te beïnvloed. Verdere skeiding van die organiese fraksie van *C. intermedia* met HPCCC het 4 fraksies opgelewer wat elkeen verskil het van die ander in terme van fenoliese samestelling en obesiteits-teenwerkende effekte. Geen van die ekstrakte of fraksies, behalwe die wateroplosbare fraksie van *C. intermedia* en die organiese fraksie van *C. maculata* wat ATP-inhoud laat daal het in 3T3-L1 vetselle, het sellewensvatbaarheid beïnvloed soos gemeet in MTT- en ATP-toetse na akute behandeling nie. Tydens chroniese behandeling van 3T3-L1 pre-vetselle, het die hoogste konsentrasies van CCC F1 en CCC F3 die ATP-inhoud verlaag. In 3T3-L1 vetselle, het die organiese fraksie van *C. intermedia* en daaropvolgende CCC-fraksies die uitdrukking van gene betrokke by vet en energie metabolisme gemoduleer terwyl die organiese fraksie van *C. intermedia* nie die uitdrukking van hierdie gene in $\text{Lepr}^{\text{db/db}}$ -muise beïnvloed het nie.

In samevatting, die organiese fraksie van *C. intermedia* het obesiteits-teenwerkende eienskappe getoon *in vitro* en *in vivo*. 'n Flavanoon met obesiteits-teenwerkende potensiaal, neo-ponsirien, is geïdentifiseer in *C. intermedia* en is vir die eerste keer gevind in *Cyclopia* spesies. Bio-aktiwiteitsgerigte fraksionering van die organiese fraksie van *C. intermedia* het CCC-fraksies gelewer wat verskillende polifenole bevat het en wat verskillende obesiteits-teenwerkende effekte getoon het. Hierdie resultate dui daarop dat die obesiteits-teenwerkende potensiaal van *C. intermedia* nie toegeken kan word aan 'n enkele fenoliese verbinding nie, maar dat sinergistiese of kumulatiewe effekte vanaf meer as een obesiteits-teenwerkende verbinding, met verskille in werkingsmeganisme, betrokke mag wees.

ACKNOWLEDGEMENTS

To the almighty God, I thank you for granting me this opportunity and for giving me strength for all my accomplishments especially throughout this study.

I would like to sincerely acknowledge the following people for their contributions:

- Dr Carmen Pheiffer, my supervisor, for her support, assistance, motivation and enthusiasm throughout the study. Thank you for your dedication, time and effort! It was a privilege to be your student;
- Dr Christiaan Malherbe, my co-supervisor, for taking his time to teach and assist me with my experiments at the Agricultural Research Council (ARC) laboratory. Thank you for your encouragement, guidance and your valuable input throughout this study;
- Prof Barbara Huisamen, my co-supervisor, for her scientific input, guidance and support throughout this study;
- Dr Christo Muller and Prof Elizabeth Joubert for their valuable input and expertise throughout this study and Dr Johan Louw, for the opportunity to conduct my PhD research at the Biomedical Research and Innovation Platform (BRIP), South African Medical Research Council (SAMRC);
- All my colleagues from BRIP (especially Dr Mazibuko, Dr Gabuza, Mr Linden) for technical, scientific and academic input and contributions ;
- The Post-Harvest and Wine Technology Division at the ARC Infruitec Nietvoorbij and Primate Unit and Delft Animal Centre (SAMRC) for using their facilities to conduct my research, as well their technical assistance;
- Dr Elize Willenburg and Dr Dalene De Beer (ARC) for the identification of neoponcirin;
- To my mother, family and friends, thank you for your unconditional love, prayers, support and encouragement; and
- This work was financially supported by the SAMRC Self-Initiated Research (SAMRC-SIR) grant BU 23143 (C Malherbe) and baseline funds from the SAMRC (C Pheiffer). Financial support from the SAMRC (Research Capacity Development), BRIP, Stellenbosch University, Harry Crossley Foundation, Ernst & Ethel Ericksen Trust, Whitehead Scientific (Travel Award) and the PSSA (Travel Award) is also acknowledged.

TABLE OF CONTENTS

Declaration	ii
ABSTRACT	iii
OPSOMMING	v
ACKNOWLEDGEMENTS	vii
TABLE OF CONTENTS	viii
LIST OF FIGURES	xiv
LIST OF TABLES	xix
ABBREVIATIONS	xxi
CHAPTER 1	1
LITERATURE REVIEW	1
1.1 Introduction	2
1.2 Assessment of obesity.....	2
1.3 Prevalence of obesity	3
1.3.1 South Africa	4
1.4 Risk factors for obesity	5
1.5 Adipose tissue	7
1.5.1 White adipose tissue	8
1.5.2 Brown adipose tissue	8
1.6 Adipogenesis.....	9
1.6.1 Transcriptional regulation of adipogenesis	11
1.6.1.1 Peroxisome proliferator activator receptor gamma (PPAR γ)	11
1.6.1.2 CCAAT/enhancer binding protein (C/EBP) family	12
1.6.1.3 Other transcription factors involved in adipogenesis	12
1.7 Adipocyte metabolism	13
1.7.1 Glucose metabolism.....	13
1.7.2 Lipogenesis.....	15
1.7.2.1 <i>De novo</i> fatty acid synthesis	15
1.7.2.2 Fatty acid uptake from circulation and transport	16
1.7.2.3 Triglyceride synthesis	17
1.7.3 Lipolysis	18
1.7.4 Fatty acid oxidation	19
1.8 Metabolic complications associated with obesity	21

1.8.1 Inflammation	22
1.8.2 Oxidative stress and mitochondrial dysfunction.....	22
1.9 Insulin Resistance	23
1.10 Obesity and the metabolic syndrome.....	25
1.11 Obesity and chronic diseases.....	27
1.11.1 Type 2 diabetes mellitus	27
1.11.2 Cardiovascular disease.....	28
1.11.3 Cancer	28
1.11.4 Non-alcoholic fatty liver disease.....	29
1.12 Current interventions against obesity.....	29
1.12.1 Lifestyle modification.....	29
1.12.2 Pharmacological drugs.....	29
1.12.3 Bariatric surgery.....	30
1.12.4 Medicinal plants and polyphenols.....	31
1.13 South African indigenous plants: Cape Fynbos	31
1.13.1 <i>Cyclopia</i> species (honeybush tea).....	32
1.13.2 Geographical distribution	33
1.13.3 Honeybush tea industry	34
1.13.4 Phenolic composition	34
1.13.5 Biological properties of <i>Cyclopia</i> species	39
1.13.5.1 Anti-obesity health effects.....	39
1.13.6 Anti-obesity phenolic compounds present in <i>Cyclopia</i>	40
1.13.6.1 Xanthones	40
1.13.6.2 Flavonoids.....	41
1.13.6.3 Other polyphenolic groups.....	42
1.14 Model systems to study obesity	46
1.14.1 3T3-L1 adipocytes	46
1.14.2 The <i>Lepr^{db/db}</i> mouse model.....	46
1.15 Motivation for the study	47
1.15.1 Problem statement and research motivation	47
1.14.2 Hypothesis	48
1.14.3 Aim	49
1.14.4 Study objectives.....	49

CHAPTER 2	51
MATERIALS AND METHODS	51
2.1 Overview of methodology	52
2.2 Plant material	54
2.2.1 Preparation of 40% aqueous methanol extracts	55
2.2.2 Liquid-liquid fractionation of 40% aqueous methanol extracts	55
2.2.3 Large scale preparation of the bioactive fraction	55
2.2.4 High performance counter-current chromatography (HPCCC)	56
2.2.5 Separation and quantification of phenolic compounds using HPLC-DAD	58
2.2.6 Identification of phenolic compounds using LC-DAD-MS and -MS/MS Detection	60
2.3 <i>In vitro</i> cell culture	61
2.3.1 Cell line	61
2.3.2 Thawing of 3T3-L1 pre-adipocytes	62
2.3.3 Subculture of 3T3-L1 pre-adipocytes	62
2.3.3.1 Trypsin treatment.....	62
2.3.3.2 Cell counting.....	63
2.3.3.3 Freezing cells	63
2.3.4 Seeding of 3T3-L1 pre-adipocytes	63
2.3.5 Differentiation of 3T3-L1 pre-adipocytes into mature adipocytes	64
2.3.6 Extract preparation and treatments	66
2.3.6.1 Acute treatment	66
2.3.6.2 Chronic treatment	66
2.3.7 <i>In vitro</i> bioassays	67
2.3.7.1 Oil Red O Assay	67
2.3.7.2 Intracellular triglycerides	68
2.3.7.3 Glycerol Release Assay.....	69
2.3.7.4 The 3-[4, 5-Dimethylthiazol-2-yl]-2, 5 diphenyltetrazolium bromide Assay	69
2.3.7.5 The adenosine-5'-triphosphate (ATP) activity Assay	70
2.3.7.6 Propidium iodide staining.....	70
2.4 <i>In vivo</i> study	71
2.4.1 Overview of study	71
2.4.2 Ethical consideration	71
2.4.3 Animal monitoring and housing	73
2.4.4 Experimental design	73
2.4.5 Preparation of dosage treatment and administration of treatment	74

2.4.6 Body weight and fasting plasma glucose.....	74
2.4.7 Food and water intake monitoring	74
2.4.8 Oral glucose tolerance test (OGTT)	75
2.4.9 Blood collection and tissue harvesting	75
2.4.10 Fasting insulin.....	75
2.5 Gene expression analysis by quantitative real time PCR.....	76
2.5.1 RNA extraction.....	76
2.5.2 RNA quantification	77
2.5.3 RNA integrity.....	78
2.5.4 DNase treatment.....	79
2.5.5 Reverse transcription	79
2.5.6 Quantitative real-time PCR.....	80
2.5.6.1 Assessment of genomic DNA contamination	81
2.5.6.2 Quantitative real-time PCR for gene expression analyses	82
2.6 Protein expression analysis	84
2.6.1 Cell collection and protein extraction.....	84
2.6.2 Quantification of protein concentration	84
2.6.3 Protein separation by electrophoresis	85
2.6.4 Transfer of proteins to a PVDF membrane.....	85
2.6.5 Ponceau S staining	86
2.6.6 Western Blot analyses	86
2.7 Statistical analysis	87
CHAPTER 3.....	89
RESULTS 1	89
3.1 Phenolic Analysis	91
3.2 <i>In vitro</i> experiments to identify the most bioactive <i>Cyclopia</i> fraction.....	97
3.2.1 Validation of the <i>in vitro</i> cell model.....	97
3.2.2 The aqueous fraction of <i>C. maculata</i> and organic fraction of <i>C. intermedia</i> dose-dependently decrease lipid content in differentiated 3T3-L1 adipocytes.....	98
3.2.3 Cytotoxicity varies according to <i>Cyclopia</i> species and their fractions	101
3.2.4 Selection of the organic fraction of <i>C. intermedia</i> for further analysis	105
3.2.4.1 Effect of the organic fraction of <i>C. intermedia</i> on gene expression	105
3.2.4.2 Effect of the organic fraction of <i>C. intermedia</i> on protein expression.....	108
3.3 Validation of phenolic content and bioactivity of the large-scale preparation.....	108

3.4 <i>In vivo</i> experiments of the organic fraction of <i>C. intermedia</i>	111
3.4.1 Validation of the Lepr ^{db/db} mouse model	111
3.4.2 The organic fraction of <i>C. intermedia</i> decreases body weight gain in obese Lepr ^{db/db} without changes in food and water consumption.....	114
3.4.3 The organic fraction of <i>C. intermedia</i> increases liver weight of obese Lepr ^{db/db} mice.....	116
3.4.4 Effect of the organic fraction of <i>C. intermedia</i> on glucose metabolism.....	118
3.4.5 Effect of the organic fraction of <i>C. intermedia</i> on adipose tissue gene expression.....	118
3.4.5.1 Subcutaneous white adipose tissue.....	119
3.4.5.2 Gonadal white adipose tissue	122
3.4.5.3 Interscapular brown adipose tissue	125
3.5 Summary of results.....	127
CHAPTER 4.....	134
RESULTS 2	134
4.1 Fractionation of the organic fraction of <i>C. intermedia</i> and phenolic analysis	136
4.2 Effect of CCC fractions in differentiating 3T3-L1 pre-adipocytes	140
4.2.1 Lipid accumulation	140
4.2.2 Triglyceride content.....	142
4.2.3 ATP content	144
4.3 Effect of CCC fractions in mature 3T3-L1 adipocytes	146
4.3.1 Lipid content	146
4.3.2 Glycerol Release.....	148
4.3.3 ATP content.....	150
4.4 Effect of the CCC fractions on gene expression in mature 3T3-L1 adipocytes.....	152
4.5 Effect of the CCC fractions on protein expression in mature 3T3-L1 adipocytes.....	160
4.6 Summary of results.....	162
CHAPTER 5.....	167
DISCUSSION.....	167
5.1 Bioactivity varies according to <i>Cyclopia</i> species and phenolic content.....	168
5.2 Evaluation of the anti-obesity effects of <i>C. intermedia</i>	173
5.3 HPLC fractionation of <i>Cyclopia intermedia</i> into four fractions with different bioactivity.....	182
5.4 Shortcomings of the study	188
5.6 Future work	189
5.7 Conclusion	190

REFERENCES.....	192
ADDENDUM 1 - Animal Ethics Approval.....	219
ADDENDUM 2 - Reagents and Buffers solutions	221
ADDENDUM 3 - Supplementary Data	224

LIST OF FIGURES

CHAPTER 1

- Figure 1.1** The global prevalence of obesity (BMI \geq 30 kg/m²) in women and men \geq 18 years of age.
- Figure 1.2** Factors contributing to the development of obesity.
- Figure 1.3** Morphological representation of adipocytes within white adipose tissue and brown adipose tissue.
- Figure 1.4** Stages in pluripotent stem cell development to mature adipocytes and transcriptional regulation of adipocyte differentiation.
- Figure 1.5** Schematic diagram depicting the process of glucose uptake, glycolysis, the tricarboxylic acid cycle and fatty acid synthesis in adipocytes.
- Figure 1.6** An illustration of fatty acid uptake, and triglyceride synthesis and storage in adipocytes.
- Figure 1.7** Regulation of lipolysis in adipocytes during fasting and basal levels.
- Figure 1.8** Schematic illustration of fatty acid oxidation in the mitochondria.
- Figure 1.9** Mechanism of inflammatory and fatty acid induced insulin resistance in adipocytes.
- Figure 1.10** Trifoliolate leaves of *Cyclopia subternata* (A), *Cyclopia maculata* (B) and *Cyclopia intermedia* (C).
- Figure 1.11** Natural distribution of *Cyclopia* species in the Western and Eastern Cape regions of South Africa.

CHAPTER 2

- Figure 2.1** Experimental outline.
- Figure 2.2** Liquid-liquid fractionation of a 40% aqueous methanol extract indicating the aqueous, water (lower) fraction and the organic, *n*-butanol (upper) fraction.
- Figure 2.3** High performance counter current chromatography (A) and an illustration of the HPCCC protocol (B).
- Figure 2.4** Protocol for chemical induction of pre-adipocytes into mature adipocytes.

- Figure 2.5** Overview of animal experimental procedure.
- Figure 2.6** Schematic illustration of the transfer sandwich assembly used for transferring proteins from SDS-PAGE gel to a PVDF membrane.

CHAPTER 3

- Figure 3.1** Phenolic profile of *C. subternata*.
- Figure 3.2** Phenolic profile of *C. intermedia*.
- Figure 3.3** Phenolic profile of *C. maculata*.
- Figure 3.4** Validation of the *in vitro* cell model.
- Figure 3.5** The effect of aqueous and organic fractions, prepared from 40% aqueous methanol extract of *C. subternata* on lipid content in 3T3-L1 adipocytes.
- Figure 3.6** The effect of aqueous and organic fractions, prepared from 40% aqueous methanol extract of *C. intermedia* on lipid content in 3T3-L1 adipocytes.
- Figure 3.7** The effect of aqueous and organic fractions, prepared from 40% aqueous methanol extract of *C. maculata* on lipid content in 3T3-L1 adipocytes.
- Figure 3.8** The effect of aqueous and organic fractions, prepared from 40% aqueous methanol extract of *C. subternata* on mitochondrial dehydrogenase activity in 3T3-L1 adipocytes.
- Figure 3.9** The effect of aqueous and organic fractions, prepared from 40% aqueous methanol extract of *C. subternata* on ATP content in 3T3-L1 adipocytes.
- Figure 3.10** The effect of aqueous and organic fractions, prepared from 40% aqueous methanol extract of *C. intermedia* on mitochondrial dehydrogenase activity in 3T3-L1 adipocytes.
- Figure 3.11** The effect of aqueous and organic fractions, prepared from 40% aqueous methanol extract of *C. intermedia* on ATP content in 3T3-L1 adipocytes.
- Figure 3.12** The effect of aqueous and organic fractions, prepared from 40% aqueous methanol extract of *C. maculata* on mitochondrial dehydrogenase activity in 3T3-L1 adipocytes.
- Figure 3.13** The effect of aqueous and organic fractions, prepared from 40% aqueous methanol extract of *C. maculata* on ATP content in 3T3-L1 adipocytes.

- Figure 3.14** The effect of the organic fraction of *C. intermedia* on the mRNA expression genes involved in lipid or fatty acid, glucose and energy metabolism in 3T3-L1 adipocytes.
- Figure 3.15** The effect of the organic fraction of *C. intermedia* on PPAR γ and PPAR α protein expression in 3T3-L1 adipocytes.
- Figure 3.16** Phenolic profile of the large-scaled preparation of *C. intermedia*.
- Figure 3.17** Metabolic characteristics of Lepr^{db/db} mice and Lepr^{db/+} mice.
- Figure 3.18** The effect of the organic fraction of *C. intermedia* on body weight gain in Lepr^{db/+} and Lepr^{db/db} mice.
- Figure 3.19** The effect of the organic fraction of *C. intermedia* on food intake and water consumption of Lepr^{db/+} and Lepr^{db/db} mice.
- Figure 3.20** The effect of the organic fraction of *C. intermedia* on liver weight of Lepr^{db/db} and Lepr^{db/+} mice.
- Figure 3.21** The effect of the organic fraction of *C. intermedia* on fasting plasma glucose concentration and glucose tolerance of Lepr^{db/+} and Lepr^{db/db} mice.
- Figure 3.22** The effect of the organic fraction of *C. intermedia* on fasting serum insulin levels of Lepr^{db/+} and Lepr^{db/db} mice.
- Figure 3.23** The effect of the organic fraction of *C. intermedia* on the mRNA expression of genes associated with lipid, fatty acid, glucose and energy metabolism in subcutaneous adipose tissue of Lepr^{db/+} and Lepr^{db/db} mice.
- Figure 3.24** The effect of the organic fraction of *C. intermedia* on the mRNA expression of genes associated with lipid, fatty acid, glucose and energy metabolism in the gonadal adipose tissue of Lepr^{db/+} and Lepr^{db/db} mice.
- Figure 3.25** The effect of the organic fraction of *C. intermedia* on the mRNA expression of on the mRNA expression of brown fat markers and energy metabolism genes in the interscapular brown adipose tissue of Lepr^{db/+} and Lepr^{db/db} mice.

CHAPTER 4

- Figure 4.1** HPLC chromatographic profile of the organic fraction of *C. intermedia*.
- Figure 4.2** Phenolic profile showing the major phenolic compounds of CCC fraction 1.
- Figure 4.3** Phenolic profile showing the major phenolic compounds of CCC fraction 2.

- Figure 4.4** Phenolic profile showing the major phenolic compounds of CCC fraction 3.
- Figure 4.5** Phenolic profile showing the major phenolic compounds of CCC fraction 4.
- Figure 4.6** The effect of CCC F1, CCC F2, CCC F3 and CCC F4 on lipid accumulation in differentiating 3T3-L1 pre-adipocytes.
- Figure 4.7** The effect of CCC F1, CCC F2, CCC F3 and CCC F4 on triglyceride content in differentiating 3T3-L1 pre-adipocytes.
- Figure 4.8** The effect of CCC F1, CCC F2, CCC F3 and CCC F4 on intracellular ATP content in differentiating 3T3-L1 pre-adipocytes.
- Figure 4.9** The effect of CCC F1, CCC F2, CCC F3 and CCC F4 on lipid content in differentiated 3T3-L1 adipocytes.
- Figure 4.10** The effect of CCC F1, CCC F2, CCC F3 and CCC F4 on glycerol release in differentiated 3T3-L1 adipocytes.
- Figure 4.11** The effect of CCC F1, CCC F2, CCC F3 and CCC F4 on intracellular ATP content in differentiated 3T3-L1 adipocytes.
- Figure 4.12** The effect of the CCC fractions on mRNA expression of genes involved in lipid or fatty acid, energy and glucose metabolism.
- Figure 4.13** The effect of CCC fractions on PPAR α and PPAR γ protein expression.

ADDENDUM 3

- Figure S1** The effect of aqueous and organic fractions, prepared from 40% aqueous methanol extracts of *C. maculata*, *C. intermedia* and *C. subternata* on cell density in 3T3-L1 adipocytes.
- Figure S2** The effect of CCC F1, CCC F2, CCC F3 and CCC F4 on cell density in differentiating 3T3-L1 pre-adipocytes.
- Figure S3** The effect of CCC F1, CCC F2, CCC F3 and CCC F4 on cell density in differentiated 3T3-L1 adipocytes.
- Figure S4** The effect of the aqueous fraction of *C. maculata* and the organic fraction of *C. intermedia* on propidium iodide staining.
- Figure S5** The effect of the old and new organic fraction of *C. intermedia* on lipid accumulation in 3T3-L1 adipocytes.

- Figure S6** The effect of the old and new organic fraction of *C. intermedia* on the mitochondrial dehydrogenase activity in 3T3-L1 adipocytes.
- Figure S7** The effect of the old and new organic fraction of *C. intermedia* on the ATP content in 3T3-L1 adipocytes.
- Figure S8** The effect of the organic fraction of *C. intermedia* and the CCC fractions on PPAR α and PPAR γ protein expression.

LIST OF TABLES

CHAPTER 1

- Table 1.1** Methods of assessment and classification of obesity, and the risk associated with metabolic disease.
- Table 1.2** World Health Organization criteria to define the metabolic syndrome.
- Table 1.3** International Diabetes Federation criteria to define the metabolic syndrome.
- Table 1.4** Chemical compounds identified in *Cyclopia* to date.
- Table 1.5** Studies demonstrating the *in vitro* anti-obesity and anti-diabetic properties of the major phenolic compounds of *Cyclopia* species and the mechanism of their biological activity.
- Table 1.6** Studies demonstrating the *in vivo* anti-obesity and anti-diabetic properties of the major phytochemicals of *Cyclopia* species and the mechanism of their biological activity.

CHAPTER 2

- Table 2.1** Information regarding the original harvestings and processing of *Cyclopia* species.
- Table 2.2** Standard calibration mixtures for *C. subternata*, *C. intermedia* and *C. maculata* phenolic standards.
- Table 2.3** Cell seeding densities and volumes used for multi-well plate culturing.
- Table 2.4** Media formulations used for adipocyte differentiation and maintenance.
- Table 2.5** Treatment groups for the mice.
- Table 2.6** Components used for the reverse transcription reaction.
- Table 2.7** Reaction components for quantitative real time PCR to assess genomic DNA content.
- Table 2.8** Reaction components for quantitative real time PCR reactions.
- Table 2.9** Taqman® gene expression assays used in this study.
- Table 2.10** Primary antibodies and dilutions used in Western blot detection.

CHAPTER 3

- Table 3.1** Quantification of major phenolic compounds in 40% aqueous methanol extracts of *C. subternata*, *C. intermedia* and *C. maculata* and their aqueous and organic fractions by HPLC-DAD.
- Table 3.2** Quantification of major phenolic compounds (g/100 g) in the upscaled 40% aqueous methanol extract of *C. intermedia* and its organic fraction by qHPLC-DAD.
- Table 3.3** Metabolic characteristics of the $\text{Lepr}^{\text{db/+}}$ and $\text{Lepr}^{\text{db/db}}$ control mice after 28 days.
- Table 3.4** Effect of the organic fraction of *C. intermedia* on body weight.
- Table 3.5** Summary of *in vitro* results for *C. subternata*.
- Table 3.6** Summary of *in vitro* results for *C. intermedia*.
- Table 3.7** Summary of *in vitro* results for *C. maculata*.
- Table 3.8** Summary of *in vitro* mRNA gene expression results.
- Table 3.9** Summary of *in vitro* protein expression results.
- Table 3.10** Summary of mRNA gene expression results in sWAT and gWAT.
- Table 3.11** Summary of mRNA gene expression results in iBAT.

CHAPTER 4

- Table 4.1** Quantification of major phenolic compounds (g/100 g organic fraction) in the CCC fractions of the organic fraction of a 40% aqueous methanol extract of *C. intermedia* by qHPLC-DAD.
- Table 4.2** Summary of results for CCC fraction screening in differentiating 3T3-L1 pre-adipocytes.
- Table 4.3** Summary of results for CCC fraction screening in differentiated 3T3-L1 adipocytes.
- Table 4.4** Summary results for the effect of CCC fractions on mRNA expression in differentiated 3T3-L1 adipocytes.
- Table 4.5** Summary results for the effect of CCC fractions on protein expression in differentiated 3T3-L1 adipocytes.

ABBREVIATIONS

Acaca	Acetyl-coenzyme A carboxylase alpha
ACC	Acetyl-coenzyme A carboxylase
Act β	Beta-actin
Adipoq	Adiponectin
ADP	Adenosine diphosphate
AMPK	Adenosine monophosphate activated protein kinase
ANOVA	Analysis of variance
ATCC	American type culture collection
ATGL	Adipose triglyceride lipase
ATP	Adenosine triphosphate
AUC	Area under the curve
B2M	Beta-2 microglobulin
BSA	Bovine serum albumin
BMI	Body mass index
BW	Body weight
cAMP	Cyclic adenosine monophosphate
CCC F1	Counter-current chromatography fraction-1
CCC F2	Counter-current chromatography fraction-2
CCC F3	Counter-current chromatography fraction-3
CCC F4	Counter-current chromatography fraction-4
C/EBP α	CCAAT/enhancer-binding protein alpha
C/EBP β	CCAAT/enhancer binding protein beta
C/EBP δ	CCAAT/enhancer binding protein delta
CD36/FAT	Fatty acid translocase
cDNA	Complementary DNA
CO ₂	Carbon dioxide
CPM	Counts per minute
CPTI α	Carnitine Palmitoyltransferase I alpha
CREB1	cAMP response element binding protein 1
Cs	Citrate synthase
Ct	Cycle threshold
CVD	Cardiovascular disease
DAG	Diacylglycerol
DMEM	Dulbecco's modified eagle's medium
DMSO	Dimethyl sulfoxide
DNA	Deoxyribonucleic acid
dNTPs	Deoxynucleotides
DPBS	Dulbecco's phosphate buffered saline
DPM	Disintegrations per minute
ECM	Extracellular matrix
EGCG	Epigallocatechin gallate
ELISA	Enzyme-linked immunosorbent assay
Ex/em	Excitation and emission

FA	Fatty acid
FAs	Fatty acids
FABP4	Fatty acid binding protein 4
FABPpm	Plasma membrane fatty acid binding protein
FABPc	Cytosolic fatty acid binding protein
FASN	Fatty acid synthase
FATP	Fatty acid transport protein
FBS	Fetal bovine serum
FFA	Free fatty acid
FGF2	Fibroblast growth factor 2
Fig	Figure
G3PDH	Glyceraldehyde-3-phosphate dehydrogenase
G6P	Glucose-6-phosphate
G6Pc	Glucose 6-phosphatase, catalytic
G6Pase	Glucose 6-phosphatase
GATA2	GATA binding protein 2
GDM	Gestational diabetes mellitus
GLUT1 or 4	Glucose transporter 1 or 4
HDL-C	High density lipoprotein cholesterol
HPCCC	High performance counter-current chromatography
HPLC-DAD	High performance liquid chromatography with diode-array detection
HRP	Horseradish peroxidase
HSL	Hormone sensitive lipase
HSP90AB1	Heat shock protein 90 alpha (cytosolic), class B member 1
HPRT1	Hypoxanthine guanine phosphoribosyl transferase 1
IBMX	Isobutyl methyl xanthine
IDF	International diabetes federation
IL-6	Interleukin-6
IRS	Insulin receptor substrate
IRS1	Insulin receptor substrate-1
LCFA	Long chain fatty acid
LC-MS/MS	Liquid chromatography tandem mass spectrometry
LPL	Lipoprotein lipase
LDL-C	Low-density lipoprotein cholesterol
MetS	Metabolic syndrome
mRNA	Messenger ribonucleic acid
MTT	3-(4,5-dimethylthiazol-2-yl)-2,5-diphenyltetrazolium bromide
NaOH	Sodium hydroxide
NBCS	New born calf serum
NEFA	Non-esterified fatty acids
NONO	Non-POU-domain-containing, octamer binding protein
NTC	No template control
OD	Optical density
OGTT	Oral glucose tolerance test

PBS	Phosphate buffered saline
PMSF	Phenylmethylsulfonyl fluoride
PGC1 α	Peroxisome proliferator-activated receptor gamma coactivator 1-alpha
PPAR α	Peroxisome proliferator-activated receptor alpha
PPAR γ	Peroxisome proliferator-activated receptor gamma
AMPK	5' AMP-activated protein kinase
PUDAC	Primate unit and delft animal centre
PVDF	Polyvinylidene difluoride
qRT-PCR	Quantitative reverse transcription polymerase chain reaction
RC/DC	Reducing agent compatible and detergent compatible
ROS	Reactive oxygen species
rpm	revolutions per minute
RPL13A	Ribosomal protein l13a
SCD1	Stearoyl-coenzyme A desaturase 1
SDS	Sodium dodecyl sulfate
SDS-PAGE	Sodium dodecyl sulfate polyacrylamide gel electrophoresis
SEM	Standard error of the mean
SIRT1	Sirtuin1
SIRT3	Sirtuin3
SREBF1	Sterol regulatory element binding transcription factor 1
SST	Serum separating tubes
STZ	Streptozotocin
T1DM	Type 1 diabetes mellitus
T2DM	Type 2 diabetes mellitus
TBST	Tris buffered saline with tween
TC	Total cholesterol
TG	Triglycerides
TNF α	Tumor necrosis factor alpha
UCP1	Uncoupling protein 1
UCP2	Uncoupling protein 2
UCP3	Uncoupling protein 3
VLDL-C	Very low density lipoprotein cholesterol
WC	Waist circumference
WHO	World health organization
WHR	Waist to hip ratio

UNITS OF MEASUREMENTS

μ L	Microliter
mL	Milliliter
L	Litre
Ng	Nanogram
μ g	Microgram
Mg	Milligram

G	Gram
kg	Kilogram
nM	Nanomolar
μ M	Micromolar
mM	Millimolar
M	Molar
mm	Millimeters
μ m	Micrometer
min	Minute
sec	Second
H	Hour
$^{\circ}$ C	Degree Celsius
$\times g$	Centrifugal gravity
%	Percentage

CHAPTER 1

LITERATURE REVIEW

1.1 Introduction

Obesity is a metabolic disorder that is characterized by the excessive accumulation of fat, to the extent that it negatively impacts health (Jung and Choi, 2014). Obese individuals have an increased risk of developing a number of chronic diseases such as type 2 diabetes mellitus (T2DM), cardiovascular diseases (CVD) and certain types of cancers (Schuklenk and Zhang, 2014), with obesity often regarded as the plague of the 21st century and the leading cause of preventable death (Rössner, 2002).

1.2 Assessment of obesity

Body mass index (BMI) is the most commonly used method to assess obesity (Nguyen and El-Serag., 2010) and is calculated by dividing weight in kilograms (kg) by height in meters squared (m^2) (Rothman, 2008). A BMI value of $30 \text{ kg}/m^2$ or more indicates obesity; BMI can also be used to determine whether individuals are underweight, normal weight or overweight (**Table 1.1**) (Aditya and Wilding, 2011). Although BMI is used globally as a marker for obesity, it is unable to distinguish between peripheral (subcutaneous) obesity and central (visceral) obesity, and fails to account for muscle mass. Subcutaneous fat is associated with fat distribution throughout the body, for example in the buttocks, thighs and arms, whereas visceral obesity occurs when excess body fat accumulates in the abdominal or chest areas, surrounding the internal organs and is often associated with metabolic disorders (Hamdy et al., 2006). For example, Asian women, despite having similar BMI to Caucasian women, have an increased risk of developing metabolic and obesity-related diseases, which could be due to increased visceral adiposity (Lim et al., 2011). A combination of BMI, waist circumference (WC), which is the measurement around the narrowest part of the abdomen above the hip, and waist-to-hip ratio (WHR), the ratio of the WC to the hip circumference, the measurement around the narrowest part of the waist and the widest area of the hips, have been suggested to more accurately predict the risk of metabolic diseases (Table 1.1). Although using a combination of these measurements is superior to using them individually, they are susceptible to ethnic variation (Chan and Woo, 2010).

Table 1.1 Methods of assessment and classification of obesity, and the risk associated with metabolic disease.

Assessment Method	Measurement and classification	Health risk
BMI (kg/m ²)	< 18.5 kg/m ² (underweight)	-
	18.5 - 24.9 kg/m ² (Normal)	Normal
	25.0 - 29.9 kg/m ² (Overweight)	Increased
	30.0 - 34.9 kg/m ² (Obesity)	High
	35.0 - 39.9 kg/m ² (High obesity)	Very high
	≥ 40.0 kg/m ² (Extreme obesity)	Extremely high
Waist-to-hip ratio Waist (cm) / Hip (cm)	Males ≥ 0.95	High
	Females ≥ 0.8	High
Waist Circumference Waist (cm)	Male < 94 cm	Low
	≥ 94 cm	High
	≥ 102 cm	Very high
	Females < 80 cm	Low
	≥ 80 cm	High
	≥ 88 cm	Very high

Adapted from the National Institutes of Health (1998).

1.3 Prevalence of obesity

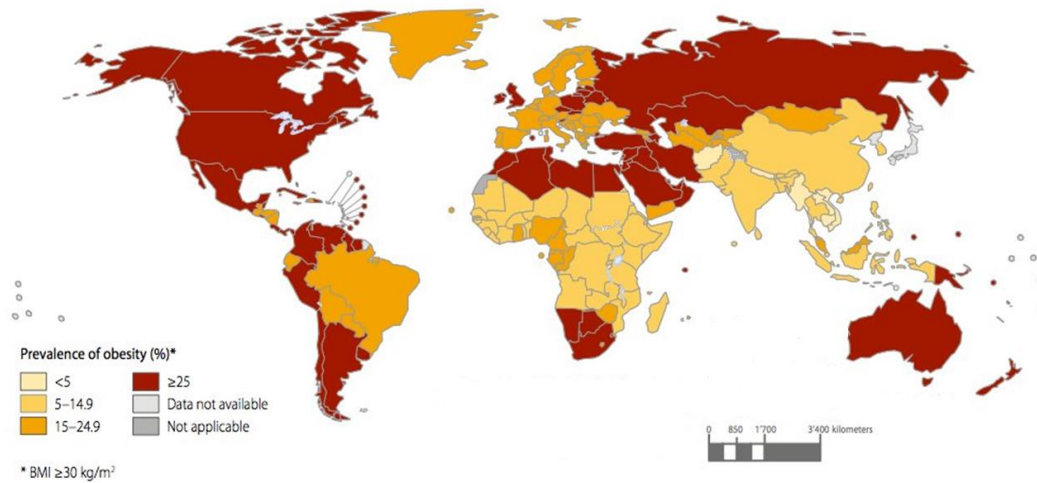
The prevalence of obesity increased rapidly during the 1980s, with the World Health Organization (WHO) classifying obesity an epidemic in 1997 (James, 2008). Recent epidemiological data show that the number of overweight and obese individuals has increased from 857 million individuals in 1980 to 2.1 billion individuals in 2013, i.e. nearly 30% of the world's population is either overweight or obese (Ng et al., 2014), and of those individuals 670 million are classified as obese (BMI ≥ 30 kg/m²) and 98 million severely obese (BMI ≥ 35 kg/m²) (World Obesity Federation, 2015). If the current trajectory continues to escalate without effective interventions, the number of obese individuals in the world could increase by up to 1.12 billion individuals by 2030 (Kelly et al., 2008). It is estimated that obesity accounted for approximately 3.4 million deaths in 2010 (Ng et al., 2014). The obesity epidemic is not restricted to adults, with an increasing number of

children classified as obese. Globally, approximately 42 million children under the age of five were overweight or obese in 2013 (WHO, 2014).

1.3.1 South Africa

Although obesity was traditionally considered a disease of developed countries, recent studies report its growing prevalence in low and middle income countries. For example, a recent survey reported that South Africa (SA), a middle income country at the southernmost tip of Africa, has amongst the highest rates of overweight and obese individuals globally (**Fig. 1.1**) (Ng et al., 2014). In particular, approximately 69.3% of South African women are overweight, of whom 42% are obese. These rates are higher than those reported for women in the United States of America (USA) (61.9% overweight, of whom 33.95% obese), a country renowned for its high overweight and obesity rates (Ng et al., 2014). Alarmingly, many of these women are of child-bearing age, and candidates for abnormal intrauterine programming, thus increasing the risk of their offspring developing obesity and metabolic disease in later life (Desai et al., 2013). Further, obesity increases the risk of non-communicable diseases, and in SA it is estimated that up to 90% of T2DM cases are attributable to being overweight (Joubert et al., 2007). This presents a major burden to an already struggling health care system, challenged with high rates of human immunodeficiency virus and acquired immune deficiency syndrome (HIV/AIDS) and tuberculosis (TB).

Age-standardized prevalence of obesity in women aged 18 years and over (BMI ≥ 30 kg/m²), 2014



Age-standardized prevalence of obesity in men aged 18 years and over (BMI ≥ 30 kg/m²), 2014

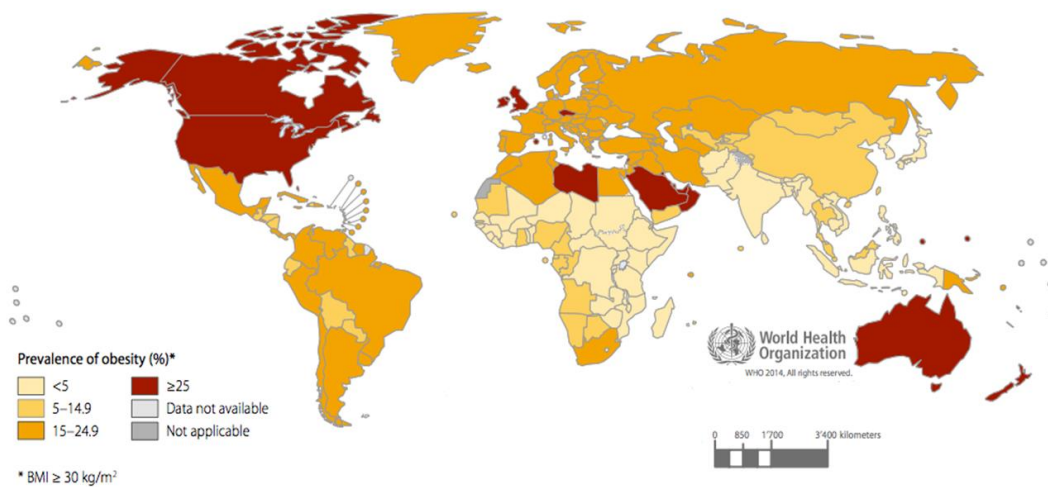


Figure 1.1 The global prevalence of obesity (BMI ≥ 30 kg/m²) in women and men ≥ 18 years of age. Adapted from WHO (2014).

1.4 Risk factors for obesity

Although obesity is a multifactorial disorder caused by a number of factors including genetics, medication, psychological, cultural and economic factors, the consumption of an unhealthy diet characterized by high-fat or high-sugar foods, and a sedentary lifestyle is thought to be the main contributors to the disease (Popkin, 2005) (**Fig. 1.2**). A number of rodent and non-human primate studies have provided direct evidence of dietary effects

on obesity and metabolic disease (Bremer et al., 2011; Yang et al., 2012). Yang et al. (2012) showed that consumption of a high fat and sucrose diet induced weight gain, hepatosteatosis, adipose tissue hypertrophy and hyperinsulinemia in male C57BL/6 J mice. In rhesus monkeys, a high-fructose diet induced insulin resistance and other features of the metabolic syndrome including central obesity, dyslipidemia, and inflammation (Bremer et al., 2011). Similarly, in human studies such as the Leeds Fat Study, obesity was 19 times higher in individuals who consumed diets high in fat compared to individuals who consumed low fat diets (Blundell and MacDiarmid, 1997). Bray et al. (2004) showed that increased consumption of high-fructose corn syrup is associated with the increased obesity epidemic. Epidemiological studies have shown that the increased prevalence of obesity is associated with reduced physical activity and increased sedentary behavior, especially amongst children and adolescents (Maffei, 2000).

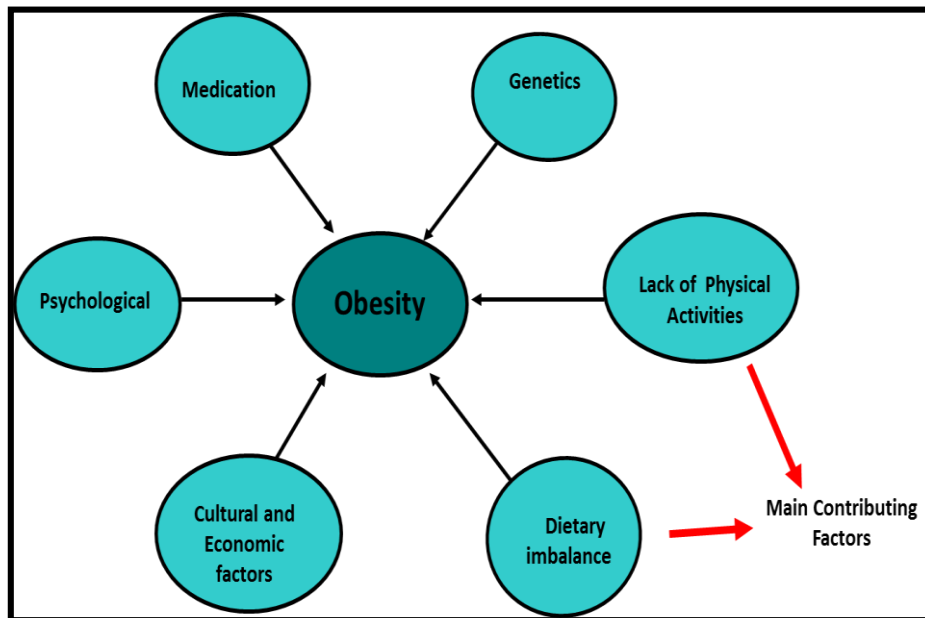


Figure 1.2 Factors contributing to the development of obesity. Adapted and modified from Popkin (2005).

1.5 Adipose tissue

There are two types of adipose tissue, white adipose tissue (WAT), whose main function is to store excess energy as fat thereby maintaining whole-body energy homeostasis, and brown adipose tissue (BAT), whose function is thought to be heat generation (Cannon and Nedergaard, 2004; Gaidhu and Ceddia, 2011). Adipocytes within these adipose depots have different cellular structures and physiological roles. Adipocytes within WAT contain a single large lipid droplet, a nucleus and a few mitochondria in the periphery of the cytoplasmic area; in contrast, adipocytes within BAT contain smaller lipid droplets and many mitochondria (**Fig. 1.3**).

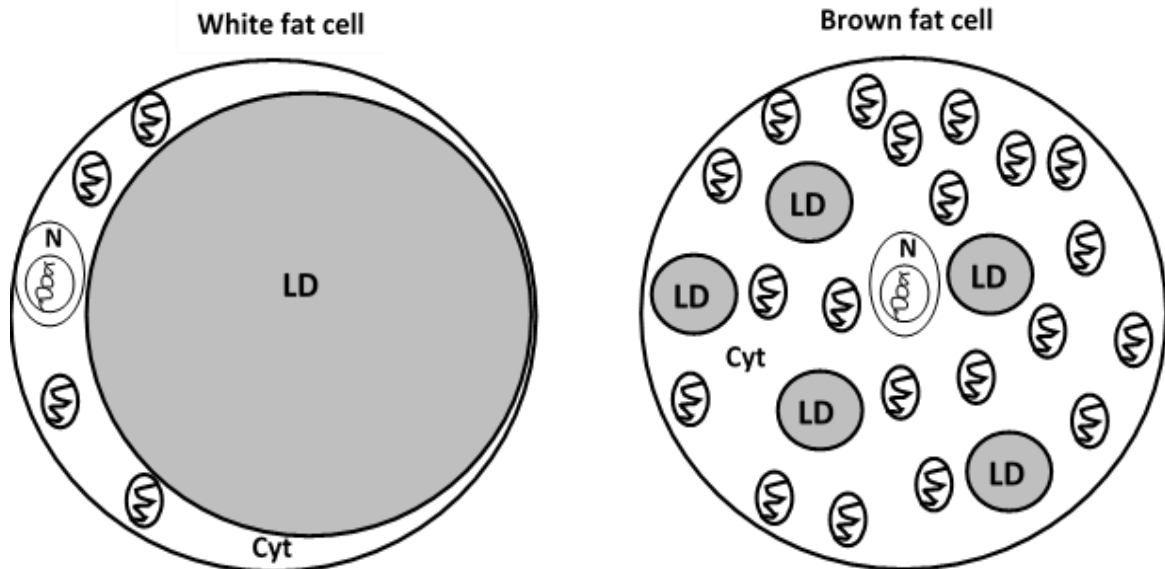


Figure 1.3 Morphological representation of adipocytes within white adipose tissue and brown adipose tissue. Adipocytes from white adipose tissue (WAT) contain a large single triglyceride-containing lipid droplet (LD), a single nucleus (N) and few mitochondria in the limited cytoplasmic (Cyt) area, whereas adipocytes from brown adipose tissue (BAT) contain a high density of mitochondria and multiple small LD. Adapted and modified from Gaidhu and Ceddia (2011).

Adipose tissue respond to excess nutrients by adipocyte hypertrophy and/or hyperplasia. Adipocyte hyperplasia refers to adipose tissue growth due to an increased number of adipocytes, whereas adipocyte hypertrophy refers to adipose tissue growth due to an

increase in adipocyte size (Jo et al., 2009). Adipocyte hypertrophy is associated with abnormal tissue remodeling, hypoxia, adipocyte cell death, increased secretion of chemokines, recruitment of macrophages and chronic inflammation (Lee et al., 2010).

1.5.1 White adipose tissue

WAT is comprised of 35% - 75% adipocytes (Gaidhu and Ceddia, 2011), which are specialized cells for the synthesis and storage of fat as triglycerides (TGs) (**Fig. 1.3**). Other cell types include small mesenchymal stem cells (MSCs), T regulatory cells, endothelial precursor cells, immune cells, macrophages and pre-adipocytes (Halberg et al., 2008). In addition to its main function to store energy and regulate energy homeostasis (Vázquez-Vela et al., 2008), WAT has also been identified as a key endocrine organ that secretes a variety of adipokines (leptin, adiponectin, interleukin 6 (IL-6) and tumor necrosis factor alpha (TNF- α)) that function as autocrine/paracrine molecules regulating metabolism within adipose and multiple other tissues (Cao, 2014). White adipose tissue can occur subcutaneously or as visceral fat (Hamdy et al., 2006).

1.5.2 Brown adipose tissue

The term BAT is derived from the brown color of this adipose tissue, which is attributed to the presence of a large number of mitochondria in these cells (**Fig. 1.3**) (Cannon and Nedergaard, 2004). Brown adipose tissue is found abundantly in infants and in small mammals, with its expression decreasing with age (Graja and Schulz, 2015). The primary function of BAT is to transform energy into heat, a term referred to as adaptive thermogenesis. During adaptive thermogenesis, the uncoupling protein 1 (UCP-1, also known as thermogenin) uncouples oxidative phosphorylation from ATP synthesis, thus generating heat and increasing energy expenditure. Adaptive thermogenesis is induced by cold (non-shivering thermogenesis) or by excess calorie intake (diet-induced thermogenesis) (Cannon and Nedergaard 2004; Wu et al., 2013). Rodent and human studies have shown that brown adipocytes are able to maintain energy balance and improve glucose metabolism compared to their white counterparts (Chondronikola et al.,

2014). Over the last few years, the conversion of white adipocytes into brown or beige adipocytes has attracted considerable interest as therapeutic targets for obesity (Wu et al., 2013).

1.6 Adipogenesis

Adipogenesis refers to adipocyte formation, a process whereby precursor cells differentiate into mature adipocytes. *In vitro* cell line models such as 3T3-L1 adipocytes, discussed in more detail in **Section 1.12**, have facilitated the elucidation of the process of adipogenesis (**Fig. 1.4**). Pluripotent stem cells differentiate into mesenchymal precursor cells that have the ability to differentiate into various cell lineages including pre-adipocytes, chondroblasts, osteoblasts or myoblasts (Gregoire et al., 1998). The process of differentiation into mature adipocytes includes growth arrest, post-confluence mitosis, clonal expansion, early differentiation and terminal differentiation (**Fig. 1.4**) (Gregoire et al., 1998). Adipogenesis is co-ordinated by a number of transcription factors that regulate the expression of genes involved in adipocyte development (**Fig. 1.4**) (Gregoire et al., 1998).

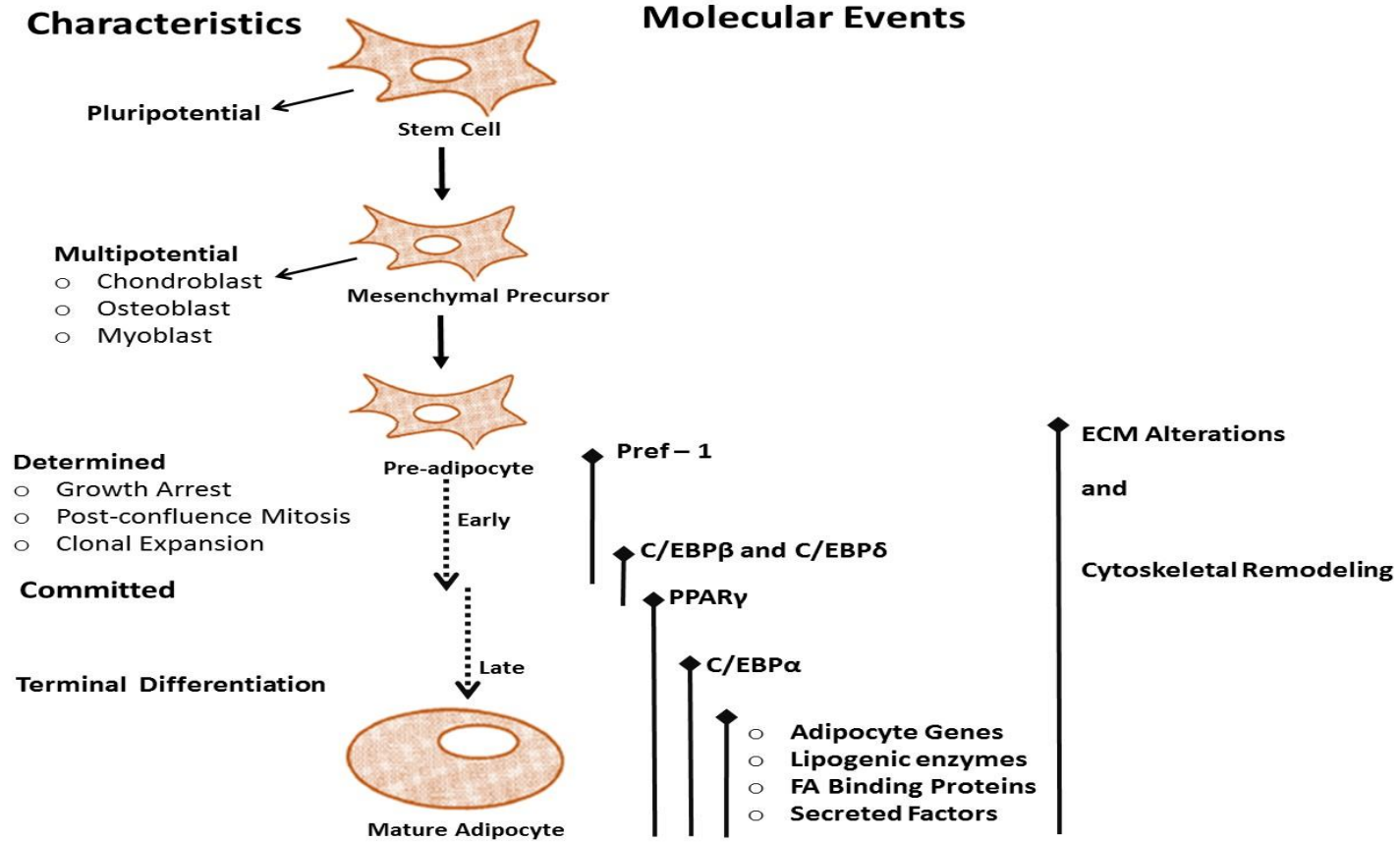


Figure 1.4 Stages in pluripotent stem cell development to mature adipocytes and transcriptional regulation of adipocyte differentiation. Adipocytes are derived from pluripotent stem cells, differentiated into mesenchymal precursor cells and pre-adipocytes. For the development of mature adipocytes, pre-adipocytes undergo four major stages including growth arrest, clonal expansion, early differentiation and terminal differentiation. This is regulated by several transcription factors. Adapted and modified from Gregoire et al. (1998).

Pref-1 - Pre-adipocyte factor 1; C/EBPβ - CCAAT/enhancer-binding protein beta; C/EBPδ - CCAAT/enhancer-binding protein delta; PPARγ - peroxisome proliferator activator receptor gamma; C/EBPα - CCAAT/enhancer-binding protein alpha; ECM - Extracellular matrix.

1.6.1 Transcriptional regulation of adipogenesis

Adipogenesis is regulated by several transcription factors, with peroxisome proliferator activator receptor gamma (PPAR γ) and members of the CCAAT/enhancer binding protein (C/EBP) family considered the most important (Cowherd et al., 1999).

1.6.1.1 Peroxisome proliferator activator receptor gamma (PPAR γ)

PPAR γ , a key regulator of adipogenesis (Rosen et al., 1999), is a member of the nuclear hormone receptor superfamily and is predominantly expressed in adipose tissue. PPAR γ exists in two isoforms, PPAR γ 1 and PPAR γ 2, due to alternative splicing or alternative promoter usage of the PPAR γ gene (Rosen et al. 2000). PPAR γ 1 is expressed in several tissues, whereas PPAR γ 2 is primarily expressed in adipocytes (Cowherd et al., 1999; Rosen et al., 2000). Both isoforms induce adipogenesis (Cowherd et al., 1999), although PPAR γ 2 is considered more essential for adipocyte differentiation than PPAR γ 1. The additional 30 amino acid residues at the N-terminal of PPAR γ 2 are thought to account for its higher transcriptional activity compared to PPAR γ 1 (Zhu et al., 1995). The expression of PPAR γ is regulated by several transcription factors which either inhibit or activate its expression. In addition to its role in adipogenesis, PPAR γ also regulates a number of genes involved in lipid and glucose metabolism such as adipocyte fatty acid binding protein (aP2), lipoprotein lipase (LPL), fatty acid transport protein (FATP), acyl-CoA synthase (ACS), fatty acid synthase (FASN), glucose transporter 4 (GLUT4), perilipin and hormone-sensitive lipase (HSL) (Savage, 2005).

PPAR γ plays an important role in regulating insulin sensitivity, and ligands that are able to activate PPAR γ have been investigated as therapeutic targets for T2DM. The most popular are the thiazolidinediones (TZDs) such as rosiglitazone and pioglitazone (Monsalve et al., 2013). Unsaturated fatty acids (oleate, linoleate, eicosapentaenoic or arachidonic acids) and their metabolites are also able to activate PPAR γ (Ferré, 2004).

Other members of the PPAR family include PPAR alpha (α) and PPAR delta (δ) (Vázquez-Vela et al., 2008). PPAR α is highly expressed in the liver, heart, kidneys and skeletal muscle, and plays an important role in fatty acid metabolism by regulating the expression

of genes involved in β -oxidation (Berger et al., 2005). PPAR α is also expressed in adipocytes where it induces adipogenesis, although not as effectively as PPAR γ 2 (Brun et al., 1996). PPAR δ is highly expressed in rodents and humans, however it is not capable of inducing adipogenesis (Cowherd et al., 1999; Vázquez-Vela et al., 2008), and has been implicated in mechanisms such as energy uncoupling and fatty acid catabolism in hepatocytes, muscles and adipocytes (Wang et al., 2003; Lee et al., 2006).

1.6.1.2 CCAAT/enhancer binding protein (C/EBP) family

Six isoforms of the C/EBP family have been identified, but only C/EBP alpha (α), C/EBP beta (β) and C/EBP delta (δ) have been reported to regulate adipocyte differentiation (Akasaka et al., 2007). The essential role of C/EBP α in adipogenesis has been demonstrated in several mouse fibroblastic cell lines where its overexpression induced adipogenesis (Freytag et al., 1994). Moreover, adipocytes of C/EBP α knockout mice failed to accumulate lipids (Wang et al., 1995), further illustrating the importance of C/EBP α in adipocyte development. Both PPAR γ and C/EBP α are essential for regulating adipogenesis (Rosen et al., 2002) and it has been suggested that they participate in a single pathway. However, Rosen et al. (2002) showed that PPAR γ is also able to stimulate adipose development independently of C/EBP α .

The pro-adipogenic role of C/EBP β and C/EBP δ has been established *in vitro* by several studies. In 3T3-L1 pre-adipocytes, the expression of both C/EBP β and C/EBP δ , stimulated adipogenesis and also induced the expression of C/EBP α (Cao et al., 1991). Similarly, the expression of C/EBP β in NIH-3T3 fibroblasts enhanced adipogenesis and increased PPAR γ expression (Wu et al., 1995). These studies suggest that C/EBP β and C/EBP δ are necessary for inducing the expression of C/EBP α and PPAR γ , which are important regulators of adipocyte differentiation.

1.6.1.3 Other transcription factors involved in adipogenesis

Other transcription factors essential for adipogenesis include the sterol regulatory element binding protein (SREBP)-1c, members of the Krüppel-like factors (KLF) proteins, and the

signal transducer and activator of transcription-5a (STAT5a) (Stephens, 2012). Several studies have demonstrated that SREBP1c stimulates adipocyte development (Kim and Spiegelman, 1996; Kim et al., 1998; Fajas et al., 1999); possibly by inducing PPAR γ expression (Kim et al., 1998). Further, SREBP1c regulates lipid metabolism by inducing the expression of genes involved in fatty acid (FA) and triglyceride (TG) synthesis (Kim and Spiegelman, 1996). KLF transcription factors such as KLF15, KLF5, KLF4, KLF6 and KLF9 are essential for adipocyte development whereas KLF2, KLF3 and KLF7 are anti-adipogenic (Wu and Wang, 2013). Transcription factors such as members of the GATA-binding (GATA2 and GATA3), the Forkhead families (Forkhead Box O1 [FOXO1] and Forkhead Box A2 [FOXA2]) and the Wnt families inhibit adipocyte differentiation (Stephens, 2012).

1.7 Adipocyte metabolism

After the ingestion of food, FAs are taken up directly from the circulation in the form of non-esterified FAs/free fatty acids (FFAs), or synthesized endogenously from excess glucose metabolites during *de novo* lipogenesis. FAs are used as an energy source or for energy storage in the form of TGs (Kersten, 2001). During nutrient deprivation, TGs are hydrolyzed, resulting in the release of FAs from adipocytes and their transport to target tissues such as the muscle or liver (Duncan et al., 2007), where they can be used for energy production through β -oxidation (Glatz et al., 2010). The processes important in glucose and FA metabolism, TG formation, storage and mobilization will be discussed below.

1.7.1 Glucose metabolism

Glucose is used primarily as a source of energy and carbon for FA synthesis and provides the glycerol backbone for TG synthesis (Guo et al., 2012). Two transport proteins, glucose transporter 1 (GLUT1), encoded by the solute carrier family 2 (facilitated glucose transporter), member 1 (SLC2A1) gene, and glucose transporter 4 (GLUT4), encoded by the solute carrier family 2 (facilitated glucose transporter), member 4 (SLC2A4) gene, are

responsible for the uptake of glucose by adipocytes. Basal glucose uptake is facilitated by GLUT1, while insulin stimulated glucose uptake is facilitated by GLUT4 (Pessin et al., 1992). After entry into the adipocyte, the majority of glucose is metabolized via glycolysis. Hexokinase (HK) catalyzes the first step of glycolysis, i.e. the phosphorylation of glucose to glucose-6-phosphate, which undergoes a number of reactions to yield pyruvate as an end product (**Fig. 1.5**) (Guo et al., 2012). Pyruvate is converted to acetyl-CoA by pyruvate dehydrogenase (PDH) and in the mitochondrial matrix. In the mitochondria, acetyl-CoA enters the tricarboxylic acid (TCA) cycle, also known as the Krebs cycle, and is metabolized to carbon dioxide (CO_2), $\text{NADH} + \text{H}^+$ and FADH_2 and to a lesser extent the TCA cycle leads to the production of adenosine triphosphate (ATP) through oxidative phosphorylation. Citrate is used for the transport of acetyl-CoA from the mitochondrial matrix into the cytoplasm using ATP citrate lyase, where acetyl-CoA is used as the substrate for endogenous FA synthesis (**Fig. 1.5**).

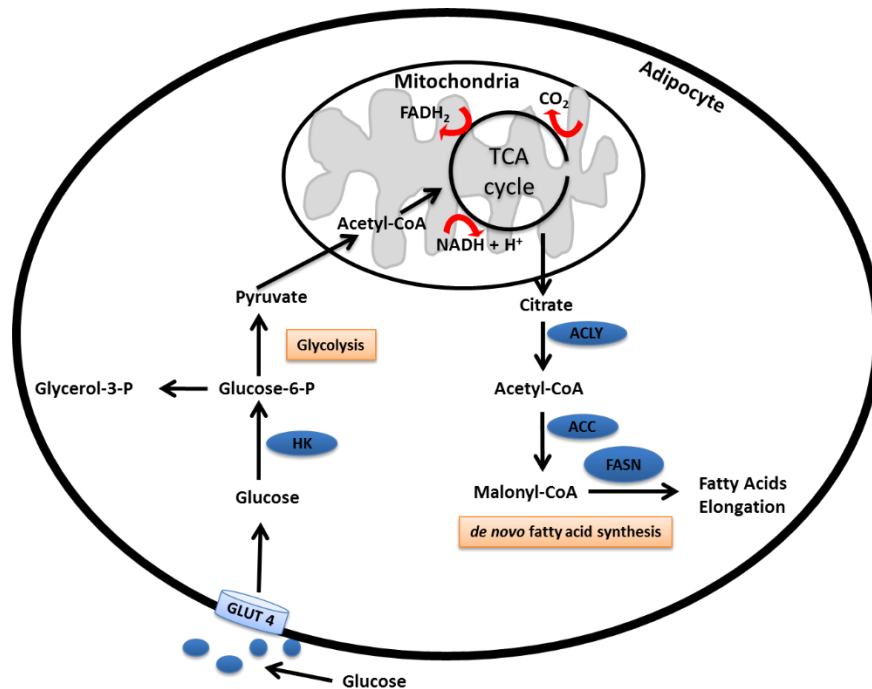


Figure 1.5 Schematic diagram depicting the process of glucose uptake, glycolysis, the tricarboxylic acid cycle and fatty acid synthesis in adipocytes. After glucose uptake by adipocytes, it is converted to pyruvate by glycolysis in the cytoplasm and thereafter pyruvate is converted to acetyl-CoA and enters the mitochondrion. Acetyl-CoA is either used for energy (ATP) production in the mitochondria or used in the cytoplasm for FA synthesis. Adapted and modified from (Ferré and Foufelle, 2007). GLUT4 - glucose transporter 4; HK - hexokinase; ACLY - ATP citrate lyase; ACC - Acetyl-CoA carboxylase; FASN - fatty acid synthase.

1.7.2 Lipogenesis

Lipogenesis refers to the formation and storage of FAs as TGs from acetyl-CoA or directly from FAs taken up directly from the circulation.

1.7.2.1 *De novo* fatty acid synthesis

As described above (**Section 1.7**), FAs can be synthesized endogenously from excess carbohydrates, during *de novo* lipogenesis or *de novo* FA synthesis (Ameer et al., 2014; Frayn et al., 2006; Kersten, 2001; Strable and Ntambi, 2010). Excess carbohydrate intake induces *de novo* lipogenesis in both adipose tissue and liver, whereas fasting decreases *de novo* lipogenesis in adipocytes by stimulating TG hydrolysis (Kersten, 2001). During

lipogenesis, citrate (derived from glucose metabolism) is converted to acetyl-CoA by ATP citrate lyase (ACLY) (**Fig. 1.5**). Acetyl-CoA carboxylase (ACC) converts acetyl-CoA to malonyl-CoA (Ameer et al., 2014; Tong and Harwood, 2006), which is then converted to long chain fatty acids, including palmitoyl-CoA, stearoyl-CoA and oleoyl-CoA, through a series of steps catalyzed by the fatty acid synthase (FASN) complex which uses NADPH as a reducing equivalent (**Fig. 1.5**). The long chain fatty acids (3 molecules of fatty acyl-CoA) are re-esterified to glycerol-3-phosphate (Glycerol-3-P) for complete TG synthesis and storage, or used for energy production (Gibson and Harris, 2002).

1.7.2.2 Fatty acid uptake from circulation and transport

The uptake of FAs from lipoproteins is the primary function of adipocytes, and FAs that are taken up directly from the circulation contribute to the majority of TG storage (Frayn et al., 2006). Triglyceride-rich lipoproteins (including the chylomicrons and the very-low density lipoproteins (VLDL)) are released into circulation from the gut and liver (Glatz et al., 2010) and hydrolyzed by lipoprotein lipase (LPL) to release FAs as FFAs, which are taken up by peripheral tissues and used either as metabolic fuels or for TG storage (Gibson and Harris, 2002). Although FAs are hydrophobic and are able to easily permeate the plasma membrane by passive diffusion (Glatz et al., 2010), FA uptake is mainly facilitated by plasma membrane-associated fatty acid transport proteins (Glatz et al., 2010). These proteins, include the plasma membrane-associated fatty acid binding protein (FABP_{pm}), the fatty acid transport protein family 1 - 6 (FATP 1 - 6) and the fatty acid translocase (FAT)/CD36 protein (Glatz et al., 2010). After FAs are taken up, they are transported into the cytoplasm by the cytoplasmic FABP (FABP_c). FAs can be used by cells for energy storage as TGs, or transported to the mitochondria for energy production via β -oxidation (**Fig. 1.6**) (Gibson and Harris, 2002).

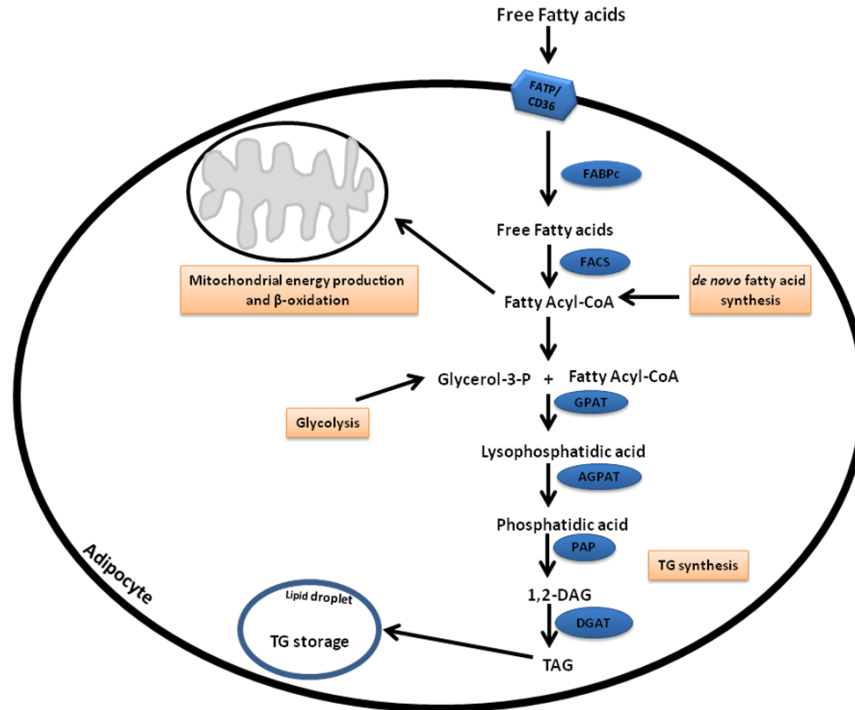


Figure 1.6 An illustration of fatty acid uptake, and triglyceride synthesis and storage in adipocytes. Adipocytes take up fatty acids (FAs) in the form of free fatty acids directly from the circulation using FA transport proteins including the fatty acid transport protein (FATP) or fatty acid translocase protein (CD36). Once inside cells, they are transported through the cytoplasm by fatty acid binding protein (FABPc) and converted to fatty acyl CoA by fatty acyl-CoA synthase (FACS) and either used for energy production by beta oxidation in the mitochondria, or converted to lysophosphatidic acid in the presence of glycerol-3-phosphate in a reaction catalyzed by glycerol-3-phosphate acyltransferase (GPAT). This leads to a stepwise synthesis of triglycerides and their storage in lipid droplets (lipogenesis). Alternatively triglycerides (TGs) can be synthesized from fatty acyl CoA derived from *de novo* fatty acid synthesis. Adapted and modified from (Ahmadian et al., 2007). AGPAT - acylglycerol-3-phosphate acyltransferase; PAP - phosphatidic acid phosphatase; DGAT - diacylglycerol acyltransferase; TAG - triacylglycerol or triglyceride (TG).

1.7.2.3 Triglyceride synthesis

Glycerol-3-phosphate (Glycerol-3-P) derived from the glycolytic pathway, is required for TG synthesis (Nye et al., 2008; Guo et al., 2012). Emerging evidence shows that glycerol is also produced by other metabolic pathways such as glyceroneogenesis, which generates glycerol from sources other than glucose (Nye et al., 2008).

During TG synthesis, the initial step involves the formation of 1-acylglycerol-3-phosphate (lysophosphatidic acid) from Glycerol-3-P and one FA molecule (fatty acyl-CoA). This

reaction is catalyzed by glycerol-3-phosphate acyltransferase (GPAT) (**Fig. 1.6**) (Ahmadian et al., 2007). Thereafter 1-acylglycerol-3-phosphate acyltransferase (AGPAT) catalyzes the esterification and conversion of lysophosphatidic acid to 1,2-diacylglycerol-3-phosphate (phosphatidic acid). Phosphatidic acid can either be used for the synthesis of various phospholipids or used for TG synthesis (Ahmadian et al., 2007). For TG synthesis, phosphatidic acid is converted to 1,2-diacylglycerol (1,2-DAG) in a reaction catalyzed by phosphatidic acid phosphatase (PAP) and thereafter diacylglycerol acyltransferase (DGAT) catalyzes the acylation of 1,2-DAG for the formation of TGs, which are stored inside lipid droplets in adipocytes (**Fig. 1.6**) (Ahmadian et al., 2007).

1.7.3 Lipolysis

Lipolysis (also known as adipolysis in adipocytes) is defined as the hydrolysis of the three ester bonds of TGs to release three FFA molecules and a glycerol molecule. These FFAs are distributed to target tissues where they serve as energy substrates (Duncan, 2007) while glycerol is transported to the liver or kidney, where it is converted to Glycerol-3-P by glycerol kinase (Hagopian et al., 2008). During lipolysis, TGs are hydrolyzed by desnutrin/adipocyte triglyceride lipase (ATGL), releasing a FFA molecule and a diacylglycerol (DAG) moiety (Villena et al., 2004). DAG is hydrolyzed to monoacylglycerol (MAG) and a free fatty acid molecule, in a reaction catalyzed by hormone sensitive lipase (HSL). Thereafter, MAG is hydrolyzed by monoacylglycerol lipase (MGL) and releases a free fatty acid molecule and glycerol (**Fig. 1.7**) (Duncan, 2007).

During fasting or exercise, lipolysis is stimulated by catecholamines. Catecholamines bind and activate β -adrenoreceptor proteins in the cell membrane, which activates adenylyl cyclase thereby increasing cyclic adenosine monophosphate (cAMP) concentrations. High levels of cAMP activate protein kinase A (PKA), whose function is to phosphorylate HSL and perilipin, therefore stimulating lipolysis (**Fig. 1.7**). Perilipin, a lipid droplet associated protein located on the outer surface of lipid droplets (Tansey et al., 2004), regulates lipolysis during both basal and stimulated conditions (Duncan, 2007). During basal conditions, perilipin restricts lipolysis by preventing entry of TG lipases into lipid

droplets (Tansey et al., 2004). Upon stimulation, perilipin is phosphorylated via the adenylyl cyclase pathway and increases lipolysis (Tansey et al., 2004).

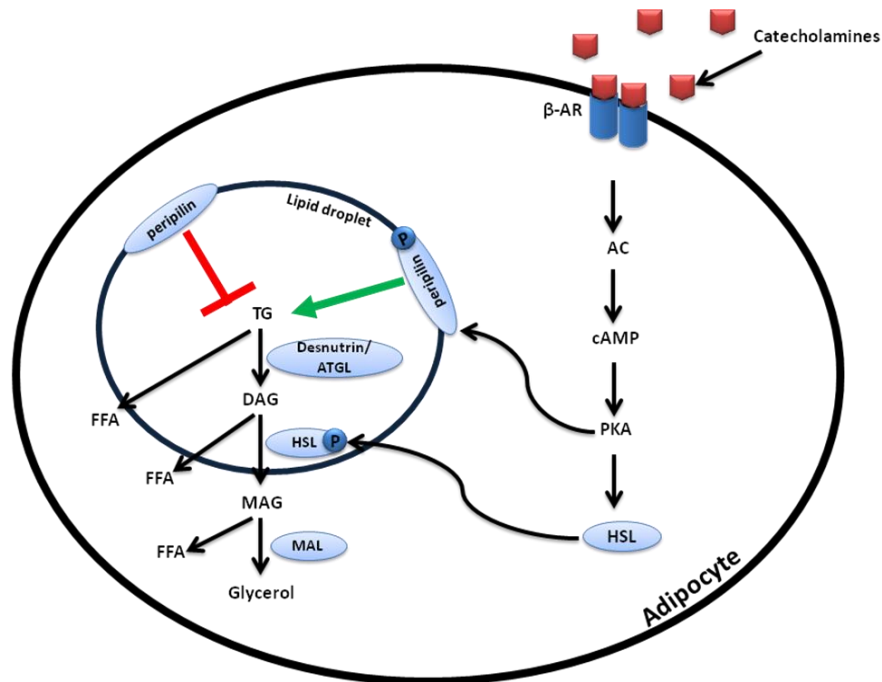


Figure 1.7 Regulation of lipolysis in adipocytes during fasting and basal levels. During fasting, catecholamines stimulate lipolysis by binding to β -adrenergic receptors (β -AR), activating adenylyl cyclase (AC) which increases cyclic adenosine monophosphate (cAMP) concentrations and activates protein kinase A (PKA). PKA phosphorylates perilipin and stimulates lipolysis. PKA also phosphorylates hormone sensitive lipase (HSL), resulting in translocation of HSL from the cytosol to the lipid droplet where it stimulates the hydrolysis of diacylglycerol (DAG) to form monoacylglycerol (MAG). MAG is further hydrolyzed to glycerol and a free fatty acid molecule. Free fatty acids generated from lipolysis are released into the circulation and used by target tissues as substrates for energy. At basal level, perilipin (unphosphorylated) inhibits lipolysis. Adapted and modified from (Duncan, 2007). TG - triglycerides; ATGL - adipose triglyceride lipase; MAL - monoacylglycerol lipase; FFA - free fatty acid.

1.7.4 Fatty acid oxidation

Fatty acid oxidation, often referred to as β -oxidation, is defined as the oxidation of FAs in order to generate the energy required for several cellular processes. Although β -oxidation

primarily occurs in the mitochondria, studies have shown that β -oxidation also occurs in peroxisomes, whereas omega (ω) oxidation occurs in the endoplasmic reticulum (Bechmann et al., 2012). After conversion of FAs into long chain fatty acids (fatty acyl-CoAs) by fatty acyl-CoA synthase (FACS) in the cytoplasm as described in **Section 1.7.2**, they are transported to the mitochondria for β -oxidation (**Fig. 1.8**) (Bechmann et al., 2012). The mitochondrial carnitine transport system transports fatty acyl-CoAs across the mitochondrial membrane into the mitochondrial matrix. Carnitine palmitoyltransferase-I (CPT-I) is located on the outer mitochondrial membrane and catalyzes the transesterification of fatty acyl-CoA to acyl-L-carnitine (Glatz et al., 2010), which is then translocated across the inner mitochondrial membrane by carnitine:acyl-L-carnitine translocase (CACT). After translocation, carnitine palmitoyltransferase-II (CPT-II) converts acyl-L-carnitine to fatty acyl-CoA in the mitochondrial matrix for oxidation (**Fig. 1.8**) (Kerner and Hoppel, 2000).

Malonyl-CoA inhibits the catalytic activity of CPT-I and hence prevents β -oxidation (Abu-Elheiga et al., 2000; McGarry and Brown, 1997). In a fed state, the expression of malonyl-CoA is increased, favoring fatty acid storage (Akkaoui et al., 2009). However, during starvation or exercise the concentration of malonyl-CoA decreases, stimulating β -oxidation (Ruderman et al., 2003). In addition to the carnitine transport system, other FA transport proteins in the mitochondrial membrane facilitate fatty acid transport into the mitochondrial matrix (Glatz et al., 2010). Peroxisome proliferator-activated receptor alpha (PPAR α) stimulates β -oxidation by inducing the expression of target genes involved in β -oxidation such as CPT-I (Goto et al., 2011)

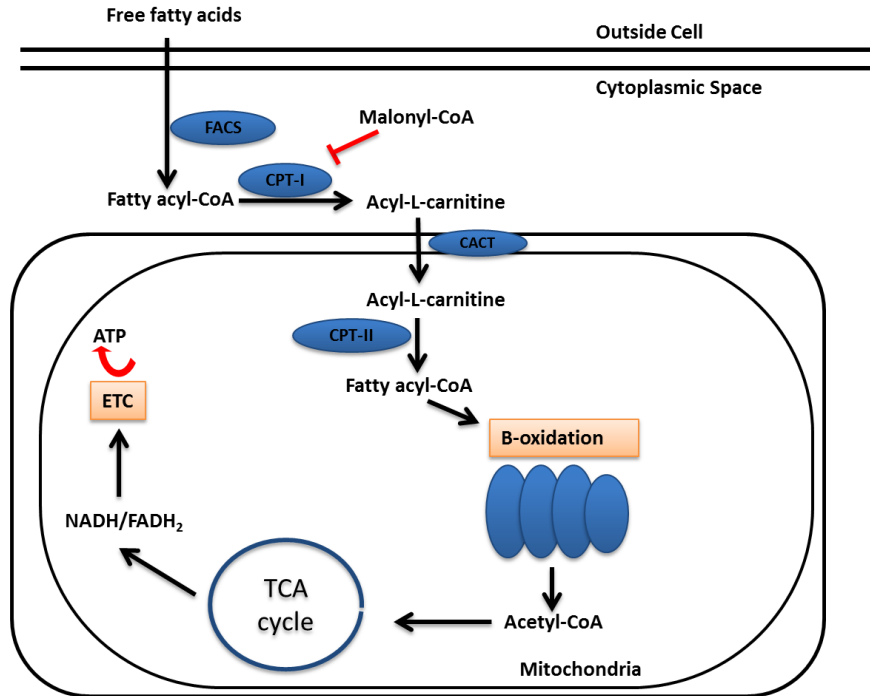


Figure 1.8 Schematic illustration of fatty acid oxidation in the mitochondria. Fatty acids are taken up from the circulation as free fatty acids and activated into long chain fatty acids (fatty acyl-CoAs) by fatty acyl-CoA synthase (FACS). Thereafter fatty acyl-CoAs are transported across the mitochondrial membrane by carnitine:acyl-L-carnitine translocase (CACT) for oxidation by the carnitine transport system consisting of carnitine palmitoyltransferase-I (CPT-I) and carnitine palmitoyltransferase-II (CPT-II). Once inside the mitochondrial matrix, fatty acyl-CoA is regenerated and undergoes β -oxidation producing acetyl-CoA which is used in the TCA cycle for energy production. Adapted and modified from (Wakil and Abu-Elheiga, 2009).

1.8 Metabolic complications associated with obesity

Increased fat storage alters adipose tissue metabolism and dysregulates energy metabolism, triggering the secretion of pro-inflammatory adipocytokines (German et al., 2010). Increased fat accumulation within adipose tissue is also associated with oxidative stress and mitochondrial dysfunction (Nassir and Ibdah, 2014; Matsuda and Shimomura, 2013). The association of obesity with chronic low-grade systematic inflammation, oxidative stress and mitochondrial dysfunction will be discussed below.

1.8.1 Inflammation

The expansion of adipose tissue (adipocyte hypertrophy) during obesity induces macrophage recruitment and infiltration, particularly M1 macrophages, regulated by the monocyte chemoattractant protein-1 (MCP-1) (German et al., 2010). Macrophage infiltration leads to the secretion of pro-inflammatory cytokines including TNF- α and interleukin 6 (IL-6) (Okabe et al., 2014). Obese individuals have high levels of circulating TNF- α and IL-6, which can be reversed by weight loss (Emanuela et al., 2012). TNF- α induces insulin resistance by inhibiting insulin receptor substrate 1 (IRS1) signaling (Hotamisligil et al., 1996), and stimulates the activation of other pro-inflammatory cytokines such as IL-6, while inhibiting the expression of adiponectin (Wang and Trayhurn, 2006; Kwon and Pessin, 2013).

Adiponectin is an anti-inflammatory adipokine that increases insulin sensitivity and inhibits inflammation (Liu and Liu, 2009). Adiponectin is expressed at high levels in adipocytes, however pro-inflammatory cytokines such as TNF- α and IL-6, and reactive oxygen molecules (ROS), inhibit its expression (Kwon and Pessin, 2013). Obese subjects have low adiponectin levels, which are inversely correlated with insulin resistance and the development of T2DM (Arita et al., 1999; Kadowaki et al., 2006).

1.8.2 Oxidative stress and mitochondrial dysfunction

Oxidative stress has been proposed as one of the mechanisms linking obesity to diabetes, hypertension, dyslipidemia, atherosclerosis and cancer (Matsuda and Shimomura, 2013). Oxidative stress occurs due to an imbalance between ROS production and scavenging (Sies, 1997). Excess intake of glucose and FAs, as a result of obesity or hyperglycemia leads to increased substrate oxidation and thus results in excessive mitochondrial ROS production (Brownlee, 2005; Matsuda and Shimomura, 2013). ROS are capable of inducing cellular damage by oxidizing cell constituents such as proteins, lipids and DNA (Matsuda and Shimomura, 2013). Obesity is associated with high levels of TNF- α and IL-6, which are responsible for inducing ROS and reactive nitrogen species (RNS) in adipocytes (Fernández-Sánchez et al., 2011).

Furukawa et al. (2004) showed that linoleate increases ROS production in 3T3-L1 adipocytes and this effect was significantly ameliorated by anti-oxidants, N-acetyl Cysteine (NAC) and apocynin, an inhibitor of nicotinamide adenine dinucleotide phosphate (NADPH) oxidase (Furukawa et al., 2004). Adipose tissue from obese mice have elevated lipid peroxidation levels, high H₂O₂ content and increased messenger RNA (mRNA) expression of NADPH oxidase subunits (Furukawa et al., 2004). In addition, increased TNF- α mRNA levels and decreased expression levels of anti-oxidant enzymes such as copper-zinc superoxide dismutase (Cu-ZnSOD), glutathione peroxidase (GPx) and catalase (CAT) were observed (Furukawa et al., 2004).

Mitochondrial dysfunction, an important pathophysiology of obesity and insulin resistance (Bournat and Brown, 2010), occurs due to decreased mitochondrial biogenesis, reduced mitochondrial content and decreased activity of oxidative proteins in the electron transport chain (ETC), thus resulting in decreased substrate oxidation (Montgomery and Turner, 2015), increased lipid accumulation and oxidative stress (Montgomery and Turner, 2015). In mature adipocytes, mitochondrial dysfunction has been associated with high levels of free fatty acids due to impaired fatty acid oxidation (Gao et al., 2010), dysregulated glucose homeostasis (Sutherland et al., 2008) and impaired adiponectin function (Koh et al., 2007). It is suggested that excessive substrates, as a result of obesity induce abnormal lipid and glucose metabolism, leading to mitochondrial dysfunction (increased ROS production, decreased energy expenditure and ATP production) (Gao et al., 2010).

1.9 Insulin Resistance

Insulin resistance (IR) is defined as the inability of peripheral tissues to respond to physiological concentrations of insulin (Choi and Kim, 2010) leading to impaired fasting glucose, impaired glucose tolerance and T2DM (**Tables 1.2 and 1.3**). IR is associated with high insulin concentration (hyperinsulinemia), due to excessive insulin secretion by β -cells, ultimately leading to β -cell dysfunction and loss (Kasuga, 2006). Visceral fat is one of the major risk factors for IR (Banerji et al., 1997), although subcutaneous adiposity has also been reported to contribute to IR (Abate et al., 1995; Patel and Abate, 2013). Obese individuals have increased levels of plasma FAs due to adipose fat storage

exceeding its capacity; hence excessive FFAs are released into the circulation (**Fig. 1.9**). A number of mechanisms whereby FAs induce IR have been proposed. Randle et al. (1963) suggested that FAs compete with glucose for substrate oxidation, thus inhibiting glucose metabolism. FAs also inhibit insulin signaling by directly decreasing insulin receptor substrate 1 (IRS1) associated phosphatidylinositol 3-kinase activity; resulting in impaired glucose uptake (Dresner et al., 1999). Abdul-Ghani and DeFronzo, 2010 showed that FAs induce IR by increasing the accumulation of intracellular lipid metabolites such as diacylglycerol or ceramides in muscle, which disrupts insulin signaling by inhibiting tyrosine phosphorylation of the IRS 1/2 (Petersen and Shulman, 2006). It has also been reported that FAs induce IR by stimulating cellular (oxidative and endoplasmic reticulum) stress, activation of inflammatory cytokines and decreasing anti-inflammatory adipokines (**Fig. 1.9**) (Boden, 2011).

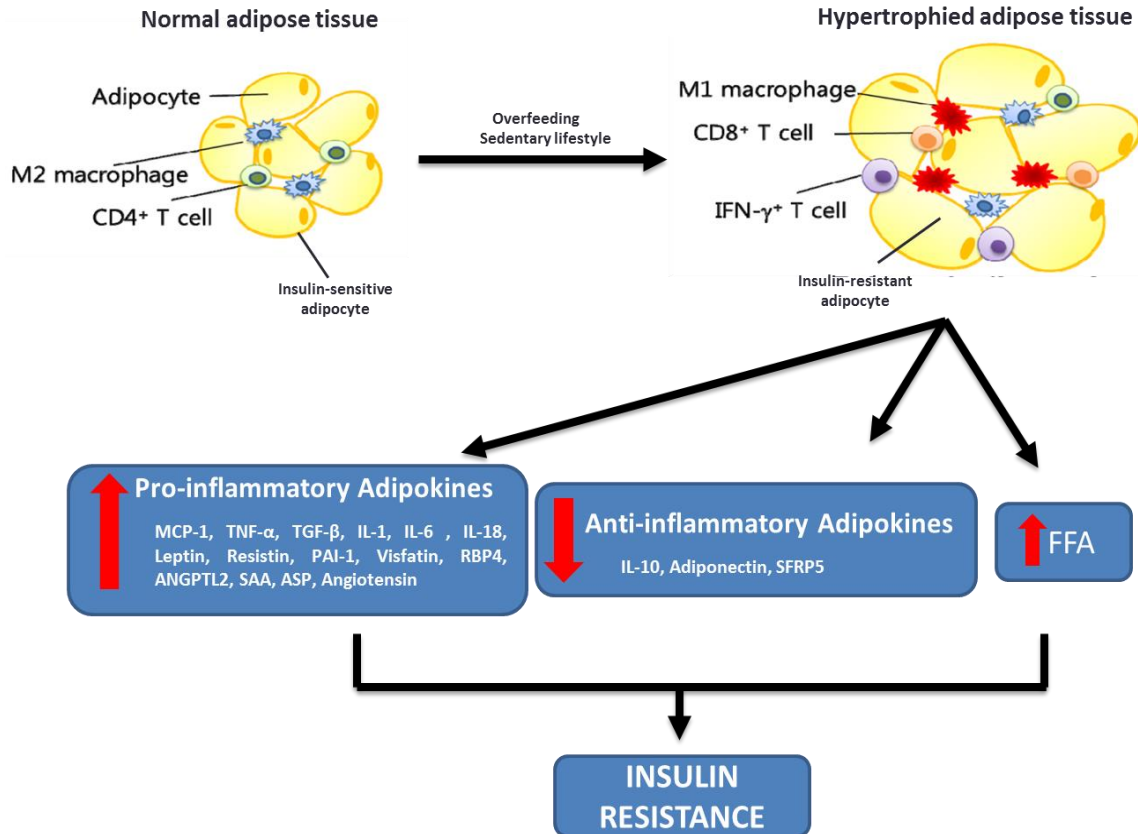


Figure 1.9 Mechanism of inflammatory and fatty acid induced insulin resistance in adipocytes. During obesity, adipose tissue increase in size by hypertrophy leading to dysregulated secretion of adipokines and an increase in the release of free fatty acids (FFAs). The FFAs and pro-inflammatory adipokines are transported from adipocytes to target tissues including the muscle and the liver, where they deregulate metabolic pathways (glucose and lipid) and also alter inflammatory responses thus inducing insulin resistance and other metabolic diseases including dyslipidemia and the non-alcoholic fatty liver disease. Adapted and modified from Jung and Choi (2014). MCP-1 - monocyte chemoattractant protein-1; TNF- α - tumor necrosis factor alpha; TGF- β - transforming growth factor beta; IL-1 - interleukin 1; IL-6 - interleukin 6; IL-18 - interleukin 18; PAI-1 - plasminogen activator inhibitor-1; RBP4 - retinol binding protein 4; ANGPTL2 - angiopoietin like protein 2; SAA - serum amyloid A; ASP - acylation stimulating protein; IL-10 – interleukin 10; SFRP5 - secreted frizzled-related protein 5.

1.10 Obesity and the metabolic syndrome

The metabolic syndrome (MetS) is a group of disorders including obesity (particularly visceral obesity), dyslipidemia, hypertension and hyperglycemia (Alberti et al., 2005; Jung and Choi, 2014) that are clinically used to assess the risk for cardiovascular diseases and T2DM. According to the International Diabetes Federation (IDF), a quarter of the world's

adult population has the metS, which is associated with the increased prevalence of obesity (Grundy et al., 2005). The diagnostic criteria for the MetS, defined by the World Health Organization (WHO) and IDF are illustrated in **Table 1.2** and **1.3**.

Dyslipidemia, due to impaired lipoprotein metabolism, is characterized by high TG levels, increased levels of total cholesterol (TC), low density lipoprotein (LDL) and very low density lipoprotein (VLDL) cholesterol, high apolipoprotein (apo) levels and decreased high density lipoprotein (HDL) cholesterol levels (Klop et al., 2013). Dyslipidemia is widely accepted as a risk factor for coronary heart diseases, particularly low HDL cholesterol levels. The increasing prevalence of obesity is accepted as one of the major risk factors for the development of hypertension (Narkiewicz, 2006).

Table 1.2 World Health Organization criteria to define the metabolic syndrome.

One of the following below:	
<ul style="list-style-type: none"> • Type 2 diabetes mellitus • Insulin resistance • Impaired fasting glucose • Impaired glucose tolerance 	
Plus any of the two below:	
Blood pressure	Systolic \geq 140 mmHg Diastolic \geq 90 mmHg
Plasma triglycerides	\geq 1.7 mmol/L
HDL-cholesterol	Males: $<$ 0.9 mmol/L Females: $<$ 1.0 mmol/L
Obesity	Males: Waist-to-hip ratio $>$ 0.9 Females: Waist-to-hip ratio $>$ 0.85 and/or BMI $>$ 30 kg/m ²
Microalbuminuria	Urinary albumin excretion rate \geq 20 mg/min Albumin:creatinine ratio \geq 30 mg/g

Adapted and modified from Alberti et al. (2006), Grundy et al. (2005) and Kassi et al. (2011)

Table 1.3 International Diabetes Federation criteria to define the metabolic syndrome.

	Ethnicity	Sex	Measurement
Waist circumference	Europids ^a (Caucasian)	Male	≥ 94 cm
		Female	≥ 80 cm
	South Asians ^b	Male	≥ 90 cm
		Female	≥ 80 cm
	Chinese	Male	≥ 90 cm
		Female	≥ 80 cm
	Japanese	Male	≥ 85 cm
		Female	≥ 90 cm
Plus any two of the following:			
Blood pressure	Systolic ≥ 130 mmHg Diastolic ≥ 85 mmHg		
Plasma triglycerides	≥ 1.7 mmol/L		
Hyperglycemia	≥ 5.6 mmol/L		

^aInclusive of Sub-Saharan Africa, Mediterranean and Middle East

^bInclusive of ethnic South and Central Americans

Adapted and modified from Alberti et al. (2006), Grundy et al. (2005) and Kassi et al. (2011).

1.11 Obesity and chronic diseases

1.11.1 Type 2 diabetes mellitus

Diabetes is a major source of morbidity and mortality worldwide. In 2013, it was estimated that 382 million adults worldwide were affected by diabetes, with the prevalence expected to rise to 592 million adults by 2035 (Guariguata et al., 2014). There are three major types of diabetes, namely type one diabetes mellitus (T1DM) which is associated with insulin deficiency as a result of autoimmune-mediated destruction of pancreatic β -cells (Yoon and Jun, 2005), T2DM which is associated with insulin resistance and pancreatic β -cell dysfunction and accounts for more than 90% of diabetes cases (Zhang and Moller, 2000), and gestational diabetes mellitus (GDM) which is a condition of glucose intolerance first diagnosed during pregnancy (Gilmartin et al., 2008). Obesity is one of the major risk factors for T2DM and up to 80% of people with T2DM are either obese or overweight

(Ross et al., 2011). In SA, a middle income country, approximately 90% of T2DM are attributable to excess weight (Joubert et al., 2007). Thus, diabetes a term coined to refer to obesity-dependent T2DM (Farag and Gaballa, 2011) is a major cause of concern for the global burden of the disease, particularly in low and middle income countries with already struggling health care systems.

1.11.2 Cardiovascular disease

Cardiovascular disease (CVD) is the leading cause of death worldwide causing approximately 17.3 million deaths per year, with rates expected to increase to more than 23.6 million deaths by 2030 (Smith et al., 2012). Obesity is associated with dyslipidemia and increased levels of pro-inflammatory cytokines, leading to endothelial damage and vascular hypertrophy, and thus increasing the risk factor for hypertension, coronary heart diseases (CHD) and heart failure (Poirier et al, 2006). Abnormal secretion of IL-6 by adipocytes has been associated with impaired endothelium-dependent dilation in human veins (Bhagat and Valance, 1997). Abnormal lipid profiles (low HDL cholesterol and increased LDL cholesterol levels) during obesity are associated with atherosclerosis (Gordon et al. 1977).

1.11.3 Cancer

Obesity is associated with an increased risk of several cancers including oesophageal, postmenopausal breast, endometrium, colon, rectum and kidney cancer (Vainio et al., 2002). In a study by Calle et al. (2003), women with a BMI > 40 kg/m² had a 62% higher risk of developing liver and pancreatic cancer, non-Hodgkin's lymphoma and myeloma compared to women with BMI < 25 kg/m². Several mechanisms, for the role of obesity in cancer development have been proposed (Basen-Engquist and Chang, 2011). Enlarged adipose tissue continually secrete inflammatory adipokines (TNF- α and IL-6) that induce tumorigenesis in various target tissues including the liver and the kidney (Stemmer et al., 2012). Stemmer et al. (2012) showed that high fat diet-induced obesity is carcinogenic in rat kidneys by inducing an inflammatory and tumor-promoting environment.

1.11.4 Non-alcoholic fatty liver disease

Non-alcoholic fatty liver disease (NAFLD) is the most common form of liver disease, characterized by a spectrum of diseases including hepatic steatosis (lipid accumulation in the liver) and non-alcoholic steatohepatitis (NASH, liver inflammation and fibrosis) (Jung and Choi, 2014). NAFLD is associated with obesity and T2DM, and previous studies have shown that NAFLD is present in up to 90% of obese people (Machado et al., 2006). NAFLD occurs due to abnormal hepatic lipid metabolism as a result of increased FA input (FA uptake, FA synthesis and FA re-esterification into TG) and decreased FA output (FA oxidation and secretion) (Fabbrini et al., 2010).

1.12 Current interventions against obesity

1.12.1 Lifestyle modification

Lifestyle modification, such as dietary intervention and increased physical activity is considered the most effective prevention and treatment strategy for obesity (Fabricatore and Wadden, 2003; Shaw et al., 2005). A very low energy density diet (≤ 800 kcal per day) demonstrated a 21.3% weight loss compared to the baseline weight after 24 weeks of dietary intervention (Anderson et al., 2004). Moreover, a combination of physical activity and dietary intervention improves weight loss compared to individual interventions (Jakicic, 2009). Wing et al. (1998) showed that interventions consisting of diet only, physical activity only or a combination of diet and physical activity induced a 9.1, 2.1 and 10.4% weight loss, respectively in obese subjects. Despite the potential success of lifestyle modification, adherence is poor, resulting in the increased reliance on pharmacological agents to manage obesity. Furthermore, studies have shown that the huge variability in individual's response to exercise and dietary intervention is likely associated with genetic variation (Bray, 2008).

1.12.2 Pharmacological drugs

According to the Food and Drug Administration (FDA), an anti-obesity drug can only be approved for clinical use when it is considered safe and shows at least a 5% reduction in

weight (FDA, 2007). Anti-obesity drugs employ several mechanisms whereby they decrease weight, for example, appetite suppression (Phentermine and Amphetamine), inhibition of intestinal lipases (Orlistat), inhibition of serotonin, dopamine and norepinephrine reuptake (Lorcaserin and sibutramine), enhancing γ -aminobutyric acid (GABA) signaling in order to promote anorexigenic signaling (Topiramate) and targeting glucagon-like peptide 1 receptor agonists (Exenatide), leptin receptor agonists and amylin analogs (Pramlintide) (Kim et al., 2014). However their clinical use is hindered by their adverse side-effects which include cardiovascular complications and psychiatric events. Anti-obesity drugs such as sibutramine, rimonabant and the amphetamine analogues have been withdrawn from the market due to their side-effects (Chaput et al., 2007; Derosa and Maffioli, 2012; Kim et al., 2014). Although Orlistat, Phentermine/Topiramate and Lorcaserin have been approved to treat obesity, they are also plagued by side-effects such as insomnia, headaches and gastrointestinal effects (Derosa and Maffioli, 2012; Adan, 2013).

1.12.3 Bariatric surgery

Bariatric surgery refers to a range of gastrointestinal surgical procedures used to treat severe obesity, and due to the increased prevalence of obesity globally, the use of bariatric procedures has increased considerably (Smith et al., 2008 and 2011). Bariatric surgery improves obesity related diseases including T2DM, hypertension and dyslipidemia. The major disadvantages of bariatric surgery include surgical complications and expense (Fabricatore and Wadden, 2003; Hoerger et al., 2010). Furthermore, increased suicidal risks have been reported following bariatric surgery (Mitchell et al., 2013), and individuals who have done this procedure usually require life-long supplementation with vitamins because of the malabsorption of essential vitamins, minerals and even pharmacological drugs (Xanthakos, 2009; Sawaya et al., 2012).

1.12.4 Medicinal plants and polyphenols

More than 80% of the world's population, particularly in developing countries, rely on traditional plant-based medicinal systems for primary healthcare (Ekor, 2014). Africa is heavily reliant on traditional medicines with about 5000 plant species used for medicinal purposes, and these medicinal plants are considered safer compared to conventional drugs, furthermore, they are easily accessible and affordable (Mahomoodally, 2013).

Polyphenols are secondary metabolites of plants produced in response to stress. They possess anti-oxidant properties and have the ability to prevent a wide range of metabolic diseases, including obesity (Hsu and Yen, 2008; Rayalam et al., 2008; Meydani and Hasan, 2010; Yun, 2010). Polyphenols are found in a variety of dietary sources including fruits, vegetables and beverages such as tea or wine (Pandey and Rizvi, 2009), and are often explored as an alternative or as an adjunct to conventional obesity treatment. Polyphenols exist in several forms, the most common types of which are the flavonoids, lignans, stilbenes and phenolic acids (Rispaill et al., 2005). Of these polyphenols, apigenin, genistein, kaempferol, resveratrol, curcumin and catechins have showed anti-obesity properties (Rayalam et al., 2008; Meydani and Hasan, 2010; Yun, 2010). These compounds prevent or decrease obesity by regulating physiological and molecular pathways such as suppression of appetite, inhibition of pancreatic lipase activity, regulating lipid metabolism by inhibiting adipogenesis and lipogenesis or stimulating lipolysis and fatty acid oxidation, and stimulating energy expenditure or thermogenesis (Rayalam et al., 2008; Meydani and Hasan, 2010; Yun, 2010). In addition to their effects against obesity, studies have also reported a number of health promoting properties against chronic diseases such as T2DM and CVD (Bahadoran et al., 2013; Trigueros et al., 2013).

1.13 South African indigenous plants: Cape Fynbos

South Africa is rich in indigenous plants with health promoting properties (Van Wyk, 2011). These plants have been used for centuries to treat disease, although scientific validation of their clinical use is often lacking. Two Cape fynbos plant genera, *Aspalathus linearis*

(rooibos) and the *Cyclopia* species (honeybush) have been consumed as herbal teas in South Africa and internationally, mainly due to their pleasant taste and aroma (Du Toit et al., 1998). Furthermore, there are a number of anecdotal reports of their health effects (Du Toit et al., 1998). The South African government, together with the Agricultural Research Council (South Africa), has spearheaded projects to exploit South Africa's vast indigenous resources to benefit the economy. Additionally, the medicinal properties of these plants make them attractive preventative or therapeutic agents against a number of health conditions. The honeybush tea industry has therefore attracted considerable interest due to its growth potential for commercialization.

1.13.1 *Cyclopia* species (honeybush tea)

The *Cyclopia* genus, commonly referred to as honeybush, belongs to the tribe Podalyrieae under the leguminous family of Fabaceae and forms part of the rich fynbos biome (Schutte, 1997). *Cyclopia* species are morphologically similar but not identical; they have woody stems with a height ranging from 1.5 m to 3 m (Bond and Goldblatt, 1984). They have trifoliolate leaves, differing in their shapes across species (**Fig. 1.10**) and are characterized by bright yellow flowers with a sweet, honey-like aroma that occurs during their flowering season, usually between September and October (Joubert et al., 2008a). More than 20 species of *Cyclopia* have been described to date (Joubert et al., 2011). *Cyclopia genistoides* was the first species of *Cyclopia* identified; it was originally termed Honigtee (Greenish, 1881). Unlike rooibos tea which is manufactured from one species only, i.e. *Aspalathus linearis*, the leaves, stems and flowers of various species of *Cyclopia* spp. are consumed as honeybush tea, with *Cyclopia genistoides*, *Cyclopia subternata* and *Cyclopia intermedia* commercialized for the production of honeybush herbal tea. Although the first branded honeybush tea product 'Caspa Cyclopia Tea' appeared on the South African market during the 1960s, the honeybush tea industry is not as established as rooibos tea (Joubert et al., 2008a). However, the demand for honeybush tea has increased both nationally and internationally (Joubert et al., 2011) mainly due to its pleasant taste, absence of caffeine (Greenish, 1881), low tannin content (Terblanche, 1982) and anecdotal and scientific reports of its medicinal properties.



Figure 1.10 Trifoliate leaves of *Cyclophia subternata* (A), *Cyclophia maculata* (B) and *Cyclophia intermedia* (C). Adapted from the South African Honeybush tea Association (SAHTA).

1.13.2 Geographical distribution

Cyclophia spp. occur in the coastal and mountainous regions of the Western and Eastern Cape provinces of South Africa (Du Toit et al., 1998) (**Fig. 1.11**). These species grow in cool, wet southern slopes and in sandy soils with low phosphorous, pH and nematode content (Schutte, 1997). Each species is locally described according to its appearance and environment (Du Toit et al., 1998).

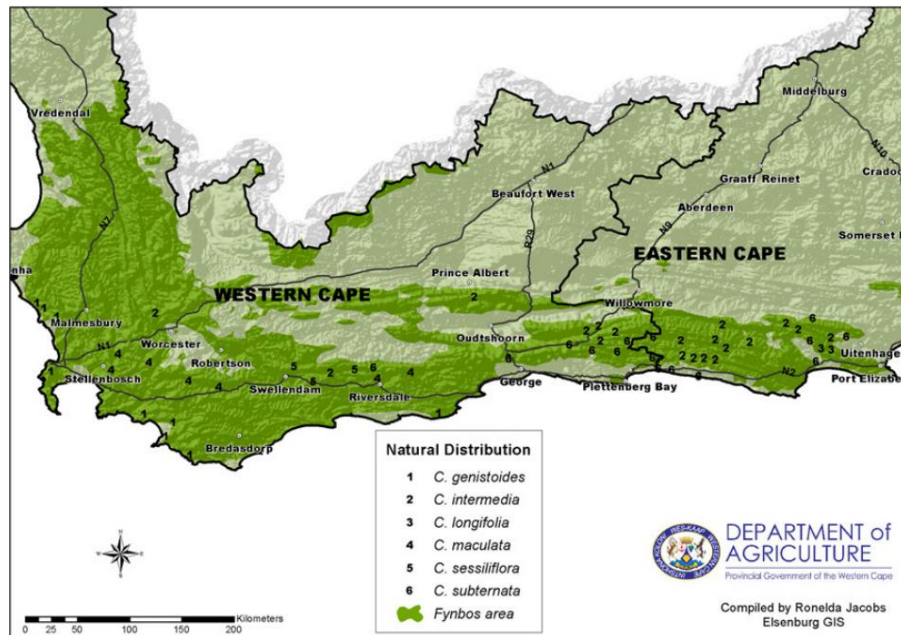


Figure 1.11 Natural distribution of *Cyclophia* species in the Western and Eastern Cape regions of South Africa. Adapted from Joubert et al. (2011).

1.13.3 Honeybush tea industry

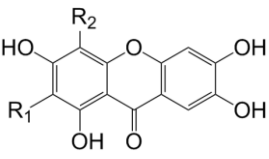
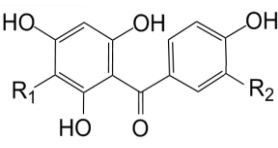
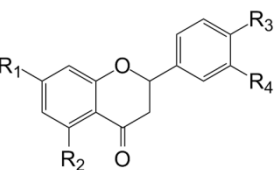
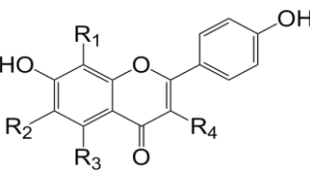
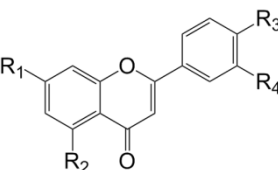
Currently three *Cyclopia* spp., *C. genistoides*, *C. subternata* and *C. intermedia* are used for the commercial production of honeybush tea. It is estimated that approximately 200 hectares are used for the commercial cultivation of the former two, while the latter, *C. intermedia* is not currently cultivated and is only wild harvested, due to its slow growth (Joubert et al., 2008a, 2011). The increased demand for honeybush tea has led to the cultivation of other members such as *C. maculata*, *C. longifolia* and *C. sessiliflora* (Joubert et al., 2011). The honeybush tea export market has grown significantly over the last ten years; approximately 200 tons of honeybush is exported annually to countries such as The Netherlands, United Kingdom (UK), United States of America (USA) and Germany (Joubert et al., 2011).

1.13.4 Phenolic composition

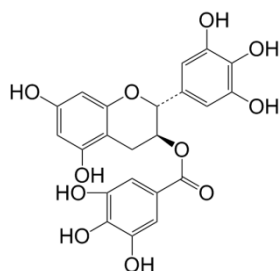
De Nysschen et al. (1996) identified three major polyphenols in the leaves of several *Cyclopia* species, including the xanthone C-glycoside (mangiferin) and the two flavanone O-glycosides, hesperitin and isosakuranetin. Thereafter, phenolic characterization of two *Cyclopia* spp., fermented *C. intermedia* (Ferreira et al., 1998; Kamara et al., 2003) and unfermented *C. subternata* (Kamara et al., 2004) showed the presence of several phenolic groups including the xanthenes, flavanones, flavonols, isoflavones, flavones, coumestans, pinitol and *p*-Coumaric (*Para*-Coumaric) acid (**Table 1.4**). Using liquid chromatography mass spectrometry (LC-MS), Joubert et al. (2008b) failed to detect isosakuranetin in extracts of several *Cyclopia* species including *C. intermedia*, *C. subternata*, *C. genistoides* and *C. sessiliflora*, as it was previously identified by De Nysschen et al. (1996). The major phenolic compounds identified in all *Cyclopia* species analyzed to date include mangiferin, isomangiferin and hesperidin (Joubert et al., 2008a; 2011). Recently, high contents of benzophenones and dihydrochalcones have been identified in *C. genistoides* and *C. subternata* species (**Table 1.4**) (De Beer et al., 2012; Kokotkiewicz et al., 2012; 2013; Malherbe et al., 2014; Beelders et al., 2014b).

Factors such as seasonal variation, geographical location and processing affect phenolic composition, thus providing an explanation for the differences in biological properties of *Cyclopia*. For example, Marnewick et al. (2009) compared the anti-mutagenic and anti-oxidant properties of fermented and unfermented teas, and showed that lower phenolic content, as a result of fermentation, was associated with decreased protective effects of these herbal teas. Fermentation was also shown to result in decreased anti-oxidant activity (Joubert et al., 2008b). Fermentation refers to the processing or oxidation of plant material, usually at high temperatures, in order to develop certain characteristics in tea infusions. In honeybush tea, fermentation is important for the development of its dark reddish brown color and its characteristic aroma and flavour (Joubert et al., 2011). The unfermented or 'green' honeybush tea has recently attracted interest, since it minimizes the oxidation of polyphenols (De Beer et al., 2012) and enhances the protective effects of honeybush (Joubert et al., 2008a).

Table 1.4 Chemical compounds identified in *Cyclopia* to date.

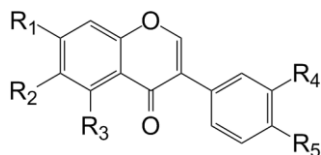
Class and structure	Compound's name and substitute
<p>Xanthone</p> 	<p>Mangiferin^a: R1 = C-β-D-glucosyl; R2 = H Isomangiferin^a: R1 = H; R2 = C-β-D-glucosyl</p>
<p>Benzophenone</p> 	<p>Iriflophenone-3-C-β-D-glucoside-4-O-β-D-glucoside^f: R1 = C-β-D-glucosyl; R2 = H, R3 = O-β-D-glucosyl Iriflophenone-3-C-β-D-glucoside^d: R1 = C-β-D-glucosyl; R2 = H Maclurin-3-C-β-glucoside^e: R1 = C-β-glucosyl; R2 = OH</p>
<p>Flavanone</p> 	<p>Hesperidin^{a,c}: R1 = O-rutinosyl; R2 = OH; R3 = OCH3; R4 = OH Hesperetin^a: R1 = R2 = OH; R3 = OCH3; R4 = OH Eriocitrin^c: R1 = O-rutinosyl; R2 = R3 = R4 = OH Eriodictyol^a: R1 = R2 = R3 = R4 = OH Naringenin^a: R1 = R2 = R3 = OH; R4 = H Narirutin^c: R1 = O-rutinosyl; R2 = R3 = OH; R4 = H Prunin^b: R1 = O-glucosyl; R2 = R3 = OH; R4 = H Naringenin-5-O-rutinoside^b: R1 = R3 = OH; R2 = O-rutinosyl; R4 = H Eriodictyol-5-O-glucoside^b: R1 = R3 = R4 = OH; R2 = O-β-D-glucosyl Eriodictyol-7-O-glucoside^b: R1 = O-β-D-glucosyl; R2 = R3 = R4 = OH</p>
<p>Flavanol</p> 	<p>Kaempferol-5-O-glucoside^b: R1 = R2 = H; R3 = O-α-D-glucosyl; R4 = OH Kaempferol-6-C-glucoside^b: R1 = H; R2 = C-β-D-glucosyl; R3 = R4 = OH Kaempferol-8-C-glucoside^b: R1 = C-β-D-glucosyl; R2 = H; R3 = R4 = OH Kaempferol-di-3-O,6-C-glucoside^b: R1 = H; R2 = C-β-D-glucosyl; R3 = OH; R4 = O-β-D-glucosyl</p>
<p>Flavone</p> 	<p>Luteolin^{a,c}: R1 = R2 = R3 = R4 = OH Diosmetin^b: R1 = R2 = R4 = OH; R3 = OCH3 5-Deoxyluteolin^c: R1 = R3 = R4 = OH; R2 = H Scolymoside^c: R1 = O-rutinosyl; R2 = R3 = R4 = OH Isorhoifolin^d: R1 = O-rutinosyl; R2 = R3 = OH; R4 = H</p>

Flavan-3-ol



(-)-epigallocatechin gallate (EGCG)^c

Isoflavone



Formononetin^a: R₁ = OH; R₂ = R₃ = R₄ = H; R₅ = OCH₃

Formononetin diglucoside^b: R₁ = O- α -apiofuranosyl-(1'''' \rightarrow 6''')- β -D-glucopyranosyl; R₂ = R₃ = R₄ = H; R₅ = OCH₃

Afrormosin^a: R₁ = OH; R₃ = R₄ = H; R₂ = R₅ = OCH₃

Calycosin^a: R₁ = R₄ = OH; R₂ = R₃ = H; R₅ = OCH₃

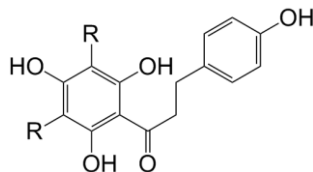
Calycosin-7-O- β -glucoside^d: R₁ = O- β -D-glucosyl; R₂ = R₃ = H; R₄ = OH; R₅ = OCH₃

Wistin^b: R₁ = O- β -D-glucosyl; R₃ = R₄ = H; R₂ = R₅ = OCH₃

Orobol^c: R₁ = R₃ = R₄ = R₅ = OH; R₂ = H

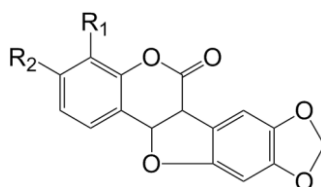
Ononin (Formononetin-7-O-glucoside)^d: R₁ = O- β -D-glucosyl; R₂ = R₃ = R₄ = H; R₅ = OCH₃

Dihydrochalcone



Phloretin-3', 5'-di-C- β -D-glucoside^d: R = C- β -D-glucosyl

Coumestans

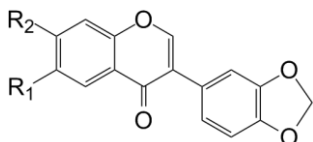


Medicagol^a: R₁ = H; R₂ = OH

Flemichapparin^a: R₁ = H; R₂ = OCH₃

Sophoracoumestan B^a: R₁ = OCH₃; R₂ = OH

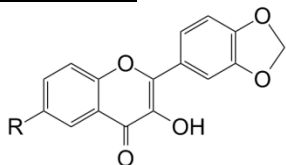
Methylendioxyisoflavone derivative



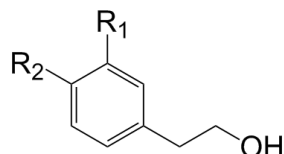
Pseudobaptigenin^a: R₁ = H; R₂ = OH

Fujikinetin^a: R₁ = OCH₃; R₂ = OH

Rothindin^d: R₁ = H; R₂ = O- β -D-glucosyl

Methylenedioxyflavonol derivative

3',4'-Methylenedioxyflavonol-6-O-apiosyl-glucoside^b: R = O- α -apiofuranosyl- (1''' \rightarrow 6'')- β -D-glucopyranosyl

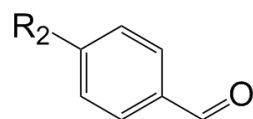
Phenylethanol derivative

Tyrosol^b: R₁ = H; R₂ = OH

3-Methoxy-tyrosol^b: R₁ = OCH₃; R₂ = OH

Tyrosol-4-O-glucoside^c: R₁ = H; R₂ = O- β -D-glucosyl

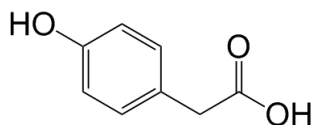
Phenylethanol-3-O-apiosyl-glucoside^b: R₁ = O- α -apiofuranosyl- (1'' \rightarrow 6')- β -D-glucopyranosyl; R₂ = H

Benzaldehyde derivative

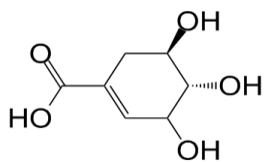
Benzaldehyde-4-O-apiosyl-glucoside^b: R = O- α -apiofuranosyl- (1'' \rightarrow 2')- β -D-glucopyranosyl

Phenolic carboxylic acid

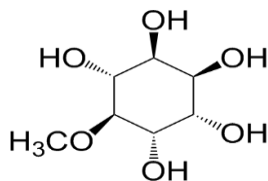
Para-Coumaric acid^{a,c}

**Organic acid**

(\pm)-Shikimic acid^c

**Inositol**

(+)-Pinitol^{a,c}



^aFerreira et al., 1998; ^bKamara et al., 2003; ^cKamara et al., 2004; ^dKokotkiewicz et al., 2012; ^eKokotkiewicz et al., 2013; ^fBeelders et al., 2014b. Table adapted from Joubert et al., 2008a.

1.13.5 Biological properties of *Cyclopia* species

A number of anecdotal claims of the medicinal properties of honeybush have been reported. Native tribes have been using honeybush infusions for the treatment of coughs and infections associated with the upper respiratory system (Dharmananda, 2004), to cure chronic catarrh and pulmonary tuberculosis (Bowie, 1830), to stimulate milk production (Terblance, 1982), and to prevent stomach ulcers, and skin problems such as psoriasis (Du Toit et al., 1998) for centuries. Furthermore, honeybush has been used as an appetite stimulant and as a sleeping remedy due to it being caffeine free (Du Toit et al., 1998).

Recently, a number of scientific studies have confirmed the health properties of honeybush tea. For example, HPLC analysis has identified pinitol, a compound which is used as an expectorant (Beecher et al., 1989) in honeybush tea extracts, thus validating the earlier reports of its use as an expectorant (Dharmananda, 2004). Furthermore, pinitol exhibited insulin-like activity by decreasing hyperglycemia in STZ-induced diabetic mice (Bates et al., 2000). Studies have demonstrated anti-oxidant (Marnewick et al., 2003; Petrova et al., 2011), anti-mutagenic (Marnewick et al., 2000; Marnewick et al., 2004; Van der Merwe et al., 2006), chemoprotective (Marnewick et al., 2005; Marnewick et al., 2009; Sissing et al., 2011), phytoestrogenic (Verhoog et al., 2007a; Verhoog et al., 2007b; Mfenyana et al., 2008; Visser et al., 2013; Mortimer et al., 2015), anti-microbial (Coetzee et al., 2008), anti-osteoclastogenic (Visagie et al., 2015) anti-diabetic (Muller et al., 2011; Chellan et al., 2014; Beelders et al., 2014b; Schulze et al., 2016) and anti-obesity (Dudhia et al., 2013; Pheiffer et al., 2013) activity of several *Cyclopia* extracts. The studies relating to the anti-obesity effects of honeybush tea extracts will be discussed below.

1.13.5.1 Anti-obesity health effects

Mechanisms whereby dietary polyphenols could mediate their anti-obesity effects include 1) inhibition of adipogenesis by decreasing the expression of PPAR γ and other pro-adipogenic transcription factors, 2) preventing lipogenesis by decreasing the expression of genes involved in FA synthesis and TG storage, 3) stimulating lipolysis by increasing the expression of HSL, as well as the rate of FA oxidation by inducing PPAR α expression

(Okabe et al., 2014), 4) inhibiting pancreatic lipase activity (Birari and Bhutani, 2007), or 5) suppressing appetite by increasing satiety (Mashmoul et al., 2013). In 2013, Dudhia et al. (2013) reported that hot water extracts of fermented and unfermented *C. maculata* and unfermented *C. subternata* inhibited adipogenesis in 3T3-L1 pre-adipocytes. Decreased adipogenesis was mediated by decreased expression of PPAR γ 2 and associated with decreased intracellular TG accumulation. The anti-obesity properties of the extracts were associated with increased leptin secretion and also adiponectin secretion in the case of unfermented *C. maculata*. Furthermore, fermented *C. maculata* stimulated lipolysis in mature 3T3-L1 adipocytes by increasing HSL and perilipin protein expression levels (Pheiffer et al., 2013).

1.13.6 Anti-obesity phenolic compounds present in *Cyclopia*

As discussed above, *Cyclopia* extracts are rich in complex polyphenols with several biological activities. Most of the polyphenols identified in *Cyclopia* extracts have shown anti-obesity activity in other plants; some of these compounds will be discussed below, as they may confer similar effects in *Cyclopia*.

1.13.6.1 Xanthones

The two most common C-glycoside xanthones, mangiferin and isomangiferin have been identified as the major compounds of several *Cyclopia* species (Joubert et al., 2009). Mangiferin (2-C- β -D-glucopyranosyl-1,3,6,7-tetrahydroxyxanthone) was first identified as the major constituent of mango (*Mangifera indica*) extracts (Mirza et al., 2013). Other sources of mangiferin include *Salacia reticulata* (Shimada et al., 2011), the Bunge rhizome (*Anemarrhena asphodeloides*) (Miura et al., 2001), the mango ginger (*Curcuma amada*) (Kullu et al., 2014) and *Swertia ciliata* (Chauhan and Dutt, 2013). Isomangiferin (4-C- β -D-glucopyranosyl-1,3,6,7-tetrahydroxyxanthone), a structural isomeric form of mangiferin has been detected in *Anemarrhena asphodeloides* (Aritomi and Kawasaki, 1969) and several *Pyrrhosia* species (Li and Tong, 1992).

Mangiferin ameliorates hyperlipidemia and hypertriglyceridemia by regulating the expression of genes involved in FA metabolism, lipid oxidation and lipogenesis (Guo et al., 2011; Niu et al., 2012) (**Table 1.5** and **Table 1.6**). The concentration of mangiferin is essential for its bioactivity. Shimada et al. (2011) showed that mangiferin at various concentrations (0.1, 1 and 10 μM) did not reduce TG content in 3T3-L1 adipocytes. However in human mesenchymal stem cells (hMSCs), mangiferin at 40 μM decreased adipocyte differentiation and lipid accumulation (Subash-babu and Alshatwi, 2015). These results could also suggest that the bioactivity of mangiferin is cell type specific. More recently Xing et al. (2014) showed that 15 mg/kg of mangiferin ameliorated hepatic steatosis by inhibiting the expression of diacylglycerol acyltransferase (DGAT)-2, and preventing TG and lipid accumulation in the liver of fructose-fed hypertensive rats (**Table 1.6**). Mangiferin, purified from *Salacia oblonga* increased glucose uptake in rat L6 myotubes and mouse 3T3-L1 adipocytes by increasing the expression and translocation of GLUT4 (Giron et al., 2009). Recently, Kumar et al. (2013) showed that mangiferin improved glucose oxidation in 3T3-L1 cells (**Table 1.5**).

1.13.6.2 Flavonoids

Hesperidin was originally identified as one of the major flavanones in citrus fruits (Babu et al., 2013) and in various species of *Cyclopia* (Joubert et al., 2009). Dietary supplementation with 0.2 g/kg of hesperidin exhibited anti-hyperlipidemic and anti-hyperglycemic effects in C57BL/KsJ-db/db mice. The anti-hyperlipidemic effects were mediated by decreased hepatic and serum TGs due to inhibition of FASN. The anti-hyperlipidemic effect of hesperidin was also demonstrated in STZ-induced diabetic rats (Akiyama et al., 2010) (**Table 1.6**).

Other examples of flavonoids in *Cyclopia* with anti-obesity health properties include hesperetin, naringenin, eriocitrin, kaempferol, luteolin, epigallocatechin gallate (EGCG) and formononetin. Hesperetin is derived from the hydrolysis of hesperidin, and together with its metabolites decreased plasma TG and cholesterol levels in rats fed a high cholesterol diet (Kim et al., 2003). Naringenin, a compound responsible for the bitter taste of grapefruit (Goldwasser et al., 2010), was shown to inhibit the apolipoprotein B (apoB)

secretion in HepG2 cells via inhibition of acyl-coenzyme A: cholesterol acyltransferase 2 (ACAT2) and microsomal triglyceride transfer protein (MTP) (Wilcox et al., 2001). Eriocitrin, a major anti-oxidant flavonoid in lemon fruit (Hiramitsu et al., 2014) showed lipid-lowering activity in rats fed a high fat and cholesterol diet (**Table 1.6**) (Miyake et al., 2006). *In vitro* studies in HepG2 liver cells also confirmed the lipid-lowering activity of eriocitrin (Hiramitsu et al., 2014) (**Table 1.5**).

Kaempferol is abundantly present in dietary sources such as apples, grapefruit and beverages such as tea. Luteolin was shown to inhibit the differentiation of 3T3-L1 pre-adipocytes by inhibiting the transcription of PPAR γ (Park et al., 2009). On the contrary, Ding et al. (2010) showed that luteolin stimulates insulin sensitivity by increasing transcription of PPAR γ in 3T3-L1 adipocytes (**Table 1.5**). Epigallocatechin gallate (EGCG) is the major flavonoid catechin in *Camellia sinensis* green tea (Lee et al., 2013), and was shown to inhibit adipogenesis in 3T3-L1 pre-adipocytes (Chan et al., 2011). Of the *Cyclopia* species investigated, this flavonoid was thus far only identified in *C. subternata* (Kamara et al., 2004).

1.13.6.3 Other polyphenolic groups

The benzophenones, iriflophenone-3-C- β -glucoside, iriflophenone-3-C- β -D-glucoside-4-O- β -D-glucoside and maclurin-3-C- β -glucoside were recently detected in *Cyclopia subternata* (Kokotkiewicz et al., 2012) and *Cyclopia genistoides* (Kokotkiewicz et al., 2013; Beelders et al., 2014b). These compounds have previously shown anti-obesity effects. Zhang et al. (2011) showed that iriflophenone-3-C- β -D-glucoside and maclurin-3-C- β -glucoside extracted from mango leaves decreased TG and free fatty acid accumulation, while increasing the expression of AMP-activated protein kinase (AMPK) in 3T3-L1 adipocytes.

Phloretin-3,5-di-C-glucoside, a dihydrochalcone compound with anti-oxidant properties (Barreca et al., 2011) was identified for the first time in *C. subternata* (Kokotkiewicz et al., 2012). Other dihydrochalcones, aspalathin and nothofagin from *A. linearis* have previously showed anti-obesity activities (Kawano et al., 2009) and therefore phloretin-3, 5-di-C-

glucoside could have similar activity in *Cyclopia*. *Para*-Coumaric acid, a major constituent of *Sasa queipaertensis* leaf extract (SQE), was previously detected in *C. intermedia* (Ferreira et al., 1998) and *C. subternata* (Kamara et al., 2004). This extract (SQE) has demonstrated anti-obesity effects in adipose tissue of high-fat diet (HFD)-induced obese C57BL/6 mice and in mature 3T3-L1 adipocytes through the AMPK pathway (Kang et al., 2012), suggesting that the presence of *p*-Coumaric acid in this extract could be responsible for its biological activity.

Table 1.5 Studies demonstrating the *in vitro* anti-obesity properties of the major phenolic compounds of *Cyclopia* species and the mechanism of their biological activity.

Bioactive Compound	Study Model and experimental methods	Mode of Activity	Reference
Mangiferin	HepG2 cells treated with 0.2 mM oleic acid (to stimulate high plasma free fatty acid levels), were treated with mangiferin (12.5, 25, 50, 100 µM) for 24 h	↑ FFA uptake and AMPK phosphorylation, CD36, CPT1 gene expression ↓ Intracellular FFA and TG and DGAT2, ACC gene expression	Niu et al., 2012
Hesperidin	3T3-L1 adipocytes pre-treated with hesperidin (50 and 100 µM) for 1h and thereafter incubated with or without TNF-α (10ng/ml) for 4 or 24 h	↓ TNF-α induced insulin resistance by inhibiting IL-6 and PGE ₂ production	Chae and Shin, 2012
Naringenin	3T3-L1 pre-adipocytes differentiated in the presence of naringenin (0, 6, 12, 25 and 50 µg/mL) Matured 3T3-L1 adipocytes treated with naringenin (0-50 µg/mL)	↓ Adipocyte differentiation by inhibiting PPARγ ↑ Insulin stimulated glucose uptake by inhibiting IRS-1 tyrosine phosphorylation	Richard et al., 2013
Eriocitrin	HepG2 cells treated with 30 µM eriocitrin for 48 h. Then exposed to 400 µM palmitate with or without eriocitrin	↓ Palmitate-induced lipid accumulation ↑ Mitochondrial size and mitochondrial DNA content ↑ mRNA ACADM expression levels (involved in lipid metabolism) ↑ mRNA TFAM, COX411 and ATP5J expression levels (mitochondrial biogenesis)	Hiramitsu et al., 2014
Kaempferol	3T3-L1 adipocytes treated with kaempferol (5, 10, 20 and 50 µM) for additional 3 days after differentiation	↑ Insulin stimulated glucose uptake in matured adipocytes ↓ Differentiation of 3T3-L1 pre-adipocytes	Fang et al., 2008
Luteolin	3T3-L1 adipocytes treated with luteolin 20 µM, for 6 or 24 h	↑ Insulin sensitivity by increasing insulin stimulated glucose uptake ↑ Insulin stimulated Akt2 phosphorylation, PPARγ, adiponectin and leptin ↓ TNF-α, IL-6 and MCP-1	Ding et al., 2010
Luteolin	3T3-L1 pre-adipocytes differentiated in the presence of luteolin (10, 25 and 50 µM)	↓ TG accumulation ↓ PPARγ and C/EBPα mRNA and protein expression levels	Park et al., 2009
<i>Para</i> -Coumaric acid	Differentiated L6 skeletal muscles exposed to <i>p</i> -Coumaric acid (12.5, 25, 50 or 100 µM) with or without oleic acid (1 mM) for 48 or 24 h	↑ AMPK phosphorylation (time and dose dependent manner), ACC phosphorylation, PPARα ↑ CPT-1 mRNA expression and Glucose uptake ↑ Oleic acid-induced TG accumulation	Yoon et al., 2013

GLUT4 - glucose transporter protein 4; FFA - free fatty acids; AMPK - AMP-activated protein kinase, CD36 - fatty acid translocase; CPT1 - carnitine palmitoyltransferase 1; TG - triglycerides; DGAT2 - diacylglycerol acyltransferase 2; ACC - acetyl-CoA carboxylase; IL-6 - interleukin 6; PGE₂ - prostaglandin E₂; PPARγ - peroxisome proliferator activator receptor gamma; IRS-1 - insulin receptor substrate 1; ACADM - acyl-CoA dehydrogenase, medium chain; TFAM - transcription factor A, mitochondrial; COX411 - cytochrome c oxidase subunit 411; ATP5J - ATP synthase, H⁺ transporting, mitochondrial Fo complex subunit F6; Akt2 - V-Akt murine thymoma viral oncogene homolog 2; TNF-α - tumor necrosis factor alpha; MCP-1 - monocyte chemoattractant protein-1; C/EBPα - CCAAT/enhancer binding protein alpha; PPARα - peroxisome proliferator activator receptor alpha.

↑Increased

↓Decreased

Table 1.6 Studies demonstrating the *in vivo* anti-obesity properties of the major phytochemicals of *Cyclopia* species and the mechanism of their biological activity.

Bioactive Compound	Study Model and experimental methods	Mode of Activity	Reference
Mangiferin	Hyperlipidemic Wistar rats on high fat diet supplemented with mangiferin (50, 100 and 150 mg/kg BW) for 6 weeks	↓ Liver and plasma FFA and TG ↑ Liver AMPK, CD36, CPT1 ↓ Liver DGAT2, ACC	Niu et al., 2012
Mangiferin	Spontaneously hypertensive rats fed fructose to induce liver steatosis were administrated mangiferin (15 mg/kg) by oral gavage for over 7 weeks	↓ Hepatic TG content and lipid content ↓ Hepatic DGAT2	Xing et al., 2014
Hesperidin	STZ T1DM rats feed a standard diet containing 10 g/kg diet hesperidin for four weeks	↓ Blood glucose, G6Pase, serum and hepatic TG, TC and serum LDL-C, VLDL-C ↑ Serum insulin, adiponectin, GK, serum HDL-C and HDL-C/TC	Akiyama et al., 2010
Hesperidin	C57BL/KsJ-db/db (T2DM) mice	↑ GK (hepatic), GLUT4 (adipocytes), PPAR γ (hepatic and adipocyte) ↓ Plasma and hepatic FFA and triglycerides; hepatic FASN, G6PD and PAP, GLUT2	Jung et al., 2006
Eriocitrin	Zebra fish on diet-induced obesity (overfeeding) obtained oral administration of eriocitrin (32 mg/kg/day) for 28 days	↓ Liver steatosis, plasma TG ↑ Hepatic mRNA ACOX1 and ACADM expression levels (lipid metabolism) ↑ Hepatic mRNA NRF1 and TFAM expression levels (mitochondrial biogenesis)	Hiramitsu et al., 2014
Eriocitrin	Rat on High fat and high cholesterol diet supplemented with 0.35% and 0.7% eriocitrin for 21 days	↓ Serum TC, TG and VLDL-C, LDL-C, phospholipids	Miyake et al., 2006
Kaempferol	Wistar rat on HFD-induced obesity were orally dosed with kaempferol (70, 150 and 300 mg/kg) once a day for 8 weeks.	↓ Body weight gain, fat pad weight, plasma and hepatic lipids, hepatic SREBP-1 and SREBP-2 protein expression ↑ Hepatic PPAR α , ACO and CYP4A protein expression	Chang et al., 2011
<i>Para</i> -Coumaric acid	Ovariectomized rats orally administered 10 mg/kg <i>p</i> -Coumaric acid daily for 4 weeks	↓ Serum cholesterol, body mass gain ↑ Serum estradiol levels	Zych et al., 2009

FFA - free fatty acids; TG - triglycerides; AMPK - AMP-activated protein kinase, CD36 - fatty acid translocase; CPT1 - carnitine palmitoyltransferase 1; DGAT2 - diacylglycerol acyltransferase 2; ACC - acetyl-CoA carboxylase; TC - total cholesterol; LDL-C - low density lipoprotein cholesterol, VLDL-C - very low density lipoprotein cholesterol; GK - glucokinase; G6Pase - glucose-6-phosphatase; HDL-C - high density lipoprotein cholesterol; GLUT4 - glucose transporter protein 4; PPAR γ - peroxisome proliferator activator receptor gamma; FASN - fatty acid synthase; G6PD - glucose-6-phosphate dehydrogenase; PAP - phosphatidate phosphohydrolase; GLUT 2 - glucose transporter protein 2; TLR2 - toll-like receptor 2; TNF- α - tumor necrosis factor alpha; MCP-1 - monocyte chemoattractant protein-1; ACADM - acyl-CoA dehydrogenase, medium chain; ACOX1 - acyl-CoA oxidase 1; TFAM - transcription factor A, mitochondrial; NRF1 - nuclear respiratory factor-1; SREBP - sterol regulatory element-binding protein 1 or 2; PPAR α - peroxisome proliferator activator receptor alpha; ACO - acyl-CoA oxidase; CYP4A - cytochrome P450 isoform 4A1.

↑ Increased

↓ Decreased

1.14 Model systems to study obesity

Understanding the pathophysiology of obesity require suitable *in vitro* and *in vivo* models that mimic disease pathogenesis. Currently, the most commonly used *in vitro* models to study obesity are 3T3-L1 cells, Ob1771 cells, 3T3F442A cells, TA1 cells and Ob17 cells, with the former being the most widely used (Ntambi and Young-Cheul, 2000). Primary adipocytes derived from the subcutaneous and visceral fat depots of animals and humans are also used to understand the pathophysiology of obesity. Rodent models including diet-induced obese, genetic obese, and genetic obese and diabetic models are commonly used for *in vivo* studies (Lutz et al., 2001). The relevance of the 3T3-L1 adipocytes and the $Lepr^{db/db}$ mouse model to study obesity will be discussed below.

1.14.1 3T3-L1 adipocytes

Although *in vitro* models do not represent the complexity of human physiology and their relevance to study disease is often questioned, they are useful for rapid and inexpensive screening of bioactive compounds. The 3T3-L1 pre-adipocyte cell line is an immortalised mouse fibroblast cell line, commonly used for *in vitro* studies associated with adipogenesis, lipid and glucose metabolism (Green and Kehinde 1976). After their differentiation into mature adipocytes, they represent similar morphology, gene expression and metabolism as normal adipocytes (Green and Kehinde, 1976). The use of chemical inducers of adipogenesis (insulin, dexamethasone and 3-isobutyl-1-methylxanthine [IBMX]), that mimic the hormonal, dietary and genetic influences of adipocyte differentiation *in vivo* has made a significant impact towards understanding molecular events involved in adipogenesis (Park et al., 2014).

1.14.2 The $Lepr^{db/db}$ mouse model

The $Lepr^{db/db}$ mouse is a model of obesity and T2DM (Srinivasan and Ramarao, 2007). This animal model has a diabetic homozygous, spontaneous glycine to threonine mutation in the leptin receptor gene on chromosome 4, which results in the expression of a non-functional leptin receptor protein (Wang et al., 2014). Leptin, a hormone secreted by

adipose tissue, regulates appetite and maintains energy homeostasis. Leptin binds to the leptin receptor in order to regulate its signaling, and loss of the leptin receptor leads to several physiological abnormalities including hypothalamus disturbance (Wang et al., 2013; 2014). The $Lepr^{db/db}$ mouse is characterized by progressive metabolic deterioration including obesity, hyperphagia, hyperglycemia, glucose intolerance, hyperinsulinemia and T2DM at a very young age (Wang et al., 2013). The use of the $Lepr^{db/db}$ mouse model allows the screening of compounds without any side effects normally associated with chemical inducers of diabetes such as alloxan and streptozotocin (STZ) (King, 2012). Furthermore the use of this *in vivo* animal model is useful in representing the complexity and heterogeneous conditions associated with obesity including IR, dyslipidemia and T2DM (Srinivasan and Ramarao, 2007). However, $Lepr^{db/db}$ mice have a short life span, making it difficult to investigate the long term complications of obesity and T2DM (Wang et al., 2013).

1.15 Motivation for the study

1.15.1 Problem statement and research motivation

Obesity, a multifactorial metabolic disorder, has been described as a global pandemic that is significantly spreading in several parts of the world. The prevalence of being overweight and obesity has rapidly increased since 1980, in both developed and developing countries, and almost 30% of the world's population is either overweight or obese (Finucane et al., 2011; Ng et al., 2014). Obesity is a complex metabolic disorder that is frequently associated with several metabolic abnormalities including low-grade inflammation, insulin resistance, dyslipidemia, hyperglycemia, glucose intolerance, hypertension and non-alcoholic fatty liver disease (Kaila and Raman, 2008). Obesity also increases the risk for chronic diseases such as T2DM, CVD and certain types of cancers (Haslam and James, 2005). These chronic diseases place a huge socioeconomic burden on countries, particularly developing countries, such as South Africa, with an already overburdened health care system.

Increased physical activity and reduced energy consumption are effective strategies for weight management and the prevention of obesity, however people are reluctant to lifestyle modification, resulting in the increased reliance on pharmacotherapy to treat obesity (Hunter et al., 2008; Lagerros and Rösner, 2013). The currently available pharmacological drugs approved by the FDA for obesity treatment (Orlistat, Phentermine/Topiramate and Lorcaserin) are not effective, and have a number of unpleasant side effects (Adan, 2013). Thus, there is an urgent need to develop effective interventions in order to prevent or better manage the rapidly increasing prevalence of obesity and obesity-related complications.

Medicinal plants and their phytochemicals, particularly polyphenols have recently received considerable attention as alternative or adjunct therapies for the treatment or prevention of chronic diseases such as obesity and T2DM. Natural medicines are used frequently all over the world and they are often considered safer than conventional medicine (Mahomoodally, 2013). Increasing evidence show that *Cyclopia* spp., indigenous South African plants used for the commercial production of honeybush herbal tea, have potential to ameliorate obesity (Dudhia et al., 2013; Pheiffer et al., 2013). Aqueous extracts of *C. maculata* and *C. subternata* inhibited adipogenesis in differentiating 3T3-L1 pre-adipocytes and stimulated lipolysis in differentiated 3T3-L1 adipocytes (Dudhia et al., 2013; Pheiffer et al., 2013). The bioactivity of these extracts is thought to be due to the high content of polyphenols, and therefore the specific roles of these polyphenols as anti-obesity agents needs to be further studied, which would guide nutraceutical development.

1.15.2 Hypothesis

Cyclopia plant extracts contain complex mixtures of polyphenolic compounds with bioactivity. Although a number of previous studies have reported that these extracts may have beneficial health effects, identification of the compound/s or sub-fractions responsible for the biological effect of these extracts is critical before it can be developed as a nutraceutical. We hypothesize that polyphenol enrichment of *Cyclopia* extracts may enhance their anti-obesity effects, and that bioactivity guided fractionation will facilitate the identification of these bioactive polyphenols.

1.15.3 Aim

The aim of this study is to investigate the anti-obesity properties of three commercially relevant *Cyclopia* spp. using polyphenol-enriched *Cyclopia* extracts and fractions, and to characterize and identify polyphenols responsible for the anti-obesity potential of *Cyclopia* using bioactivity guided fractionation.

1.15.4 Study objectives

Objective 1: To prepare 40% aqueous methanol extracts of *C. maculata*, *C. intermedia* and *C. subternata*, and to separate these extracts into aqueous and organic fractions for further enrichment of the phenolic content of the organic fraction. To identify and compare the polyphenolic composition of the aqueous methanol extracts, and their aqueous and organic fractions using liquid chromatography tandem mass spectrometry (LC-MS/MS) and quantitative high performance liquid chromatography-diode array detector (HPLC-DAD).

Objective 2: Screening of aqueous and organic fractions of the aqueous methanol extracts of *C. maculata*, *C. intermedia* and *C. subternata* for their effect on lipid content and cell viability in differentiated 3T3-L1 adipocytes in order to select the most bioactive *Cyclopia* fraction. Further analysis of the bioactive fraction, for its effect on the expression of genes relevant to lipid, glucose and energy metabolism in differentiated 3T3-L1 adipocytes.

Objective 3: To prepare the bioactive *Cyclopia* fraction on large scale and confirm its activity in obese $Lepr^{db/db}$ mice. Further elucidation of its effect on the expression of genes associated with lipid, glucose and energy metabolism in various adipose fat depots.

Objective 4: To further fractionate the selected *Cyclopia* fraction into four sub-fractions using high performance counter-current chromatography (HPLCCC), and determination of their polyphenolic composition using LC-MS/MS and quantitative HPLC.

Objective 5: To determine the effect of the fractions obtained from HPLC on lipid content and TG accumulation, lipolysis and ATP content in differentiating 3T3-L1 pre-adipocytes and in differentiated 3T3-L1 adipocytes in order to facilitate the identification of anti-obesity polyphenols. Determine the effect of these fractions on the expression of genes relevant to lipid, glucose and energy metabolism in mature 3T3-L1 adipocytes.

CHAPTER 2

MATERIALS AND METHODS

2.1 Overview of methodology

Aqueous methanol (40% methanol) extracts of three *Cyclopia* species (*C. subternata*, *C. intermedia* and *C. maculata*) were prepared, and subsequently separated into aqueous and organic fractions to further enrich the phenolic content of the organic fraction. LC-MS/MS and HPLC-DAD were used to determine the polyphenolic composition of these extracts and fractions. The aqueous and organic fractions of the 40% aqueous methanol extracts were thereafter screened for their effect on lipid content and cell viability in mature 3T3-L1 adipocytes. The mechanism of action of the most bioactive fraction was assessed by measuring the messenger RNA (mRNA) expression of known lipid, glucose and energy metabolism genes, using quantitative real-time PCR (qRT-PCR). The expression of PPAR γ and PPAR α was assessed by western blot analysis. The anti-obesity effects of the selected bioactive fraction were evaluated in an obese Lepr^{db/db} mouse model, where after the mRNA expression of genes involved in lipid, glucose and energy metabolism was assessed in various adipose fat depots. The bioactive fraction was further separated into four major sub-fractions (CCC fractions) using HPLC, and LC-MS/MS and quantitative HPLC-DAD were used to determine the polyphenolic composition of the CCC fractions. CCC fractions were tested *in vitro* for their effect on lipid content, TG accumulation, lipolysis and ATP content in both differentiating 3T3-L1 pre-adipocytes and differentiated 3T3-L1 adipocytes. The expression of genes and proteins, as described previously, were investigated after treatment of differentiated 3T3-L1 adipocytes with optimized concentrations of CCC fractions using qRT-PCR and western blot analysis. A schematic diagram of the experimental outline is illustrated in **Fig. 2.1**.

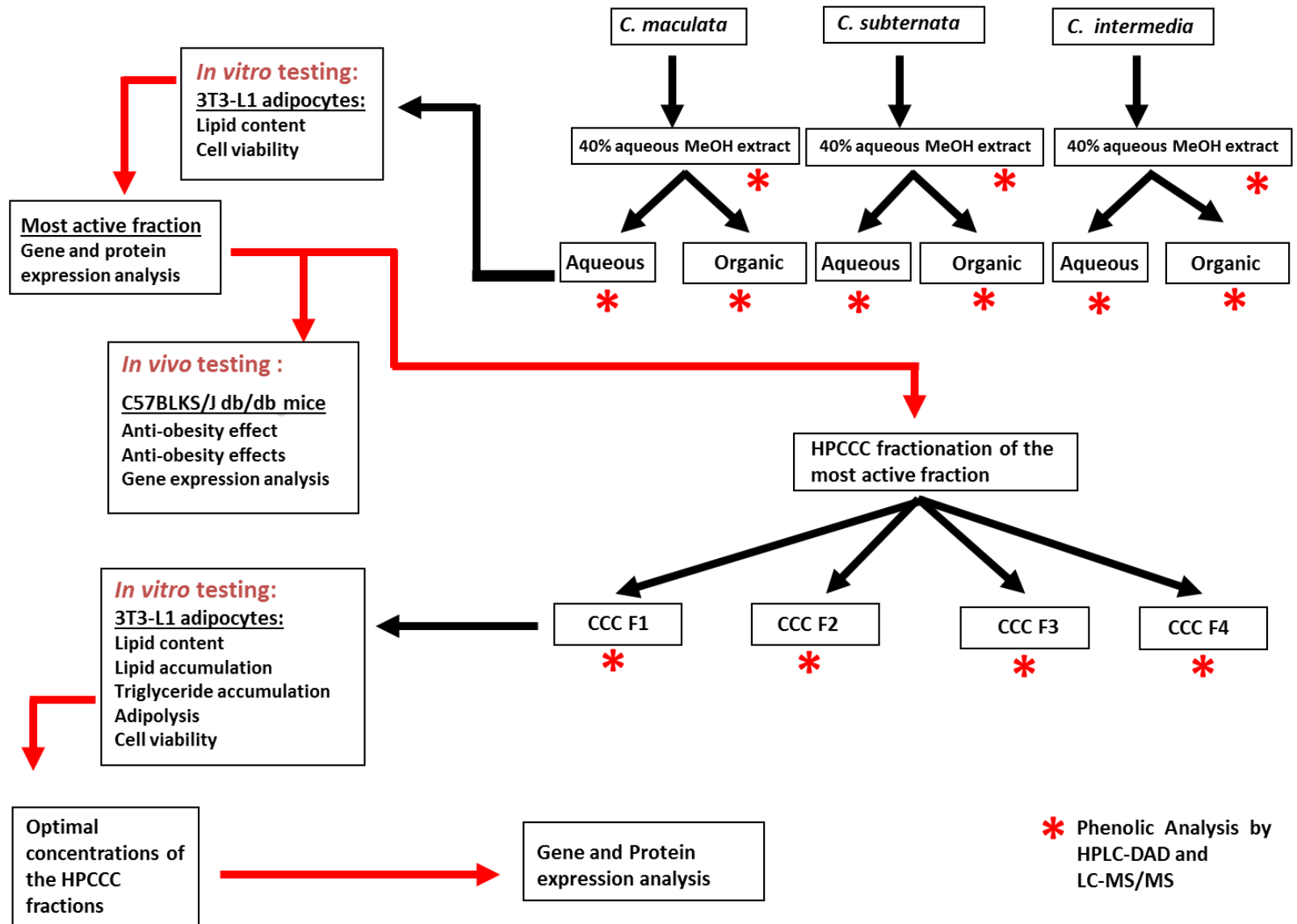


Figure 2.1 Experimental outline.

Reagents used in this study and their suppliers are listed in **Addendum 2** unless otherwise stated in the experimental protocols. Buffers and solutions used are also listed in **Addendum 2**.

2.2 Plant material

The information regarding the harvesting and processing of *C. subternata*, *C. intermedia* and *C. maculata* is described in **Table 2.1**. The plant material was processed using standard processing procedures for the unfermented 'green' honeybush tea. Briefly, shoots (leaves and stems) of these plants (> 4 kg/species) were harvested from commercial or experimental plantations in the Western Cape, South Africa, from January to June 2013. The unfermented plant material was prepared by drying the intact fresh plant material at 40°C to less than 10% moisture content, whereafter it was pulverized with a Retsch mill (1 mm sieve; Retsch Technology GmbH, Haan, Germany) and stored in sealed plastic containers at room temperature in the dark.

Table 2.1 Information regarding the original harvestings and processing of *Cyclopia* species.

Species	Harvested Area	Description	Harvest Date	ARC Sample Code
<i>C. subternata</i>	Barrydale	Unfermented; Whole dried Milled Retsch	31 January 2013 /12 March 2013	ARC 180 (40% aqueous methanol extract)
				ARC 184_P (aqueous fraction)
				ARC 184_NP (organic fraction)
<i>C. intermedia</i>	Barrydale	Unfermented; Whole dried Milled Retsch	03 June 2013	ARC 181 (40% aqueous methanol extract)
				ARC 185_P (aqueous fraction)
				ARC 185_NP (organic fraction)
<i>C. maculata</i>	Beriaville	Unfermented; Whole dried Milled Retsch	06 May 2013	ARC 182 (40% aqueous methanol extract)
				ARC 186_P (aqueous fraction)
				ARC 186_NP (organic fraction)

2.2.1 Preparation of 40% aqueous methanol extracts

Aqueous methanol extracts of each *Cyclopia* species were prepared by adding 1500 mL of 40% methanol (v/v, prepared in deionized water) to 150 g dried, milled plant material in 2 L Schott bottles. Each bottle was placed in a water bath at 70°C for 30 minutes, while swirling the contents every 5 minutes. The warm extracts were filtered using a stainless steel mesh, followed by vacuum filtration through Whatman no. 4 filter paper. Methanol was evaporated under vacuum at 40°C, using a rotary evaporator (Buchi Labortechnik, Postfach, Flawil, Switzerland) and the plant extracts were frozen and freeze-dried using a Virtis Advantage Plus freeze-drier (SP Scientific, Warminster, PA, USA).

2.2.2 Liquid-liquid fractionation of 40% aqueous methanol extracts

Freeze-dried 40% aqueous methanol extracts were separated into aqueous and organic fractions by liquid-liquid partitioning, using water and *n*-butanol. Briefly, 3 g of each extract was dissolved in 200 mL of deionized water by sonication, transferred into a separating funnel and 100 mL of *n*-butanol was added. Fractionation was achieved by inverting the funnel five times (with the pressure within the separating funnel released after every invert) to ensure distribution of the compounds between the two layers, which represented the aqueous (lower) and organic (upper) fractions (**Fig. 2.2**). Both fractions were collected into separate bottles and *n*-butanol partitioning of each dissolved 3 g extract was repeated four times with 100 mL of *n*-butanol to achieve exhaustive fractionation. Liquid-liquid fractionation was repeated using five different 3 g aliquots of the 40% aqueous methanol extract prepared above (**section 2.2.1**). Butanol was evaporated under vacuum by rotary evaporation at 40°C and the fractions were frozen and freeze-dried.

2.2.3 Large scale preparation of the bioactive fraction

The most bioactive *Cyclopia* fraction was prepared on a large scale to obtain a yield sufficient for animal experiments and HPLC fractionation. This required preparation of several batches of the 40% aqueous methanol extract of the selected *Cyclopia* species as described in **Section 2.2.1** (21 batches of 150 g plant material). Liquid-liquid

fractionation was conducted as described in **Section 2.2.2**, using 15 g of the extract (which is 5 times more of the extract than used above), dissolved in 1000 mL deionized water and mixed with 500 mL *n*-butanol, as described above.

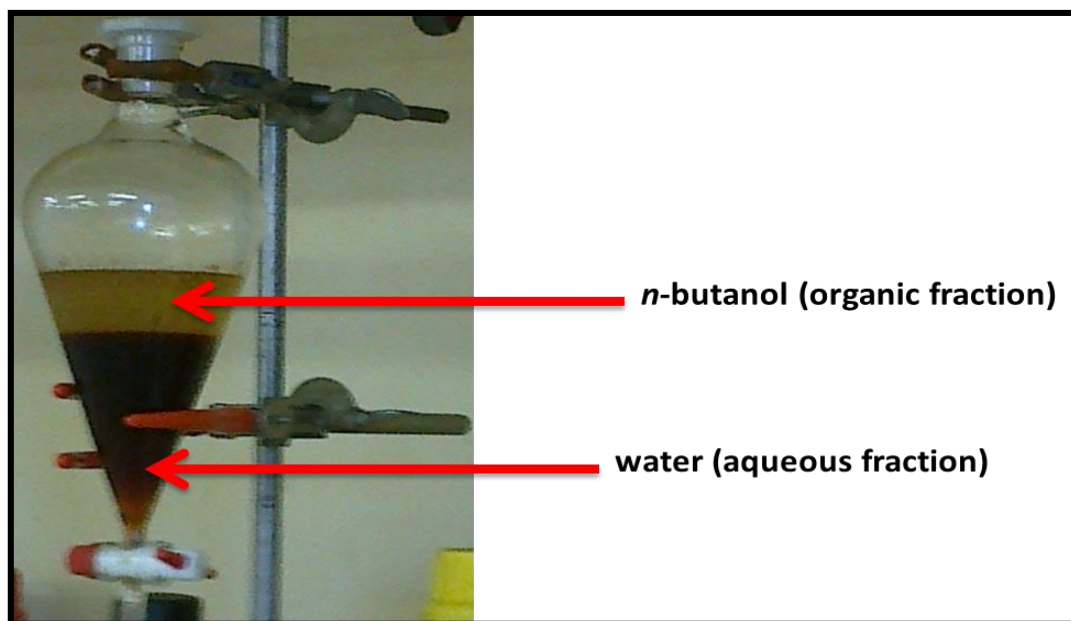


Figure 2.2 Liquid-liquid fractionation of a 40% aqueous methanol extract indicating the aqueous, water (lower) fraction and the organic, *n*-butanol (upper) fraction.

2.2.4 High performance counter-current chromatography (HPCCC)

The most bioactive fraction, selected from *in vitro* screening experiments and confirmed in obese *Lepr^{db/db}* mice was separated into four sub-fractions using HPCCC. HPCCC is a preparative purification chromatographic technique that separates compounds using two immiscible liquids under a centrifugal force, with one liquid acting as a stationary phase and the other as a mobile phase (**Fig 2.3**). Compounds are separated based on their affinity for the mobile and stationary phases (Berthod et al., 2009). HPCCC fractionation was carried out using a multilayer coil, planetary J-type centrifuge spectrum model (Dynamic Extraction, Slough, United Kingdom). Fractionation was carried out at 28°C and the coil system (the column) was filled with the stationary phase solution using a Gilson 305 HPLC pump (Gilson Inc., Middleton, WI, USA) (**Fig. 2.3B**). The rotation speed was

set at 1 600 rpm. The βr values for the preparative coil were measured as 0.52 at the internal end of the coil and 0.86 at the external end of the coil (equation $\beta r = r/R$, with r = spool radius measured at the nearest and farthest layer of the coil; and R = rotor radius). At least 2 L of solvent mixture containing tert-butyl methyl ether–*n*-butanol–acetonitrile–water, in a ratio of 1:3:1:5 (v/v/v) was prepared in a separating funnel, allowed to equilibrate at room temperature, and separated into two layers; the upper organic layer (stationery phase) and the lower aqueous layer (mobile phase), that were both degassed by sonication after collecting into separate bottles.

The sample was prepared by dissolving 60 mg of the plant extract in 6 mL of a 1:1 mixture containing the stationary phase and the mobile phase, by sonication. Thereafter, the sample was injected into the column using a manual low-pressure sample injection valve. The mobile phase was pumped through the column at a flow rate of 7.5 mL/min using the Gilson 305 HPLC pump in a head-to-tail direction. Separation was monitored using the Waters 2996 diode array detector (Waters, Milford, MA, USA) and the MassLynx v4.1 software (Waters), and recording the HPCCC chromatograms at 288 and 320 nm. Fractions were collected into test tubes at 1 minute intervals using the Gilson FC204 fraction collector (Gilson, Inc.). Each separation took approximately 45 minutes, where after the sample that remained in the column was extruded by pumping the stationery phase (10 mL/min), thus re-filling the coils in preparation for the next fractionation. The fractions (CCC fractions) collected into test tubes were pooled into four major fractions based on the clustering of their peaks in the chromatograms. HPCCC fractionation was repeated several times in order to obtain a sufficient yield for cell culture screening experiments, and the collected fractions were evaporated under vacuum at 40°C, using a rotary evaporator and frozen before freeze-drying.

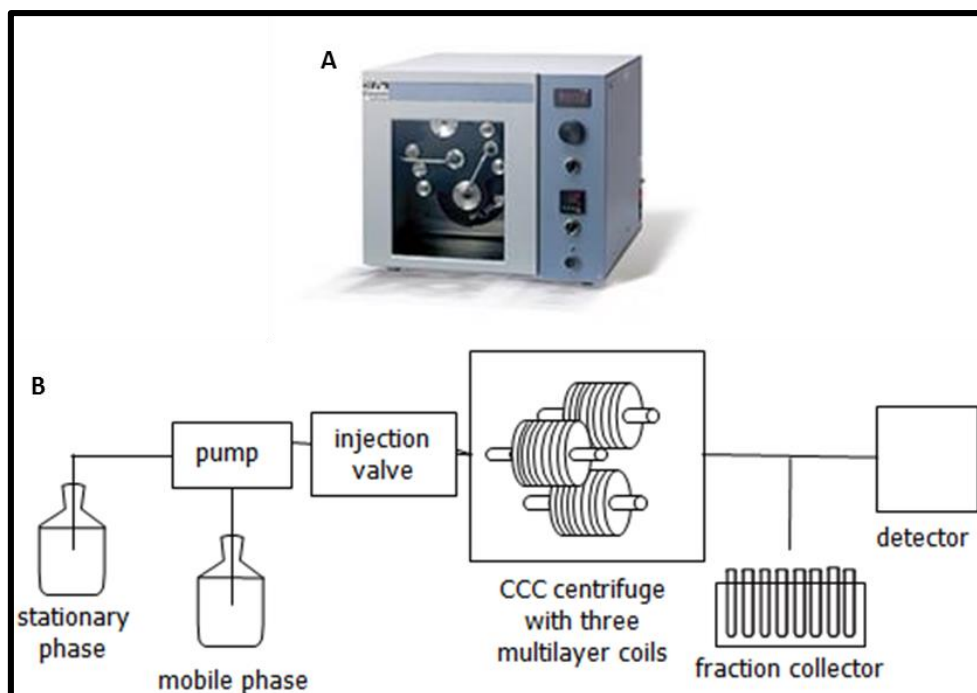


Figure 2.3 High performance counter current chromatography (A) and an illustration of the HPCCC protocol (B).

2.2.5 Separation and quantification of phenolic compounds using HPLC-DAD

HPLC is an analytical technique used for separation, identification and quantification of individual compounds in complex mixtures (Siddiqui et al., 2013). HPLC with diode array detection (DAD) (Abad-García et al., 2009) was used for the quantification of major phenolic compounds. The analysis was performed using an Agilent 1200 series HPLC system consisting of an in-line degasser, quaternary pump, autosampler, column thermostat and DAD controlled by OpenLAB Chemstation software (Agilent Technologies Inc., Santa Clara, CA, USA). Samples were prepared in 10% aqueous DMSO (to a final concentration of 6 mg/mL) by dissolving the samples first in the equivalent of 10% of the final volume in DMSO. Subsequently, Milli-Q water was added to reach the final volume and concentration. Thereafter, samples were filtered through 0.22 μm Millex-HV membrane syringe filters (Millipore, Bedford, MA, USA) and analyzed in duplicate. The standard phenolic compounds were also analyzed in duplicate. Ascorbic acid, to a final concentration of 9 mg/mL was added to samples and standards prior to filtration in order to prevent oxidative degradation of the phenolic compounds during analysis. The injection

volumes for the standards and samples ranged from 10 - 20 μL and from 1 - 25 μL , respectively depending on the assumed phenolic concentration.

HPLC-analysis of the *C. subternata* and *C. maculata* extracts and fractions was performed using the validated species-specific HPLC methods as described by De Beer et al. (2012) and Schulze et al. (2014). A Gemini-NX C18 (150 x 4.6 mm; 3 μm , 110 \AA) column from Phenomenex (Santa Clara, CA, USA) and a solvent gradient consisting of acetonitrile (Solvent B) and 2% (v/v) acetic acid (Solvent A) as mobile phase, with a flow rate of 1 mL/min and temperature of 30°C was maintained. The mobile phase gradient for *C. subternata* was: 0 - 2 min (8% B), 2 - 27 min (8% - 38% B), 27 - 28 min (38% - 50% B), 28 - 29 min (50% B), 29 - 30 (50% - 8% B), 30 - 40 min (8% B). The mobile phase gradient for *C. maculata* was 0 - 2 min (8% B), 2 - 31 min (8% - 38% B), 31 - 32 min (38% - 50% B), 32 - 33 min (50% B), 33 - 34 min (50% - 8% B), 34 - 44 min (8% B). For *C. intermedia*, a new method was developed and validated by slight modification of the method described in Schulze et al. (2015) for *C. longifolia* polyphenols. Briefly, separation was achieved on a 2.6 μm Kinetex C18 core-shell column (150 x 4.6 mm; Phenomenex, Torrance, CA, USA), using a mobile phase consisting of 0.1% (v/v) aqueous formic acid (A) and acetonitrile (B) in a multilinear gradient: 0 - 4 min (4.5% B), 4 - 22 min (4.5% - 8% B), 22 - 49 min (8% - 20% B), 49 - 60 min (20% - 50% B), 60 - 62 min (50% B), 62 - 63 min (50% - 4.5% B), 63 - 69 min (4.5% B). A flow rate of 1 mL/min and column temperature at 30°C was maintained throughout the analysis.

The xanthones (mangiferin and isomangiferin), one benzophenone (maclurin-3-C- β -glucoside), flavones (luteolin, scolymoside and vicianin-2) and the hydroxycinnamic acid (*p*-Coumaric acid) were quantified at 320 nm, the flavanones (eriocitrin, an eriodictyol-*O*-deoxyhexoside-*O*-hexoside and hesperidin), benzophenones (iriflophenone-3-C- β -D-glucoside and iriflophenone-3-C- β -D-glucoside-4-*O*- β -D-glucoside) and dihydrochalcones (phloretin-3',5'-di-C- β -D-glucoside and 3-hydroxyphloretin-3',5'-di-C-hexoside) at 288 nm and the hydroxybenzoic acid (protocatechuic acid) at 255 nm. The phenolic compounds were quantified using calibration curves for authentic reference standards whereas compounds with no authentic standards were quantified as equivalents of related compounds. Calibration curves were set up for selected standard compounds to test the

linearity of their UV-DAD responses. The linearity ranges (μg on-column) for the three different *Cyclopia* species are described in **Table 2.2**.

Table 2.2 Standard calibration mixtures for *C. subternata*, *C. intermedia* and *C. maculata* phenolic standards.

Compound	Wavelength	Linearity Range μg on-column		Regression Equation	Correlation Coefficient, R^2
		Minimum	Maximum		
<i>C. subternata</i>					
Mangiferin	320 nm	0.0098	2.4429	$y = 2187.6x + 0.6778$	0.9999
Vicenin-2	320 nm	0.0026	0.6611	$y = 1856.9x - 0.5761$	0.9999
Luteolin	320 nm	0.0083	2.0800	$y = 2843.1x - 33.396$	0.9999
<i>p</i> -Coumaric acid	320 nm	0.0043	0.8667	$y = 6203.0x + 1.3646$	0.9999
Eriocitrin	288 nm	0.0066	1.6607	$y = 1593.9x + 0.4689$	0.9999
Hesperidin	288 nm	0.0078	1.9580	$y = 1619.4x + 1.4078$	0.9999
Iriflophenone-3-C- β -D-glucoside	288 nm	0.0052	3.2697	$y = 1714.3x + 0.8972$	0.9999
Protocatechuic acid	288 nm	0.0044	0.8869	$y = 3340.4x + 0.8257$	0.9999
<i>C. intermedia</i>					
Mangiferin	320 nm	0.0064	1.6000	$y = 2139.3x - 21.749$	0.9998
Maclurin-3-C- β -glucoside	320 nm	0.0027	0.6723	$y = 2015.0x - 2.5742$	0.9999
Vicenin-2	320 nm	0.0027	0.6819	$y = 1730.9x - 2.5173$	0.9999
Luteolin	320 nm	0.0007	0.1656	$y = 2504.7x - 16.664$	0.9983
Eriocitrin	288 nm	0.0026	0.6620	$y = 1556.6x - 4.5363$	0.9999
Narirutin	288 nm	0.0027	0.6627	$y = 1468.2x - 0.4057$	0.9999
Hesperidin	288 nm	0.0052	1.3115	$y = 1594.1x - 3.0581$	0.9999
Iriflophenone-3-C- β -D-glucoside	288 nm	0.0028	0.6906	$y = 1873.5x + 0.8460$	0.9999
Neoponcirin	288 nm	0.0330	1.6480	$y = 1480.4x + 1.6936$	0.9999
<i>C. maculata</i>					
Mangiferin	320 nm	0.0195	4.8857	$y = 2173.2x + 16.827$	0.9999
Vicenin-2	320 nm	0.0026	0.6611	$y = 1856.2x - 1.7048$	0.9999
Luteolin	320 nm	0.0083	2.0800	$y = 2818.5x - 24.149$	0.9999
<i>p</i> -Coumaric acid	320 nm	0.0043	0.8667	$y = 6193.9x - 0.2402$	0.9999
Eriocitrin	288 nm	0.0066	1.6607	$y = 1569.5x + 0.9647$	0.9999
Hesperidin	288 nm	0.0091	2.2844	$y = 1612.3x + 1.9152$	0.9999
Iriflophenone-3-C- β -D-glucoside	288 nm	0.0065	1.6348	$y = 1841.6x + 2.7270$	0.9999
Protocatechuic acid	288 nm	0.0044	0.8869	$y = 3336.8x + 0.5268$	0.9999

2.2.6 Identification of phenolic compounds using LC-DAD-MS and -MS/MS Detection

Like HPLC, LC-MS is a sensitive and specific analytical technique used to detect biochemical compounds, but in addition also gives the molecular mass of compounds using tandem mass spectrometry (MS) (Pitt, 2009). In this study, LC-DAD-MS and -

MS/MS detection was conducted using conditions previously described by De Beer et al. (2012) and Schulze et al. (2014) for *C. subternata* and *C. maculata*, respectively. LC analysis was performed on a Waters Acquity ultra-performance liquid chromatography (UPLC) system consisting of an in-line degasser, DAD detector, column oven and binary pump (Waters). This system was coupled to a Synapt G2 quadrupole time of flight (QTOF) mass spectrometer equipped with electrospray ionisation (ESI) (Waters). An injection volume of 10 µL was used for both the standard and samples (aqueous fractions of *C. subternata*, *C. intermedia* and *C. maculata*), whereas 2-5 µL of the organic fractions were injected. UV-Vis spectra were recorded from 215 to 500 nm and the MS and MS^E scan ranges were from 155 to 1000 m/z and from 40 to 1000 m/z, respectively. Prior to introduction into the ionisation chamber, the eluant was split in a ratio of 3:2. MS results were acquired in both positive and negative ionisation mode with MS and MS^E for each sample. For MS^E a collision energy ramp from 20 to 60 V was used. The parameters used for MS were as follows: capillary voltage 2 500 V, cone voltage 15 V, desolvation temperature 275°C, source temperature 120°C and nitrogen flow rate 650 L/h. MassLynx v4.1 software (Waters) was used for data acquisition and analysis. Peaks were identified by comparing LC-MS spectra for both positive and negative ionisation, UV-Vis spectra and retention times to those of authentic reference standards. For peaks with no authentic standards available, LC-MS and - MS^E spectra were confirmed based on data from previous literature (De Beer et al., 2012; Schulze et al., 2014).

2.3 *In vitro* cell culture

2.3.1 Cell line

Murine 3T3-L1 pre-adipocytes (American Type Culture Collection, VA, USA) were used for *in vitro* experiments. The passage number was kept below 20 for all experiments in order to maintain consistency between experiments and to prevent the depletion of specific cell phenotypes such as the ability of these cells to differentiate due to excessive passage.

2.3.2 Thawing of 3T3-L1 pre-adipocytes

Cryo-preserved cells (2×10^6 cells/mL) in freezing media containing Dulbecco's Modified Eagle's Medium (DMEM), 10% newborn calf serum (NBCS) and 7% (v/v) dimethyl sulfoxide (DMSO) were removed from liquid nitrogen. Cells were thawed by placing the cryotubes in a 37°C water bath. Immediately after thawing, the cell suspension was transferred into a 75 cm² tissue culture flask containing 17 mL of pre-warmed pre-adipocyte growth media (90% DMEM and 10% NBCS). The cells were incubated overnight at 37°C in humidified air with 5% CO₂. Twenty-four hours after seeding, the media was refreshed with pre-warmed pre-adipocyte growth media. Pre-adipocyte growth media was supplemented with 100 U/mL penicillin and 100 µg/mL streptomycin until the cells were passaged twice.

2.3.3 Subculture of 3T3-L1 pre-adipocytes

2.3.3.1 Trypsin treatment

Cells were trypsinized when 70 - 80% confluency was reached. Pre-adipocyte growth media was completely aspirated and cells were rinsed with 8 mL of warm Dulbecco's phosphate buffered saline (DPBS). Thereafter, cells were incubated with 2 mL of trypsin-versene at 37°C in humidified air with 5% CO₂ for 5 - 7 minutes until the cells were dislodged from the cell culture flask; visual observation with an inverted light microscope (CKX 41, Olympus; Melville, NY, USA). Trypsinization was stopped by adding 8 mL of pre-warmed pre-adipocyte growth media, and the cell suspension was pipetted up and down briefly to disaggregate cell clumps and ensure single cell suspension. Thereafter, the cell suspension was centrifuged at $800 \times g$ (SL 16R Thermo Fisher Scientific, Waltham, MA, USA) for five minutes and the cell pellet was resuspended in 10 mL of pre-warmed pre-adipocyte growth media. Approximately 200 µL of the cell suspension was removed for cell counting.

2.3.3.2 Cell counting

Cells were counted using the Countess® Automated Cell Counter (Invitrogen, Carlsbad, CA, USA). Briefly, 10 µL of the cell suspension was thoroughly mixed with 10 µL of a 0.4% solution of trypan blue prepared in phosphate buffered saline (Invitrogen). Ten microliters of the mixture was transferred onto the counting chamber, which was then inserted into the Countess Automated Cell Counter, following the manufacture's guidelines. The total number of viable cells (cells/mL) was generated by the cell counter and used for either freezing cells, or preparing seeding densities for subculturing experiments (in 75 cm² tissue culture flask or multi-well plates) only if their viability was 70% or more.

2.3.3.3 Freezing cells

After counting, cells were harvested by centrifugation at 800 × *g* for five minutes. The supernatant was discarded and the cells were resuspended in sterile cold freezing media containing DMEM, 10% NBCS and 7% DMSO, at a volume required to achieve 2 × 10⁶ cells/mL. The resuspended cell suspension was aliquoted as 1 mL per cryotube and placed on ice. The cells were stored at -80°C overnight and transferred to liquid nitrogen the following day for long term storage.

2.3.4 Seeding of 3T3-L1 pre-adipocytes

After trypsin treatment (**Section 2.3.3.1**) and cell counting (**Section 2.3.3.2**), cells were diluted to 2 × 10⁴ cells/mL and seeded into multi-well plates as demonstrated in **Table 2.3**. Cells were maintained in pre-adipocyte growth media until adipocyte differentiation was induced. Cells were randomly assessed for mycoplasma contamination using the MycoAlert™ Mycoplasma Detection Kit, according to the manufacturer's instructions (Lonza, Basel, Switzerland).

Table 2.3 Cell seeding densities and volumes used for multi-well plate culturing.

Type of multi-well plate	Cell Concentration	Culturing volume	Cell Density
96 well	2×10^4 cells/mL	200 μ L	4×10^3 cells/well
24 well	2×10^4 cells/mL	1000 μ L	2×10^4 cells/well
6 well	2×10^4 cells/mL	3000 μ L	6×10^4 cells/well

2.3.5 Differentiation of 3T3-L1 pre-adipocytes into mature adipocytes

Adipocyte differentiation was conducted in accordance with the ATCC protocol, with slight modifications (**Fig. 2.4**). Fully confluent (100% confluent) pre-adipocytes were induced to differentiate by adding differentiation media (ADM) containing DMEM supplemented with 10% fetal bovine serum (FBS), 0.5 mM 3-isobutyl-1-methylxanthine (IBMX), 1 μ M dexamethasone (Dex) and 1 μ g/mL insulin (**Table 2.4**). Cells were incubated at 37°C in humidified air with 5% CO₂ for 72 hours. After 72 hours, (day 3) the differentiation media was replaced with adipocyte maintenance media (AMM1) (**Table 2.4**) containing DMEM, 10% FBS and 1 μ g/mL insulin, and incubated for two days. Thereafter (day 5), adipocytes were maintained in DMEM and 10% FBS media (AMM2) (**Table 2.4**) until they were fully differentiated (Day 7) (confirmed by observation of 80% or more lipid droplets under the inverted light microscope).

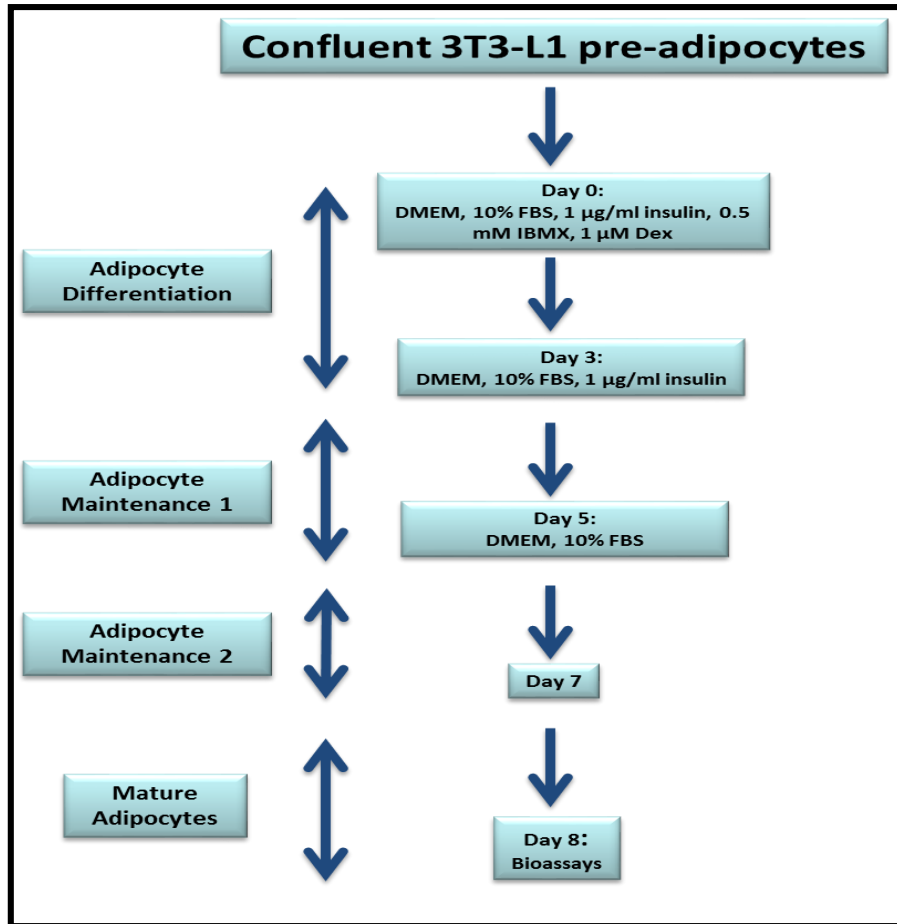


Figure 2.4 Protocol for chemical induction of pre-adipocytes into mature adipocytes.

Table 2.4 Media formulations used for adipocyte differentiation and maintenance.

Media	Formulation
Adipocyte differentiation media (ADM)	DMEM, 10% Fetal Bovine Serum (FBS), 0.5 mM 3-isobutyl-1-methylxanthine (IBMX), 1 µM dexamethasone and 1 µg/mL insulin
Adipocyte maintenance media (AMM1)	DMEM, 10% FBS and 1 µg/mL insulin
Adipocyte maintenance media (AMM2)	DMEM and 10% FBS

2.3.6 Extract preparation and treatments

2.3.6.1 Acute treatment

The liquid-liquid fractions or the CCC fractions were each prepared fresh in 10% DMSO to yield a stock concentration of 100 mg/mL. This was followed by preparation of a 1 mg/mL stock in 8.3 g/L DMEM media without phenol red, and supplemented with 3.7 g/L sodium bicarbonate (NaHCO_3), 0.1% bovine serum albumin (BSA) and either 4.5 g/L or 8 mM D-Glucose (depending on the assay to be conducted). The liquid-liquid or CCC fractions were then diluted to 100 $\mu\text{g/mL}$ from the 1 mg/mL stock using the same DMEM media (without phenol red) as above, and filter sterilized using a 0.22 μm pore-size Millex-GP Polyethersulfone (PES) membrane syringe filter before subsequent dilutions (50, 10 and 1 $\mu\text{g/mL}$) were prepared. Isoproterenol (10 μM), a β -adrenergic agonist with lipolytic activity (Ranjit et al., 2011), and mangiferin (0.01 μM), a major phenolic compound in *Cyclopia* species with anti-obesity activity (Subash-babu and Alshatwi, 2015), were used as positive controls. Differentiated adipocytes (day 7) were treated with the liquid-liquid or CCC fractions for 24 hours, followed by experimental assays on day 8. The final concentration of DMSO added to the cells was less than 0.01%, and therefore 0.01% (v/v) DMSO was used as a vehicle control (Sengupta et al., 2011). As organic extracts are insoluble in water, DMSO was used as a solubilizing agent.

2.3.6.2 Chronic treatment

For chronic treatment, CCC fractions were prepared as described above (**Section 2.2.6.1**) in ADM, AMM1 and AMM2 media (**Section 2.3.5** and **Table 2.3**), and cells were treated with these extract supplemented media, daily during differentiation (from day 0 to day 7). On day 7, cells were treated with extracts prepared in DMEM without phenol red as described in **Section 2.3.6.1**, followed by experimental assays on day 8. Chronic treatment was conducted to assess the ability of the CCC fractions to inhibit adipogenesis.

2.3.7 *In vitro* bioassays

2.3.7.1 Oil Red O Assay

After treatment with the aqueous and organic fractions of the 40% methanol extracts or the CCC fractions, intracellular lipid content was assessed using Oil Red O (ORO) staining. ORO is a hydrophobic dye that stains and quantifies neutral intracellular lipids (Ramirez-Zacarias et al., 1992). After treatment, cells were washed with pre-warmed DPBS, fixed with 10% (v/v) neutral buffered formalin for 15 minutes at room temperature, and rinsed twice with DPBS. This was followed by staining with 0.7% (v/v) ORO working solution (prepared by diluting a 1% stock (w/v in 100% isopropanol) with distilled water) for 30 minutes. After incubation, the staining solution was removed and cells were washed three times with sterile water to remove unbound dye. Images of the cells were taken using the NIS elements software with a Nikon Eclipse Ti inverted microscope (Nikon, Kanagawa, Japan) at 20 × magnification. The amount of lipid accumulated in cells was quantified by eluting the dye retained in the cells with 200 µl of 100% isopropanol and measuring optical density (OD) at 570 nm using a BioTek® ELx800 plate reader equipped with Gen 5® software for data acquisition (BioTek Instruments Inc., Winooski, VT, USA).

Lipid content was normalized to cell density as described by Sanderson et al. (2014). Briefly, after extraction of the ORO staining solution with isopropanol, cells were washed with 70% (v/v) ethanol, and 400 µL of 0.5% (v/v) crystal violet (CV) solution (prepared by diluting a 1% (w/v) stock with distilled water), was added to the cells and incubated for 5 minutes. After incubation, the CV dye was removed, cells were washed three times with DPBS and allowed to dry completely. Cell density was quantified by eluting the CV dye retained in the cells with 70% (v/v) ethanol and measuring optical density (OD) at 570 nm using a BioTek® ELx800 plate reader equipped with Gen 5® software for data acquisition. The ORO/CV values were calculated and expressed as a percentage relative to the vehicle control.

2.3.7.2 Intracellular triglycerides

Intracellular triglycerides (TGs) were quantified to assess the effect of the CCC fractions on lipid accumulation during adipogenesis. After treatment in 24 well plates, cells were washed and scraped into DPBS, pooling three replicates, and centrifuged at $800 \times g$ for 5 minutes at 4°C , to collect the cells. Thereafter, cells were resuspended in 5% (v/v) Triton X100 and transferred to a 2 mL Eppendorf tube containing a stainless steel bead. The cells were lysed and homogenized for two minutes at 25 Hz using a Tissue lyser (Qiagen, Hilden, Germany). Intracellular TGs were quantified using a TG quantification colorimetric/fluorometric kit (Biovision, Milpitas, CA, USA) according to the manufacturer's instructions. TG samples were prepared by heating the cell homogenates at 100°C for 5 minutes, then cooling at room temperature. The heating and cooling was repeated one more time in order to solubilize all TGs. Subsequently, samples were centrifuged for 2 minutes at $16\ 100 \times g$ (Centrifuge 5415R, Eppendorf, Westbury, NY, USA) to remove insoluble material, and the supernatants were transferred into new 1.5 mL Eppendorf tubes.

Standards were prepared from a TG stock (1 mM) supplied with the kit and further diluted to 0, 2, 4, 6, 8 and 10 nM concentrations, in duplicate (0 nM was used as a background control). Ten-fold diluted samples and standards were transferred to a clear 96 well assay plate, and 2 μL of lipase enzyme was added to each well followed by incubation for 20 minutes at room temperature, in order to convert TG into glycerol and free fatty acids. Samples (without lipase) were included as controls for all samples analyzed. Fifty microliters of a reaction mix containing 2 μL TG enzyme mix, 2 μL TG probe and 46 μL TG assay buffer (scaled up depending on number of samples analyzed), was added to each well (samples and the standards), and incubated for 60 minutes at room temperature, protected from light. TG content was measured using a colorimetric plate reader (BioTek® plate reader ELx800 and the Gen 5 software) at 570 nm. TG concentration was calculated from the standard curve taking into account sample dilution and volume as indicated in the formula below and represented as mM concentration.

$$\text{TG concentration} = \frac{\text{Amount of TG from the standard (nmol)} \times \text{Sample dilution factor}}{\text{Sample volume added into the reaction well } (\mu\text{l})}$$

2.3.7.3 Glycerol Release Assay

The effect of the CCC fractions on glycerol releases, a marker of lipolysis, was assessed using the free glycerol colorimetric/fluorometric assay Kit (Biovision, Milpitas, CA, USA) according to the manufacturer's instructions. Briefly, after 24 hour treatment, 200 μL of the cell culture supernatant was transferred into a clear 96 well plate and stored at -20°C until further analysis.

A standard curve was prepared by pipetting duplicate volumes of 0, 2, 4, 6, 8, and 10 μL of a 1 mM glycerol standard into a clear 96 well plate and the volumes were adjusted to 50 μL using glycerol assay buffer. Fifty microliters of the undiluted culture supernatant were added to the 96 well plate and a reaction mix containing 2 μL glycerol enzyme mix, 2 μL glycerol probe and 46 μL glycerol assay buffer (scaled up depending on number of samples analyzed) was added to the sample and standard wells. The plate was incubated for 30 minutes at room temperature, protected from light. During the incubation, glycerol is enzymatically oxidized to a product that reacts with the probe to generate a colour. After incubation, absorbance was measured at 570 nm using the BioTek® plate reader ELx800 and the Gen 5 software. The glycerol concentration was calculated from the standard curve taking into account sample volume as indicated in the formula below and represented as a percentage relative to the vehicle control at 100%.

$$\text{Glycerol concentration} = \frac{\text{Glycerol amount from the standard (nmol)}}{\text{Sample volume (before dilution) added into the reaction well } (\mu\text{l})}$$

2.3.7.4 The 3-[4, 5-Dimethylthiazol-2-yl]-2, 5 diphenyltetrazolium bromide Assay

A method for assessing mitochondrial dehydrogenase activity, using 3-[4, 5-Dimethylthiazol-2-yl]-2, 5 diphenyltetrazolium bromide (MTT) was adapted from Mosmann

(1983). The MTT assay is a colorimetric based assay, in which MTT is reduced by mitochondrial dehydrogenase, thus producing a purple formazan product (Mosmann, 1983; Weyermann et al., 2005). After cells were treated as described previously (**Section 2.3.6.1**), the media was aspirated and replaced with 200 μ L of fresh media. Fifty microliters of 2 mg/mL MTT solution (prepared in DPBS) was added to each well and the cells were incubated at 37°C in humidified air with 5% CO₂ for one hour. The cell supernatant was aspirated and 200 μ L of 100% DMSO and 25 μ L of Sorenson's glycine Buffer (0.1 M glycine and 0.1 M NaCl, pH 10.5) added, and the plate was gently shaken to dissolve the formazan product. Absorbance was measured at 570 nm using the BioTek® plate reader ELx800 and the Gen 5 software. The absorbance values were used to quantify the MTT content and results were expressed as a percentage relative to the control at 100%.

2.3.7.5 The adenosine-5'-triphosphate (ATP) activity Assay

Cells seeded and differentiated in 96 well plates (white walled luminescence plates) were treated as described previously, and the ATP content was quantified using the ViaLight™ Plus cell proliferation and cytotoxicity assay kit (Lonza, Basel, Switzerland) according to the manufacturer's instructions, with minor modifications. Briefly, cells were lysed by adding 50 μ L of lysis reagent to each well of a 96 well plate and incubating for at least 15 minutes at room temperature. Thereafter, 100 μ L of the ATP monitoring reagent plus was added to the cell lysate, and the reaction was incubated for 2 minutes at room temperature in order to generate a luminescence signal. After incubation, luminescence was measured with a luminometer (BioTek® plate reader FLx800) and Gen 5 Software. The ATP content was expressed as a percentage relative to the control at 100%.

2.3.7.6 Propidium iodide staining

The effect of plant extracts on propidium iodide staining, a marker of cellular necrosis, was assessed. Briefly, following 24 hour treatment of mature adipocytes in 96 well, black walled cell culture plates, the cells were washed with warm DPBS, followed by incubation with 1 μ g/mL of propidium iodide (prepared in DPBS) for 15 minutes at 37°C in humidified

air containing 5% CO₂. After incubation, cells were washed with warm DBPS and resuspended in DPBS. Thereafter, fluorescence was measured at ex/em 540/608 nm using the BioTek® FLx800 plate reader and the Gen 5 software.

2.4 *In vivo* study

2.4.1 Overview of study

The anti-obesity potential of the most bioactive fraction from *in vitro* screening, was assessed *in vivo*, using Lepr^{db/db} mice and their heterozygous controls (Lepr^{db/+} mice). Six to seven week old female mice, comprising 24 obese (Lepr^{db/db}) and 24 lean controls (Lepr^{db/+} mice) were divided into six groups (n = 8) and treated with either vehicle control (1% DMSO prepared in distilled water) or two concentrations of the organic fraction of *C. intermedia* (70.5 and 351.5 mg/kg prepared in 1% DMSO), daily by oral gavage for 28 days. The experimental outline is shown in **Fig. 2.4**. Body weight, fasting plasma glucose and, food and water consumption were measured weekly. On day 27 of treatment, the oral glucose tolerance test (OGTT) was performed on 16 hours fasted mice, followed by blood collection and tissue harvesting (liver, subcutaneous, gonadal and brown adipose fat depots) for gene expression analysis on day 28.

2.4.2 Ethical consideration

Ethical approval for the animal work was granted by the Research Ethics Committee: Animal Care and Use of the University of Stellenbosch (protocol number: SU-ACUM13-00028) and the ethics committee of the South African Medical Research Council (protocol number: ECRA 10/13), **Addendum 1**. The study was performed in accordance with the principles and guidelines of the South African Medical Research Council Ethics for Medical Research: use of animals in research and training, and the South African National Standard (SANS 10386: 2008) for the Care and Use of Animals for Scientific Purpose.

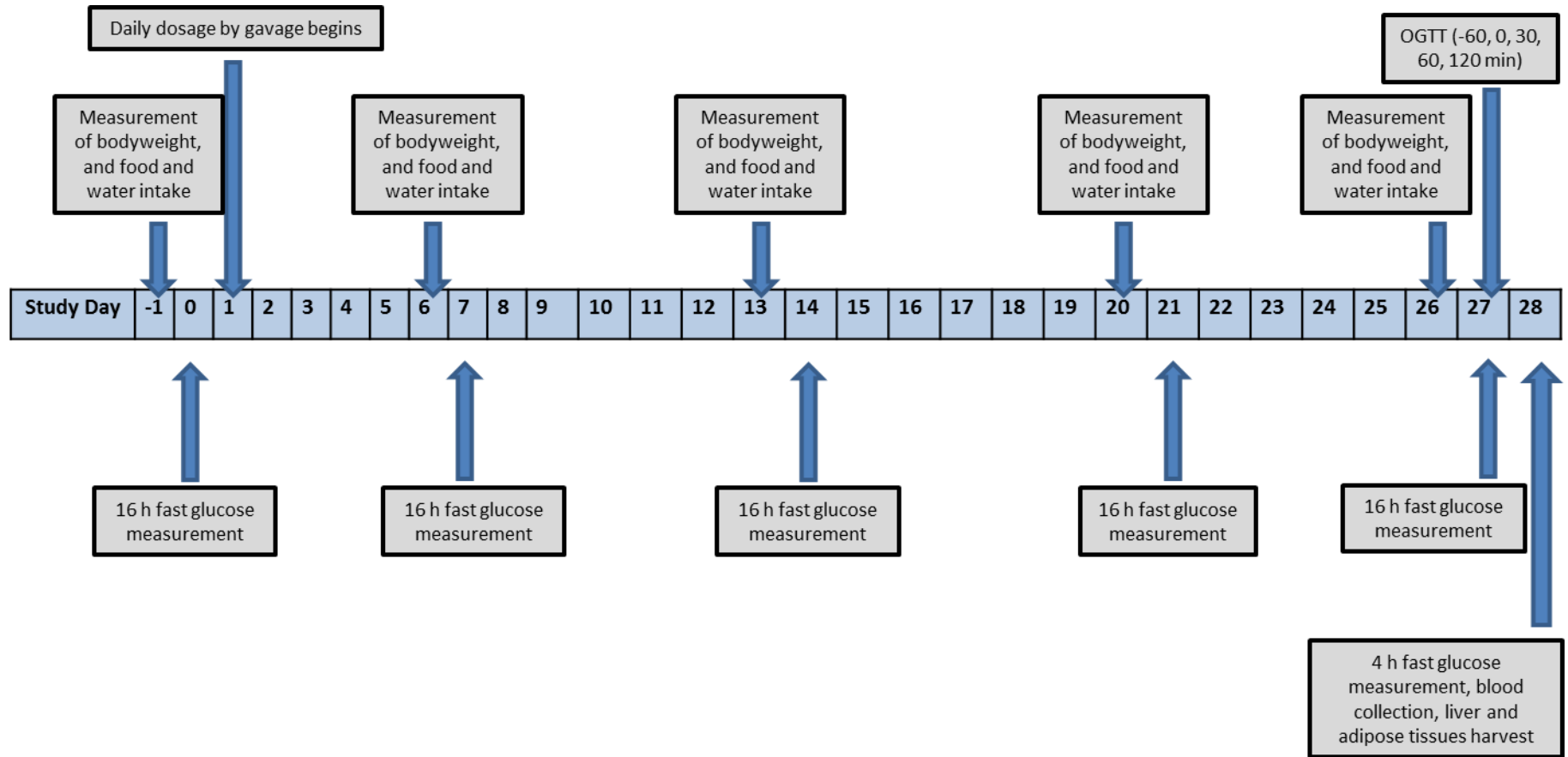


Figure 2.5 Overview of animal experimental procedure. Adapted and modified from Jackson laboratory standard protocol for Type 2 diabetes mellitus. www.jax.org/jaxservices/invivo-type2diabetes

2.4.3 Animal monitoring and housing

All procedures were carried out at the Primate Unit and Delft Animal Centre (PUDAC) of the South African Medical Research Council (Tygerberg, South Africa). Female C57BL/KsJ-*Lepr*^{db/db} mice (*Lepr*^{db/db} mice) and their heterozygous lean controls, C57BL/KsJ- *Lepr*^{db/+} mice (*Lepr*^{db/+} mice) were maintained according to standard operating procedures of PUDAC. Animals were housed (up to 10 mice per cage) under controlled environmental conditions in a temperature regulated room of 24 - 26°C and ± 55% humidity with a 12-hour light/dark cycle and ventilation of 15 - 20 air changes per hour. The mice were allowed access to a normal standard laboratory diet and water, *ad libitum*. Animals were transferred to individual cages when they were six to seven weeks of age (phenotypic differences between groups) for experimentation.

2.4.4 Experimental design

The animals were divided into 6 groups as illustrated in **Table 2.5** to ensure similar baseline fasting plasma glucose and body weight values between groups.

Table 2.5 Treatment groups for the mice.

Groups (n = 8)	Treatment	Treatment Route	Treatment Schedule	Treatment duration
Group 1 <i>Lepr</i> ^{db/+} (lean) control mice	1% DMSO vehicle	Oral gavage	Daily	28 days
Group 2 <i>Lepr</i> ^{db/+} (lean) treated mice	70.5 mg/kg - organic <i>C. intermedia</i> fraction	Oral gavage	Daily	28 days
Group 3 <i>Lepr</i> ^{db/+} (lean) treated mice	351.5 mg/kg - organic <i>C. intermedia</i> fraction	Oral gavage	Daily	28 days
Group 4 <i>Lepr</i> ^{db/db} (obese) control mice	1% DMSO vehicle	Oral gavage	Daily	28 days
Group 5 <i>Lepr</i> ^{db/db} (obese) treated mice	70.5 mg/kg - organic <i>C. intermedia</i> fraction	Oral gavage	Daily	28 days
Group 6 <i>Lepr</i> ^{db/db} (obese) treated mice	351.5 mg/kg - organic <i>C. intermedia</i> fraction	Oral gavage	Daily	28 days

2.4.5 Preparation of dosage treatment and administration of treatment

The two concentrations (70.5 and 351.5 mg/kg) of the organic fraction of *C. intermedia* were extrapolated to 11.43 mg/kg and 57.15 mg/kg daily intake in humans respectively, calculated based on body surface area dose translation from humans to mice (Reagan-Shaw et al., 2007). Due to the insolubility of the organic fraction of *C. intermedia* in aqueous solvents, DMSO at a final concentration of 1% was used to solubilize the fraction and sonication was used to aid with the solubility. Treatments were prepared daily and administered by oral gavage. Animals were monitored during and after gavage for any signs of discomfort.

2.4.6 Body weight and fasting plasma glucose

Body weight of mice were monitored once a week using a calibrated scale. The total weight gain and the percentage weight increase were determined at the end of the study. For the assessment of fasting plasma glucose, the mice were fasted for 16 hours or 4 hours (with only access to drinking water, *ad libitum*) before glucose measurement. The second drop of blood was collected from the tip of the tail by tail prick and glucose concentration was determined using a calibrated glucometer (OneTouch Select®, LifeScan Inc., Milipitas, CA, USA).

2.4.7 Food and water intake monitoring

Food and water intake was monitored weekly during the treatment period. The amount of food falling inside the cages was taken into consideration.

Estimated water consumption (mL) per week, was calculated as follows:

Water intake per week (mL) = water (mL) given at the beginning of the week - water remaining in the water bottle (mL) at last day of the week,

Estimated food consumption (g) per week was calculated as follows:

Food intake per week (g) = food (g) given at the beginning of the week - food (g) remaining in the cage at last day of the week.

2.4.8 Oral glucose tolerance test (OGTT)

The OGTT was performed after a 16 hour overnight fast, on day 27 of the study period. Mice were gavaged with plant material (**Section 2.4.4**), one hour later, glucose (Sigma-Aldrich, St Louis, MO, USA), dissolved in distilled water to a final concentration of 2 g/kg was administered via oral gavage (0.2 - 0.5 mL depending on body weight) to the mice and glucose concentrations were measured by tail prick immediately ($t = 0$) and after 30, 60, and 120 minutes as described in **Section 2.4.6**.

2.4.9 Blood collection and tissue harvesting

After 4 hour fasting, mice were anaesthetized by inhaling 98% oxygen and 2% fluothane (AstraZeneca Pharmaceuticals, Johannesburg, South Africa) and the paddle reflex non-response was used to confirm anaesthesia. A mid-line abdominal incision was made and blood was collected from the abdominal aorta and transferred to a serum separating tube (SST). Serum was separated by centrifugation at $3\ 220 \times g$ (5810R, Eppendorf, Hamburg, Germany) for 15 minutes at 4°C and serum aliquots stored at -80°C until analysis. Liver, subcutaneous white adipose tissue (sWAT), gonadal white adipose tissue (gWAT) and the interscapular brown adipose tissue (iBAT) (Lim et al., 2012) were harvested and stored in RNA $later$. Tissues in RNA $later$ were stored at -20°C until analysis.

2.4.10 Fasting insulin

Serum insulin was assessed by insulin radioimmunoassay using the Linco Kit, according to the manufacturer's instructions (Microsep RI-13K, Billerica, MA, USA). Standards, quality controls and samples were prepared in duplicate. Two hundred microliters of assay buffer was added to borosilicate tubes followed by 100 μ L of serum samples. One hundred microliters of 125 I-insulin was then added to standards and samples. Thereafter, 100 μ L of mouse insulin antibody was added to all the tubes. Tubes were vortexed, covered and incubated overnight (20 - 24 hour) at 4°C. The following day, 1 mL of precipitating reagent was added, the tubes vortexed and incubated for 20 minutes at 4°C. Samples were centrifuged at 4°C for 30 minutes at $4\ 000 \times g$ (5810R, Eppendorf). The supernatant was aspirated and the visible pellet

remaining in tube was counted using a gamma counter (Perkin-Elmer Wizard 1470 automatic gamma counter, Monza, Italy), and the results were expressed in ng/mL.

2.5 Gene expression analysis by quantitative real time PCR

Quantitative real-time polymerase chain reaction (qRT-PCR) was used to assess the effect of plant extracts on the expression of genes involved in lipid, glucose and energy metabolism.

2.5.1 RNA extraction

For extraction of total RNA from 3T3-L1 adipocytes, cells were seeded and treated in 6 well plates for 24 hours (as described in **Section 2.3.6.1**) and washed with warm DPBS. Thereafter approximately 300 μ L per well of QIAzol lysis reagent (Qiagen) was added to wells and incubated for 5 minutes, cells were scraped from the plates, and triplicate wells were pooled into a sterile 2 mL Eppendorf tube containing a stainless steel bead (Qiagen). Cells were homogenized using the Qiagen Tissue Lyser for 2 minutes at 25 Hz and centrifuged at $15\,000 \times g$ (5415R, Eppendorf) for 10 minutes at 4°C. For extraction of RNA from tissue, approximately 100 mg of tissue was weighed using sterile conditions, and transferred to a 2 mL Eppendorf tube containing 1 mL of QIAzol lysis reagent and a stainless steel bead (Qiagen), followed by homogenization at 25 Hz for 2 minutes. Homogenization was repeated three times, and samples were homogenized by altering between 2 minutes in the Tissue Lyser using pre-cooled adapters and 1 minute on ice. Homogenized tissues were centrifuged at $15\,000 \times g$ for 10 minutes, at 4°C. Hereafter, RNA was extracted from cells and tissue using the same protocol as described below.

The supernatant was carefully removed and transferred to a new 1.5 mL Eppendorf tube, 200 μ L of chloroform was added and mixed for 3 minutes, followed by centrifugation for 15 minutes at $15\,000 \times g$ and 4°C. The upper aqueous phase containing the RNA was transferred to a new 1.5 mL Eppendorf tube (this was done carefully without disturbing the white interphase or organic phase) and 0.5 mL of isopropanol was added and samples were incubated overnight at -20°C to precipitate

the RNA. The following day, samples were centrifuged at $15\ 000 \times g$ for 30 minutes at 4°C to pellet the RNA. The supernatant was discarded and the RNA pellet was washed with 70% (v/v) ethanol and centrifuged at $15\ 000 \times g$ for 15 minutes at 4°C . This wash step was repeated twice. After the final wash, ethanol was drained from the Eppendorf tubes by blotting on a paper towel, and the pellet was allowed to air dry. After drying, the RNA pellet was redissolved in 100 μL of RNase-free water, mixed by pipetting up and down several times, and then incubated at 55°C for 10 minutes in order to aid resuspension.

RNA was cleaned up using the RNeasy Mini kit (Qiagen) according to the manufacturer's instructions. To each RNA sample, 350 μL of the RTL buffer was added and mixed by pipetting up and down several times, followed by the addition of 250 μL of 100% ethanol and mixing as described above. The samples were transferred to RNeasy spin columns in 2 mL collection tubes. Spin columns were centrifuged at $13\ 000 \times g$ for 15 seconds at room temperature to bind the RNA and the flow through was discarded. A volume of 500 μL RPE buffer (diluted with 4 volumes of 96 - 100% ethanol) was added to the column and centrifuged at $13\ 000 \times g$ for 15 seconds at room temperature, and the flow through was discarded. This step was repeated and thereafter the column was transferred to a new 2 mL collection tube and centrifuged for 1 minute at $16\ 100 \times g$, to completely dry the column. The RNA was eluted by placing the column into a clean 1.5 mL collection tube, 50 μL of RNase-free water was added directly to the column membrane, and centrifuged for 1 minute at $13\ 000 \times g$. The elution step was repeated in a separate 1.5 mL collection tube to ensure that all the RNA in the membrane column was retrieved. The eluted RNA samples were placed on ice for RNA quantification.

2.5.2 RNA quantification

RNA concentration and purity was assessed by measuring the absorbance at 260 nm (A_{260}) and 280 nm (A_{280}) using a Nanodrop ND 1000 spectrophotometer (Nanodrop Technologies, Wilmington, DE, USA). Nucleic acids (RNA and DNA) absorb at 260 nm whereas proteins and other contaminants absorb at A_{280} . Thus, the ratio of 260 nm to 280 nm ($A_{260/280}$) is used to assess the purity of a sample. For RNA, a ratio of 2 is

generally accepted as being sufficiently pure. The ratio of 260 nm to 230 nm ($A_{260/230}$) is used as a secondary measure of purity and indicates contaminants that absorb at or near 230 nm. The spectrophotometer was initialized by pipetting 2 μ L RNase-free water onto the pedestal of the spectrophotometer, and 2 μ L RNase-free water was used as blank. Thereafter, 2 μ L of each RNA sample was pipetted onto the pedestal and the absorbance measured. Each sample was read in duplicate and the average of the two readings was used.

2.5.3 RNA integrity

High quality RNA (RNA integrity) is essential for accurate gene expression results (Fliege and Pfaffl, 2006). The Agilent 2100 bioanalyser is an analytical tool used to assess the quality and integrity of RNA. Compared to traditional methods, such as gel electrophoresis, the Agilent Bioanalyser is more sensitive, convenient and uses small quantities of RNA samples (Fliege and Pfaffl, 2006). The integrity of RNA is assessed by visualization of the 28S and 18S ribosomal RNA bands; a 28S:18S ratio of 2 indicates intact RNA, whereas lower ratios indicate RNA degradation. Furthermore, the software calculates the RNA Integrity number (RIN) which is based on a numbering system of 1 to 10, with 1 representing a degraded RNA and 7 - 10 RIN number representing an intact good quality RNA (Mueller et al., 2004). In this study, RNA integrity was assessed by the Centre for Proteomic and Genomic Research (CPGR), Observatory, Western Cape, South Africa, using the Agilent 2100 bioanalyser (Agilent technologies Inc.) and the Agilent RNA 6000 Nano kit.

Control RNA (100 ng/ μ L, included as an internal reference), RNA samples and the Agilent RNA Nano Ladder were heat denatured at 70°C for 2 minutes, briefly centrifuged and immediately placed on ice. After priming the chip on the chip priming station with Agilent RNA Nano gel-dye mix, 5 μ L of Agilent RNA Nano Marker was added to all wells including the RNA ladder well. One microliter of control, sample or RNA ladder was then added to respective wells. The chip was mixed on a vortex mixer for 1 minute at 2 400 \times g using a IKA vortex mixer (IKA, Staufen, Germany), and immediately loaded and analyzed on an Agilent 2100 Bioanalyser. RNA integrity was

assessed based on the RIN number and its quality assessed on an electropherogram and a gel image.

2.5.4 DNase treatment

RNA samples were treated with DNase in order to remove any contaminating genomic DNA that might be present in samples that would interfere with gene expression analysis. DNase treatment was conducted using the Turbo DNase kit (Ambion Inc., Austin, TX, USA) according to the manufacturer's instructions. Briefly, 5 μL of $10 \times$ DNase buffer and 1 μL of DNase I was added to the 20 μg of RNA to a final volume of 50 μL . Samples were mixed and incubated at 37°C for 30 minutes; whereafter another 1 μL of DNase I was added and incubated at 37°C for a further 30 minutes. The reaction was stopped by adding 5 μL of DNase inactivation reagent and mixed by placing tubes on an orbital shaker for 5 minutes at 37°C. Thereafter, the tubes were centrifuged at $10\,000 \times g$ for 1.5 minutes and the supernatant was transferred to a new 1.5 mL Eppendorf tube, carefully without disturbing the pellet. RNA concentrations were quantified using a Nanodrop ND 1000 spectrophotometer.

2.5.5 Reverse transcription

Total RNA was reverse transcribed into a single-stranded complimentary DNA (cDNA) using the High-Capacity cDNA kit (Applied Biosystems, Foster City, CA, USA), according to the manufacturer's instructions. Briefly, nuclease-free water was added to 0.4 μg (sWAT, gWAT and iBAT) or 1 μg (3T3-L1 adipocytes) of DNase treated RNA samples (prepared in duplicate) to a final volume of 10 μL and kept on ice. A reverse transcription (RT) plus reaction mix consisting of reaction buffer, dNTPs, random primers, RNase-inhibitor, reverse transcriptase and nuclease-free water was prepared, while a RT minus was prepared as above, but without reverse transcriptase (**Table 2.6**). The reactions were scaled up depending on the number of samples. Thereafter, 10 μL of plus or minus RT reaction components were added to their respective 0.2 mL tubes containing RNA samples. The tube content was mixed by pipetting, briefly centrifuged and placed in a 2720 thermal cycler (Applied Biosystems). Reactions were

incubated at 25°C for 10 minutes, 37°C for 120 minutes and 85°C for 5 seconds, to inactivate the reverse transcriptase. Nuclease-free water was used as a negative control.

Table 2.6 Components used for the reverse transcription reaction.

Component	Volume (µL)	
	Plus RT	Minus RT
0.4 µg or 1 µg DNase-treated RNA in RNase-free water	10	10
10 × RT buffer	2	2
25 × dNTPs mix	0.8	0.8
10 × random primers	2	2
RNase inhibitor	1	1
Nuclease-free water	3.2	4.2
Reverse Transcriptase (50 U/µL)	1	0
Total volume	20	20

2.5.6 Quantitative real-time PCR

Quantitative real-time PCR (qRT-PCR) is one of the most sensitive and specific techniques commonly used to study gene expression (Arya et al., 2005). In this study, TaqMan® Gene Expression Assays from Applied Biosystems were used to assess the effects of the plant extracts on the expression of genes associated with lipid, glucose and energy metabolism. The TaqMan® Gene Expression assays consist of a TaqMan® probe with a FAM™ or VIC® fluorescent reporter dye on the 5' end and a non-fluorescent quencher dye (NFQ) on the 3' end of the probe. The TaqMan® probes do not fluoresce when the reporter and quencher dyes are in close proximity, thus suppressing the reporter's fluorescence. During a PCR reaction, the *Taq* polymerase, after primer and probe binding, cleaves the probe to release the fluorescent reporter from the quencher dye, thereby allowing the detection of the reporter dye fluorescence (Arya et al., 2005). SYBR green is a non-sequence specific fluorescent dye that intercalates double-stranded DNA (dsDNA). SYBR green dye, when unbound in solution exhibits little fluorescence but emits a strong fluorescent signal when bound to a dsDNA (Arya et al., 2005). This dye can be used with any pair of primers for any target but its specificity is low due to binding to nonspecific PCR products and primer-dimers.

2.5.6.1 Assessment of genomic DNA contamination

To assess the extent of genomic DNA contamination in RNA samples, cDNA generated from the plus and minus reverse transcription reactions were both amplified with exon spanning primers for beta-actin (*ACTβ*) that would amplify both cDNA and genomic DNA. Amplification was quantified using the DNA binding dye SYBR Green. A reaction mix consisting of 12.5 μL SYBR Green master mix (Applied Biosystems), 1 μL of 10 μM *ACTβ* forward primer, 1 μL of 10 μM *ACTβ* reverse primer and water to a final volume of 24 μL was prepared (**Table 2.7**). The reaction mix was scaled up depending on the number of samples. Twenty-four microliters of reaction mix was aliquoted into the PCR plate, followed by 1 μL of undiluted cDNA (plus or minus RT reactions), or water as a no template control. The plate was sealed with adhesive film, mixed on a plate shaker (IKA) for 10 minutes and briefly centrifuged at 3 000 × *g*. The PCR reactions were conducted on the ABI 7500 Sequence Detection System Instrument (Applied Biosystems) using the Absolute Quantification (AQ) Software (SDS V1.4). The following universal cycling conditions; 50°C for 2 minutes and 95°C for 10 minutes, followed by 40 cycles of 95°C for 15 seconds and 60°C for 1 minute were used. A dissociation curve was added for secondary product detection. Data was acquired during the extension step (60°C for 1 minute). After the run, default settings for the threshold cycle (Ct) and baseline were used, and Ct values were exported to Microsoft Excel® for analysis.

Table 2.7 Reaction components for quantitative real time PCR to assess genomic DNA content.

Component	Volume (μL)	Final concentration
2 × Master Mix	12.5	1 ×
<i>ACTβ</i> Forward Primer (10 μM)	1	0.4 μM
<i>ACTβ</i> Reverse Primer (10 μM)	1	0.4 μM
Water	9.5	-
cDNA	1	20 - 50 ng ^a
Total volume	25	-

^a20 ng (sWAT, gWAT and iBAT) and 50 ng (3T3-L1 cells)

2.5.6.2 Quantitative real-time PCR for gene expression analyses

For qRT-PCR, a reaction mixture consisting of 5 μL of TaqMan® universal PCR master mix II (Applied Biosystems), 0.5 μL of pre-developed TaqMan® gene expression assays and water to a final volume of 9 μL was prepared (**Table 2.8**). The reaction mix was scaled up based on the number of samples to be analyzed. A standard curve was prepared by mixing the cDNA aliquots of all the test samples and making a ten-fold dilution series (neat to 10^{-5}). Nine microliter aliquots of the reaction mix were transferred into the wells of the PCR plate, followed by 1 μL of the standard curve dilution series, or test samples cDNA. A “no template control” (NTC) i.e. without the cDNA, was used as a negative control in all PCR reactions and all samples were analyzed in duplicate. The PCR plates were covered with adhesive film and briefly centrifuged at $3\,000 \times g$. Thereafter, plates were placed in a shaker (IKA) for 5 minutes followed by centrifugation at $3\,000 \times g$. The PCR reactions were conducted on the ABI 7500 sequence detection system instrument using universal cycling conditions as described in **Section 2.5.7**, except that the dissociation curve was omitted. Data generated on the ABI 7500 instrument was analyzed with the ABI standard quantification (AQ) software (SDS V1.4) using a Ct threshold of 0.1 and a baseline between 3 and 13 cycles. The TaqMan® gene expression assays used in this study are listed in **Table 2.9**. A panel of seven endogenous control genes (**Table 2.9**) was evaluated to determine the most stably expressed endogenous genes for normalization for each tissue (sWAT, gWAT, iBAT) or for 3T3-L1 adipocytes. NormFinder, an algorithm based tool (Andersen et al., 2004) was used to compare the seven candidate genes and identify the best or most suitable combination of two genes for each tissue or cells.

Table 2.8 Reaction components for quantitative real time PCR reactions.

Component	Volume (μL)
2 \times Master mix	5
TaqMan Gene Expression Assay	0.5
Water	3.5
cDNA (2 - 5 ng) ^a	1
Total volume	10

^a2 ng (sWAT, gWAT and iBAT) and 5 ng (3T3-L1 cells)

Table 2.9 Taqman® gene expression assays used in this study.

TaqMan gene expression assays	Assay ID
Acetyl-Coenzyme A carboxylase alpha (<i>ACACA</i>)	Mm01304257_m1
Adiponectin (<i>ADIPOQ</i>)	Mm00456425_m1
cAMP responsive element binding protein 1 (<i>CREB1</i>)	Mm00501607_m1
Carnitine palmitoyltransferase 1 alpha (<i>CPT1α</i>)	Mm01231183_m1
CCAAT/enhancer binding protein (C/EBP), alpha (<i>CEBPα</i>)	Mm00514283_s1
Citrate synthase (<i>Cs</i>)	Mm00466043_m1
Fatty acid binding protein 4 (<i>FABP4</i>)	Mm00445878_m1
Fatty acid synthase (<i>FASN</i>)	Mm00662319_m1
Fibroblast growth factor 2 (<i>FGF2</i>)	Mm01285715_m1
GATA binding protein 2 (<i>GATA2</i>)	Mm00492301_m1
Glucose-6-phosphatase, catalytic (<i>G6Pc</i>)	Mm00839363_m1
Hormone sensitive lipase (<i>LIPE/HSL</i>)	Mm00495359_m1
Insulin receptor substrate 1 (<i>IRS1</i>)	Mm01278327_m1
Lipoprotein lipase (<i>LPL</i>)	Mm00434764_m1
Peroxisome proliferator activated receptor alpha (<i>PPARα</i>)	Mm00440939_m1
Peroxisome proliferator activated receptor gamma (<i>PPARγ</i>)	Mm00440940_m1
Peroxisome proliferative activated receptor, gamma, coactivator 1 alpha (<i>PGC1α</i>)	Mm01208835_m1
Protein kinase, AMP-activated, alpha 2 catalytic subunit (<i>PRKAA2/AMPK</i>)	Mm01264789_m1
Sirtuin1 (<i>SIRT1</i>)	Mm01168521_m1
Sirtuin3 (<i>SIRT3</i>)	Mm00452131_m1
Solute carrier family 2 (facilitated glucose transporter), member 4 (<i>GLUT4</i>)	Mm01245502_m1
Stearoyl-Coenzyme A desaturase 1 (<i>SCD1</i>)	Mm00772290_m1
Sterol regulatory element binding transcription factor 1 (<i>SREBF1</i>)	Mm00550338_m1
Tumor necrosis factor (<i>TNFα</i>)	Mm00443258_m1
Uncoupling protein 1 (<i>UCP1</i>)	Mm01244861_m1
Uncoupling protein 2 (<i>UCP2</i>)	Mm00627599_m1
Uncoupling protein 3 (<i>UCP3</i>)	Mm00494077_m1
Endogenous Control Genes	
Beta-actin (<i>ACTβ</i>)	Mm02619580_g1
Beta-2 microglobulin (<i>B2M</i>)	Mm00437762_m1
Glyceraldehyde-3-phosphate dehydrogenase (<i>GAPDH</i>)	Mm99999915_g1
Heat shock protein 90 alpha (cytosolic), class B member 1 (<i>HSP90AB1</i>)	Mm00833431_g1
Hypoxanthine guanine phosphoribosyl transferase (<i>HPRT</i>)	Mm01545399_m1
Non-POU-domain-containing, octamer binding protein (<i>NONO</i>)	Mm00834875_g1
Ribosomal protein L13A (<i>RPL13A</i>)	Mm01612986_gH

2.6 Protein expression analysis

Western blot analysis was used to assess the effect of the plant extracts on PPAR γ and PPAR α protein expression in mature 3T3-L1 adipocytes.

2.6.1 Cell collection and protein extraction

Cells seeded in 6 well plates and treated as described previously (**Section 2.3.6.1**), were rinsed with warm DPBS and lysed with 400 μ L of commercial lysis buffer (Invitrogen) supplemented with 1 mM of phenyl methane sulfonyl fluoride (PMSF), and scraped from the plate surface using a cell scraper. Six replicates of a six well plate, representing a single treatment were pooled together and transferred to a 2 mL Eppendorf tube and stored at -20°C until extraction. For protein extraction, cells were thawed on ice, and a stainless bead (Qiagen) was added to the Eppendorf tube and transferred into pre-cooled Tissue lyser blocks. The cells were then homogenized using a Tissue lyser (Qiagen) at 25 Hz for 1 minute. Cells were homogenized by alternating between 1 minute in the Tissue lyser and 1 minute on ice, 5 times. The cell lysate was centrifuged at $15\ 890 \times g$ for 10 minutes at 4°C . The supernatant was carefully removed and transferred into a clean 1.5 mL Eppendorf tube. This step was done twice and thereafter the supernatant was stored at -20°C until use.

2.6.2 Quantification of protein concentration

Protein quantification was performed using the reducing agent compatible and detergent compatible (RC/DC) protein determination kit according to the manufacturer's recommendations (Bio-Rad, Hercules, CA, USA). Five microliters of BSA standards (0, 0.2, 0.5, 1, 1.4 and 2.0 mg/mL) and 5 μ L of a 1:10 dilution of each protein sample were added to wells in a 96 well assay plate, in duplicate. Twenty-five microliters of the kit's reagent A was added to each well containing the sample or BSA standards. Thereafter, 200 μ L of reagent B was added and the 96 well plate was mixed for 10 seconds using a plate shaker (IKA). Absorbance was measured at 695 nm on a BioTek® ELx800 plate reader using the Gen5 software. Protein concentration of the samples was extrapolated from the BSA standard curve.

2.6.3 Protein separation by electrophoresis

Thirty microgram of protein sample was diluted 1:1 with sample buffer (Bio-Rad) and denatured by heating at 95°C for 5 minutes. Thereafter, protein samples were loaded onto a 12% SDS-polyacrylamide gel electrophoresis (SDS-PAGE) precast gel (Bio-Rad), and 5 µL (for gel profiling) or 12 µL (for western blot analysis) of the molecular weight standard marker was also loaded onto the first well of each gel. Electrophoresis was performed at a constant voltage of 150 V until the dye reached the bottom of the gel. For protein profiling, the gel was stained with a Coomassie brilliant blue stain overnight. The following day, the gel was incubated with a destaining solution until clear bands were visible; the gel profile was captured using Bio-Rad Chemidoc image analysis (Bio-Rad).

2.6.4 Transfer of proteins to a PVDF membrane

After protein separation by electrophoresis, gels were equilibrated in 1 × transfer buffer by incubating for 5 minutes on a shaker. The polyvinylidene fluoride (PVDF) membrane and Whatman paper were carefully cut to a size of 8 cm × 6 cm. Membrane activation was performed by incubating in methanol for 15 seconds, followed by incubation in MilliQ water for 15 seconds, and 1 minute of incubation in 1 × transfer buffer. The Whatman paper, filter pads, protein gels and the activated PVDF membranes were then equilibrated in 1× transfer buffer for 20 minutes by shaking, prior to assembling the transfer sandwich. The transfer sandwich was assembled as demonstrated in **Fig. 2.6** by stacking the following in an order of negative electrode (cathode) to positive electrode (anode): fiber pad, 2 × Whatman papers, SDS-PAGE gel, PVDF membrane, 2 × Whatman papers and fiber pad in a transfer cassette. The cassette was then placed in the holding cassette with the cassette facing the corresponding colour coded electrode, black to black and red to red, and ice packs were inserted in between the cassette to maintain the cold temperature. The tank was filled with cold 1 × transfer buffer, enough to cover the cassette, and proteins were transferred for 80 minutes at 160 V at 4°C, using a magnetic stirrer.

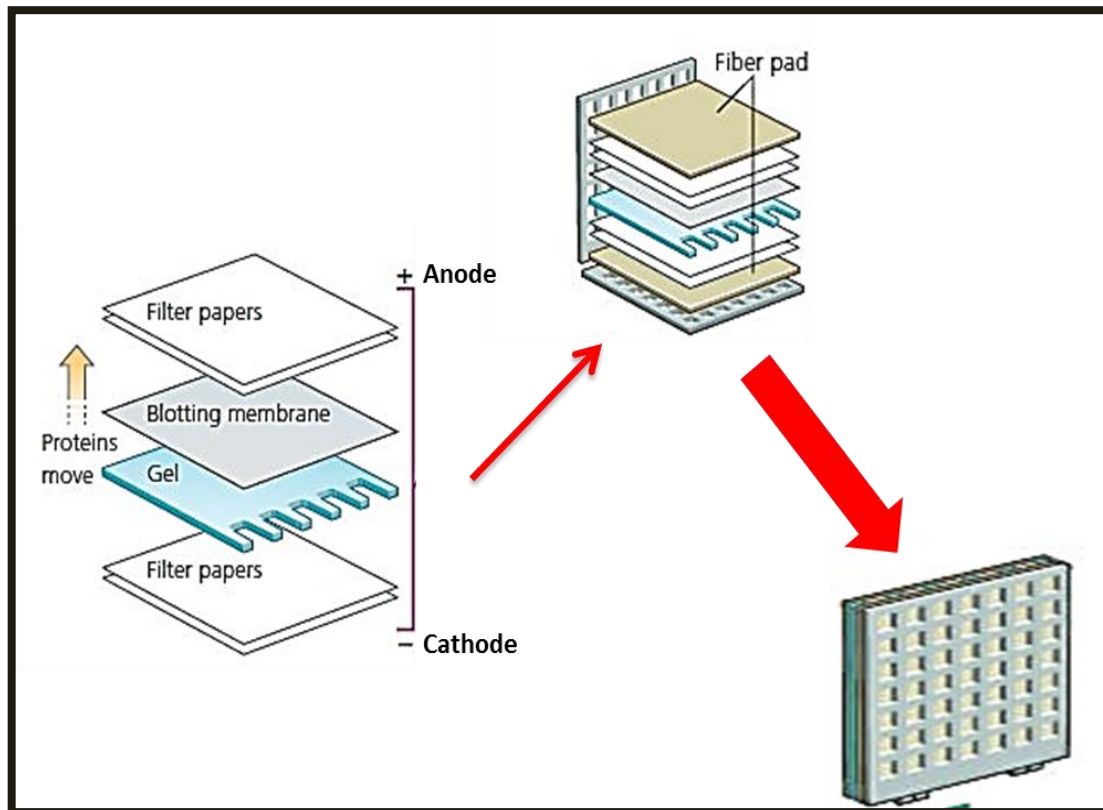


Figure 2.6 Schematic illustration of the transfer sandwich assembly used for transferring proteins from SDS-PAGE gel to a PVDF membrane.

2.6.5 Ponceau S staining

Following transfer, the PVDF membrane was stained with Ponceau S stain, to assess the efficiency of protein transfer from the SDS-PAGE gel to the membrane. The membrane was removed from the sandwich and placed in a container with the Ponceau S stain, and incubated for 5 minutes at room temperature. The staining solution was removed and the membrane was rinsed with distilled water until the background of the membrane was clear and transferred proteins were visible. To remove the staining solution, the membrane was washed with 1× Tris-buffered saline (TBS) 0.1% Tween 20 (TBST) by incubating for 10 minutes at room temperature. This was repeated three times.

2.6.6 Western Blot analyses

Following removal of the Ponceau S stain, the PVDF membrane was incubated with 5% (w/v) fat-free milk powder prepared in 1 × TBST at room temperature, with gentle

shaking for 90 minutes, in order to block non-specific protein binding. Thereafter the membrane was incubated with primary antibody (**Table 2.10**) diluted with 1 × TBST and incubated overnight at 4°C. The following day, the membrane was washed three times with 1 × TBST for 10 minutes each. This was followed by incubation with the horseradish peroxidase (HRP) labeled secondary antibody (anti-rabbit IgG) prepared in 1 × TBST with 2.5% (w/v) fat-free milk (1:4000 dilution) for 90 minutes at room temperature. The membrane was then washed with 1 × TBST, three times for 10 minutes each. A chemiluminescent substrate detection kit (Bio-Rad) was used to visualize proteins of interest. Briefly, 2 mL of chemiluminescent substrate was added to the membrane and incubated for 5 minutes. After incubation, the membrane was blotted on an absorbent paper towel to remove excess substrate. Proteins of interest were detected and quantified using the Bio-Rad Chemidoc-XRS imager and Quantity One 1-D software, respectively. Protein levels were normalized to the reference protein, Act-β (**Table 2.10**).

Table 2.10 Primary antibodies and dilutions used in Western blot detection.

Antibody	Dilution	Specificity
Peroxisome proliferator-activated receptor gamma (PPAR γ)	1:1000	Polyclonal antibody
Peroxisome proliferator-activated receptor alpha (PPAR α)	1:1000	Monoclonal antibody
Beta-actin (ACT β)	1:1000	Monoclonal antibody

2.7 Statistical analysis

Microsoft Excel® 2010 (Microsoft Office) was used for data analysis. For *in vitro* experiments, data represent three independent experiments done in three or five replicates per treatment ± standard error of the mean (SEM), and data is represented as a percentage relative to the vehicle control (0.01% DMSO set at 100%). For *in vivo* animal experiments, results are expressed as the mean ± SEM of six - eight animals per group. The sample size was determined using supporting literature (Xie et al., 2002) and a biostatistician from the South African Medical Research Council was consulted to validate the sample size. Arbitrary units (relative mRNA expression) was used to represent data for qRT-PCR, while fold change was used to represent data for Western blot analysis. Statistical analysis was conducted using GraphPad Prism®

version 5.04 (GraphPad Software Inc., La Jolla, USA). Differences between multiple groups were analyzed by one-way ANOVA and the Tukey post hoc test. A Student's t-test (unpaired) was used to analyze differences between two groups. A P-value of < 0.05 was considered to be statistically significant. Area under the curve values were calculated using the trapezoidal method with Graphpad Prism version 5.04.

CHAPTER 3

RESULTS 1

The polyphenolic characterization of plant extracts, and results for *in vitro* and *in vivo* experiments to select the most bioactive fraction for HPLC fractionation are presented in this chapter. Part of this work has been published in the South African Journal of Botany for publication entitled “A polyphenol-enriched fraction of *Cyclopia intermedia* decreases lipid content in 3T3-L1 adipocytes and reduces body weight gain of obese diabetic mice” with myself (Babalwa Jack) as the first author.

The results in this section describes the assessment of the anti-obesity potential of polyphenol-enriched extracts and fractions of three commercially relevant *Cyclopia* spp. using *in vitro* and *in vivo* model systems. Aqueous methanol extracts of *C. subternata*, *C. intermedia* and *C. maculata* were separated into aqueous and organic fractions for further enrichment of the phenolic content of the organic fraction, and their polyphenolic composition was determined by LC-MS/MS and quantitative HPLC-DAD. The effect of the aqueous and organic fractions on lipid content and cytotoxicity in 3T3-L1 adipocytes were determined using the ORO assay, and the MTT and ATP assays, respectively. The anti-obesity and anti-diabetic activity of the most bioactive fraction was assessed in obese $Lepr^{db/db}$ mice. The effect of the most bioactive fraction on the expression of genes relevant to lipid, glucose and energy metabolism in 3T3-L1 adipocytes, and in subcutaneous (sWAT) and gonadal (gWAT) white adipose tissue, and interscapular brown adipose tissue (iBAT) of obese $Lepr^{db/db}$ mice and their heterozygous lean controls ($Lepr^{db/+}$ mice) was measured using qRT-PCR. The effect of the extract on protein expression of PPAR γ and PPAR α was assessed using western blot analysis.

3.1 Phenolic Analysis

LC-MS/MS analysis and quantitative HPLC-DAD were used to identify and quantify phenolic compounds in the 40% aqueous methanol extracts, and aqueous and organic fractions of *C. subternata*, *C. intermedia* and *C. maculata*. Their phenolic profiles and content varied according to species and type of fraction (**Figs. 3.1 - 3.3** and **Table 3.1**). Considering the aqueous methanol extracts, the xanthenes, mangiferin and isomangiferin, were present in the highest levels for *C. maculata*, followed by *C. subternata* and *C. intermedia*, while the benzophenones were predominant in the *C. subternata* extract followed by *C. intermedia* and *C. maculata*. The dihydrochalcones, 3-hydroxy-phloretin-3',5'-di-C-hexoside and phloretin-3',5'-di-C- β -D-glucoside were not detected in *C. intermedia*, whereas two flavanones, neoponcirin and an eriodictyol derivative were only detected in *C. intermedia*. The eriodictyol derivative was tentatively identified as eriodictyol-O-deoxyhexoside-O-hexoside based on the mass spectrum and UV-Vis spectrum for eriocitrin (eriodictyol-7-O-rutinoside) as published in Schulze et al. (2014).

The major compounds identified in the *C. subternata* extract was mangiferin (2.680 g/100g extract), followed by iriflophenone-3-C- β -D-glucoside-4-O- β -D-glucoside, phloretin-3',5'-di-C- β -D-glucoside, scolymoside, hesperidin, iriflophenone-3-C- β -D-glucoside, isomangiferin and eriocitrin (**Fig. 3.1** and **Table 3.1**). These compounds were all present at > 0.5 g/100g extract. Vicenin-2, 3-Hydroxy-phloretin-3',5'-di-C-hexoside and maclurin-3-C- β -glucoside were present at low concentrations < 0.18 g/100g extract, moreover luteolin was identified in trace amounts. Liquid-liquid fractionation resulted in the aqueous fraction of *C. subternata* retaining iriflophenone-3-C- β -D-glucoside-4-O- β -D-glucoside as the major compound, whilst the other compounds were present as minor constituents (**Fig. 3.1** and **Table 3.1**). The organic fraction of *C. subternata* retained all the major compounds present in the extract, resulting in a fraction enriched in all the compounds, except iriflophenone-3-C- β -D-glucoside-4-O- β -D-glucoside compared to the original extract (**Fig.3.1** and **Table 3.1**).

The major compounds present in the *C. intermedia* extract was mangiferin (2.181 g/100g extract), followed by neoponcirin, hesperidin, iriflophenone-3-C- β -D-glucoside-4-O- β -D-glucoside, isomangiferin and eriodictyol-O-deoxyhexoside-O-hexoside. The

individual compounds were present at > 0.5 g/100g extract. Iriflophenone-3-C- β -D-glucoside and vicenin-2 were present at a concentration < 0.18 g/100g extract, whereas maclurin-3-C- β -glucoside was not detected (**Fig. 3.2** and **Table 3.1**). Once again as for *C. subternata*, the concentration of iriflophenone-3-C- β -D-glucoside-4-O- β -D-glucoside in the extract and fractions did not differ notably. Iriflophenone-3-C- β -D-glucoside and neoponcirin were not detected in the aqueous fraction of *C. intermedia* whereas the other compounds were present at low concentrations relative to the extract and its organic fraction (**Fig. 3.2** and **Table 3.1**). The organic fraction was enriched in mangiferin, neoponcirin, hesperidin, isomangiferin, eriodictyol-O-deoxyhexoside-O-hexoside, iriflophenone-3-C- β -D-glucoside and vicenin-2 compared to the original extract (**Fig. 3.2** and **Table 3.1**).

Similar to the *C. subternata* and *C. intermedia* extracts, mangiferin (5.366 g/100g extract) was the major compound in the *C. maculata* extract (**Fig. 3.3** and **Table 3.1**) and present in a substantially higher quantity than in the other extracts. Two of the benzophenones (maclurin-3-C- β -glucoside and iriflophenone-3-C- β -D-glucoside-4-O- β -D-glucoside) were not detected. Hesperidin and isomangiferin were also more prevalent in the *C. maculata* extract than the other extracts. Other compounds including vicenin-2, scolymoside, luteolin, iriflophenone-3-C- β -D-glucoside, 3-hydroxy-phloretin-3',5'-di-C-hexoside, eriocitrin and phloretin-3',5'-di-C- β -D-glucoside were detected as relatively minor compounds (< 0.5 g/100g extract). The aqueous fraction of *C. maculata* contained only low concentrations (< 0.1 g/100g extract) of the compounds present in the extract or, in the case of luteolin and phloretin-3',5'-di-C- β -D-glucoside were not detected in this fraction (**Fig. 3.3** and **Table 1**). The organic fraction of *C. maculata* was enriched in all compounds, with mangiferin, isomangiferin, hesperidin, eriocitrin, iriflophenone-3-C- β -D-glucoside and 3-hydroxy-phloretin-3',5'-di-C-hexoside present at concentrations ranging from 14.847 g/100g extract for mangiferin to 0.711 g/100g extract for the dihydrochalcone. Vicenin-2, scolymoside, luteolin and phloretin-3',5'-di-C- β -D-glucoside were detected as minor compounds present at concentrations < 0.5 g/100g extract (**Fig. 3.3** and **Table 3.1**).

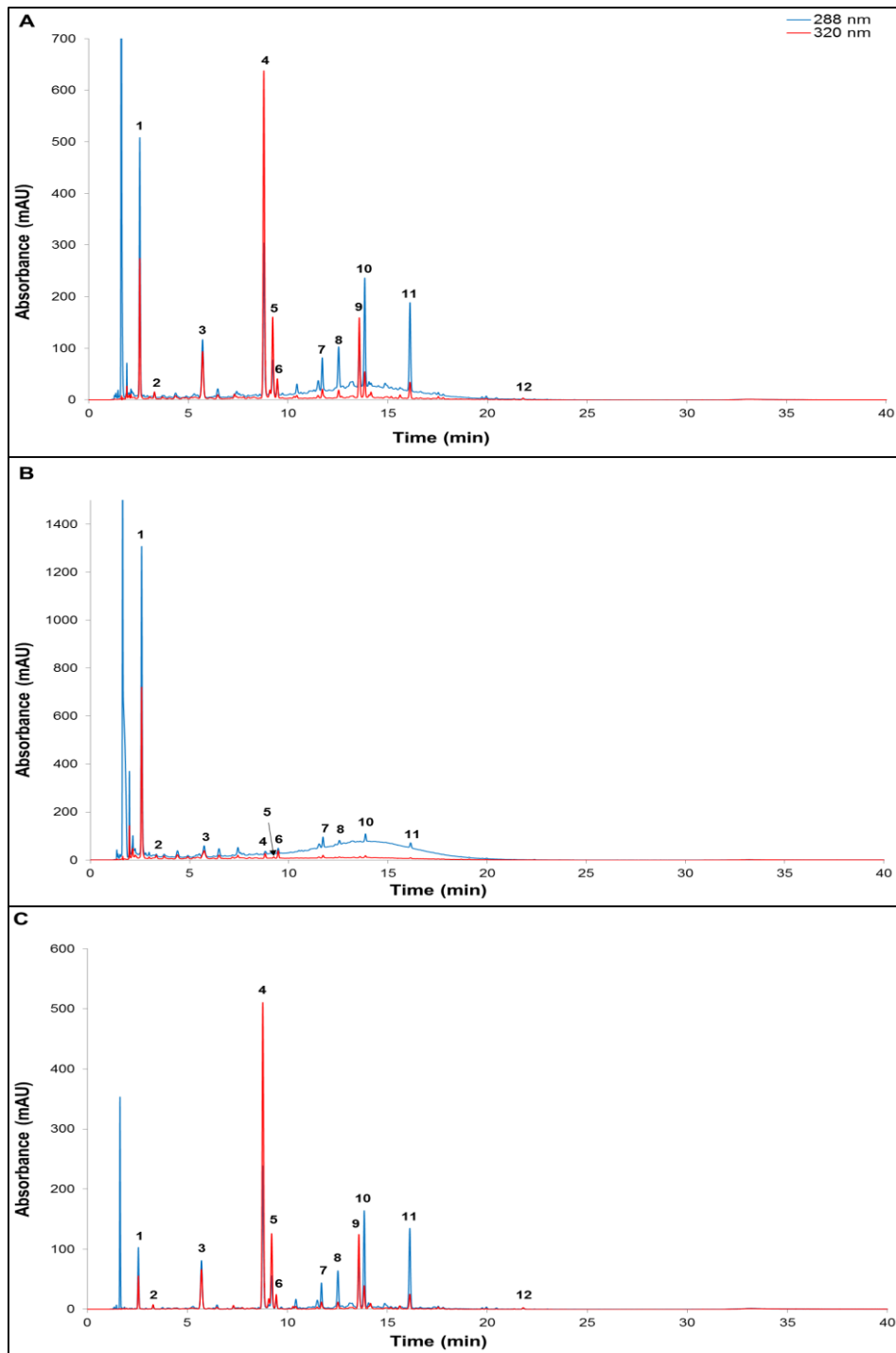


Figure 3.1 Phenolic profile of *C. subternata*. The phenolic profile showing the major phenolic compounds of a 40% aqueous methanol (40% MeOH) extract of unfermented *C. subternata* (A), aqueous fraction of 40% MeOH extract of *C. subternata* (B) and organic fraction of 40% methanol extract of *C. subternata* (C). The first peak (not numbered) represents ascorbic acid, which was added to prevent oxidation. Peak 1: Iriflophenone-3-C-β-D-glucoside-4-O-β-D-glucoside; 2: Maclurin-3-C-β-glucoside; 3: Iriflophenone-3-C-β-D-glucoside; 4: Mangiferin; 5: Isomangiferin; 6: Vicenin-2; 7: 3-Hydroxy-phloretin-3',5'-di-C-hexoside; 8: Eriocitrin; 9: Scolymoside; 10: Phloretin-3',5'-di-C-β-D-glucoside; 11: Hesperidin; 12: Luteolin.

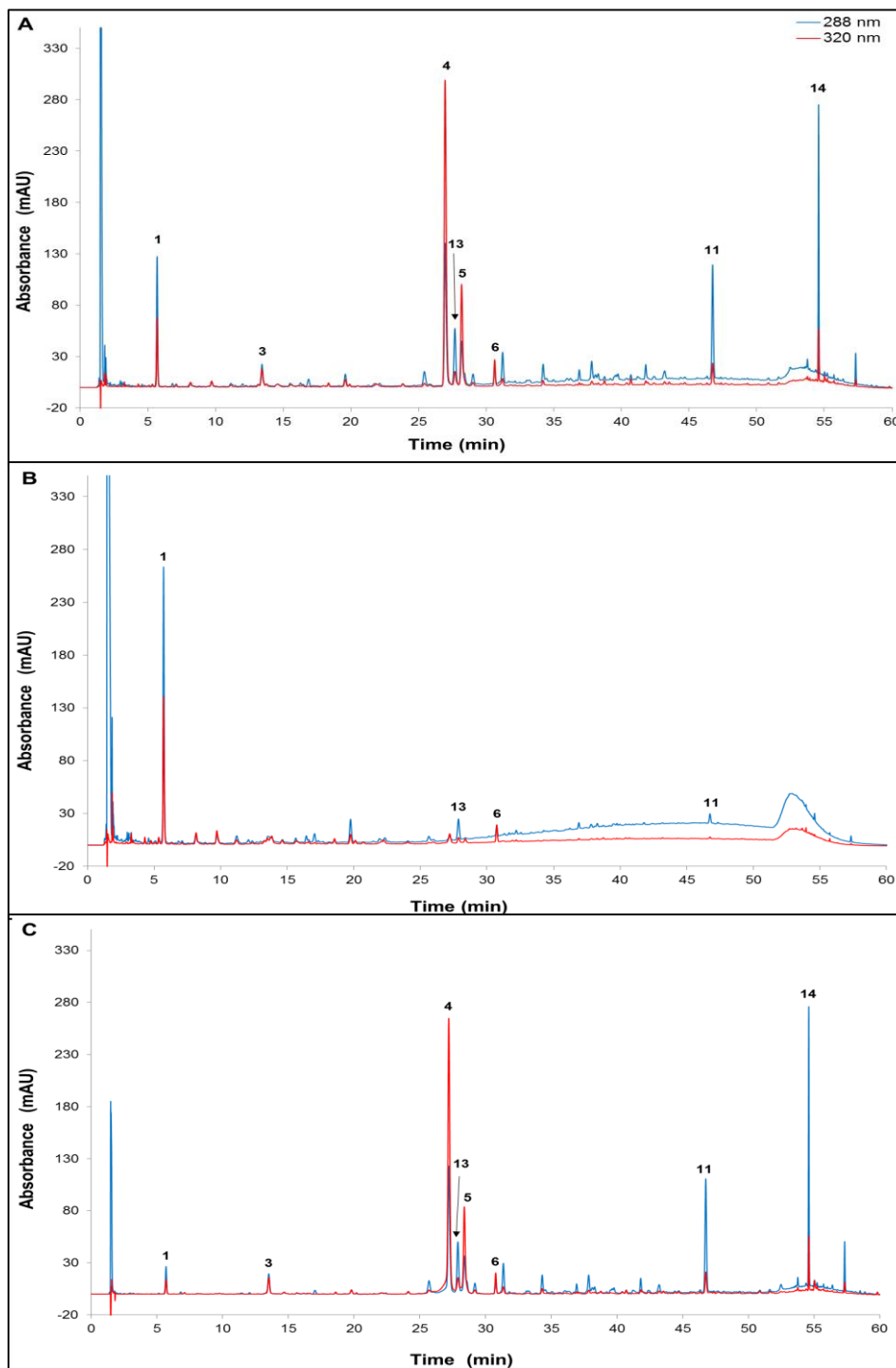


Figure 3.2 Phenolic profile of *C. intermedia*. The phenolic profile showing the major phenolic compounds of a 40% aqueous methanol (40% MeOH) extract of unfermented *C. intermedia* (A), aqueous fraction of 40% MeOH extract of *C. intermedia* (B) and organic fraction of 40% methanol extract of *C. intermedia* (C). The first peak (not numbered) represents ascorbic acid, which was added to prevent oxidation. Peak 1: Iriflophenone-3-C- β -D-glucoside-4-O- β -D-glucoside; 3: Iriflophenone-3-C- β -D-glucoside; 4: Mangiferin; 5: Isomangiferin; 6: Vicenin-2; 11: Hesperidin; 13: Eriodictyol-O-deoxyhexoside-O-hexoside; 14: Neoponcirin.

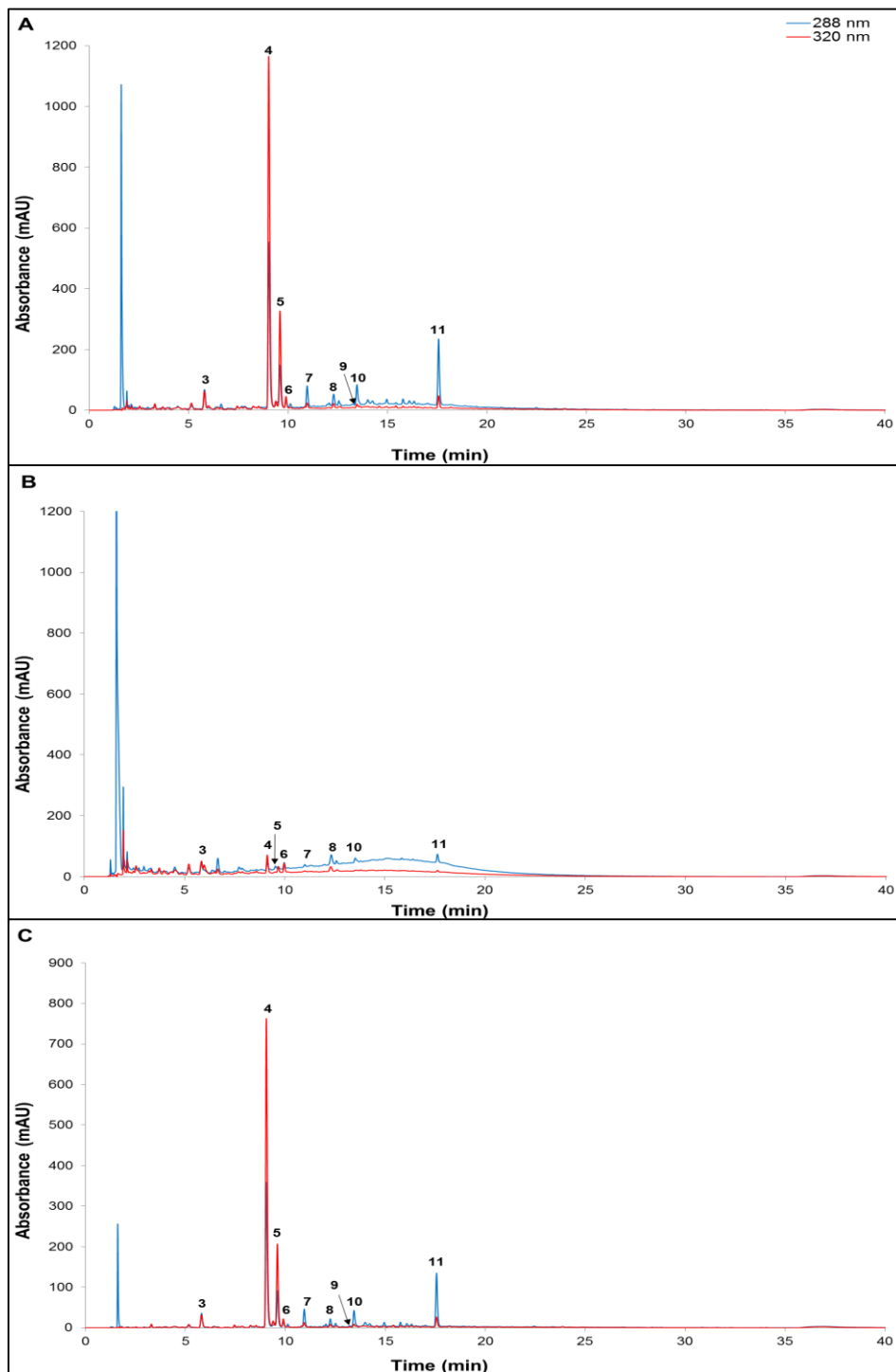


Figure 3.3 Phenolic profile of *C. maculata*. The phenolic profile showing the major phenolic compounds of a 40% aqueous methanol (40% MeOH) extract of unfermented *C. maculata* (A), aqueous fraction of 40% MeOH extract of *C. maculata* (B) and organic fraction of 40% methanol extract of *C. maculata* (C). The first peak (not numbered) represents ascorbic acid, which was added to prevent oxidation. Peak **3**: Iriflophenone-3-C- β -D-glucoside; **4**: Mangiferin; **5**: Isomangiferin; **6**: Vicenin-2; **7**: 3-Hydroxy-phloretin-3',5'-di-C-hexoside; **8**: Eriocitrin; **9**: Scolymoside; **10**: Phloretin-3',5'-di-C- β -D-glucoside; **11**: Hesperidin.

Table 3.1 Quantification of major phenolic compounds in 40% aqueous methanol extracts of *C. subternata*, *C. intermedia* and *C. maculata* and their aqueous and organic fractions by HPLC-DAD.

Compound ^a	Methanol Extract		Aqueous Fraction		Organic Fraction	
	g/100 g ^c	factor ^d	g/100 g ^c	factor ^d	g/100 g ^c	factor ^d
<i>C. subternata</i>						
Iriflophenone-3-C-β-D-glucoside-4-O-β-D-glucoside (1)	2.395	1.000	2.467	1.030	2.333	0.974
Maclurin-3-C-β-glucoside (2)	0.081	1.000	0.036	0.444	0.216	2.667
Iriflophenone-3-C-β-D-glucoside (3)	0.744	1.000	0.136	0.183	2.538	3.411
Mangiferin (4)	2.680	1.000	0.030	0.011	10.344	3.860
Isomangiferin (5)	0.566	1.000	0.008	0.014	2.182	3.855
Vicenin-2 (6)	0.159	1.000	0.055	0.346	0.476	2.994
3-Hydroxy-phloretin-3',5'-di-C-hexoside (7)	0.177	1.000	0.050	0.282	0.601	3.395
Eriocitrin (8)	0.538	1.000	0.038	0.071	1.884	3.502
Scolymoside (9)	1.067	1.000	0.016	0.015	4.137	3.877
Phloretin-3',5'-di-C-β-D-glucoside (10)	1.468	1.000	0.085	0.058	5.365	3.655
Hesperidin (11)	0.985	1.000	0.044	0.045	3.709	3.765
<i>C. intermedia</i>						
Iriflophenone-3-C-β-D-glucoside-4-O-β-D-glucoside (1)	0.783	1.000	0.794	1.014	0.752	0.960
Iriflophenone-3-C-β-D-glucoside (3)	0.172	1.000	nd ^e	nd ^e	0.611	3.552
Mangiferin (4)	2.181	1.000	0.044	0.020	8.635	3.959
Isomangiferin (5)	0.607	1.000	0.017	0.028	2.336	3.848
Vicenin-2 (6)	0.163	1.000	0.047	0.288	0.511	3.135
Hesperidin (11)	0.822	1.000	0.031	0.038	3.267	1.000
Eriodictyol-O-deoxyhexoside-O-hexoside ^b (13)	0.553	1.000	0.090	0.163	2.000	3.617
Neoponcirin (14)	0.893	1.000	nd ^e	nd ^e	3.629	4.064
<i>C. maculata</i>						
Iriflophenone-3-C-β-D-glucoside (3)	0.385	1.000	0.098	0.255	0.969	2.517
Mangiferin (4)	5.366	1.000	0.098	0.018	14.847	2.767
Isomangiferin (5)	1.277	1.000	0.033	0.026	3.750	2.937
Vicenin-2 (6)	0.175	1.000	0.060	0.343	0.413	2.360
3-Hydroxy-phloretin-3',5'-di-C-hexoside (7)	0.288	1.000	0.073	0.253	0.711	2.469
Eriocitrin (8)	0.419	1.000	0.034	0.081	1.246	2.974
Scolymoside (9)	0.036	1.000	0.009	0.25	0.065	1.806
Phloretin-3',5'-di-C-β-D-glucoside (10)	0.158	1.000	nd ^e	nd ^e	0.489	3.095
Hesperidin (11)	1.315	1.000	0.065	0.049	3.826	2.910
Luteolin (12)	0.025	1.000	nd ^e	nd ^e	0.111	4.440

^a Peak number on HPLC chromatogram in brackets^b Expressed as eriocitrin equivalent^c g/100 g refers to the amount of the compound (g) in 100 g extract or fraction^d Concentration factor refers to the amount of a compound in the extract/fraction divided by the amount of the compound in the extract^e nd - polyphenols not detected or only present in trace amounts

3.2 *In vitro* experiments to identify the most bioactive *Cyclopia* fraction

3.2.1 Validation of the *in vitro* cell model

Although 3T3-L1 adipocytes are commonly used as an *in vitro* model for obesity studies, experiments to validate the model, and to test the effect of DMSO on lipid content were performed. Lipid content in undifferentiated 3T3-L1 pre-adipocytes, differentiated 3T3-L1 adipocytes and differentiated 3T3-L1 adipocytes treated with 0.01% of DMSO for 24 hours was assessed using the ORO assay. Microscopic images of ORO stained cells showed increased lipid content (indicated by high intensity of ORO staining) in differentiated adipocytes (**Fig. 3.4B**) compared to undifferentiated pre-adipocytes (**Fig. 3.4A**). DMSO treatment did not affect lipid content in differentiated adipocytes (**Fig. 3.4C**). Quantification of these results showed that lipid content was increased 1.7-fold after differentiation ($100 \pm 2.6\%$ in undifferentiated pre-adipocytes vs. $174.2 \pm 14.7\%$ in differentiated adipocytes, $P < 0.001$) (**Fig. 3.5D**). No significant difference was observed between differentiated adipocytes and DMSO treated adipocytes, suggesting that the concentration of DMSO used in this study had no effect on lipid content. These results show that differentiation of 3T3-L1 pre-adipocytes into mature adipocytes using IBMX, Dex and insulin, significantly induces excessive lipid accumulation. Moreover, the use of DMSO as a vehicle did not affect lipid content.

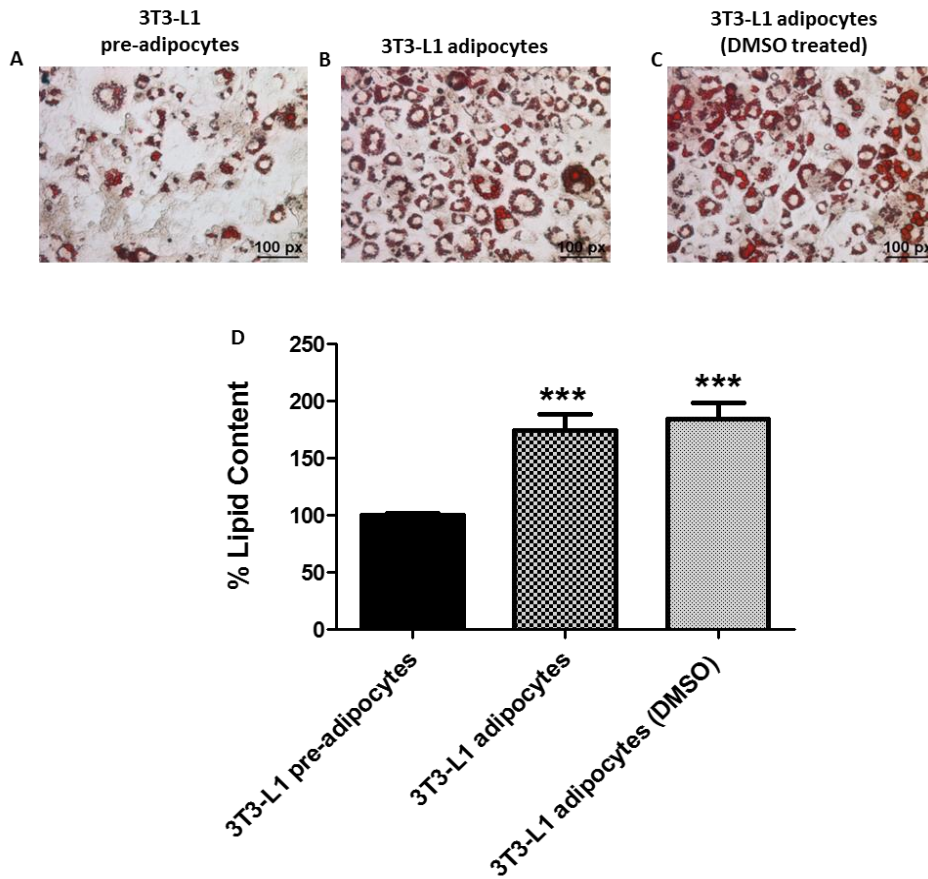


Figure 3.4 Validation of the *in vitro* cell model. Oil Red O staining of undifferentiated 3T3-L1 pre-adipocytes (A), differentiated 3T3-L1 adipocytes (B) and differentiated 3T3-L1 adipocytes treated with DMSO (C). The quantification of these results are shown in D. Pre-adipocytes were cultured to confluence in DMEM media and induced to differentiate into matured adipocytes in media containing IBMX, Dex and insulin, or left in DMEM media for undifferentiated adipocytes. DMSO treated adipocytes were incubated with 0.01% DMSO for 24 hours after differentiation. Results are expressed as the mean of three independent experiments with eight repeats per treatment, and expressed relative to undifferentiated adipocytes at 100% \pm SEM; ***P < 0.001.

3.2.2 The aqueous fraction of *C. maculata* and organic fraction of *C. intermedia* dose-dependently decrease lipid content in differentiated 3T3-L1 adipocytes

The ability of the aqueous and organic fractions of *C. subternata*, *C. intermedia* and *C. maculata* to decrease lipid content was determined by treating differentiated 3T3-L1 adipocytes with various concentrations of these fractions (1, 10, 50 and 100 μ g/mL) for 24 hours, and lipid content assessed using the ORO assay. The concentrations used in this study were in the concentration range that decreased lipid accumulation without inducing effects on cytotoxicity in 3T3-L1 pre-adipocytes differentiated in the presence

of aqueous hot water extracts of *C. subternata* and *C. maculata* (Dudhia et al., 2013). The effect on lipid content varied according to *Cyclopia* spp. and type of fraction. For example, the aqueous fraction of *C. subternata* decreased lipid content in differentiated 3T3-L1 adipocytes by $16.1 \pm 3.1\%$ ($P < 0.05$) and $25 \pm 2.3\%$ ($P < 0.001$) at 50 and 100 $\mu\text{g/mL}$, respectively, compared to untreated adipocytes, whereas no effect was observed for the organic *C. subternata* fraction (**Fig. 3.5**). In contrast, the organic fraction of *C. intermedia* decreased lipid content by $12.5 \pm 4.5\%$, $16.8 \pm 4.8\%$ ($P < 0.01$), $22.8 \pm 3.7\%$ ($P < 0.001$) and $26.7 \pm 2.6\%$ ($P < 0.001$) at 1, 10, 50 and 100 $\mu\text{g/mL}$, respectively, whereas its aqueous fraction did not significantly decrease lipid content compared to control adipocytes (**Fig. 3.6**). Similarly to *C. subternata*, the aqueous fraction of *C. maculata* reduced lipid content by $16 \pm 4.3\%$ ($P < 0.05$), $17.8 \pm 3.8\%$ ($P < 0.01$), $20.9 \pm 3.0\%$ ($P < 0.001$) and $28.7 \pm 3.3\%$ ($P < 0.001$) at 1, 10, 50 and 100 $\mu\text{g/mL}$, respectively, whereas the organic fraction of *C. maculata* did not have any significant effect on lipid content compared to untreated adipocytes (**Fig. 3.7**). Isoproterenol, used as a positive control (10 μM), decreased lipid content ($P < 0.001$) compared to control adipocytes.

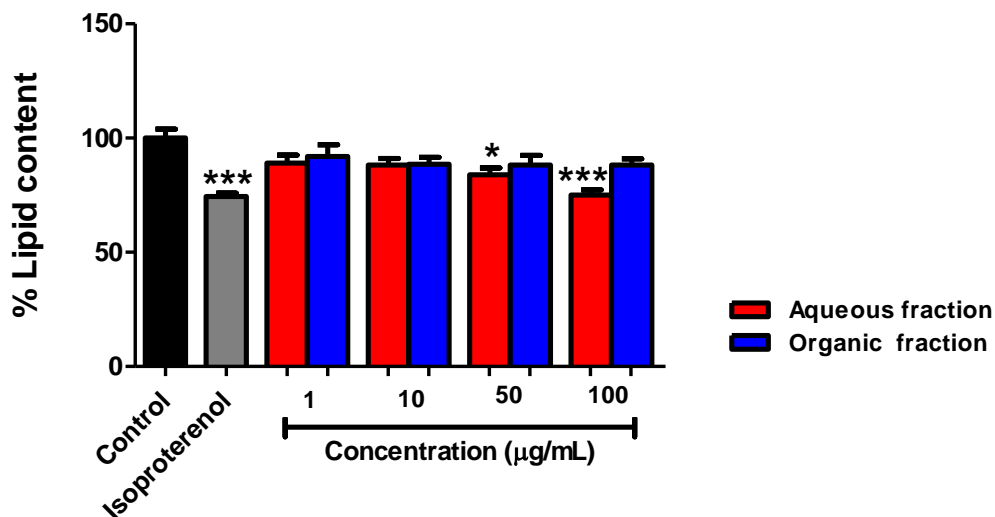


Figure 3.5 The effect of aqueous and organic fractions, prepared from 40% aqueous methanol extract of *C. subternata* on lipid content in 3T3-L1 adipocytes. Differentiated 3T3-L1 adipocytes were exposed to aqueous and organic fractions of *C. subternata* at various concentrations, vehicle control or isoproterenol for 24 hours. Lipid content was quantified using Oil Red O staining. Results are expressed as a percentage relative to the vehicle control (set at 100%), and are shown as the mean \pm SEM for three independent experiments, each performed in triplicate. Significance is depicted as * $P < 0.05$, and *** $P < 0.001$ vs. vehicle control.

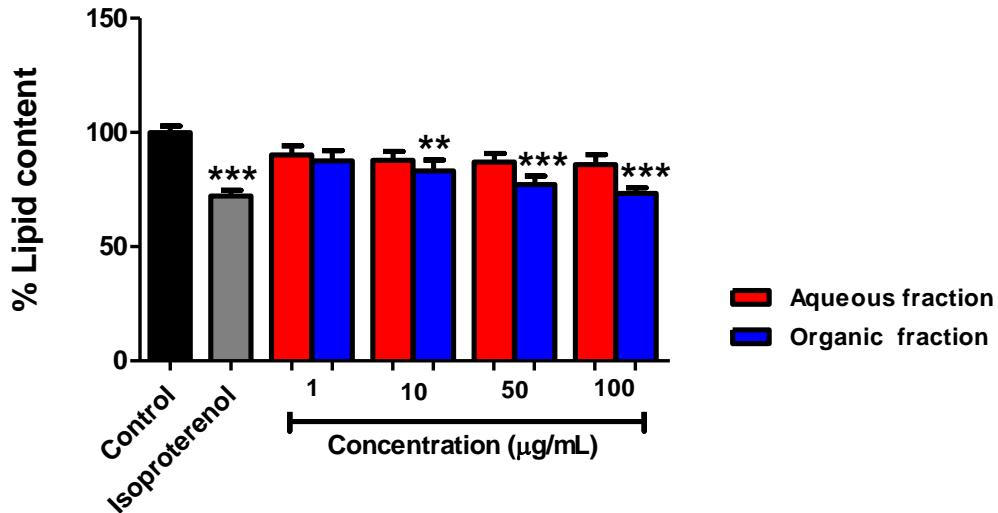


Figure 3.6 The effect of aqueous and organic fractions, prepared from 40% aqueous methanol extract of *C. intermedia* on lipid content in 3T3-L1 adipocytes. Differentiated 3T3-L1 adipocytes were exposed to aqueous and organic fractions of *C. intermedia* at various concentrations, vehicle control or isoproterenol for 24 hours. Lipid content was quantified using Oil Red O staining. Results are expressed as a percentage relative to the vehicle control (set at 100%), and are shown as the mean \pm SEM for three independent experiments, each performed in triplicate. Significance is depicted as **P < 0.01 and ***P < 0.001 vs. vehicle control.

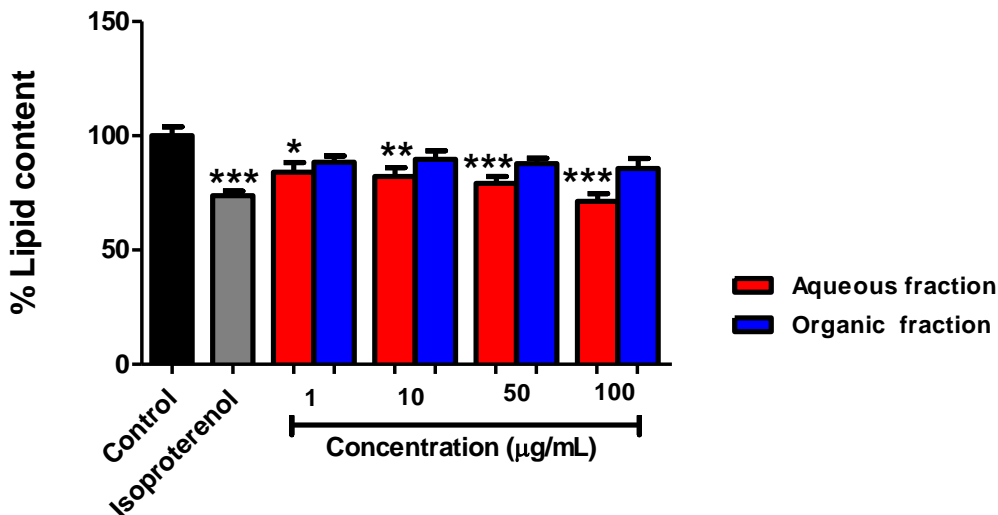


Figure 3.7 The effect of aqueous and organic fractions, prepared from 40% aqueous methanol extract of *C. maculata* on lipid content in 3T3-L1 adipocytes. Differentiated 3T3-L1 adipocytes were exposed to aqueous and organic fractions of *C. maculata* at various concentrations, vehicle control or isoproterenol for 24 hours. Lipid content was quantified using Oil Red O staining. Results are expressed as a percentage relative to the vehicle control (set at 100%), and are shown as the mean \pm SEM for three independent experiments, each performed in triplicate. Significance is depicted as *P < 0.05, **P < 0.01 and ***P < 0.001 vs. vehicle control.

3.2.3 Cytotoxicity varies according to *Cyclopia* species and their fractions

The effect of the aqueous and organic fractions of *C. subternata*, *C. intermedia* and *C. maculata* on cell viability was assessed by treating 3T3-L1 adipocytes with various concentrations of these fractions (1, 10, 50 and 100 µg/mL) for 24 hours and determining mitochondrial dehydrogenase activity (MTT assay) (**Figs. 3.8, 3.10 and 3.12**) and intracellular ATP content (**Figs. 3.9, 3.11 and 3.13**). As observed for lipid content, varying effects on cell viability were observed, depending on species and type of fraction, as well as the assay type. Both the aqueous and organic fractions of *C. subternata* increased MTT activity, at all concentrations tested ($P < 0.05$ and $P < 0.001$) (**Fig. 3.8**). However, no significant effect on ATP content was observed when cells were treated with the aqueous and organic fractions of *C. subternata* (**Fig. 3.9**).

The aqueous fraction of *C. intermedia* increased mitochondrial dehydrogenase activity by $24.7 \pm 3.9\%$ ($P < 0.001$) and $22.4 \pm 4.6\%$ ($P < 0.001$) at 50 and 100 µg/mL (**Fig. 3.10**), respectively, and the organic fraction of *C. intermedia* increased mitochondrial dehydrogenase activity by $30.4 \pm 4.0\%$ ($P < 0.001$) and $21.8 \pm 5.3\%$ ($P < 0.001$) at 50 and 100 µg/mL (**Fig. 3.10**), respectively. In contrast, treatment with 50 and 100 µg/mL of the aqueous fraction of *C. intermedia* decreased intracellular ATP content by $21.0 \pm 6.3\%$ ($P < 0.01$) and $19.3 \pm 3.8\%$ ($P < 0.05$) (**Fig. 3.11**), respectively, whereas the organic fraction had no significant effect on intracellular ATP content (**Fig. 3.11**). Treatment with the aqueous and organic fractions of *C. maculata* had no significant effect on cell viability as measured using the MTT assay (**Fig. 3.12**). In contrast, intracellular ATP content was decreased by $18.1 \pm 5.4\%$ ($P < 0.05$), $23.7 \pm 6.4\%$ ($P < 0.01$), $30.3 \pm 6.9\%$ ($P < 0.001$) and $33.8 \pm 5.8\%$ ($P < 0.001$) after treatment with 1, 10, 50 and 100 µg/mL of the organic *C. maculata* (**Fig. 3.13**), respectively, whereas its aqueous fraction had no significant effect on intracellular ATP content compared to control adipocytes (**Fig. 3.13**). Isoproterenol (10 µM) had no significant effect on the MTT activity and ATP content compared to control adipocytes.

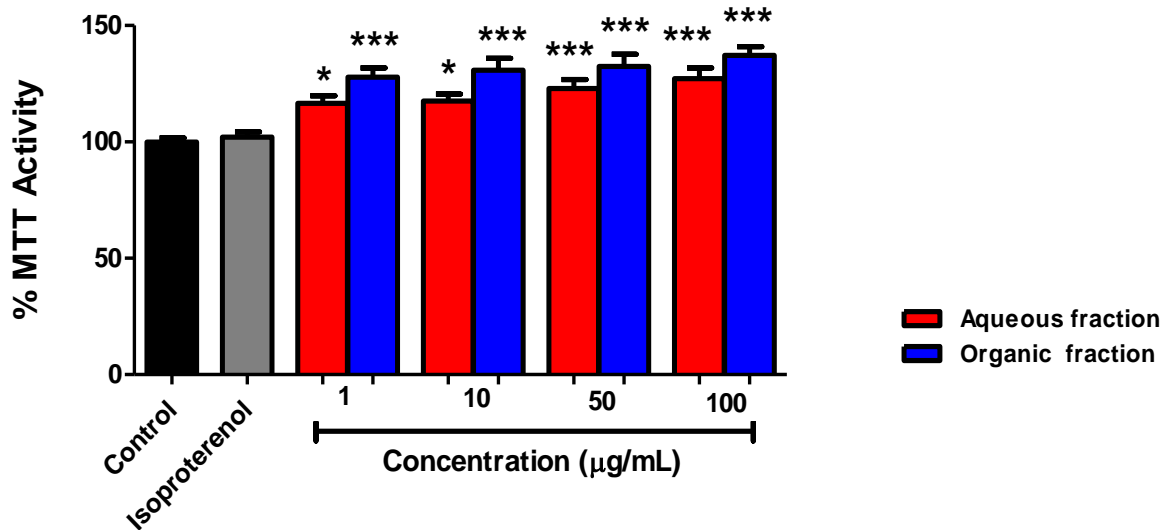


Figure 3.8 The effect of aqueous and organic fractions, prepared from 40% aqueous methanol extract of *C. subternata* on mitochondrial dehydrogenase activity in 3T3-L1 adipocytes. Differentiated 3T3-L1 adipocytes were exposed to the aqueous and organic fractions of *C. subternata* at various concentrations, vehicle control or isoproterenol for 24 hours. Mitochondrial dehydrogenase was measured using the MTT assay. Results are expressed as a percentage relative to the vehicle control (set at 100%) and are shown as mean \pm SEM for three independent experiments, each performed in triplicate. Significance is depicted as * $P < 0.05$ and *** $P < 0.001$ vs. vehicle control.

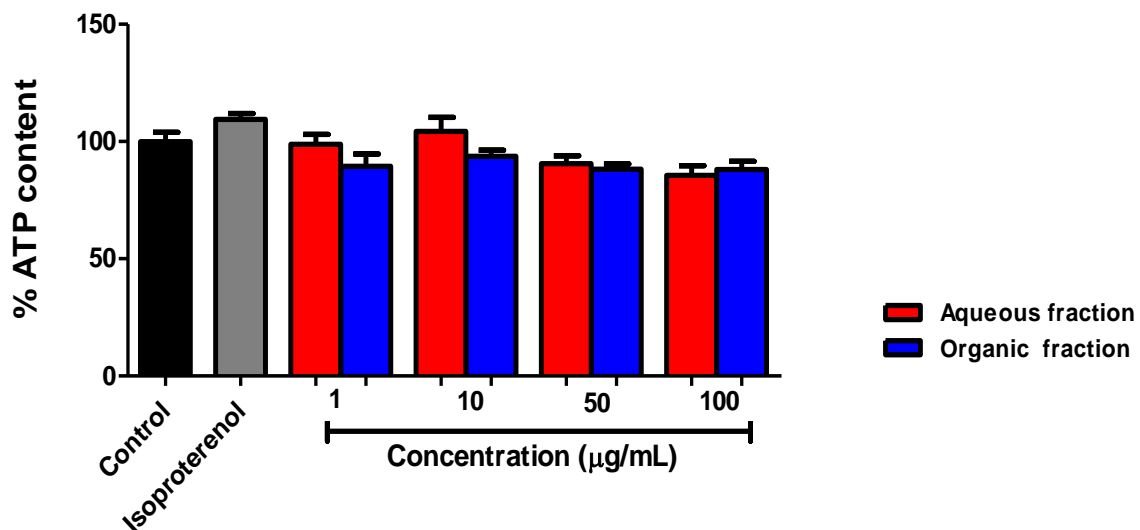


Figure 3.9 The effect of aqueous and organic fractions, prepared from 40% aqueous methanol extract of *C. subternata* on ATP content in 3T3-L1 adipocytes. Differentiated 3T3-L1 adipocytes were exposed to the aqueous and organic fractions of *C. subternata* at various concentrations, vehicle control or isoproterenol for 24 hours. Intracellular ATP content was assessed using an ATP luminescence kit. Results are expressed as a percentage relative to the vehicle control (set at 100%) and are shown as mean \pm SEM for three independent experiments, each performed in triplicate.

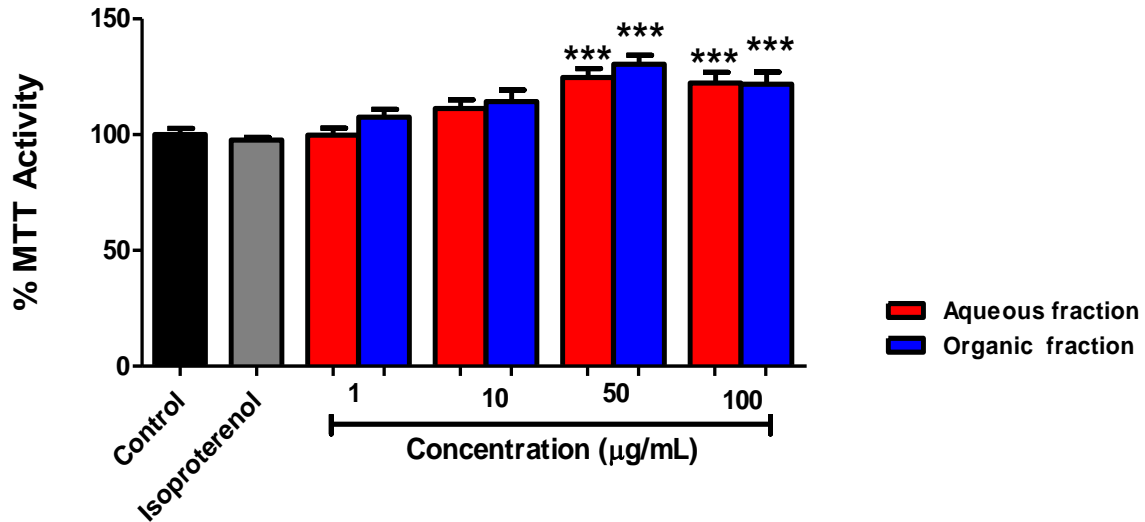


Figure 3.10 The effect of aqueous and organic fractions, prepared from 40% aqueous methanol extract of *C. intermedia* on mitochondrial dehydrogenase activity in 3T3-L1 adipocytes. Differentiated 3T3-L1 adipocytes were exposed to the aqueous and organic fractions of *C. intermedia* at various concentrations, vehicle control or isoproterenol for 24 hours. Mitochondrial dehydrogenase was measured using the MTT assay. Results are expressed as a percentage relative to the vehicle control (set at 100%) and are shown as mean \pm SEM for three independent experiments, each performed in triplicate. Significance is depicted as *** $P < 0.001$ vs. vehicle control.

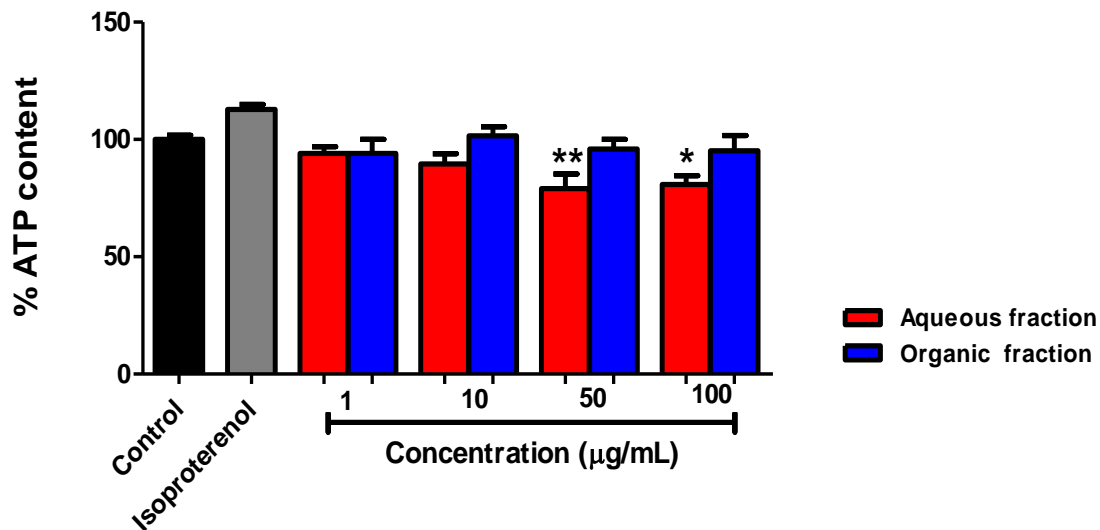


Figure 3.11 The effect of aqueous and organic fractions, prepared from 40% aqueous methanol extract of *C. intermedia* on ATP content in 3T3-L1 adipocytes. Differentiated 3T3-L1 adipocytes were exposed to the aqueous and organic fractions of *C. intermedia* at various concentrations, vehicle control or isoproterenol for 24 hours. Intracellular ATP content was assessed using an ATP luminescence kit. Results are expressed as a percentage relative to the vehicle control (set at 100%) and are shown as mean \pm SEM for three independent experiments, each performed in triplicate. Significance is depicted as * $P < 0.05$ and ** $P < 0.01$ vs. vehicle control.

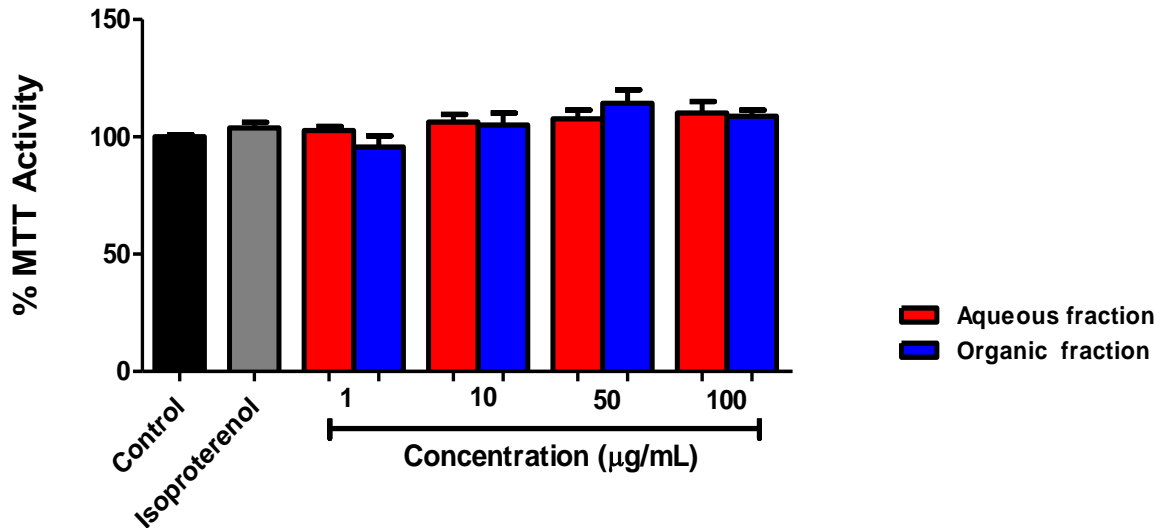


Figure 3.12 The effect of aqueous and organic fractions, prepared from 40% aqueous methanol extract of *C. maculata* on mitochondrial dehydrogenase activity in 3T3-L1 adipocytes. Differentiated 3T3-L1 adipocytes were exposed to the aqueous and organic fractions of *C. maculata* at various concentrations, vehicle control or isoproterenol for 24 hours. Mitochondrial dehydrogenase was measured using the MTT assay. Results are expressed as a percentage relative to the vehicle control (set at 100%) and are shown as mean \pm SEM for three independent experiments, each performed in triplicate.

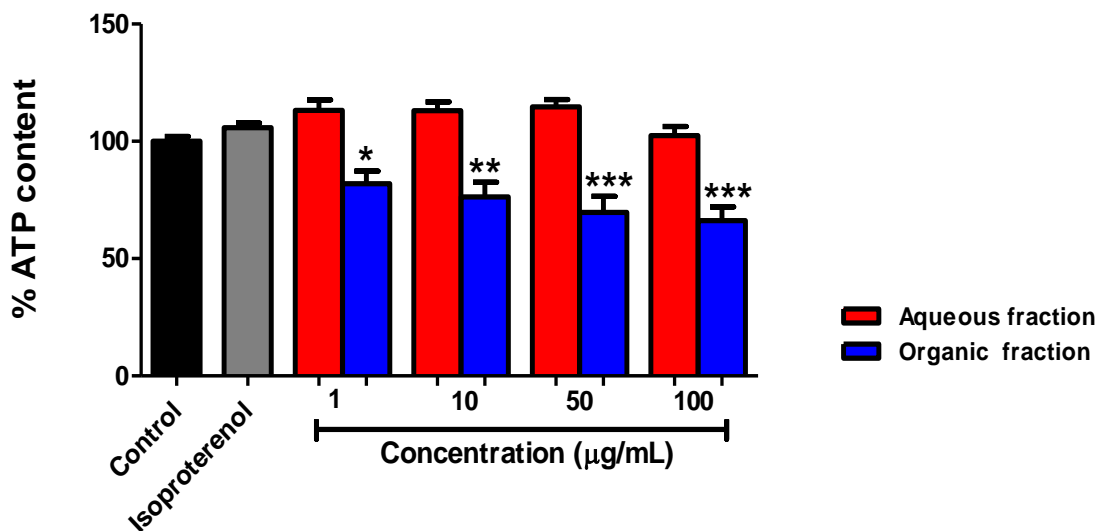


Figure 3.13 The effect of aqueous and organic fractions, prepared from 40% aqueous methanol extract of *C. maculata* on ATP content in 3T3-L1 adipocytes. Differentiated 3T3-L1 adipocytes were exposed to the aqueous and organic fractions of *C. maculata* at various concentrations, vehicle control or isoproterenol for 24 hours. Intracellular ATP content was assessed using an ATP luminescence kit. Results are expressed as a percentage relative to the vehicle control (set at 100%) and are shown as mean \pm SEM for three independent experiments, each performed in triplicate. Significance is depicted as * $P < 0.05$, ** $P < 0.01$ and *** $P < 0.001$ vs. vehicle control.

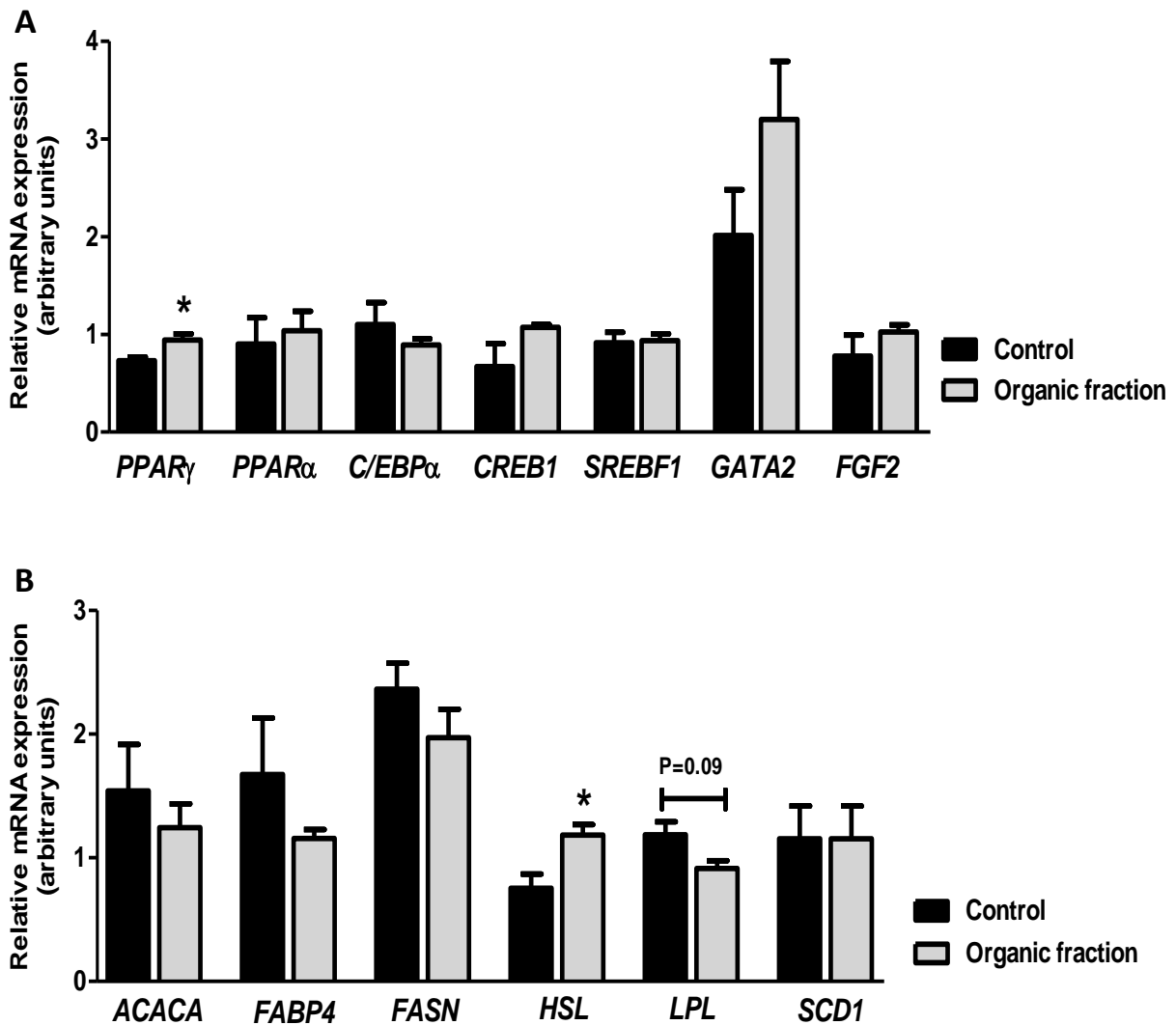
3.2.4 Selection of the organic fraction of *C. intermedia* for further analysis

The aqueous fraction of *Cyclopia maculata* and the organic fraction of *Cyclopia intermedia*, demonstrated the highest anti-obesity activity, as measured with the ORO assay, without affecting cell viability. Both fractions did not affect cell necrosis, assessed with propidium iodide staining (**Addendum 3**), further confirming that these fractions were not cytotoxic. Identification of phenolic compounds revealed the presence of neoponcirin and eriodictyol-*O*-deoxyhexoside-*O*-hexoside, polyphenols not previously detected in *Cyclopia*, in the organic fraction of *C. intermedia*. Furthermore, aqueous fractions may contain monosaccharides and methanol soluble polysaccharides, which would add to calorie intake and therefore may have the potential to be detrimental to individuals with T2DM. Based on these findings, the organic fraction of *C. intermedia* was selected for further analysis.

3.2.4.1 Effect of the organic fraction of *C. intermedia* on gene expression

To assess the effect of the organic fraction of *C. intermedia* on gene expression, experiments were scaled up and the most bioactive concentration (50 µg/mL), was selected for investigation of the molecular mechanism underlying the inhibitory effect of this fraction on lipid content. The expression of genes involved in lipid, FA, glucose and energy metabolism were measured using qRT-PCR. NormFinder, an algorithm used for identifying the optimal normalization gene (Anderson et al., 2004), identified beta-2 microglobulin (*B2M*) and the ribosomal protein L13a (*RPL13A*) as the most stably expressed endogenous controls (**Table 2.9, Chapter 2**), and therefore the combination of these genes was used for normalization of gene expression. Treatment of 3T3-L1 adipocytes with the organic fraction of *C. intermedia* increased the mRNA expression of *PPAR γ* (1.3 fold, $P < 0.05$) (**Fig. 3.14A**) and *HSL* (1.6 fold, $P < 0.05$) (**Fig. 3.14B**) compared to control adipocytes, whereas the expression of *LPL* was remained unaffected (0.7 fold, $P = 0.09$) in *C. intermedia* treated adipocytes (**Fig. 3.14B**). Treatment of 3T3-L1 adipocytes with this fraction did not have any effect on the mRNA expression of *PPAR α* , *C/EBP α* , *CREB1*, *SREBF1*, *GATA2* and *FGF2* (**Fig. 3.14A**), nor the mRNA expression of *ACACA*, *FASN* and *FABP4* (**Fig. 3.14B**) compared to the vehicle treated adipocytes.

Considering genes involved in energy metabolism, mRNA expression of *UCP3* was increased (1.5 fold, $P < 0.05$) in *C. intermedia* treated adipocytes (**Fig. 3.14C**), while no significance was observed for *SIRT1* expression (1.5 fold increase, $P = 0.07$) in *C. intermedia* treated adipocytes (**Fig. 3.14C**). Compared to control adipocytes, no significant effect in mRNA levels of *AMPK*, *SIRT3*, *PGC1 α* and *UCP2* was observed in *C. intermedia* treated adipocytes (**Fig. 3.14C**). In addition, the mRNA expression of *IRS1*, *GLUT4*, *G6PC*, *ADIPOQ*, *CPT1 α* and *Cs* was not significantly affected by treatment with the organic fraction of *C. intermedia* (**Figs. 3.14D**). The expression of *UCP1* was undetectable in 3T3-L1 adipocytes.



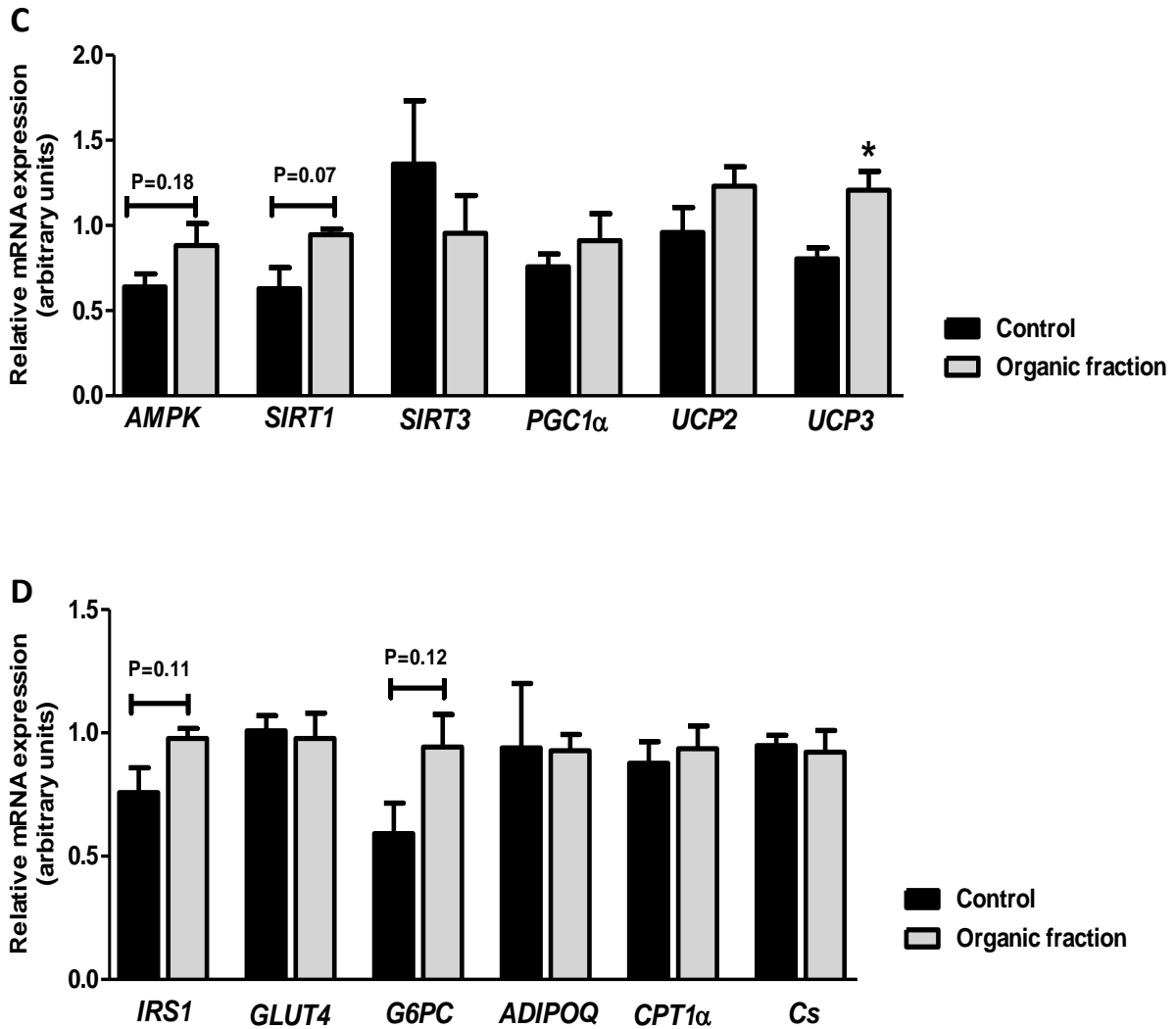


Figure 3.14 The effect of the organic fraction of *C. intermedia* on the mRNA expression genes involved in lipid or fatty acid, glucose and energy metabolism in 3T3-L1 adipocytes. Differentiated 3T3-L1 adipocytes were treated with the vehicle control or the organic fraction of *C. intermedia* at 50 $\mu\text{g}/\text{mL}$ for 24 hours. Total RNA was extracted and gene expression was analyzed by qRT-PCR (A-D). Results are represented as mRNA expression relative to the mRNA expression of endogenous controls (*B2M* and *RPL13A*) and expressed as mean \pm SEM for three independent experiments. Statistical significance is depicted as * $P < 0.05$ vs. vehicle control.

3.2.4.2 Effect of the organic fraction of *C. intermedia* on protein expression

To assess the effect of the organic fraction of *C. intermedia* on protein expression, experiments were scaled up and the most bioactive concentration (50 $\mu\text{g/mL}$) was selected for investigation of PPAR γ and PPAR α protein expression using western blot analysis. Images were cut from the original blot (Fig. S8 A and B, supplementary data) to only represent samples used in this chapter. Compared to control 3T3-L1 adipocytes, the protein expression of PPAR α and PPAR γ was not affected by treatment with the organic fraction of *C. intermedia* (Figs. 3.15 A and B).

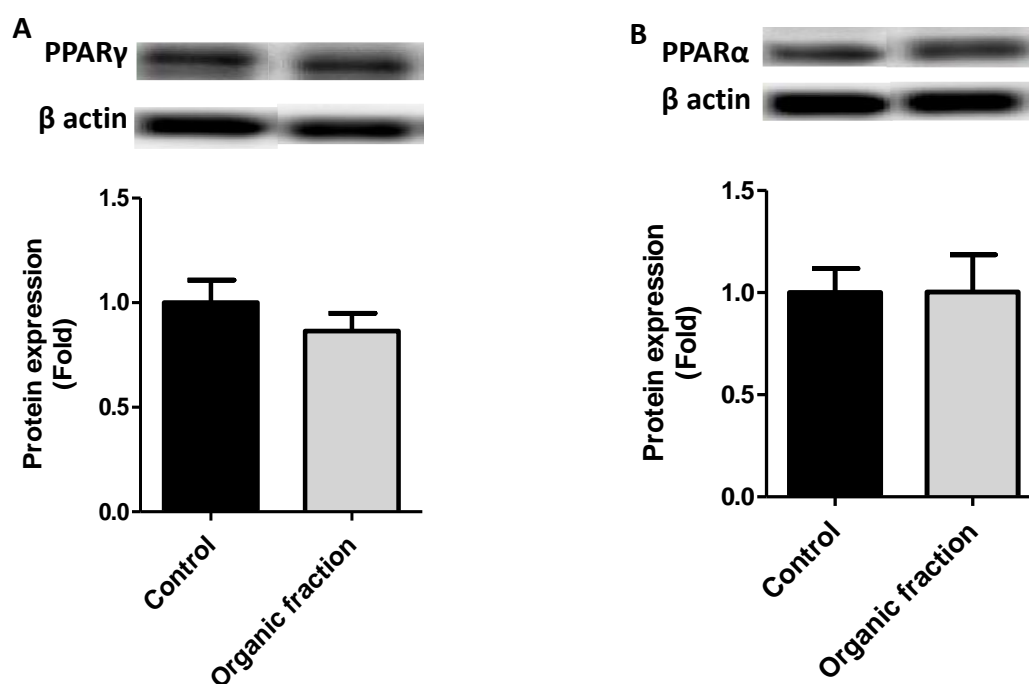


Figure 3.15 The effect of the organic fraction of *C. intermedia* on PPAR γ and PPAR α protein expression in 3T3-L1 adipocytes. Differentiated 3T3-L1 adipocytes were treated with the vehicle control or the organic fraction of *C. intermedia* at 50 $\mu\text{g/mL}$ for 24 hours. Proteins were extracted and the expression of PPAR γ (A) and PPAR α (B) were analyzed by western blot analysis. Results are expressed as the fold change relative to the vehicle control and represented as the mean \pm SEM for three independent experiments.

3.3 Validation of phenolic content and bioactivity of the large-scale preparation

After confirming the bioactivity of the small-scale prepared extract of the organic fraction of *C. intermedia* *in vitro*, the extraction of this fraction was upscaled to facilitate animal experiments and HPLC fractionation. LC-MS/MS analysis and qHPLC-DAD

were used to determine the phenolic composition of the large-scale preparation of the 40% aqueous methanol extract of *C. intermedia* and its organic fraction. The quantity and quality of the major polyphenols in the large-scale aqueous methanol extract of *C. intermedia* and its organic fraction (**Fig. 3.16** and **Table 3.2**) was similar to the previously small-scaled prepared aqueous methanol extract of *C. intermedia* and its organic fraction (**Fig. 3.2** and **Table 3.1**), thus demonstrating that the upscaled fractionation did not significantly change phenolic content. Furthermore, the *in vitro* bioactivity of the upscaled organic fraction of *C. intermedia* was compared to the previous organic fraction of *C. intermedia*. Both fractions decreased lipid content, increased MTT activity and did not have any significant effect on intracellular ATP content compared to control adipocytes (**Addendum 3**), thus confirming similar biological effects.

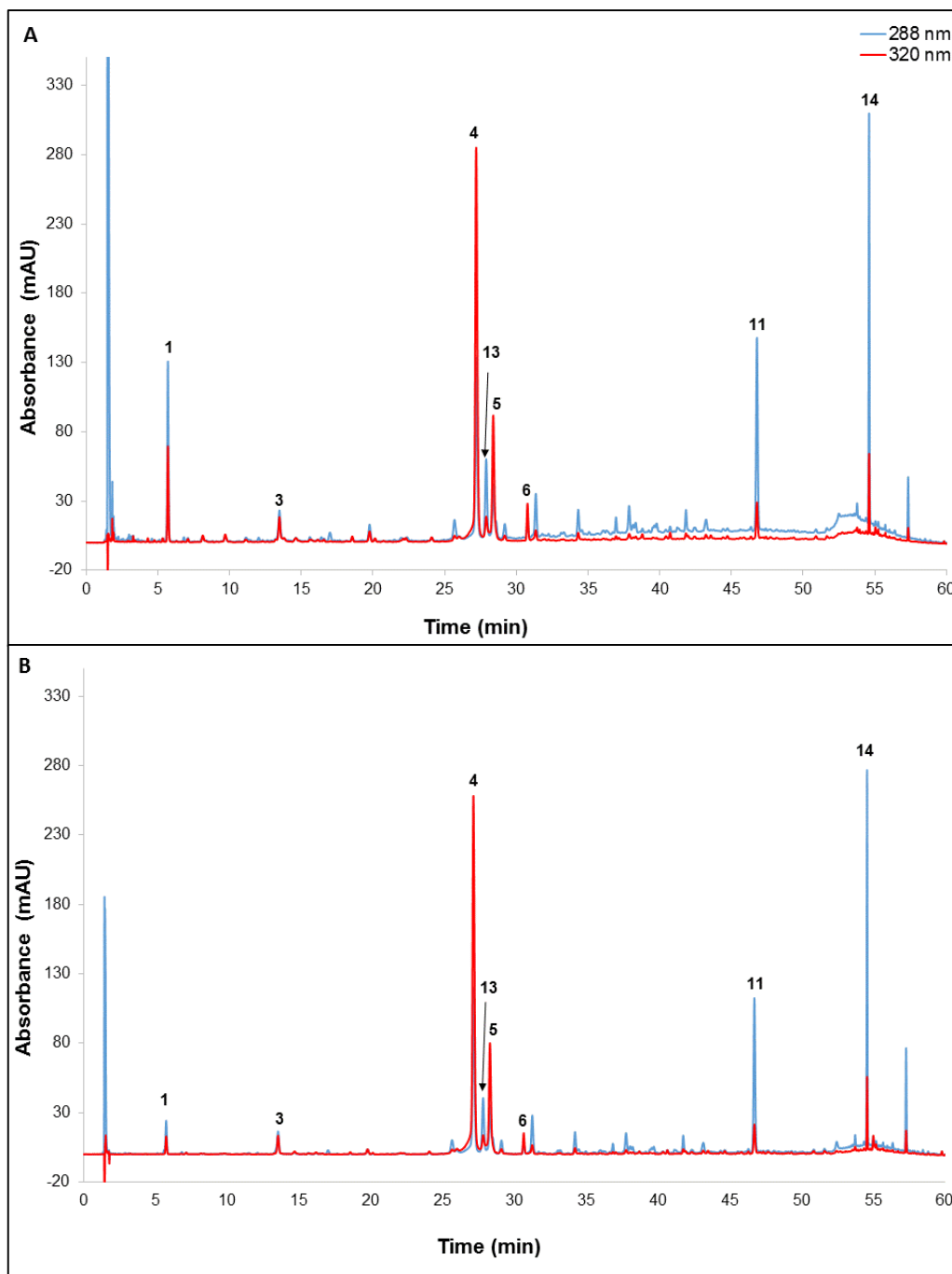


Figure 3.16 Phenolic profile of the large-scaled preparation of *C. intermedia*. The phenolic profile showing the major phenolic compounds of a 40% aqueous methanol extract of unfermented *C. intermedia* (A) and the organic fraction of a 40% methanol extract of *C. intermedia* (B), both prepared on large scale. The first peak (not numbered) represents ascorbic acid, which was added to prevent oxidation. Peak **1**: Iriflophenone-3-*C*- β -D-glucoside-4-*O*- β -D-glucoside; **3**: Iriflophenone-3-*C*- β -D-glucoside; **4**: Mangiferin; **5**: Isomangiferin; **6**: Vicenin-2; **11**: Hesperidin; **13**: Eriodictyol-*O*-deoxyhexoside-*O*-hexoside; **14**: Neoponcirin.

Table 3.2 Quantification of major phenolic compounds (g/100 g) in the upscaled 40% aqueous methanol extract of *C. intermedia* and its organic fraction by qHPLC-DAD.

Compound ^a	Aqueous methanol extract of <i>C. intermedia</i>	Organic fraction
Iriflophenone-3-C-β-D-glucoside-4-O-β-D-glucoside (1)	0.790	0.674
Iriflophenone-3-C-β-D-glucoside (3)	0.189	0.565
Mangiferin (4)	2.303	8.259
Isomangiferin (5)	0.626	2.181
Vicenin-2 (6)	0.168	0.388
Hesperidin (11)	1.029	3.318
Eriodictyol-O-deoxyhexoside-O-hexoside ^b (13)	0.582	1.484
Neoponcirin (14)	1.003	3.609

^a Peak number on HPLC chromatogram in brackets

^b Expressed as eriocitrin equivalent

3.4 *In vivo* experiments of the organic fraction of *C. intermedia*

3.4.1 Validation of the Lepr^{db/db} mouse model

Body weight, fasting blood glucose concentrations, food and water consumption of Lepr^{db/db} mice and their heterozygous Lepr^{db/+} controls were monitored on a weekly basis to evaluate the characteristics of the Lepr^{db/db} mouse model. During the 28-day study period, body weight of Lepr^{db/db} mice increased more than the body weight of Lepr^{db/+} mice ($P < 0.0001$) (**Fig. 3.17A**). The final body weight of Lepr^{db/db} mice was significantly higher (42.7 ± 1.8 g, $P < 0.001$) compared to Lepr^{db/+} mice (20.5 ± 0.6 g) (**Table 3.3**), illustrating that the Lepr^{db/db} mice are obese compared to Lepr^{db/+} mice. At day 7 of the study period, fasting plasma glucose concentrations of Lepr^{db/db} mice increased more than fasting plasma glucose concentrations of Lepr^{db/+} mice ($P < 0.05$, $P < 0.01$ and $P < 0.0001$) (**Fig. 3.17B**). At the end of 28-day study period, fasting glucose concentrations of Lepr^{db/db} mice were higher (21.9 ± 2.6 mmol/L, $P < 0.001$) than that of the Lepr^{db/+} mice (6.9 ± 1.0 mmol/L) (**Table 3.3**), demonstrating that the Lepr^{db/db} mice are hyperglycemic compared to Lepr^{db/+} mice.

During the course of the study, food intake was significantly higher ($P < 0.0001$) in Lepr^{db/db} mice compared to Lepr^{db/+} mice (**Fig. 3.17C**). At the end of the study period, total food consumption was higher in Lepr^{db/db} mice compared to Lepr^{db/+} mice (77.3 ± 2.5 g in Lepr^{db/+} mice vs. 169.7 ± 11.1 g in Lepr^{db/db} mice, $P < 0.001$), showing that the Lepr^{db/db} mice are hyperphagic compared to Lepr^{db/+} mice (**Table 3.3**). No significant

change was observed in water intake between the mice, during the first week of the study, however from weeks 2 - 4, water intake levels were significantly higher in $Lepr^{db/db}$ mice ($P < 0.01$ and $P < 0.0001$) compared to $Lepr^{db/+}$ mice (**Fig. 3.17D**). Total water intake was increased from 98.6 ± 9.5 mL in $Lepr^{db/+}$ mice to 325.3 ± 45.4 mL ($P < 0.001$) in $Lepr^{db/db}$ mice, illustrating that the $Lepr^{db/db}$ mice are polydipsic compared to $Lepr^{db/+}$ mice (**Table 3.3**).

Table 3.3 Metabolic characteristics of the $Lepr^{db/+}$ and $Lepr^{db/db}$ control mice after 28 days.

Parameter	$Lepr^{db/+}$	$Lepr^{db/db}$
Body weight (g)	20.5 ± 0.6	$42.7 \pm 1.8^{***}$
Fasting glucose concentration (mmol/L)	6.9 ± 1.0	$21.9 \pm 2.6^{***}$
Total food consumption (g)	77.3 ± 2.5	$169.7 \pm 11.1^{***}$
Total water consumption (mL)	98.6 ± 9.5	$325.3 \pm 45.4^{***}$

Statistical significance is depicted as $^{***}P < 0.05$ for $Lepr^{db/db}$ vs. $Lepr^{db/+}$ control

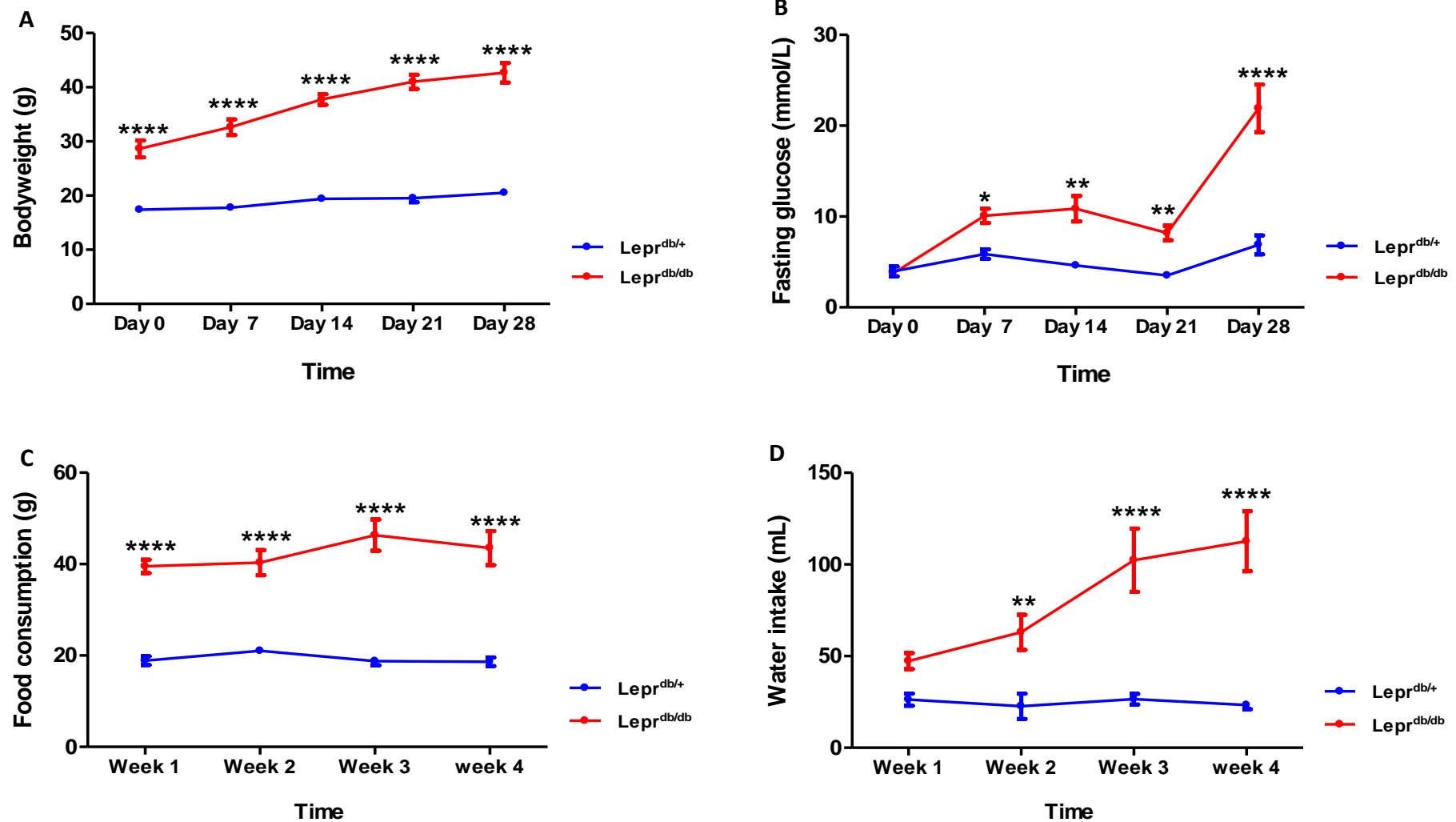


Figure 3.17 Metabolic characteristics of Lepr^{db/db} mice and Lepr^{db/+} mice. Graphs represent body weight (A), fasting plasma glucose (B), food consumption (C) and water intake (D). Results are expressed as the mean \pm SEM ($n = 6 - 8$ per group). Statistical significance is depicted as * $P < 0.05$, ** $P < 0.01$ and **** $P < 0.0001$ for Lepr^{db/db} vs. Lepr^{db/+}.

3.4.2 The organic fraction of *C. intermedia* decreases body weight gain in obese $\text{Lepr}^{\text{db/db}}$ without changes in food and water consumption

The anti-obesity effect of the organic fraction of *C. intermedia* was confirmed by treating obese $\text{Lepr}^{\text{db/db}}$ mice and their lean controls ($\text{Lepr}^{\text{db/+}}$ mice) with 70.5 mg/kg and 351.5 mg/kg of the fraction for 28 days. The percentage body weight gain was increased by $18 \pm 1.3\%$ in $\text{Lepr}^{\text{db/+}}$ mice compared to a $54.6 \pm 7.6\%$ increase in $\text{Lepr}^{\text{db/db}}$ mice ($P < 0.001$) (**Fig. 3.18** and **Table 3.4**). Daily treatment of obese $\text{Lepr}^{\text{db/db}}$ mice with the organic fraction of *C. intermedia* decreased body weight gain by 14.2% ($P = 0.1892$) and 21.7% ($P < 0.05$) at 70.5 mg/kg and 351.5 mg/kg, respectively compared to $\text{Lepr}^{\text{db/db}}$ control mice (**Fig. 3.18** and **Table 3.4**). In contrast, no changes in body weight gain were observed in $\text{Lepr}^{\text{db/+}}$ mice treated with these fractions (**Fig. 3.18**). No significant difference in total food intake and water consumption was observed in *C. intermedia* treated $\text{Lepr}^{\text{db/db}}$ mice and $\text{Lepr}^{\text{db/+}}$ mice (**Figs. 3.19A** and **3.19B**).

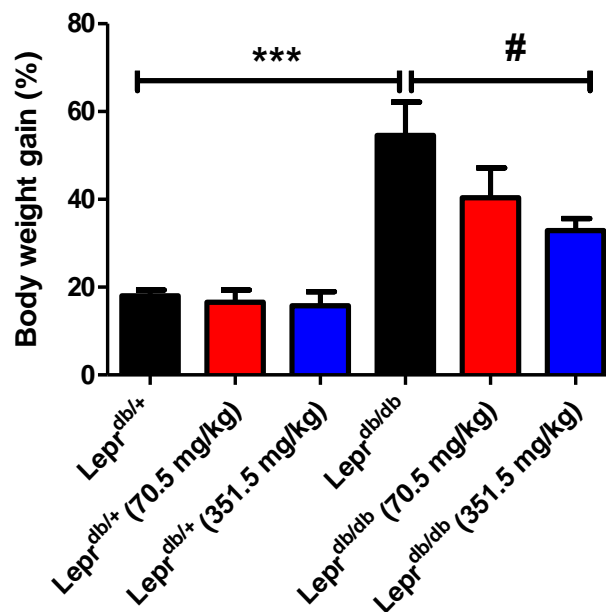


Figure 3.18 The effect of the organic fraction of *C. intermedia* on body weight gain in $\text{Lepr}^{\text{db/+}}$ and $\text{Lepr}^{\text{db/db}}$ mice. Mice were treated with vehicle control, 70.5 or 351.5 mg/kg of the organic *C. intermedia* fraction by oral gavage daily for 28 days. Body weight gain was assessed after day 28 of treatment. Values are expressed as the mean \pm SEM ($n = 6 - 8$). Significance is depicted as *** $P < 0.001$ $\text{Lepr}^{\text{db/+}}$ vs. $\text{Lepr}^{\text{db/db}}$ and # $P < 0.05$ $\text{Lepr}^{\text{db/db}}$ control vs. $\text{Lepr}^{\text{db/db}}$ 351.5 mg/kg.

Table 3.4 Effect of the organic fraction of *C. intermedia* on body weight.

Treatment Group	Initial BW (g)	Final BW (g)	Weight Gain (g) ^a	% Gain ^b
Lepr ^{db/+} control	17.9 ± 0.5	20.5 ± 0.6	3.1	18 ± 1.3 ^{***}
Lepr ^{db/+} (70.5 mg/kg)	17.5 ± 0.4	20.4 ± 0.6	2.9	16.6 ± 2.8
Lepr ^{db/+} (351.5 mg/kg)	17.4 ± 0.6	20.1 ± 0.8	2.7	15.5 ± 3.1
Lepr ^{db/db} control	28.6 ± 1.6	42.7 ± 1.8	14.0	54.6 ± 7.6 ^{***}
Lepr ^{db/db} (70.5 mg/kg)	28.5 ± 1.6	39.4 ± 1.2	10.9	38.2 ± 6.8 ^{***}
Lepr ^{db/db} (351.5 mg/kg)	29.1 ± 0.99	38.4 ± 1.3	9.3	32.0 ± 2.7 ^{***#}

^a Weight gain was calculated by subtracting initial body weight (g) from final body weight (g)

^b Percentage (%) weight gain was calculated by dividing weight gain (g) of individual mice by their initial body weight (g) multiplied by 100

Statistical significance is depicted as ^{***}P < 0.05 Lepr^{db/+} vs. Lepr^{db/db} and #P < 0.05 Lepr^{db/db} control vs. Lepr^{db/db} 351.5 mg/kg.

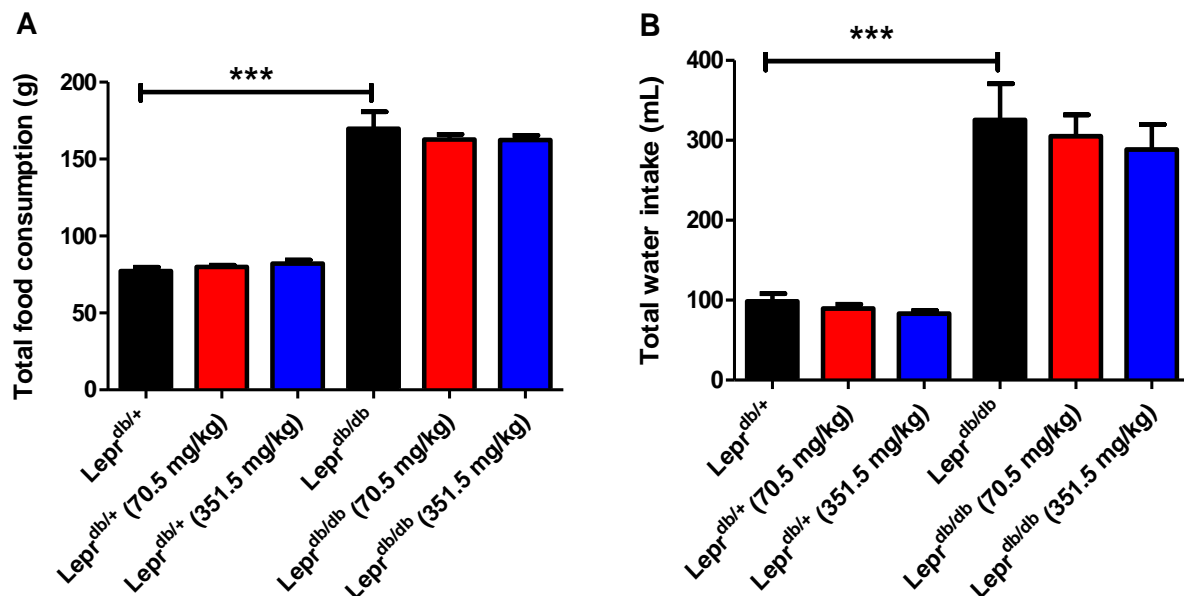


Figure 3.19 The effect of the organic fraction of *C. intermedia* on food intake and water consumption of Lepr^{db/+} and Lepr^{db/db} mice. Mice were treated with vehicle control, 70.5 or 351.5 mg/kg of organic *C. intermedia* fraction by oral gavage daily for 28 days. Total food consumption (A) and total water intake (B) were assessed after day 28 of treatment. Values are expressed as the mean ± SEM (n = 6 - 8). Significance is depicted as ^{***}P < 0.001 Lepr^{db/+} vs. Lepr^{db/db}.

3.4.3 The organic fraction of *C. intermedia* increases liver weight of obese $Lepr^{db/db}$ mice

The relative liver weight of $Lepr^{db/db}$ mice was significantly increased ($P < 0.05$) compared to $Lepr^{db/+}$ control mice (**Fig. 3.20**). Treatment with the organic fraction of *C. intermedia* at 351.5 mg/kg increased ($P < 0.05$) liver weight in $Lepr^{db/db}$ mice, whereas treatment did not affect the liver weight in the $Lepr^{db/+}$ mice (**Fig. 3.20**).

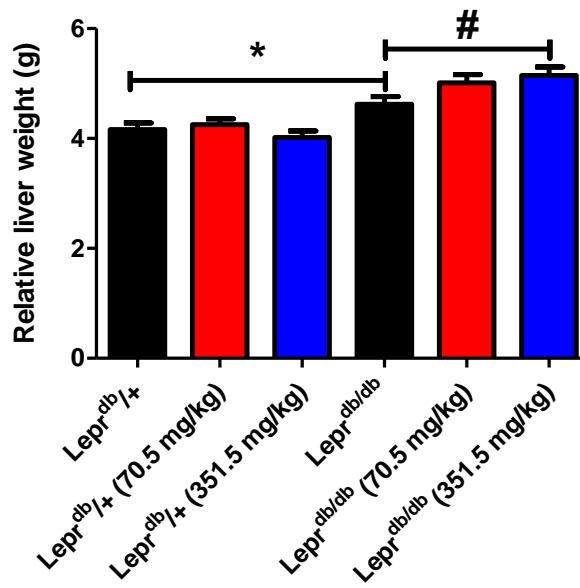


Figure 3.20 The effect of the organic fraction of *C. intermedia* on liver weight of $Lepr^{db/db}$ and $Lepr^{db/+}$ mice. At the end of the study, livers were harvested, weighed and the liver weight, relative to body weight was calculated. Results are expressed as the mean \pm SEM ($n = 6 - 8$). Significance is depicted as * $P < 0.05$ $Lepr^{db/+}$ vs. $Lepr^{db/db}$ and # $P < 0.05$ $Lepr^{db/db}$ control vs. $Lepr^{db/db}$ 351.5 mg/kg.

3.4.4 Effect of the organic fraction of *C. intermedia* on glucose metabolism

The 16 hour fasting plasma glucose concentration of $Lepr^{db/db}$ mice was increased compared to that of $Lepr^{db/+}$ mice ($P < 0.001$) (**Fig. 3.21A**). Treatment with the organic fraction of *C. intermedia* at 70.5 and 351.5 mg/kg did not have any significant effect on the glucose levels in both $Lepr^{db/+}$ and $Lepr^{db/db}$ mice (**Fig. 3.21A**). The effect of the organic fraction of *C. intermedia* on glucose tolerance was assessed using the OGTT. During the OGTT, glucose concentrations remained significantly high ($P < 0.0001$) in the $Lepr^{db/db}$ control mice compared to $Lepr^{db/+}$ control mice (**Fig. 3.21B**). Both the

OGTT (Fig. 3.21B) and the area under curve (AUC) (Fig. 3.21C) showed that treatment with the organic fraction of *C. intermedia* did not improve glucose tolerance in both $Lepr^{db/db}$ and $Lepr^{db/+}$ mice.

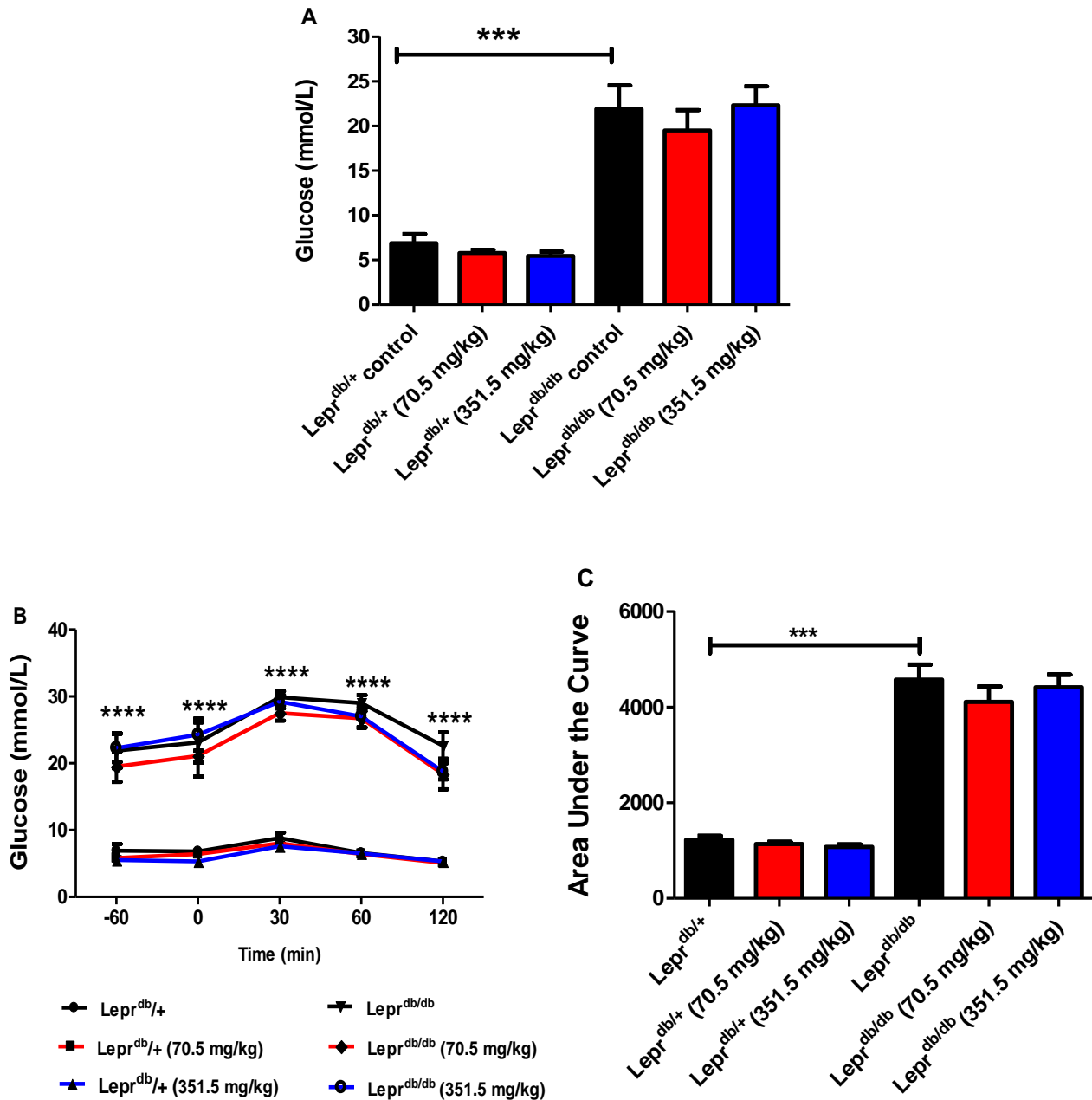


Figure 3.21 The effect of the organic fraction of *C. intermedia* on fasting plasma glucose concentration and glucose tolerance of $Lepr^{db/+}$ and $Lepr^{db/db}$ mice. Mice were fasted for 16 hours and glucose levels were measured at $t = -60$ (A). Thereafter treatment was gavaged and an hour later glucose (2 g/kg) was administered to the mice and blood glucose levels were measured at baseline ($t = 0$ min), 30, 60 and 120 minutes (B). The area under the curve (AUC) of the glucose tolerance was calculated (C). Results are expressed as the mean \pm SEM ($n = 6 - 8$). Significance is depicted as $***P < 0.001$ and $****P < 0.0001$ $Lepr^{db/+}$ vs. $Lepr^{db/db}$ mice.

At termination, blood was collected after a 4 hour fast, serum was prepared and insulin levels were measured. Results showed that serum insulin levels were significantly increased (11.3 ± 4.6 ng/mL, $P < 0.05$) in $\text{Lepr}^{\text{db/db}}$ mice compared to $\text{Lepr}^{\text{db/+}}$ control mice (0.5 ± 0.2 ng/mL). Treatment with 351.5 mg/kg of the organic fraction of *C. intermedia* did not significantly affect insulin concentrations in obese $\text{Lepr}^{\text{db/db}}$ (Fig. 3.22).

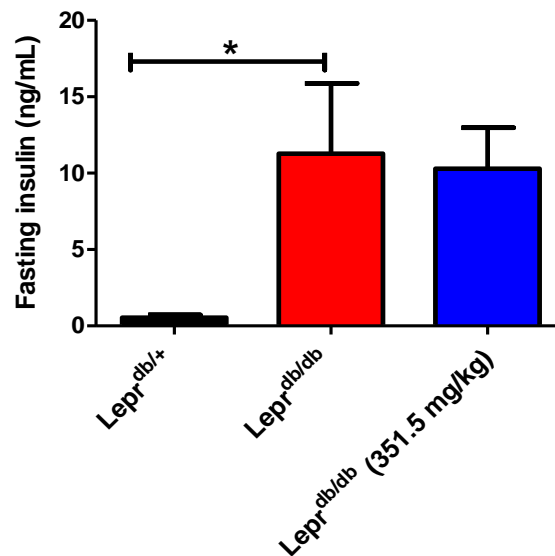


Figure 3.22 The effect of the organic fraction of *C. intermedia* on fasting serum insulin levels of $\text{Lepr}^{\text{db/+}}$ and $\text{Lepr}^{\text{db/db}}$ mice. Serum insulin levels were determined from blood collected at termination, following a 4 hour fast. Results are expressed as the mean \pm SEM ($n = 6 - 8$). Significance is depicted as * $P < 0.05$ $\text{Lepr}^{\text{db/+}}$ vs. $\text{Lepr}^{\text{db/db}}$ mice.

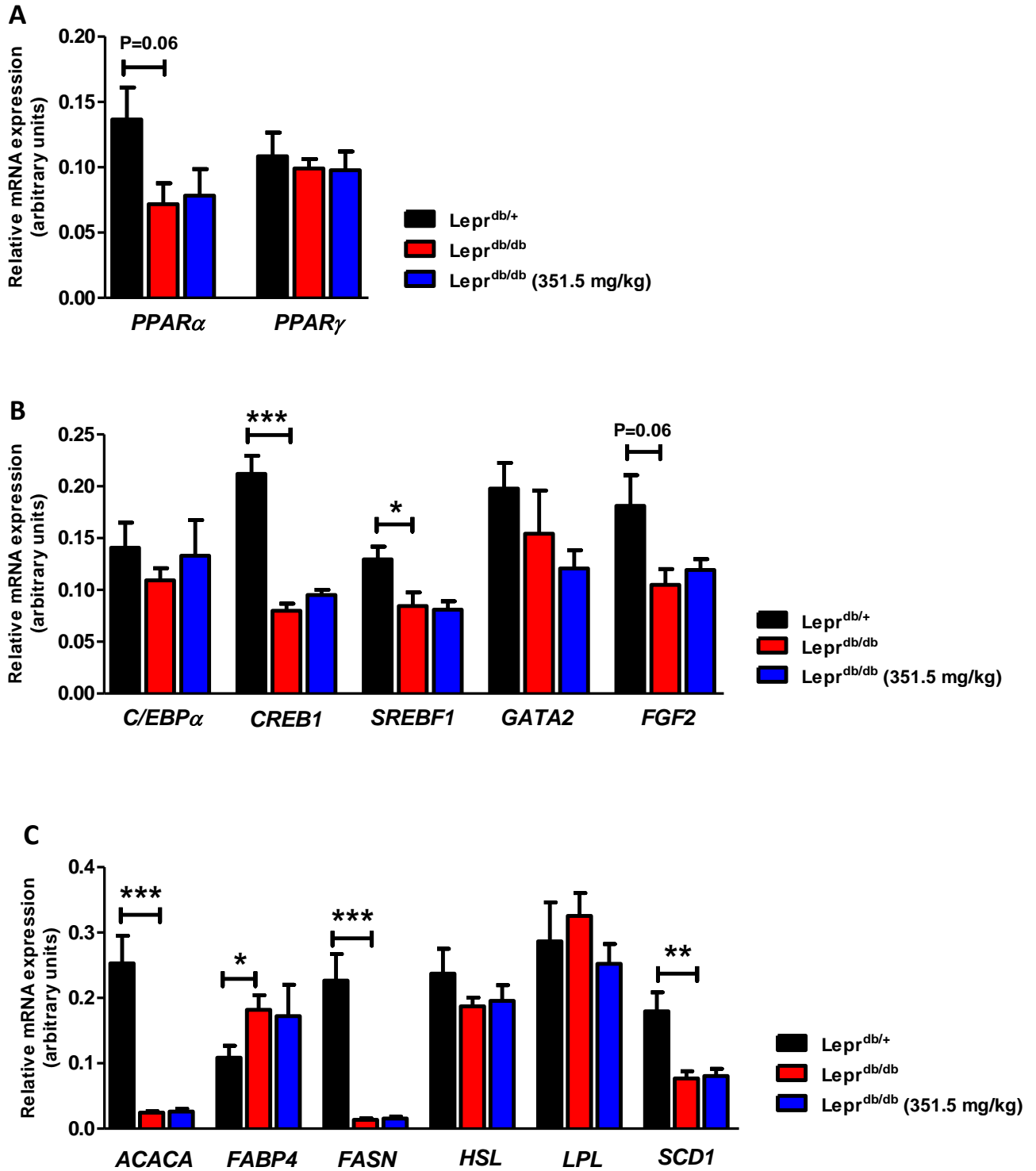
3.4.5 Effect of the organic fraction of *C. intermedia* on adipose tissue gene expression

The mechanism by which the organic fraction of *C. intermedia* decreases body weight gain in obese $\text{Lepr}^{\text{db/db}}$ mice was investigated by measuring the expression of genes associated with lipid, FA, glucose and energy metabolism in (sWAT) and gonadal (gWAT) white adipose tissues and the interscapular brown adipose tissue (iBAT) using qRT-PCR.

3.4.5.1 Subcutaneous white adipose tissue

NormFinder showed that (*ACTβ*) and the ribosomal protein L13a (*RPL13A*) were the most stable genes amongst the seven endogenous genes assessed in sWAT (**Table 2.9, Chapter 2**), therefore the combination of these genes was used for normalization of gene expression in sWAT. The mRNA expression of *PPARα*, *CREB1*, *SREBF1* and *FGF2* was decreased by 1.9-fold ($P = 0.06$), 2.7-fold ($P < 0.001$), 1.53-fold ($P < 0.05$) and 1.7-fold ($P = 0.06$), respectively, in the sWAT of obese *Lepr^{db/db}* mice compared to *Lepr^{db/+}* control mice, whereas the expression of *PPARγ*, *C/EBPα* and *GATA2* was not significantly changed between the two genotypes (**Figs. 3.23A and 3.23B**). Treatment of *Lepr^{db/db}* mice with the organic fraction of *C. intermedia* did not affect the expression of these genes (**Figs. 3.23A and 3.23B**).

The mRNA expression of *ACACA*, *FASN*, *SCD1*, *PGC1α* and *UCP3* was decreased by 10.5-fold ($P < 0.001$), 16.2-fold ($P < 0.001$), 2.3-fold ($P < 0.01$), 3.4-fold ($P < 0.05$) and 5.3-fold ($P < 0.001$), respectively, in the sWAT of obese *Lepr^{db/db}* mice compared to *Lepr^{db/+}* control mice, whereas the expression of *FABP4* was increased (1.7-fold, $P < 0.05$) in *Lepr^{db/db}* mice compared to *Lepr^{db/+}* control mice (**Figs. 3.23C and 3.23D**). The mRNA expression of *HSL*, *LPL*, *AMPK*, *SIRT1*, *SIRT3*, *UCP1* and *UCP2* was not significantly changed between the two genotypes. Furthermore, treatment with the organic fraction of *C. intermedia* did not have any significant effect on the expression of these genes (**Figs. 3.23C and 3.23D**). The mRNA expression of *ADIPOQ*, *TNFα* and *G6PC* remained unchanged between *Lepr^{db/db}* and the *Lepr^{db/+}* control mice, and in response to treatment with the organic fraction of *C. intermedia* (**Fig. 3.23E**).



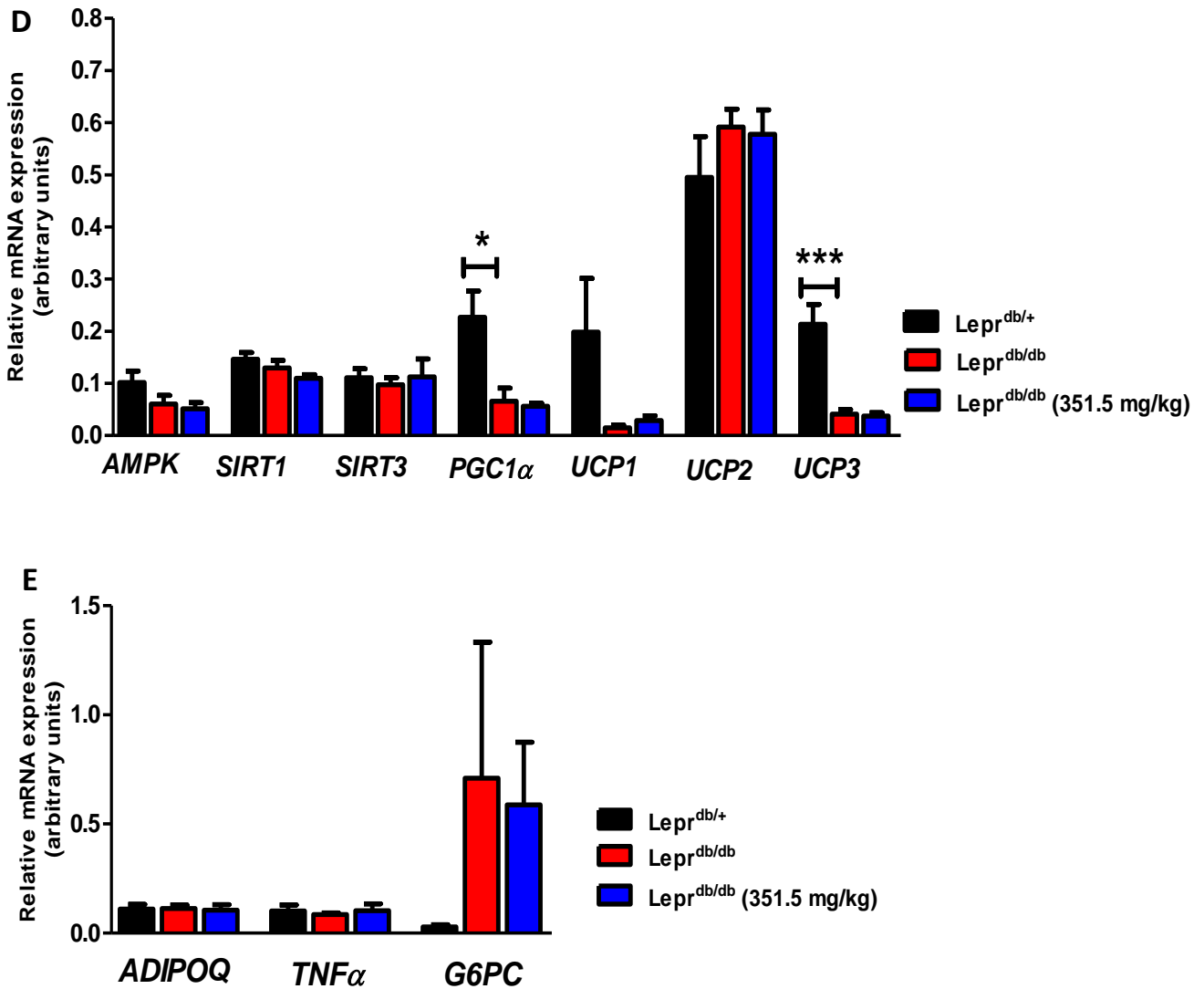
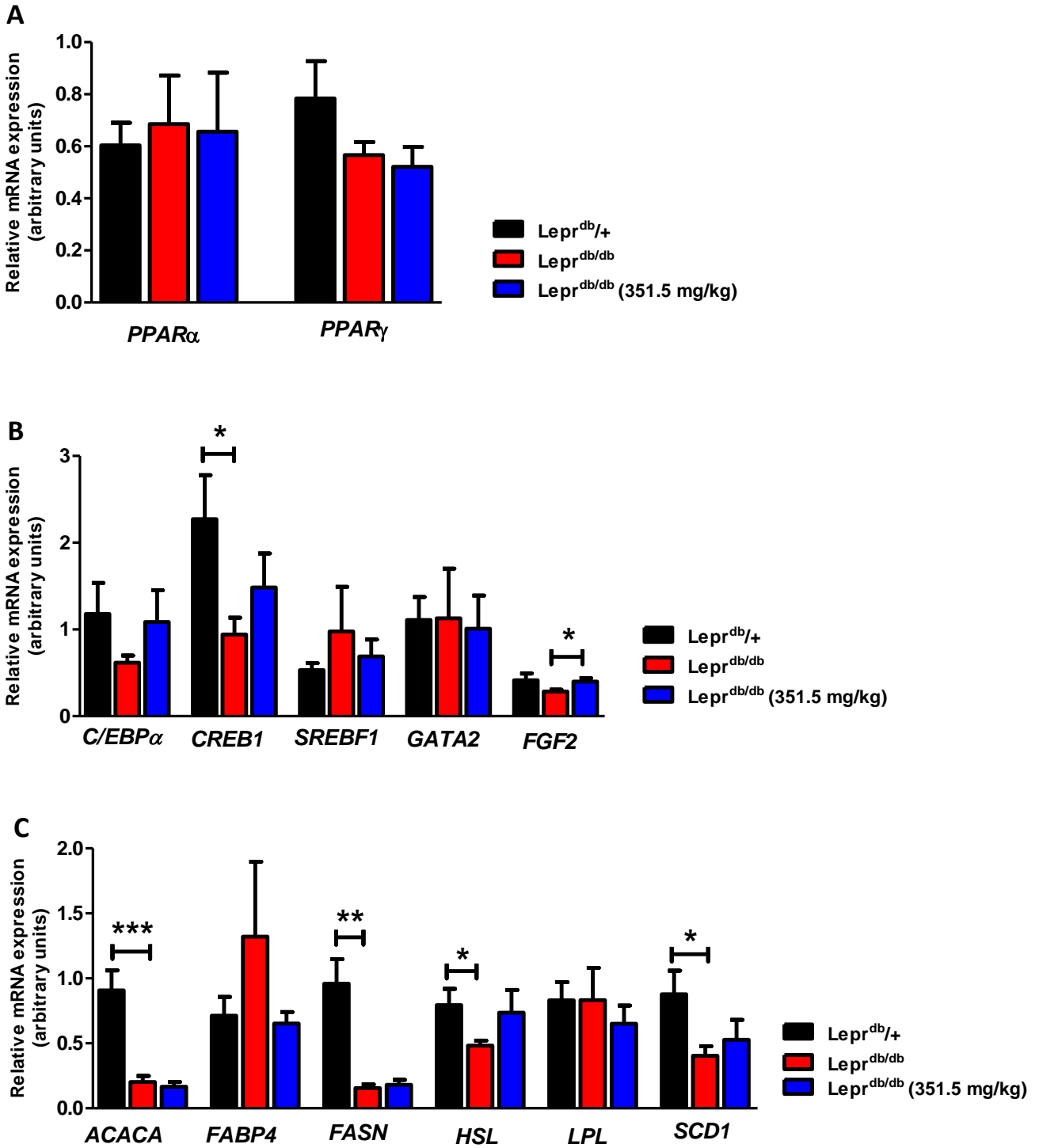


Figure 3.23 The effect of the organic fraction of *C. intermedia* on the mRNA expression of genes associated with lipid, fatty acid, glucose and energy metabolism in subcutaneous adipose tissue of Lepr^{db/+} and Lepr^{db/db} mice. Mice were treated with vehicle control or 351.5 mg/kg (for the Lepr^{db/db} mice) of the organic *C. intermedia* fraction by oral gavage daily for 28 days. Total RNA was extracted and gene expression was analyzed by qRT-PCR (A - E). Results are represented as mRNA expression relative to the mRNA expression of endogenous controls (*Act β* and *Rpl13a*), and expressed as mean \pm SEM (n = 6 - 8). Statistical significance is depicted as *P < 0.05, **P < 0.01 and ***P < 0.001 Lepr^{db/+} vs. Lepr^{db/db} mice.

3.4.5.2 Gonadal white adipose tissue

Similar to sWAT, NormFinder showed that beta-actin(*ACTB*) and the ribosomal protein L13a (*RPL13A*) were the most stable genes amongst the seven endogenous genes assessed in the gWAT (**Table 2.9, Chapter 2**), and therefore the combination of these genes was used for normalization of gene expression in gWAT. The mRNA expression of *CREB1* was decreased (2.4-fold, $P < 0.05$) in obese *Lepr^{db/db}* mice compared to *Lepr^{db/+}* control mice, whereas the expression of other genes (*PPAR γ* , *PPAR α* , *CEBP α* , *SREBF1*, *GATA2* and *FGF2*) remained unaffected between the two genotypes (**Figs. 3.24A and 3.24B**). The organic fraction of *C. intermedia* increased the mRNA expression of *FGF2* (1.4-fold, $P < 0.05$) in gWAT of *Lepr^{db/db}* mice (**Fig. 3.24B**), whereas the expression of other genes were unaffected by treatment (**Figs. 3.24A and 3.24B**).

Similar to the sWAT, the mRNA expression of *ACACA*, *FASN*, *HSL* and *SCD1* was decreased by 4.5-fold ($P < 0.001$), 6.17-fold ($P < 0.01$), 1.65-fold ($P < 0.05$) and 2.17-fold ($P < 0.05$), respectively, in the gWAT of obese *Lepr^{db/db}* mice compared to *Lepr^{db/+}* control mice, whereas *UCP2* mRNA expression was increased (2.24-fold, $P < 0.01$) in *Lepr^{db/db}* mice compared to *Lepr^{db/+}* control mice (**Figs. 3.24C and 3.24D**). Compared to *Lepr^{db/+}* control mice, the mRNA expression of *FABP4*, *LPL*, *AMPK*, *SIRT1*, *SIRT3*, *PGC1 α* , *UCP1* and *UCP3* was not changed in *Lepr^{db/db}* mice. Treatment of obese *Lepr^{db/db}* control mice with the organic fraction of *C. intermedia* did not significantly change the expression of these genes (**Figs. 3.24C and 3.24D**). The mRNA expression of *ADIPOQ*, *TNF α* and *G6PC* remained unchanged in gWAT of *Lepr^{db/db}* and *Lepr^{db/+}* control mice, and in response to treatment with the organic fraction of *C. intermedia* (**Fig. 3.24E**).



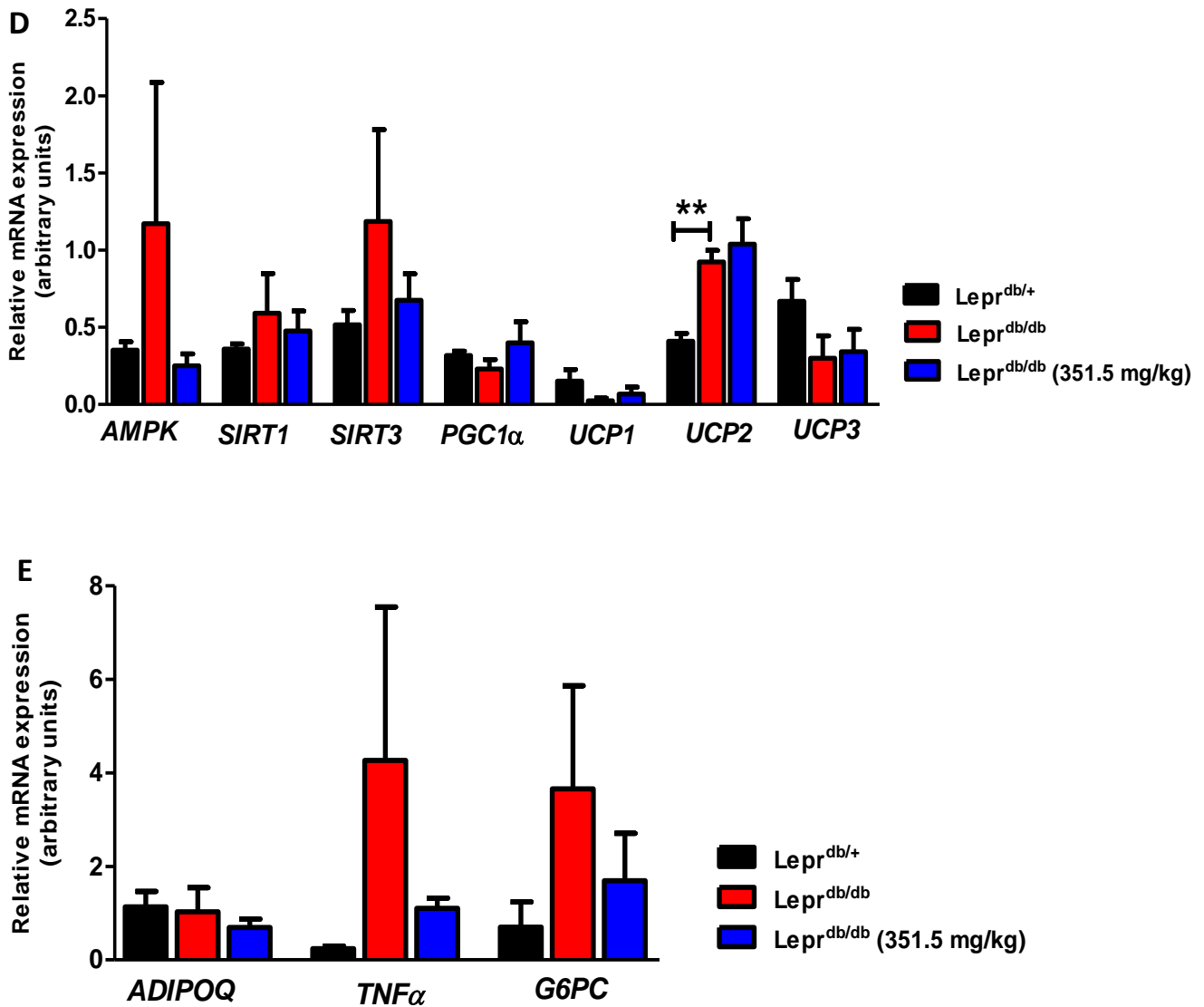
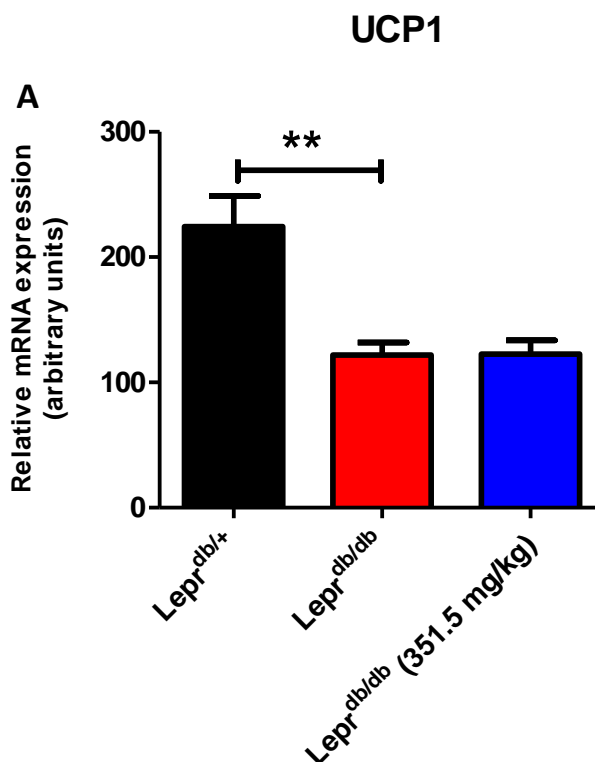


Figure 3.24 The effect of the organic fraction of *C. intermedia* on the mRNA expression of genes associated with lipid, fatty acid, glucose and energy metabolism in the gonadal adipose tissue of Lepr^{db/+} and Lepr^{db/db} mice. Mice were treated with vehicle control or 351.5 mg/kg (for the Lepr^{db/db} mice) of organic *C. intermedia* fraction by oral gavage daily for 28 days. Total RNA was extracted and gene expression was analyzed by qRT-PCR (A - E). Results are represented as mRNA expression relative to the mRNA expression of endogenous controls (*ACT β* and *RPL13A*), and expressed as mean \pm SEM (n = 6 - 8). Statistical significance is depicted as *P < 0.05, **P < 0.01 and ***P < 0.001 Lepr^{db/+} vs. Lepr^{db/db} mice or Lepr^{db/db} control mice vs. Lepr^{db/db} 351.5 mg/kg.

3.4.5.3 Interscapular brown adipose tissue

NormFinder showed that beta-2 microglobulin (*B2M*) and hypoxanthine guanine phosphoribosyl transferase 1 (*HPRT1*) were the most stable genes amongst the seven endogenous genes assessed in the iBAT (**Table 2.9, Chapter 2**), and therefore the combination of these genes was used for normalization of gene expression in iBAT. Compared to *Lepr^{db/+}* control mice, the mRNA expression of *UCP1* was decreased (1.84-fold, $P < 0.01$) in the iBAT of obese *Lepr^{db/db}* mice. Treatment with the organic fraction of *C. intermedia* did not affect the expression of *UCP1* (**Fig. 3.25A**). The mRNA expression of *PPAR γ* , *AMPK*, *SIRT3* and *UCP3* was decreased by 1.28-fold ($P = 0.07$), 1.47-fold ($P < 0.01$), 1.34-fold ($P < 0.05$) and 1.84-fold ($P < 0.01$), respectively, in iBAT of obese *Lepr^{db/db}* mice compared to *Lepr^{db/+}* control mice, whereas the mRNA expression of *UCP2* (3.5-fold, $P < 0.001$) and *CPT1 α* (2.4-fold, $P < 0.01$) was increased (**Figs. 3.25B** and **3.25C**). The expression of *SIRT1*, *PPAR α* and *PGC1 α* remained unchanged between the genotypes. No significant effect was observed in the expression of these genes in response to treatment with the organic fraction of *C. intermedia* (**Figs. 3.25A** and **3.25B**).



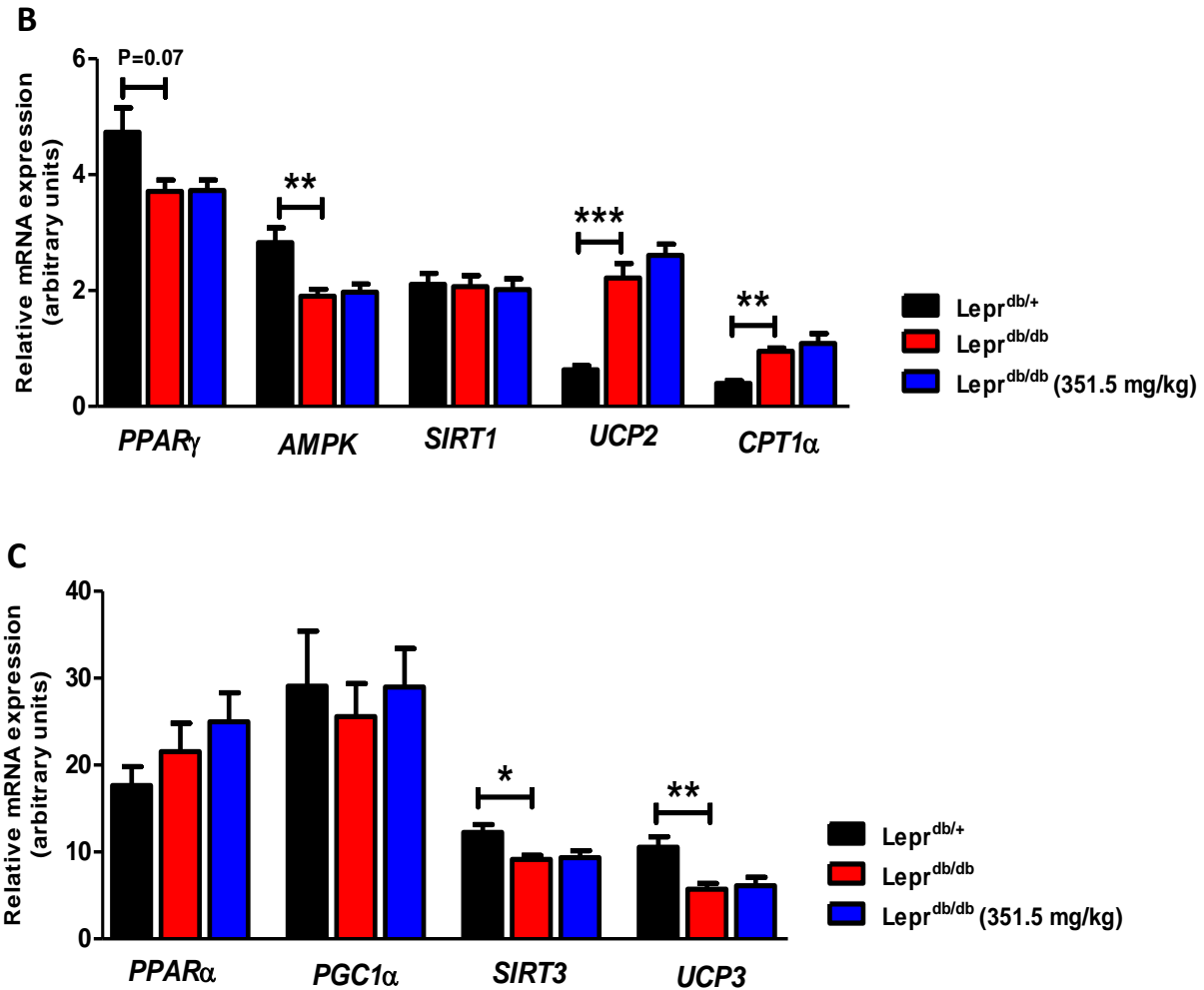


Figure 3.25 The effect of the organic fraction of *C. intermedia* on the mRNA expression of brown fat markers and energy metabolism genes in the interscapular brown adipose tissue of Lepr^{db/+} and Lepr^{db/db} mice. Mice were treated with vehicle control or 351.5 mg/kg (for the Lepr^{db/db} mice) of organic *C. intermedia* fraction by oral gavage daily for 28 days. Total RNA was extracted and gene expression was analyzed by qRT-PCR (A-C). Results are represented as mRNA expression relative to the mRNA expression of endogenous controls (*B2M* and *HPRT1*), and expressed as mean ± SEM (n = 6 - 8). Statistical significance is depicted as *P < 0.05, **P < 0.01 and ***P < 0.001 Lepr^{db/+} vs. Lepr^{db/db} mice.

3.5 Summary of results

The results described in this chapter are summarized in the tables below. The aqueous fraction of *C. maculata* (**Table 3.7**) and the organic fraction of *C. intermedia* (**Table 3.6**) dose-dependently decreased lipid content in differentiated 3T3-L1 adipocytes, whereas treatment with the aqueous fraction of *C. subternata* decreased lipid content at the highest concentrations only (**Table 3.5**). No significant effect on lipid content was observed in adipocytes treated with the organic fractions of *C. subternata* (**Table 3.5**) and *C. maculata* (**Table 3.7**) and the aqueous fraction of *C. intermedia* (**Table 3.6**). Cell viability as assessed with the MTT assay, was increased by the aqueous and organic fractions of *C. subternata* (**Table 3.5**) and *C. intermedia* (at 50 and 100 µg/mL) (**Table 3.6**), while no significant effect was observed in adipocytes treated with the aqueous and organic fractions of *C. maculata* (**Table 3.7**). Assessment of cell viability using the ATP assay showed that treatment with the aqueous and organic fraction of *C. subternata* did not affect ATP content (**Table 3.5**). The aqueous fraction of *C. intermedia* (**Table 3.6**) and the organic fraction of *C. maculata* (**Table 3.7**) decreased ATP content, whereas no effect on ATP content was observed in adipocytes treated with the organic fraction of *C. intermedia* (**Table 3.6**) and the aqueous fraction of *C. maculata* (**Table 3.7**).

The mRNA expression of *HSL*, *PPAR γ* and *UCP3* were increased in *C. intermedia* treated adipocytes compared to control adipocytes (**Table 3.8**), whereas no changes were observed in the protein expression of *PPAR γ* and *PPAR α* in adipocytes treated with the organic fraction of *C. intermedia* (**Table 3.9**). *In vivo* studies showed that the organic fraction of *C. intermedia* decreased body weight gain in obese *Lepr^{db/db}* mice without modulation of food and water consumption and glucose metabolism. Treatment with the organic fraction of *C. intermedia* did not affect gene expression in sWAT, gWAT and iBAT (**Tables 3.10** and **3.11**) of *Lepr^{db/db}* mice although the mRNA expression of *FGF2* was increased in gWAT of *Lepr^{db/db}* mice treated with the organic fraction of *C. intermedia* (**Table 3.10**). A number of changes in gene expression between the obese *Lepr^{db/db}* and *Lepr^{db/+}* mice were observed (**Tables 3.10** and **3.11**).

Table 3.5 Summary of *in vitro* results for *C. subternata*.

Experimental Assay	Aqueous fraction				Organic fraction			
	1 µg/mL	10 µg/mL	50 µg/mL	100 µg/mL	1 µg/mL	10 µg/mL	50 µg/mL	100 µg/mL
Oil Red O	↓11	↓ 12	↓ 17*	↓ 25***	↓ 9	↓ 11.5	↓ 12	↓ 12
MTT	↑16.6*	↑17.5*	↑22.9***	↑27***	↑27.8***	↑30.8***	↑32***	↑37***
ATP	↓2	↑4	↓9.5	↓15	↓11	↓6.4	↓11	↓12

↓: Decrease in percentage (%) vs. control

↑: Increase in percentage (%) vs. control

Significance depicted as: *P < 0.05, **P < 0.01 and ***P < 0.001 vs. vehicle control

nt: not tested

Table 3.6 Summary of *in vitro* results for *C. intermedia*.

Experimental Assay	Aqueous fraction				Organic fraction			
	1 µg/mL	10 µg/mL	50 µg/mL	100 µg/mL	1 µg/mL	10 µg/mL	50 µg/mL	100 µg/mL
Oil Red O	↓ 10	↓ 12.1	↓ 13	↓ 14.1	↓ 12.5	↓ 18**	↓ 23***	↓ 27***
MTT	↓0.2	↑11	↑24.7***	↑22***	↑7.6	↑14.3	↑30.4***	↑21.8***
ATP	↓6	↓10.4	↓21**	↓19.2*	↓6	↑1.5	↓4	↓5

↓: Decrease in percentage (%) vs. control

↑: Increase in percentage (%) vs. control

Significance depicted as: *P < 0.05, **P < 0.01 and ***P < 0.001 vs. vehicle control

nt: not tested

Table 3.7 Summary of *in vitro* results for *C. maculata*.

Experimental Assay	Aqueous fraction				Organic fraction			
	1 µg/mL	10 µg/mL	50 µg/mL	100 µg/mL	1 µg/mL	10 µg/mL	50 µg/mL	100 µg/mL
Oil Red O	↓ 16*	↓ 18**	↓ 21***	↓ 29***	↓ 12	↓ 10.3	↓ 12.2	↓ 14.4
MTT	↑ 2.6	↑ 6	↑ 7.7	↑ 10	↓ 4.3	↑ 5	↑ 14.3	↑ 8.8
ATP	↑ 13	↑ 13	↑ 14.6	↑ 2	↓ 18*	↓ 24**	↓ 30***	↓ 34*

↓: Decrease in percentage (%) vs. control

↑: Increase in percentage (%) vs. control

Significance depicted as: *P < 0.05, **P < 0.01 and ***P < 0.001 vs. vehicle control

nt: not tested

Table 3.8 Summary of *in vitro* mRNA gene expression results.

Genes	Organic <i>C. intermedia</i> fraction
ACACA	↓ 0.8
ADIPOQ	↔
CREB1	↑ 1.6
CPT1α	↔
CEBPα	↓ 0.8
Cs	↔
FABP4	↓ 0.7
FASN	↓ 0.8
FGF2	↑ 1.3
GATA2	↑ 1.6
GLUT4	↔
G6PC	↑ 1.6
HSL	↑ 1.6*
IRS1	↑ 1.3
LPL	↓ 0.7
PPARα	↑ 1.15
PPARγ	↑ 1.3*
PGC1α	↑ 1.2
AMPK	↑ 1.4
SIRT1	↑ 1.5
SIRT3	↓ 0.7
SCD1	↔
SREBF1	↔
UCP2	↑ 1.3
UCP3	↑ 1.5*

↓: Decrease in fold change vs. control

↑: Increase in fold change vs. control

↔: No significant fold change vs. control

Significance depicted as: *P < 0.05 vs. vehicle control

Table 3.9 Summary of *in vitro* protein expression results.

Proteins	Organic <i>C. intermedia</i> fraction
PPAR α	↓ 0.86
PPAR γ	↔

↓: Decrease in fold change vs. control

↔: No significant fold change vs. control

Table 3.10 Summary of mRNA gene expression results in sWAT and gWAT.

Genes	sWAT		gWAT	
	Lepr ^{db/+} / Lepr ^{db/db}	Lepr ^{db/db} / Lepr ^{db/db} + (351.5 mg/kg)	Lepr ^{db/+} / Lepr ^{db/db}	Lepr ^{db/db} / Lepr ^{db/db} + (351.5 mg/kg)
<i>ACACA</i>	↓ 10.5***	↔	↓ 4.5***	↓ 1.2
<i>ADIPOQ</i>	↔	↔	↔	↓ 1.48
<i>CREB1</i>	↓ 2.7***	↑ 1.19	↓ 2.4*	↑ 1.57
<i>CEBPα</i>	↓ 1.28	↑ 1.22	↓ 1.9	↑ 1.76
<i>FABP4</i>	↑ 1.7*	↔	↑ 1.86	↓ 2.0
<i>FASN</i>	↓ 16.2***	↑ 1.14	↓ 6.17***	↑ 1.16
<i>FGF2</i>	↓ 1.7	↑ 1.13	↓ 1.45	↑ 1.4*
<i>GATA2</i>	↓ 1.29	↓ 1.27	↔	↓ 1.1
<i>G6PC</i>	↑ 25.0	↓ 1.2	↑ 5.3	↓ 2.16
<i>HSL</i>	↓ 1.27	↔	↓ 1.65*	↑ 1.52
<i>LPL</i>	↑ 1.14	↓ 1.3	↔	↓ 1.28
<i>PPARα</i>	↓ 1.9	↔	↑ 1.13	↔
<i>PPARγ</i>	↔	↔	↓ 1.39	↔
<i>PGC1α</i>	↓ 3.4*	↓ 1.8	↓ 1.38	↑ 1.74
<i>AMPK</i>	↓ 1.7	↓ 1.18	↑ 3.34	↓ 4.68
<i>SIRT1</i>	↓ 1.13	↓ 1.18	↑ 1.64	↓ 1.23
<i>SIRT3</i>	↓ 1.12	↑ 1.15	↑ 2.29	↓ 1.76
<i>SCD1</i>	↓ 2.3**	↔	↓ 2.17*	↑ 1.3
<i>SREBF1</i>	↓ 1.53*	↔	↑ 1.84	↓ 1.4
<i>TNFα</i>	↓ 1.18	↑ 1.2	↑ 17.8	↓ 3.9
<i>UCP1</i>	↓ 13.7	↑ 1.97	↓ 6.6	↑ 2.8
<i>UCP2</i>	↑ 1.2	↔	↑ 2.24**	↑ 1.12
<i>UCP3</i>	↓ 5.3***	↔	↓ 2.23	↑ 1.14

↓: Decrease in fold change vs. control

↑: Increase in fold change vs. control

↔: No significant fold change vs. control

Fold change calculated by dividing highest value (relative mRNA expression) with the lowest value
Significance depicted as: *P < 0.05, **P < 0.01 and ***P < 0.001 vs. vehicle control

Table 3.11 Summary of mRNA gene expression results in iBAT.

Genes	Lepr ^{db/+} / Lepr ^{db/db}	Lepr ^{db/db} / Lepr ^{db/db} + (351.5 mg/kg)
<i>CPT1α</i>	↑ 2.4**	↑ 1.14
<i>PPARα</i>	↑ 1.22	↑ 1.16
<i>PPARγ</i>	↓ 1.28	↔
<i>PGC1α</i>	↓ 1.13	↑ 1.13
<i>AMPK</i>	↓ 1.47**	↔
<i>SIRT1</i>	↔	↔
<i>SIRT3</i>	↓ 1.34*	↔
<i>UCP1</i>	↓ 1.84**	↔
<i>UCP2</i>	↑ 3.5***	↑ 1.17
<i>UCP3</i>	↓ 1.84**	↔

↓: Decrease in fold change vs. control

↑: Increase in fold change vs. control

↔: No significant fold change vs. control

Fold change calculated by dividing highest value (relative mRNA expression) with the lowest value
Significance depicted as: *P < 0.05, **P < 0.01 and ***P < 0.001 vs. vehicle control

CHAPTER 4

RESULTS 2

The results for fractionation of the organic fraction of *C. intermedia* into four fractions using high performance counter-current chromatography, and the phenolic analysis and *in vitro* testing of these fractions are presented in this chapter.

The results in this section describe bioactivity guided fractionation of the organic fraction of *C. intermedia* to identify anti-obesity phenolic compounds. The organic fraction of *C. intermedia* was fractionated into four major fractions (CCC fractions) using HPCCC. The phenolic composition of the CCC fractions was determined by LC-MS/MS and quantitative HPLC-DAD. Thereafter, the effect of the CCC fractions on lipid content, TG accumulation, lipolysis and cytotoxicity in 3T3-L1 pre-adipocytes and 3T3-L1 adipocytes were determined using the ORO, TG, glycerol release, MTT and ATP assays, respectively. The effect of the optimized concentrations of the CCC fractions on the expression of genes relevant to lipid, glucose and energy metabolism in 3T3-L1 adipocytes was measured using qRT-PCR. Western blot analysis was used to assess the effect of the CCC fractions on PPAR γ and PPAR α protein expression.

4.1 Fractionation of the organic fraction of *C. intermedia* and phenolic analysis

The organic fraction of *C. intermedia* was separated into smaller fractions to facilitate the identification of compounds responsible for its anti-obesity effects using HPLC. Fractionation of the organic fraction of *C. intermedia* resulted in four major fractions, and for the purpose of this study these fractions are referred to as CCC fractions 1- 4 (F1 - 4) (**Fig. 4.1**). Fractionation resulted in four different CCC fractions enriched in specific polyphenols compared to the original organic *C. intermedia* fraction. LC-MS/MS and qHPLC-DAD showed that CCC F1 retained iriflophenone-3-C- β -D-glucoside-4-O- β -D-glucoside (1.943 g/100g organic fraction) and vicenin-2 (0.932 g/100g organic fraction) (**Fig. 4.2** and **Table 4.1**), whereas CCC F2 was enriched in iriflophenone-3-C- β -D-glucoside (1.689 g/100g organic fraction), hesperidin (12.714 g/100g organic fraction) and eriodictyol-O-deoxyhexoside-O-hexoside (5.636 g/100g organic fraction) (**Fig. 4.3** and **Table 4.1**). CCC F3 was enriched with the xanthenes, mangiferin (44.281 g/100g organic fraction) and isomangiferin (12.863 g/100g organic fraction) (**Fig. 4.4** and **Table 4.1**). The flavanone, neoponcirin (15.758 g/100g organic fraction) was retained in CCC F4 (**Fig. 4.5** and **Table 4.1**).

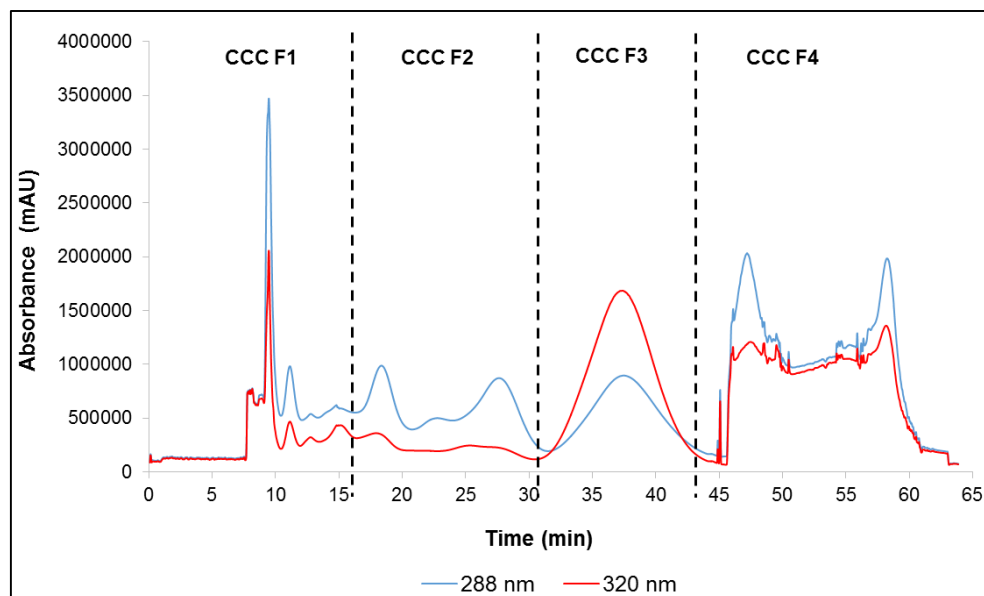


Figure 4.1 HPLC chromatographic profile of the organic fraction of *C. intermedia*. The organic fraction of *C. intermedia* was separated into four major fractions, indicated by the dashed lines, using HPLC.

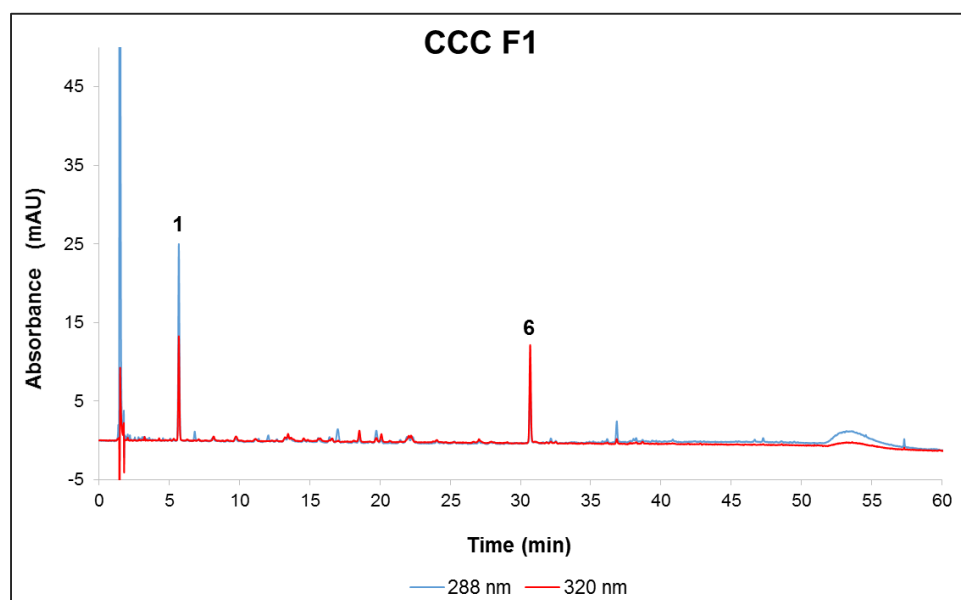


Figure 4.2 Phenolic profile showing the major phenolic compounds of CCC fraction 1. CCC F1 was isolated from the organic fraction of a 40% aqueous methanol extract of *C. intermedia* using high performance counter-current chromatography. The first peak (not numbered) represents ascorbic acid, which was added to prevent oxidation. Peak 1: Iriflophenone-3-C- β -D-glucoside-4-O- β -D-glucoside; 6: Vicenin-2.

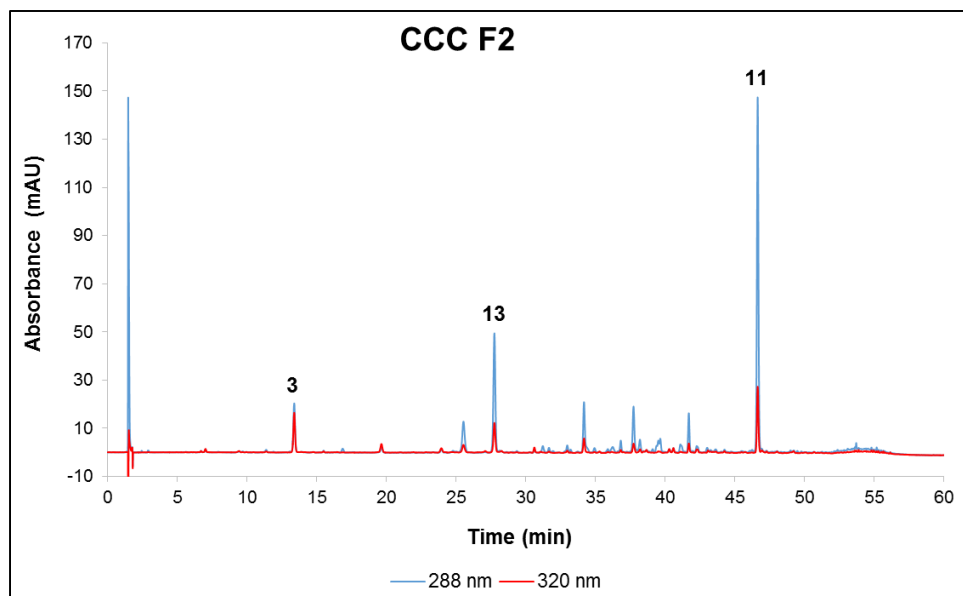


Figure 4.3 Phenolic profile showing the major phenolic compounds of CCC fraction 2. CCC F2 was isolated from the organic fraction of a 40% aqueous methanol extract of *C. intermedia* using high performance counter-current chromatography. The first peak (not numbered) represents ascorbic acid, which was added to prevent oxidation. Peak **3**: Iriflophenone-3-C- β -D-glucoside; **11**: Hesperidin; **13**: Eriodictyol-O-deoxyhexoside-O-hexoside.

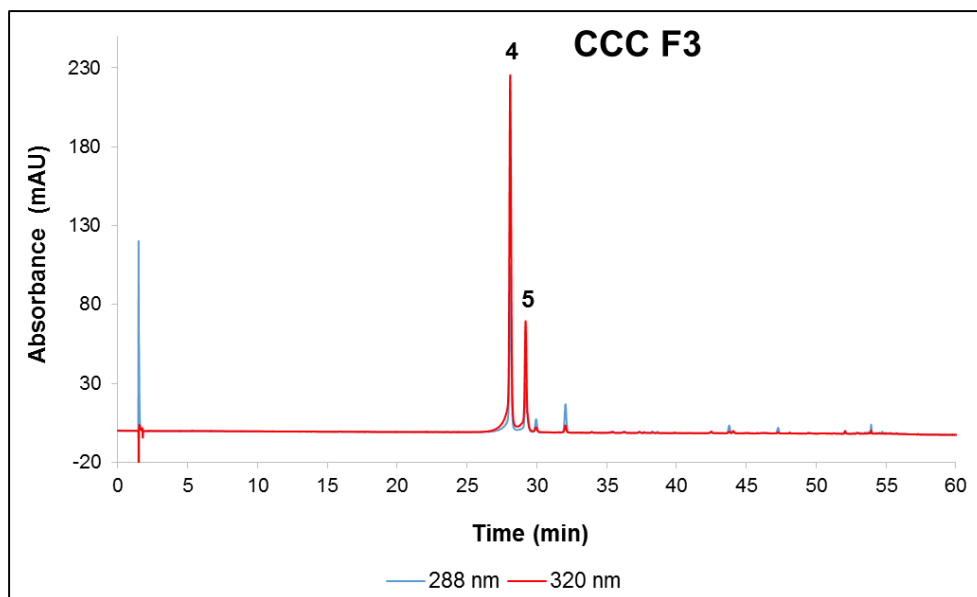


Figure 4.4 Phenolic profile showing the major phenolic compounds of CCC fraction 3. CCC F3 was isolated from the organic fraction of a 40% aqueous methanol extract of *C. intermedia* using high performance counter-current chromatography. The first peak (not numbered) represents ascorbic acid, which was added to prevent oxidation. Peak **4**: Mangiferin; **5**: Isomangiferin.

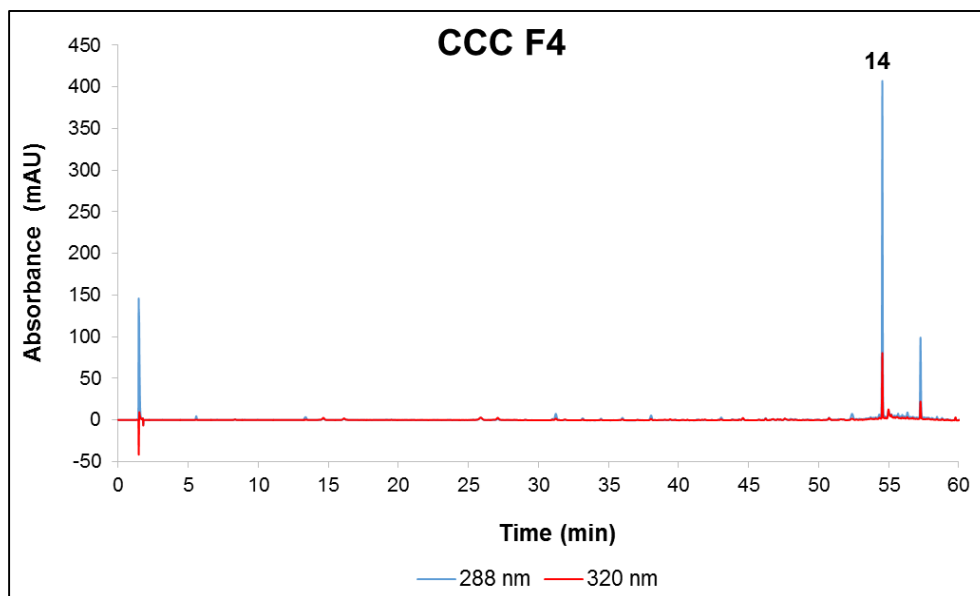


Figure 4.5 Phenolic profile showing the major phenolic compounds of CCC fraction 4. CCC F4 was isolated from the organic fraction of a 40% aqueous methanol extract of *C. intermedia* using high performance counter-current chromatography. The first peak (not numbered) represents ascorbic acid, which was added to prevent oxidation. Peak **14**: Neoponcirin.

Table 4.1 Quantification of major phenolic compounds (g/100 g organic fraction) in the CCC fractions of the organic fraction of a 40% aqueous methanol extract of *C. intermedia* by qHPLC-DAD.

Compound ^a	Organic fraction	CCC F1	CCC F2	CCC F3	CCC F4
Iriflophenone-3-C-β-D-glucoside-4-O-β-D-glucoside (1)	0.674	1.943	nd	nd	nd
Iriflophenone-3-C-β-D-glucoside (3)	0.565	nd ^c	1.689	nd	nd
Mangiferin (4)	8.259	nd	nd	44.281	nd
Isomangiferin (5)	2.181	nd	nd	12.863	nd
Vicenin-2 (6)	0.388	0.932	nd	nd	nd
Hesperidin (11)	3.318	nd	12.714	nd	nd
Eriodictyol-O-deoxyhexoside-O-hexoside ^b (13)	1.484	nd	5.636	nd	nd
Neoponcirin (14)	3.609	nd	nd	nd	15.758

^a Peak number on HPLC chromatogram in brackets

^b Expressed as eriocitrin equivalent

^c nd - polyphenols not detected or only present in trace amounts

4.2 Effect of CCC fractions in differentiating 3T3-L1 pre-adipocytes

4.2.1 Lipid accumulation

The ability of the CCC fractions to inhibit lipid accumulation in differentiating 3T3-L1 pre-adipocytes was assessed by treating cells with the CCC fractions at various concentrations (1, 10, 50 and 100 µg/mL), daily for eight days and measuring lipid content using the ORO assay. The different CCC fractions exerted varied effects on lipid accumulation. Compared to control adipocytes, CCC F1 inhibited lipid accumulation in differentiating 3T3-L1 pre-adipocytes by $33.5 \pm 3.6\%$ ($P < 0.001$) and $19.2 \pm 3.6\%$ ($P < 0.01$) at 1 and 10 µg/mL (**Fig. 4.6A**), whereas no significant effect on lipid accumulation was observed in response to treatment with CCC F2 (**Fig. 4.6B**). CCC F3 inhibited lipid accumulation in differentiating pre-adipocytes by $24.1 \pm 3.1\%$ ($P < 0.01$), $22.9 \pm 3.3\%$ ($P < 0.01$), $20.6 \pm 4.1\%$ ($P < 0.05$) and $23.9 \pm 5.9\%$ ($P < 0.01$) at 1, 10, 50 and 100 µg/mL, respectively compared to control adipocytes (**Fig. 4.6C**). Furthermore, CCC F4 reduced lipid accumulation in differentiating 3T3-L1 pre-adipocytes by $27.4 \pm 3.8\%$ ($P < 0.001$), $15.3 \pm 4.1\%$ ($P < 0.05$) and $15 \pm 2.8\%$ ($P < 0.05$) at 1, 10 and 50 µg/mL, respectively compared to control adipocytes (**Fig. 4.6D**). Treatment with mangiferin, also decreased lipid accumulation ($P < 0.01$, $P < 0.001$) compared to control adipocytes. The results for the ORO assay in differentiating pre-adipocytes are summarized in **Table 4.2**.

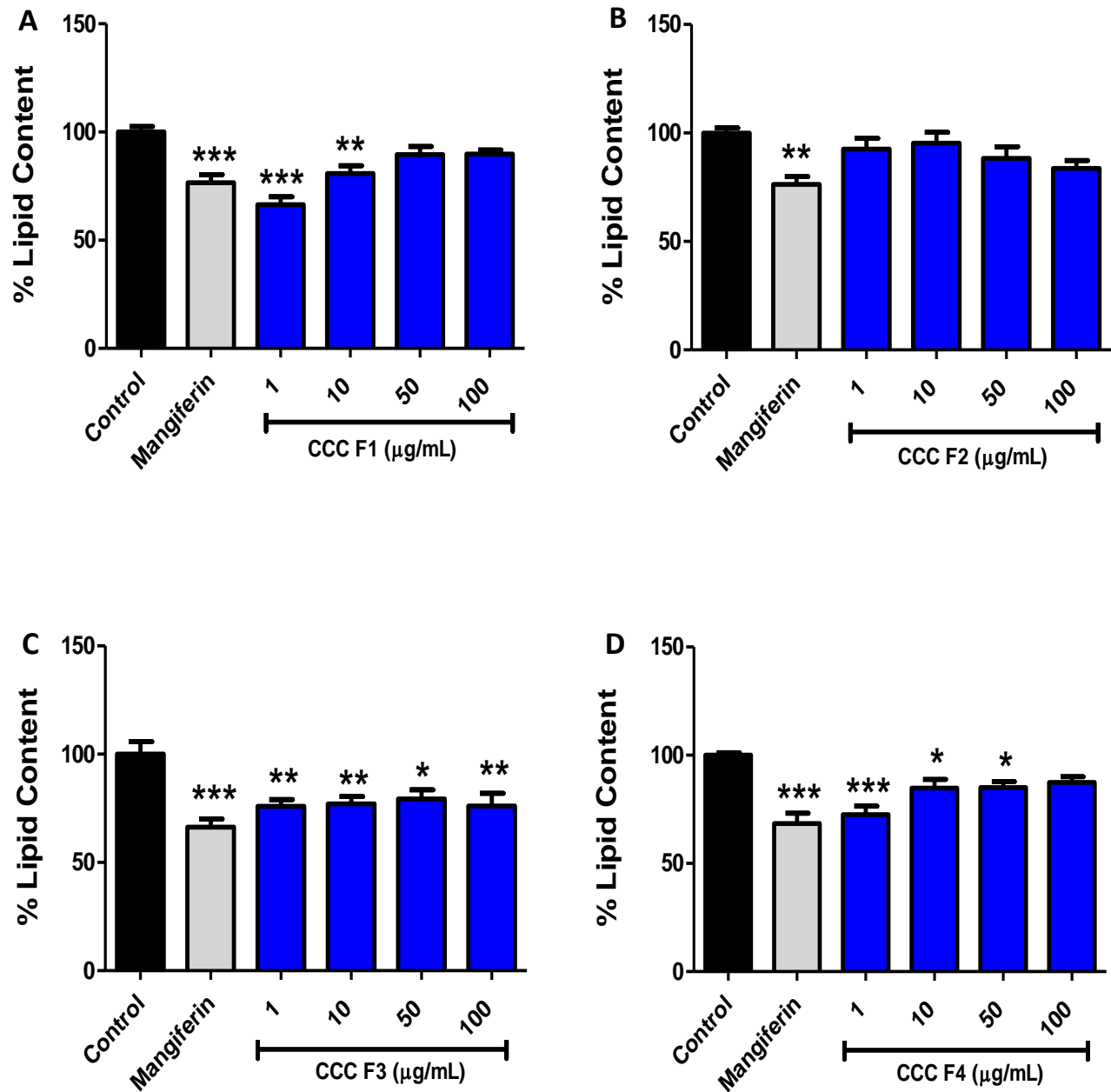


Figure 4.6 The effect of CCC F1, CCC F2, CCC F3 and CCC F4 on lipid accumulation in differentiating 3T3-L1 pre-adipocytes. Differentiating 3T3-L1 pre-adipocytes were exposed to the vehicle control, CCC F1 (A), CCC F2 (B), CCC F3 (C) or CCC F4 (D) (at various concentrations), or mangiferin daily for eight days. Lipid content was quantified using Oil Red O staining. Results are expressed as a percentage relative to the vehicle control (set at 100%), and are shown as mean \pm SEM for three independent experiments, each performed in triplicate. Significance is depicted as *P < 0.05, **P < 0.01 and ***P < 0.001 vs. vehicle control.

4.2.2 Triglyceride content

In addition to the ORO assay, intracellular TG quantification was used to assess the effect of the CCC fractions on lipid accumulation. Treatment of differentiating pre-adipocytes with CCC F1, CCC F2, CCC F3 and CCC F4 did not have any significant effect on TG accumulation compared to untreated controls (**Figs. 4.7A - D**). Similarly, mangiferin did not demonstrate any significant effects on TG accumulation.

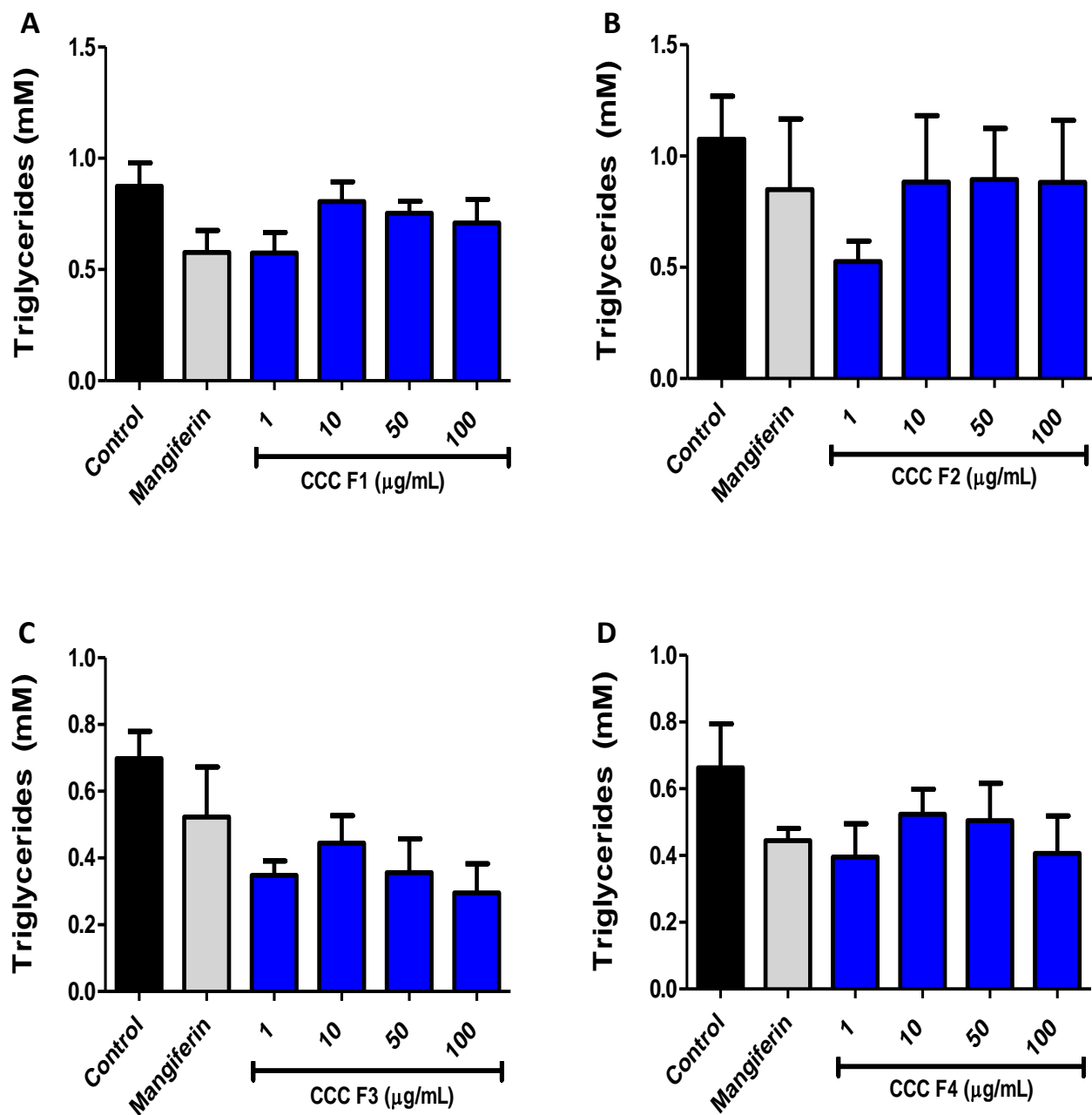


Figure 4.7 The effect of CCC F1, CCC F2, CCC F3 and CCC F4 on triglyceride content in differentiating 3T3-L1 pre-adipocytes. Differentiating 3T3-L1 pre-adipocytes were exposed to the vehicle control, CCC F1 (A), CCC F2 (B), CCC F3 (C) or CCC F4 (D) (at various concentrations), or mangiferin daily for eight days. Intracellular triglycerides were quantified using a triglyceride quantification assay kit. Results are expressed as the concentration derived from the standard curve, and are shown as mean \pm SEM for three independent experiments, each performed in triplicate.

4.2.3 ATP content

The effect of CCC fractions on cell viability was assessed by treating differentiating 3T3-L1 pre-adipocytes with various concentrations of these fractions (1, 10, 50 and 100 µg/mL), daily for eight days and measuring intracellular ATP content. Varying effects on cell viability were observed for the different CCC fractions. Compared to the untreated controls, treatment with CCC F1 decreased ATP content by $24.4 \pm 2.9\%$ ($P < 0.001$) at 100 µg/mL (**Fig. 4.8A**), whereas CCC F3 decreased ATP content by $21.5 \pm 4.2\%$ ($P < 0.05$) at 100 µg/mL (**Fig. 4.8C**). CCC F2 and CCC F4 had no significant effect on cell viability compared to untreated controls (**Figs. 4.8B** and **4.8D**). Mangiferin increased the intracellular ATP content ($P < 0.05$) compared to control adipocytes. The results for the ATP assay in differentiating pre-adipocytes are summarized in **Table 4.2**.

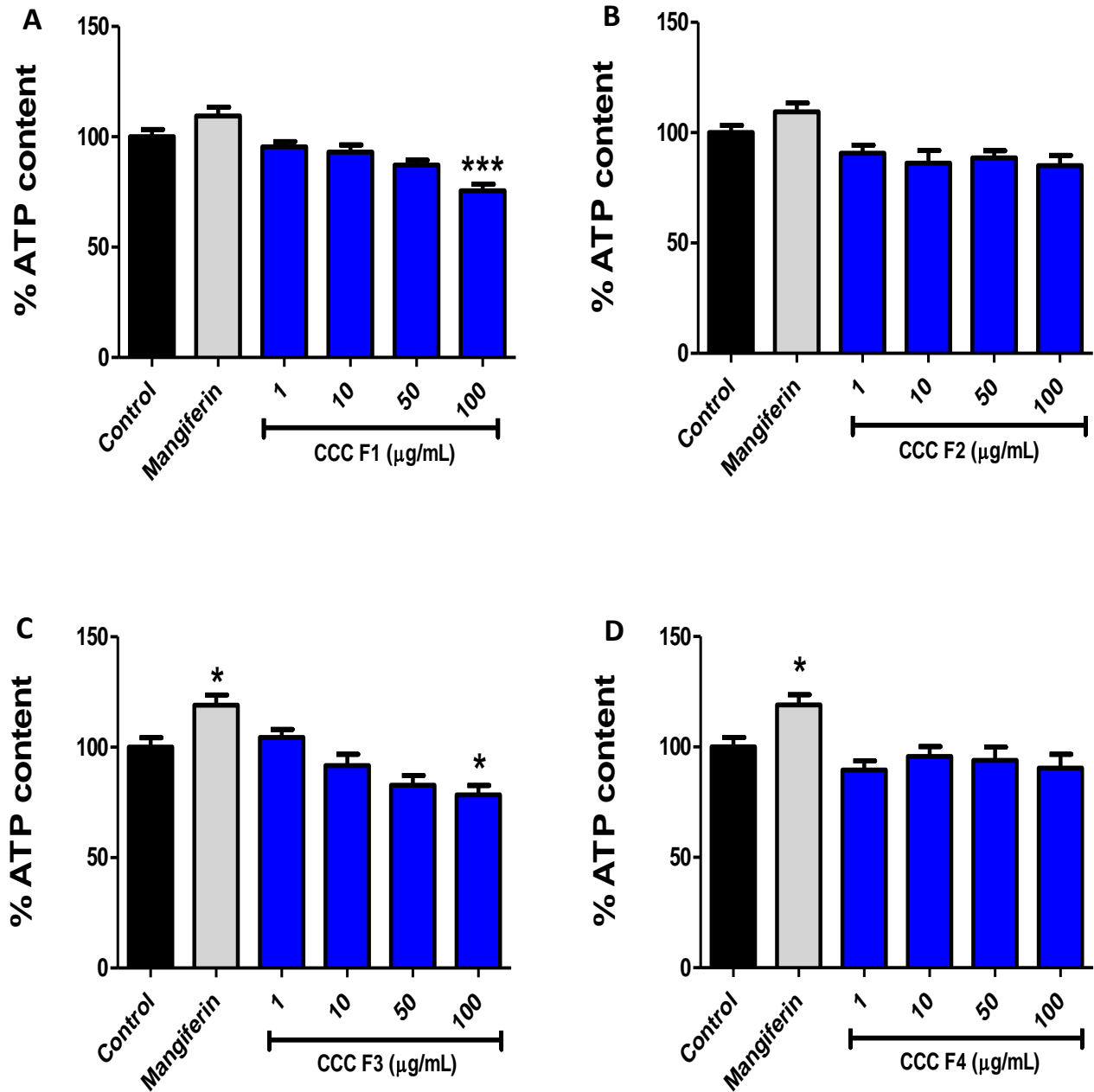


Figure 4.8 The effect of CCC F1, CCC F2, CCC F3 and CCC F4 on intracellular ATP content in differentiating 3T3-L1 pre-adipocytes. Differentiating 3T3-L1 pre-adipocytes were exposed to the vehicle control, CCC F1 (A), CCC F2 (B), CCC F3 (C) or CCC F4 (D) (at various concentrations) or mangiferin daily for eight days. Intracellular ATP content was measured using a bioluminescence assay kit. Results are expressed as a percentage relative to the vehicle control (set at 100%) and are shown as mean \pm SEM for three independent experiments, each performed in triplicate. Statistical significance is depicted as * $P < 0.05$ and *** $P < 0.001$ vs. vehicle control.

4.3 Effect of CCC fractions in mature 3T3-L1 adipocytes

4.3.1 Lipid content

To evaluate the ability of the CCC fractions on lipid content, differentiated 3T3-L1 adipocytes were treated with the CCC fractions at various concentrations (1, 10, 50 and 100 µg/mL) for 24 hours. The ability of these fractions to reduce intracellular lipid content was assessed using ORO staining. Similar to adipogenesis, the effect of treatment on lipid content varied for the different fractions. Compared to control adipocytes, CCC F1 decreased lipid content by $27.1 \pm 4.8\%$ at 100 µg/mL ($P < 0.01$) (**Fig. 4.9A**). Similarly, CCC F2 decreased lipid content by $23 \pm 5.3\%$ ($P < 0.01$) at 100 µg/mL compared to control adipocytes (**Fig. 4.9B**). No significant effect was observed on lipid content in adipocytes treated with CCC F3 (**Fig. 4.9C**), whereas CCC F4 decreased lipid content by $23.4 \pm 2.0\%$ ($P < 0.05$) and $22.5 \pm 5.4\%$ ($P < 0.05$) at 10 and 100 µg/mL, respectively compared to control adipocytes (**Fig. 4.9D**). Both isoproterenol and mangiferin decreased lipid content ($P < 0.05$, $P < 0.01$, $P < 0.001$) compared to control adipocytes. The results for the ORO assay in mature adipocytes are summarized in **Table 4.3**.

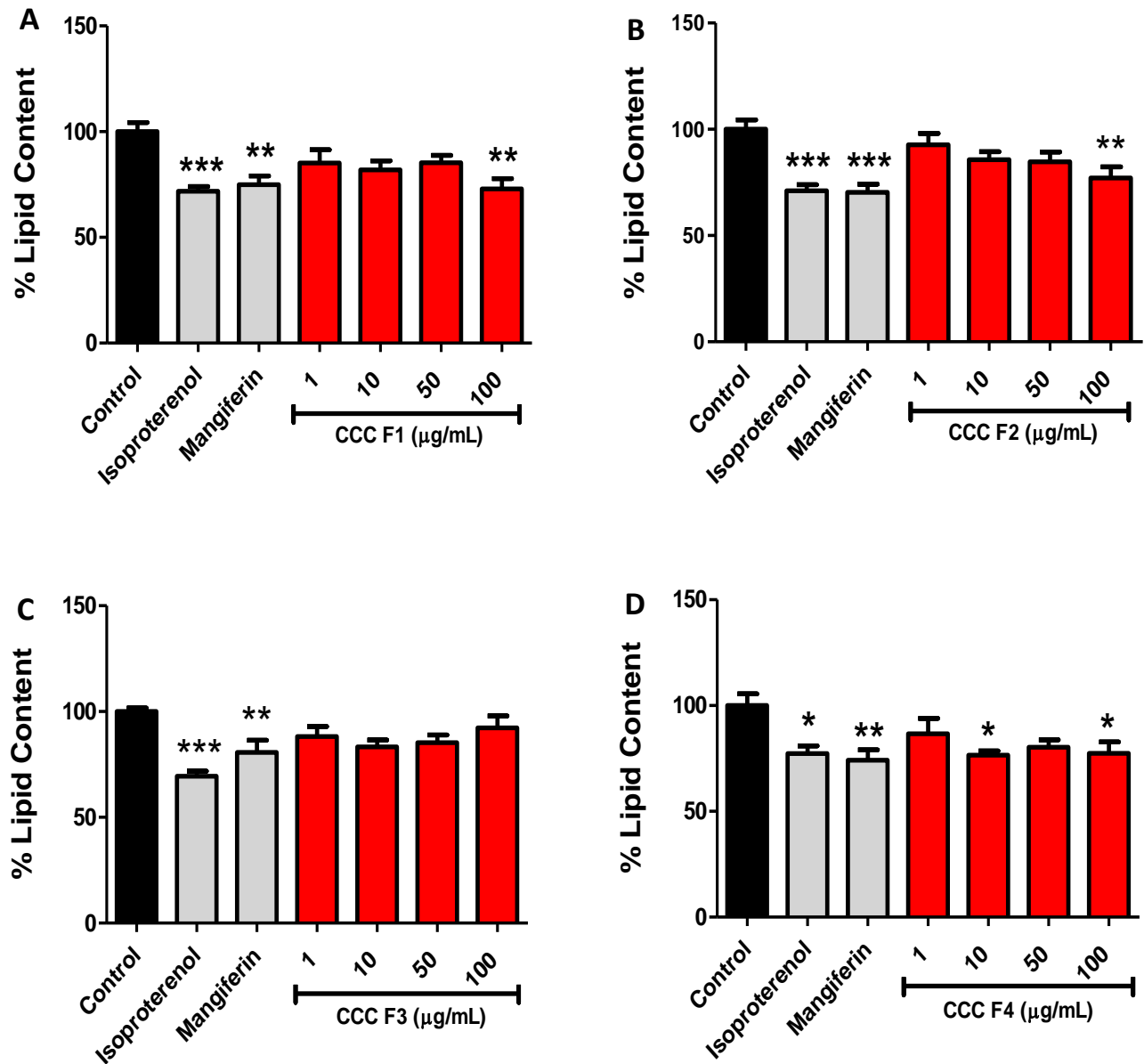


Figure 4.9 The effect of CCC F1, CCC F2, CCC F3 and CCC F4 on lipid content in differentiated 3T3-L1 adipocytes. Differentiated 3T3-L1 adipocytes were exposed to the vehicle control, CCC F1 (A), CCC F2 (B), CCC F3 (C) or CCC F4 (D) (at various concentrations), isoproterenol or mangiferin for 24 hours. Lipid content was quantified using Oil Red O staining. Results are expressed as the percentage relative to the vehicle control (set at 100%), and are shown as mean \pm SEM for three independent experiments, each performed in triplicate. Significance is depicted as * $P < 0.05$, ** $P < 0.01$ and *** $P < 0.001$ vs. vehicle control.

4.3.2 Glycerol Release

To evaluate the effect of the CCC fractions on lipolysis, differentiated 3T3-L1 adipocytes were treated with the CCC fractions at various concentrations (1, 10, 50 and 100 µg/mL) for 24 hours, and glycerol release, a marker of lipolysis, was assessed in culture supernatants. The four CCC fractions exhibited different effects on glycerol release. Compared to control adipocytes, CCC F1 increased glycerol release by $38.9 \pm 5.4\%$ ($P < 0.05$) and $39.1 \pm 13.6\%$ ($P < 0.05$) at 1 µg/mL and 50 µg/mL, respectively (**Fig. 4.10A**), whereas CCC F2 increased glycerol release by $46.3 \pm 13.6\%$ ($P < 0.05$) at 50 µg/mL (**Fig. 4.10B**). CCC F3 increased glycerol release by $24.6 \pm 3.0\%$ ($P < 0.05$) at 1 µg/mL compared to control adipocytes (**Fig. 4.10C**), while no significant effect was observed in adipocytes treated with CCC F4 (**Fig. 4.10D**). Isoproterenol increased glycerol release ($P < 0.001$), whereas mangiferin had no effect. The results for the glycerol release assay in mature adipocytes are summarized in **Table 4.3**.

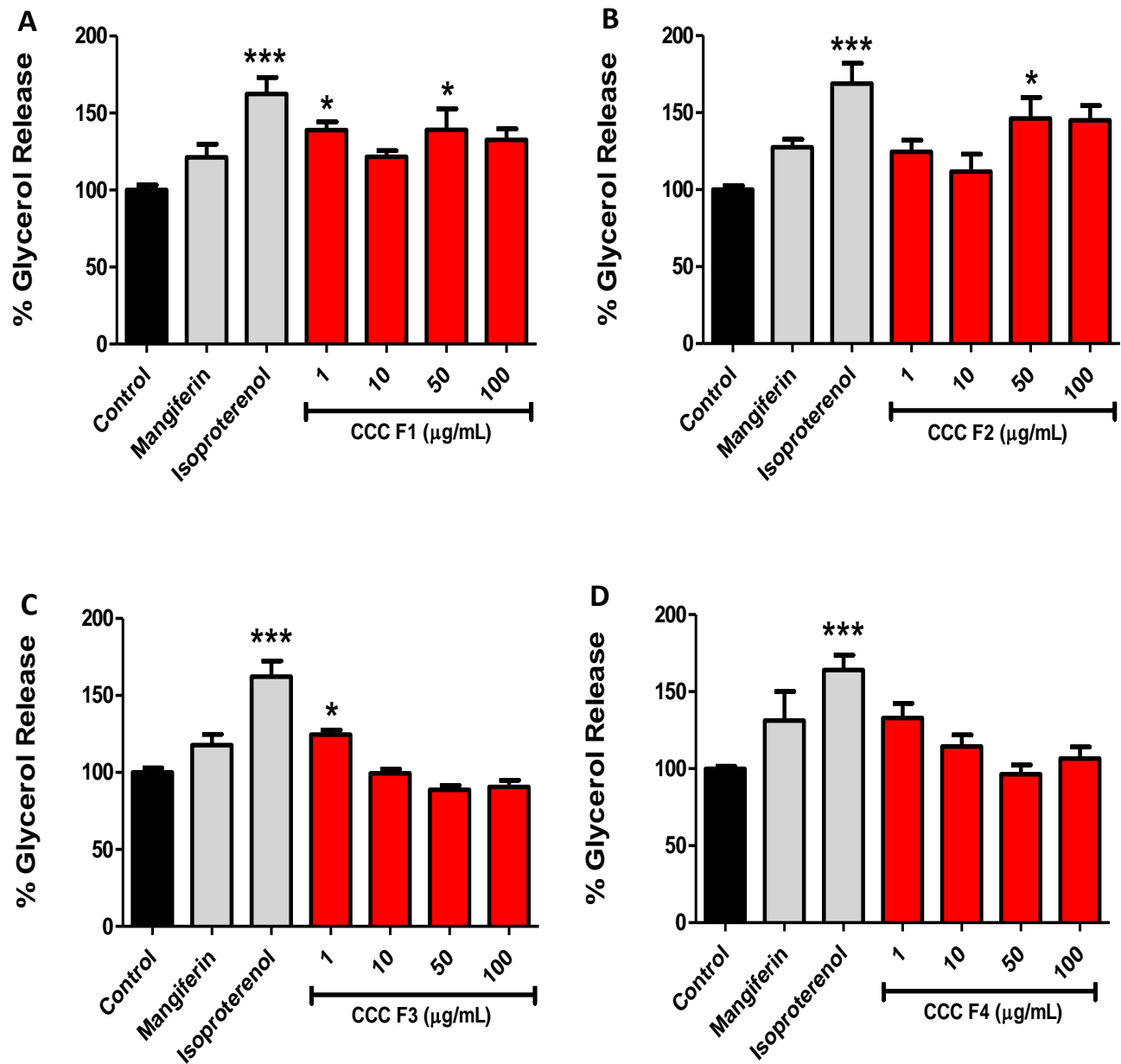


Figure 4.10 The effect of CCC F1, CCC F2, CCC F3 and CCC F4 on glycerol release in differentiated 3T3-L1 adipocytes. Differentiated 3T3-L1 adipocytes were exposed to the vehicle control, CCC F1 (A), CCC F2 (B), CCC F3 (C) or CCC F4 (D) (at various concentrations), isoproterenol or mangiferin for 24 hours. Glycerol release content was quantified using a free glycerol release assay kit. Results are expressed as the percentage relative to the vehicle control (set at 100%), and are shown as mean \pm SEM for three independent experiments, each performed in triplicate. Significance is depicted as * $P < 0.05$ and *** $P < 0.001$ vs. vehicle control.

4.3.3 ATP content

The effect of the CCC fractions on cell viability was assessed by treating differentiated 3T3-L1 adipocytes with various concentrations (1, 10, 50 and 100 µg/mL) of these fractions for 24 hours and measuring intracellular ATP content. As observed with lipid content, varying effects on cell viability were observed for the different CCC fractions. Treatment with CCC F1, CCC F2 and CCC F3 had no significant effect on cell viability as measured with the ATP assay, compared to control adipocytes (**Figs. 4.11A, 4.11B and 4.11C**). In contrast, CCC F4 increased ATP content by $9.3 \pm 3.8\%$ and 14.9 ± 4.9 ($P < 0.05$) at 50 and 100 µg/mL, respectively compared to control adipocytes (**Fig. 4.11D**). Both isoproterenol and mangiferin increased ATP content ($P < 0.05$, < 0.01 , < 0.001) compared to control adipocytes. Results for the ATP assay in mature adipocytes are summarized in **Table 4.3**.

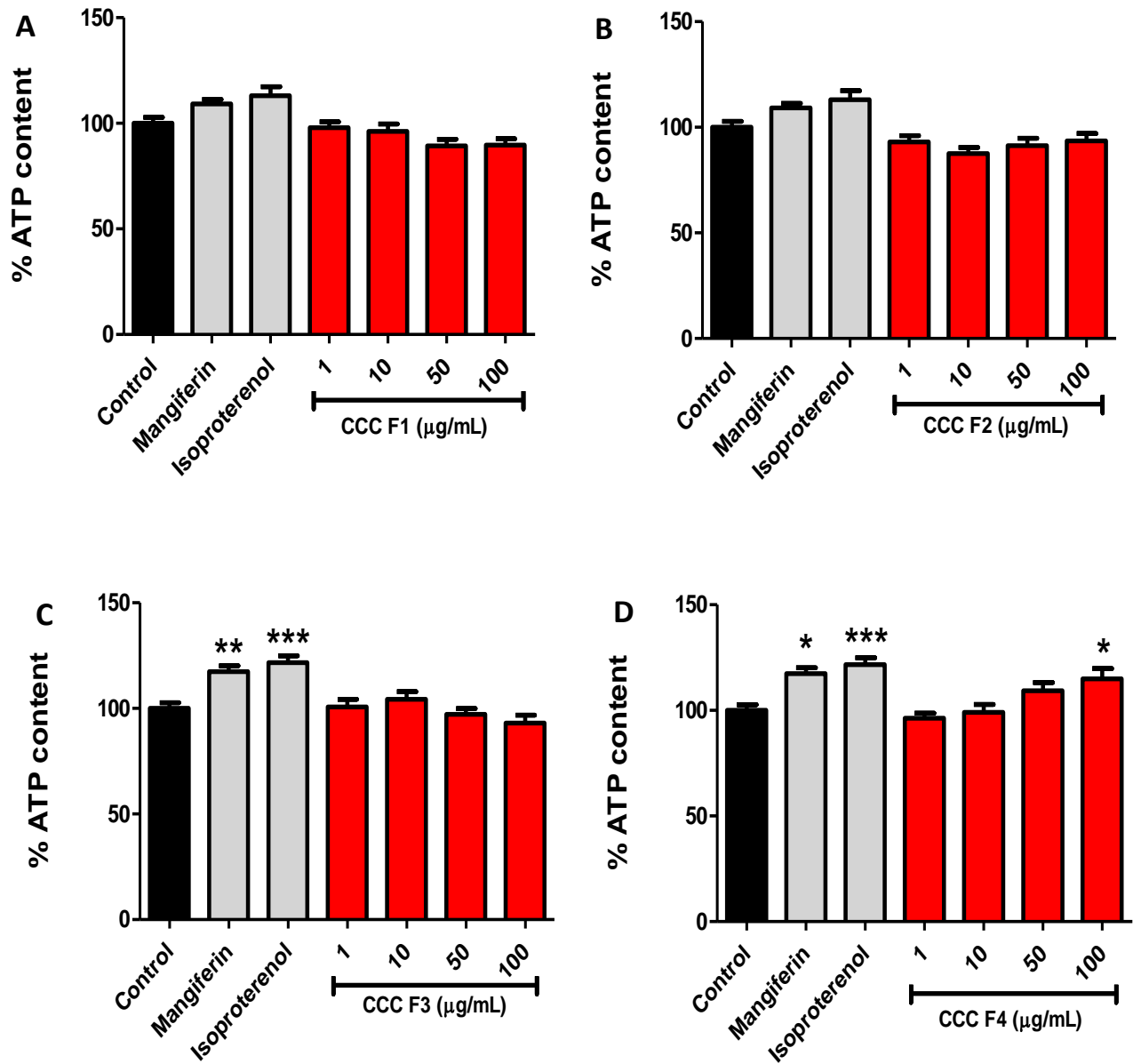


Figure 4.11 The effect of CCC F1, CCC F2, CCC F3 and CCC F4 on intracellular ATP content in differentiated 3T3-L1 adipocytes. Differentiated 3T3-L1 adipocytes were exposed to the vehicle control, CCC F1 (A), CCC F2 (B), CCC F3 (C) or CCC F4 (D) (at various concentrations) or mangiferin daily for eight days. Intracellular ATP content was measured using a bioluminescence assay kit. Results are expressed as a percentage relative to the vehicle control (set at 100%) and are shown as mean \pm SEM for three independent experiments, each performed in triplicate.

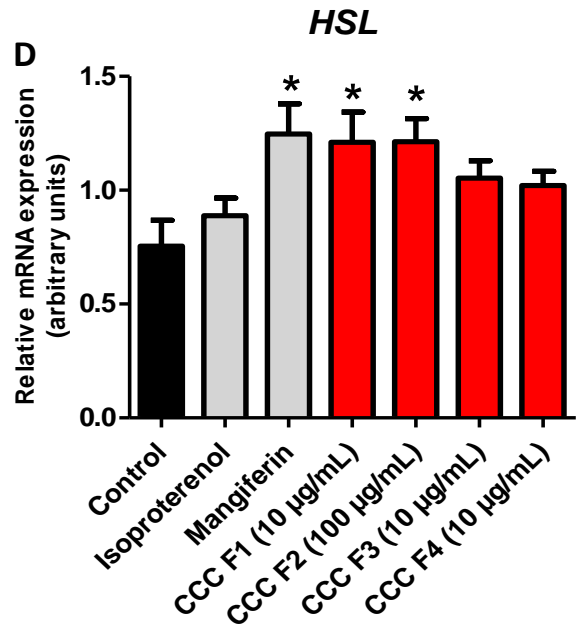
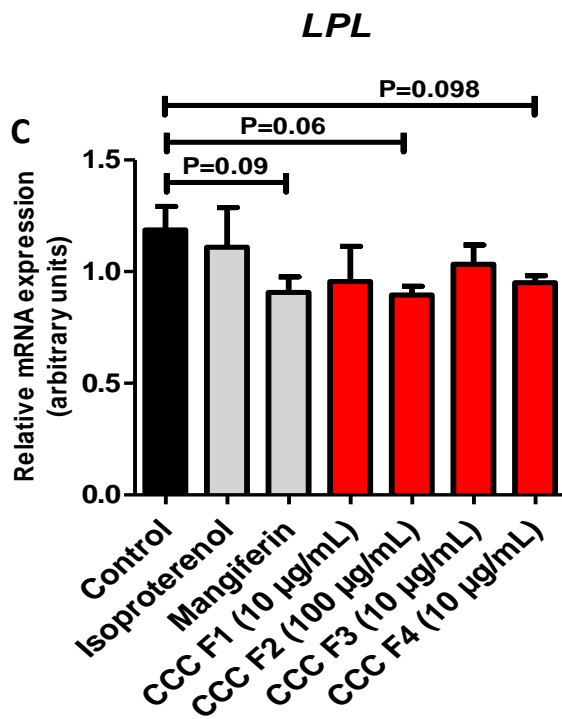
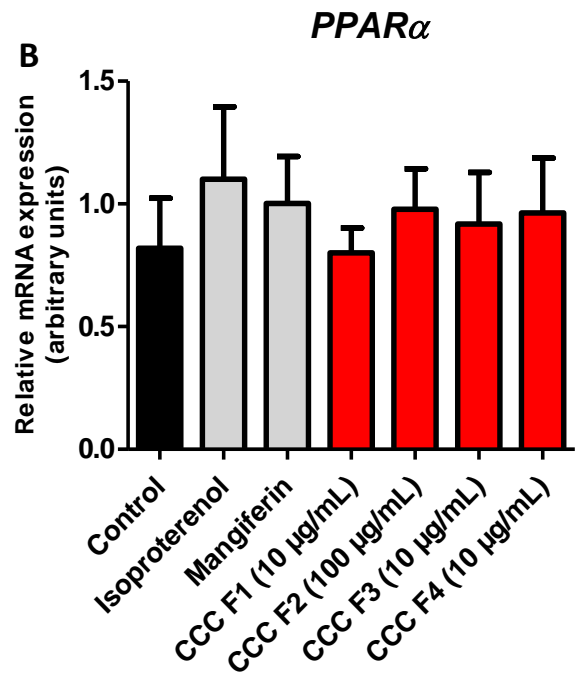
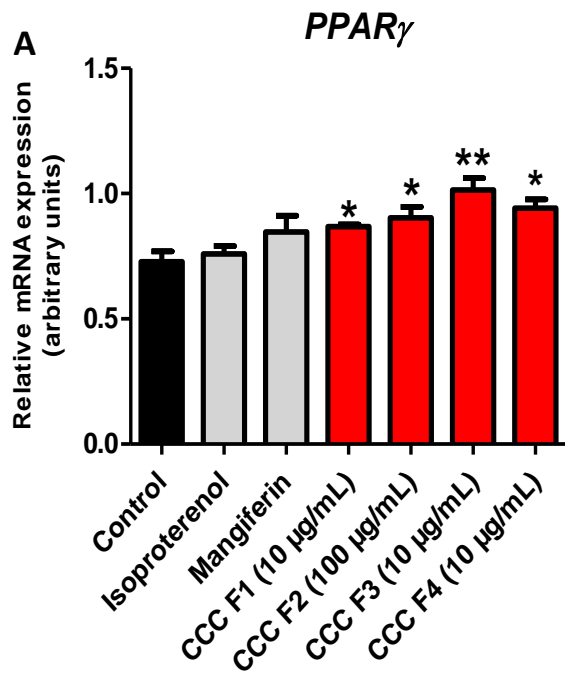
4.4 Effect of the CCC fractions on gene expression in mature 3T3-L1 adipocytes

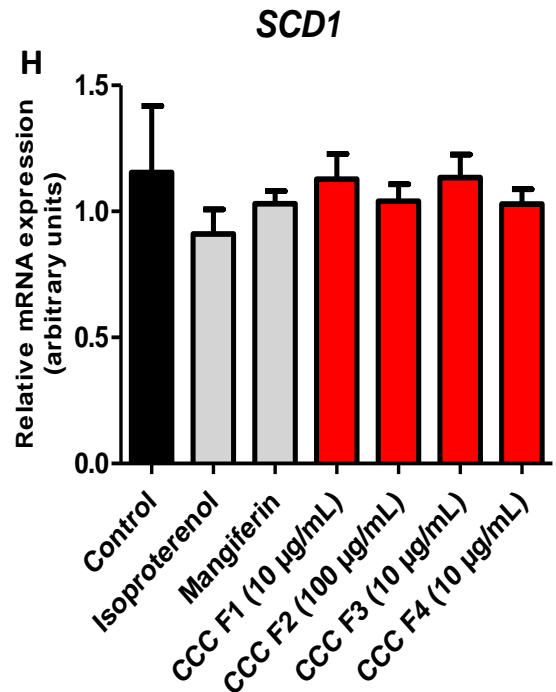
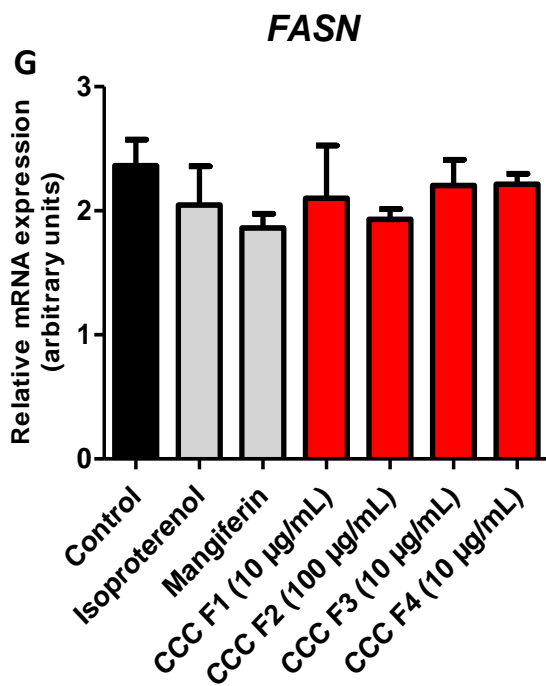
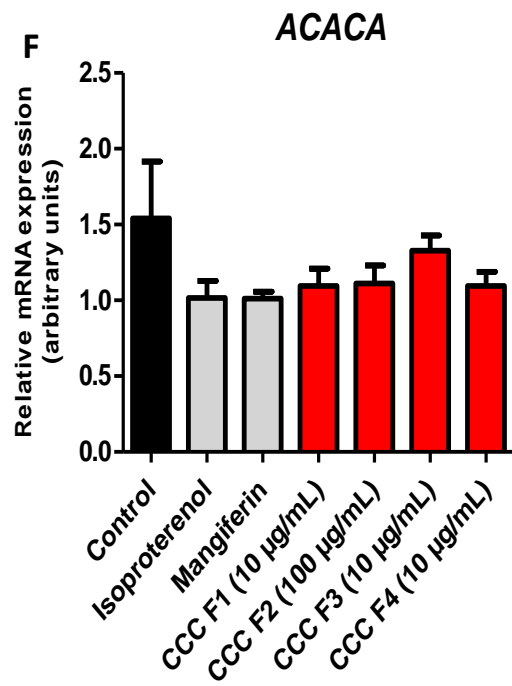
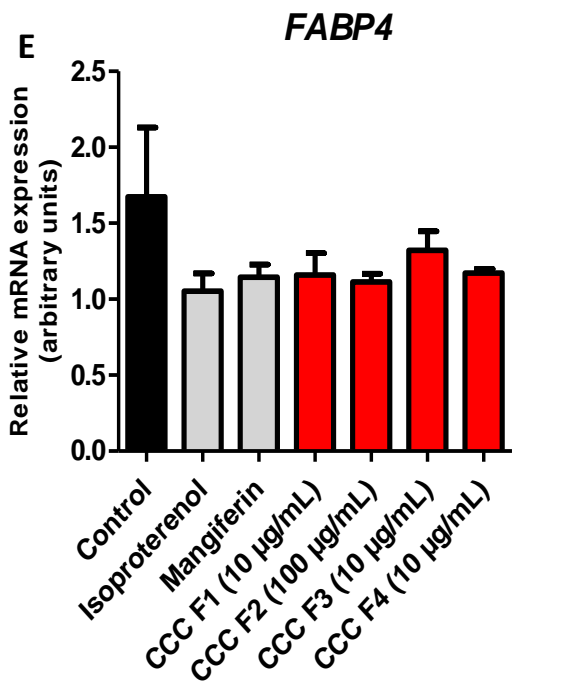
To investigate the molecular mechanisms whereby the CCC fractions mediated their functions, experiments were scaled up and the effect of these fractions on the expression of genes involved in lipid or fatty acid, glucose and energy metabolism was measured using qRT-PCR. The concentration of fractions with the highest bioactivity, without being cytotoxic, was used for gene expression experiments. NormFinder, showed beta-2 microglobulin (*B2M*) and the ribosomal protein L13a (*RPL13A*) to be the most stable genes amongst the seven candidate genes assessed (**Table 2.9, Chapter 2**), and therefore the combination of these genes was used for normalization of gene expression. Treatment of 3T3-L1 adipocytes with CCC F1, CCC F2, CCC F3 and CCC F4 increased the mRNA expression of *PPAR γ* by 1.19 fold ($P < 0.05$), 1.24 fold ($P < 0.05$), 1.39 fold ($P < 0.01$) and 1.29 fold ($P < 0.05$), respectively compared to the control adipocytes (**Fig. 4.12A**). The expression of *PPAR γ* was not changed in isoproterenol or mangiferin treated adipocytes, compared to control adipocytes (**Fig. 4.12A**). No significant changes were observed in the mRNA expression of *PPAR α* in adipocytes treated with the CCC fractions, isoproterenol or mangiferin (**Fig. 4.12B**). No significance was observed in the mRNA expression of *LPL* in adipocytes treated with CCC F2 (0.76 fold decrease, $P = 0.06$), and the mRNA expression of *LPL* in adipocytes treated with either CCC F1, CCC F3, CCC F4, isoproterenol or mangiferin, was not significantly changed compared to control adipocytes (**Fig. 4.12C**). The mRNA expression of *HSL* was increased in adipocytes treated with mangiferin (1.65 fold, $P < 0.05$), CCC F1 (1.60 fold, $P < 0.05$) and CCC F2 (1.61 fold, $P < 0.05$) compared to control adipocytes, and treatment with isoproterenol, CCC F3 or CCC F4, did not affect the expression of *HSL* (**Fig. 4.12D**). No significant changes were observed in the mRNA expression of *FABP4*, *ACACA*, *FASN* and *SCD1* in adipocytes treated with CCC F1, CCC F2, CCC F3, CCC F4, isoproterenol or mangiferin compared to control adipocytes (**Figs. 4.12E - H**).

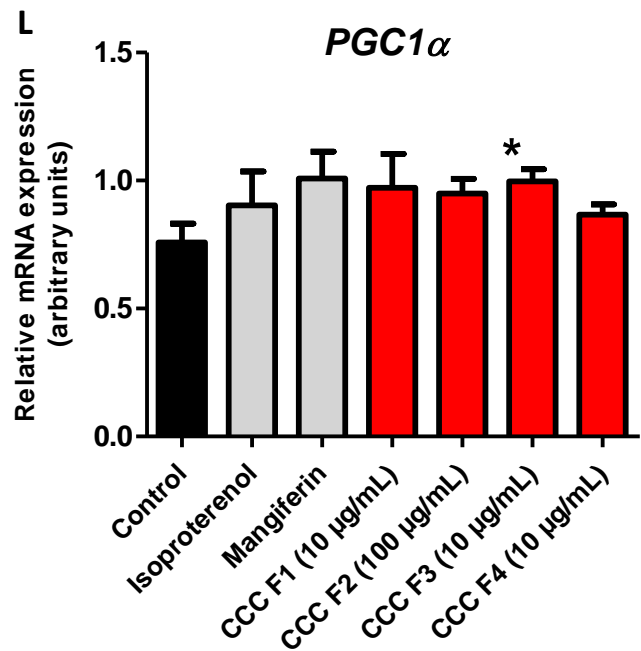
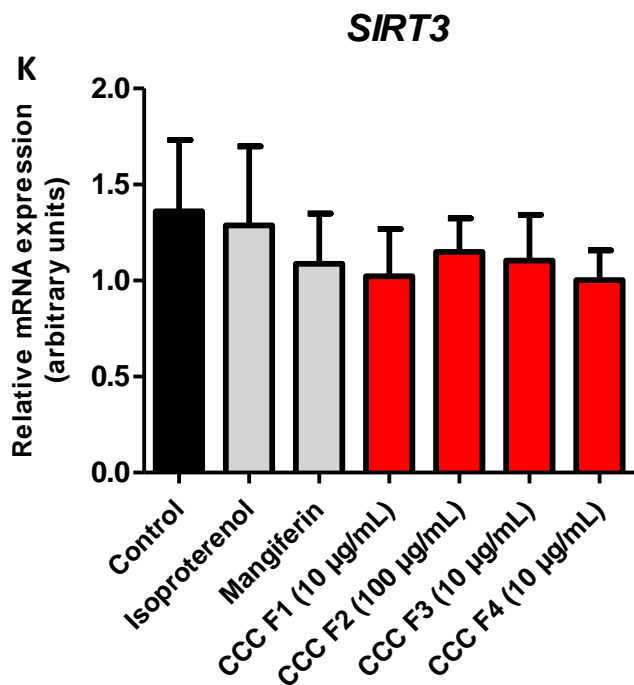
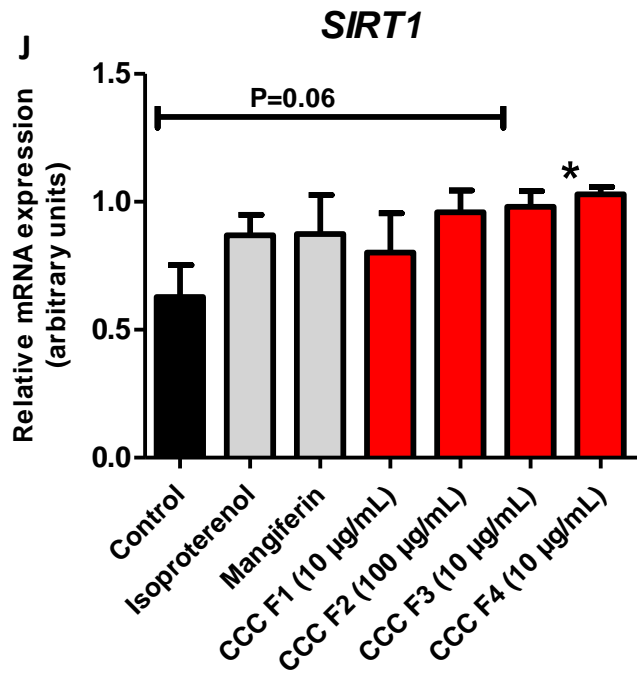
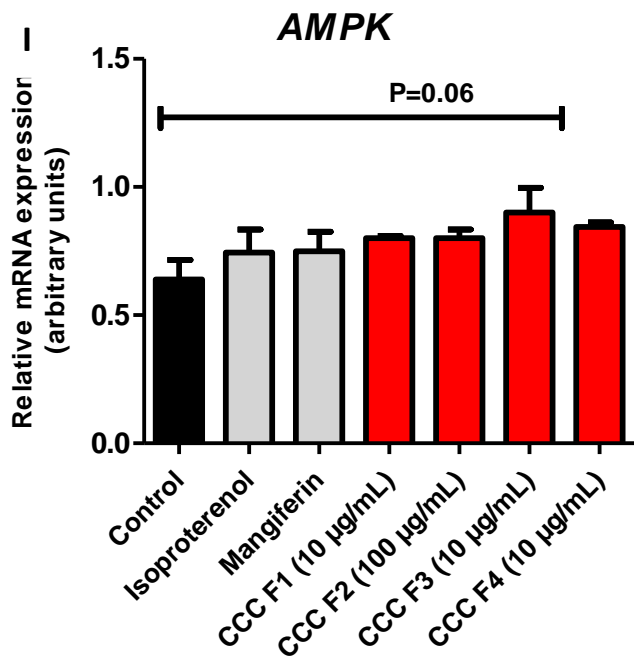
Considering energy regulating genes, treatment of differentiated 3T3-L1 adipocytes with CCC F4 resulted in increased mRNA expression of *AMPK* (1.32 fold, $P = 0.06$) although this was not statistically significant compared to control adipocytes. Isoproterenol, mangiferin, CCC F1, CCC F2 or CCC F3 did not affect the expression of *AMPK* (**Fig.**

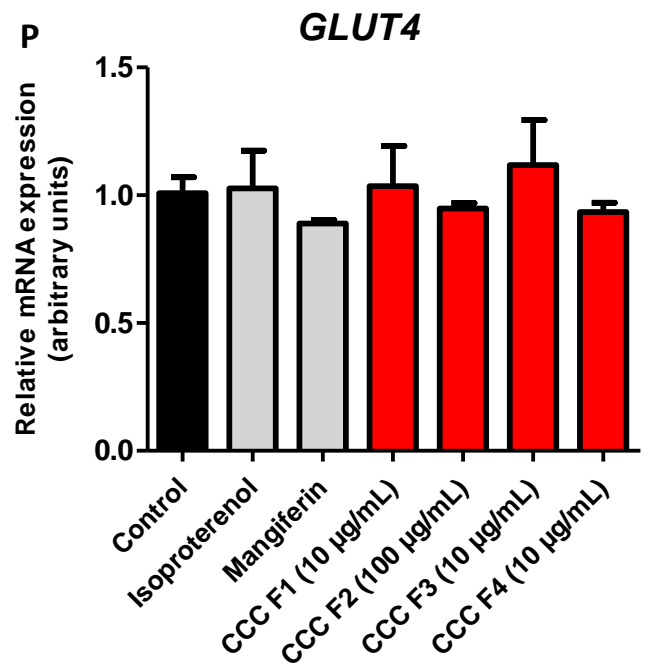
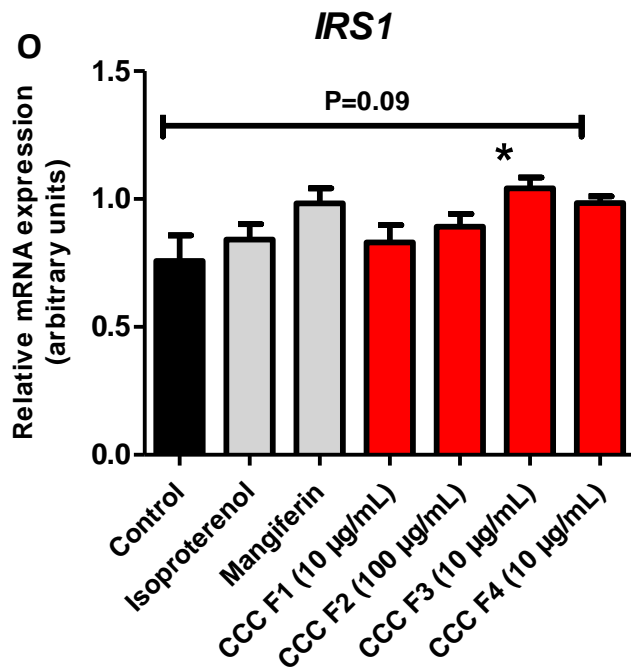
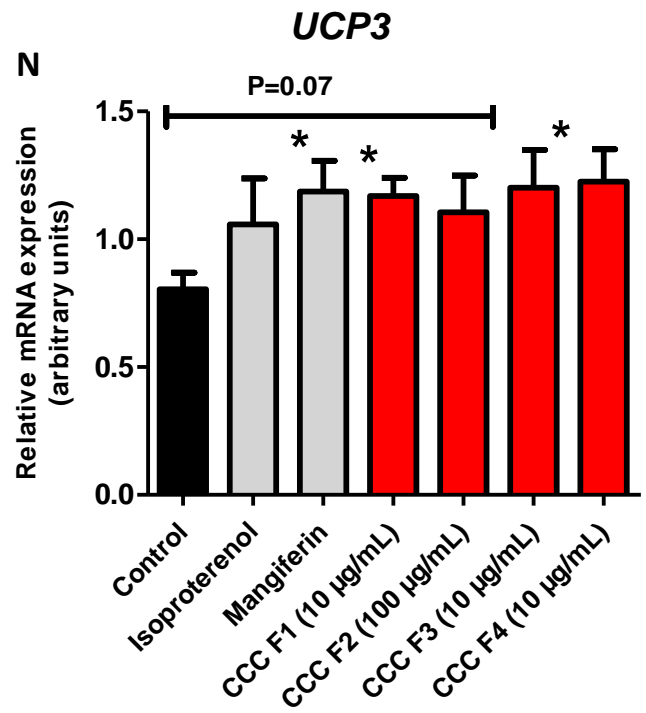
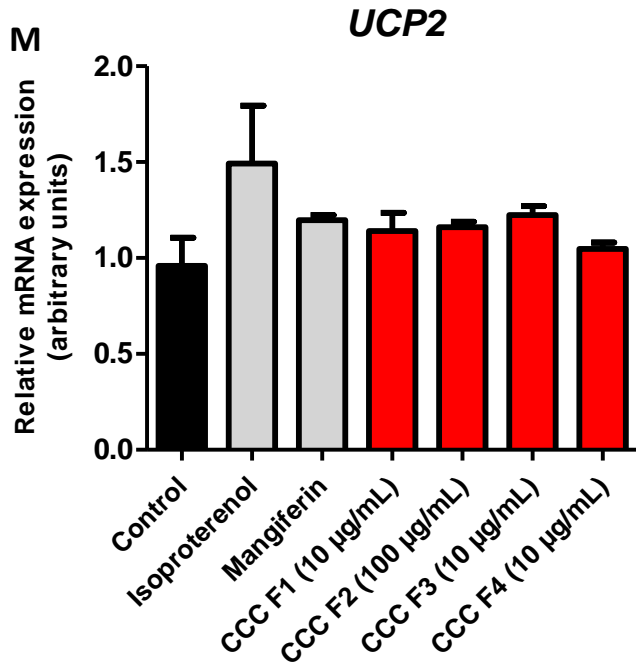
4.12I). CCC F4 increased the mRNA expression of *SIRT1* (1.64 fold, $P < 0.05$), and a non-significant increase was observed for *SIRT1* expression in adipocytes treated with CCC F3 (1.56 fold, $P = 0.06$). *SIRT1* mRNA expression was not changed in adipocytes treated with isoproterenol, mangiferin, CCC F1 or CCC F2 (**Fig. 4.12J**). Treatment with CCC F3 increased *PGC1 α* expression (1.32 fold, $P < 0.05$) compared to control adipocytes, whereas the expression of this gene remained unchanged in response to treatment with CCC F1, CCC F2, CCC F4, isoproterenol or mangiferin (**Fig. 4.12L**). Treatment with mangiferin, CCC F1 and CCC F4 increased *UCP3* mRNA expression by 1.47 fold ($P < 0.05$), 1.45 fold ($P < 0.05$) and 1.52 fold ($P < 0.05$), respectively compared to control adipocytes. A trend toward non-significant increase was observed for *UCP3* expression in CCC F3 treated adipocytes (1.49 fold, $P = 0.07$) (**Fig. 4.12N**). The mRNA expression of *SIRT3* and *UCP2* did not significantly change in adipocytes treated with isoproterenol, mangiferin or the CCC fractions (**Figs. 4.12K - M**).

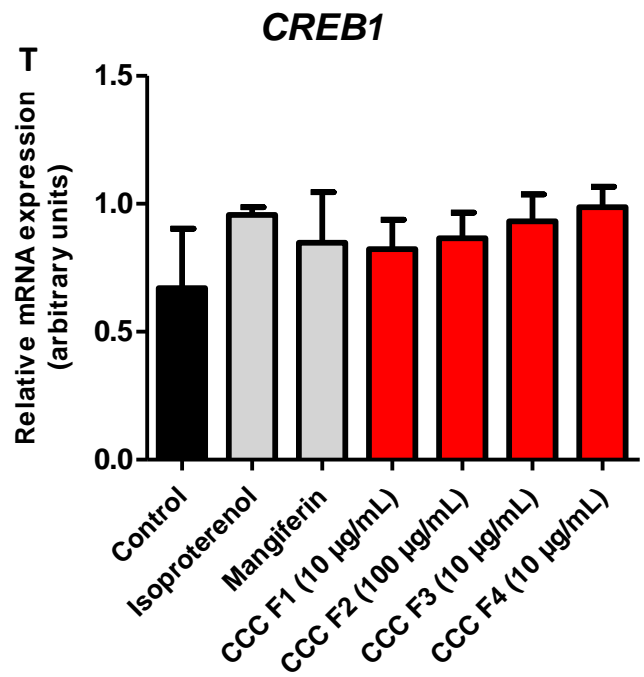
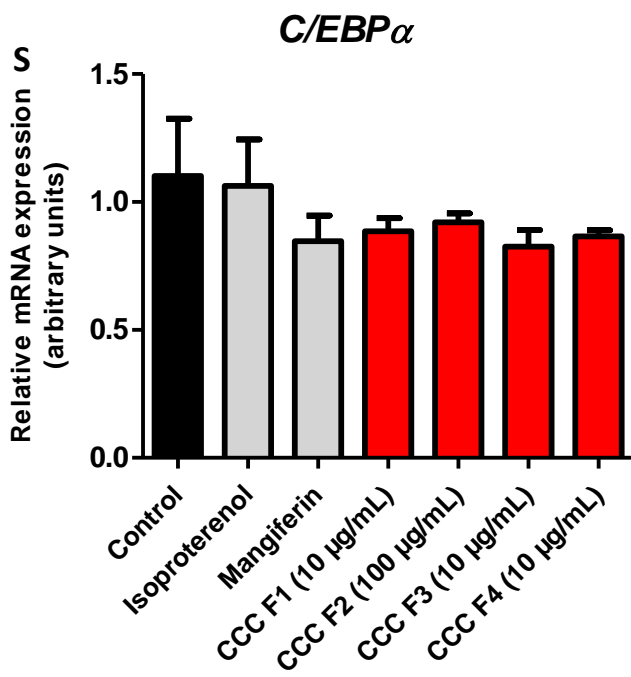
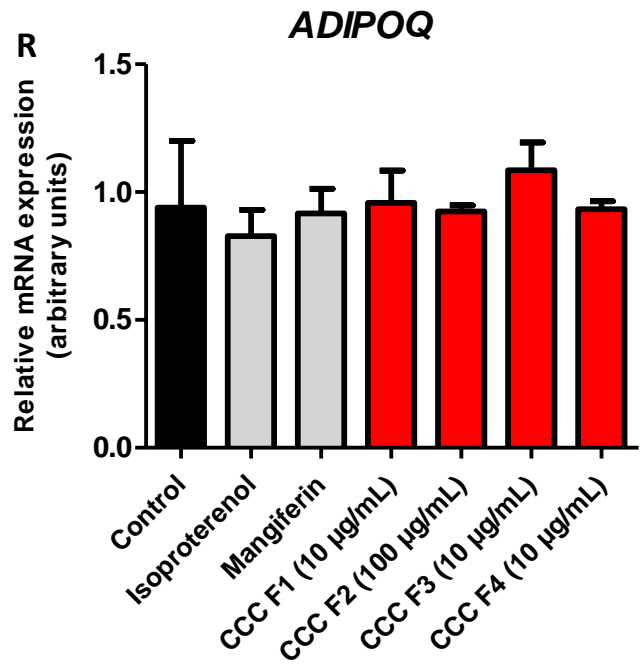
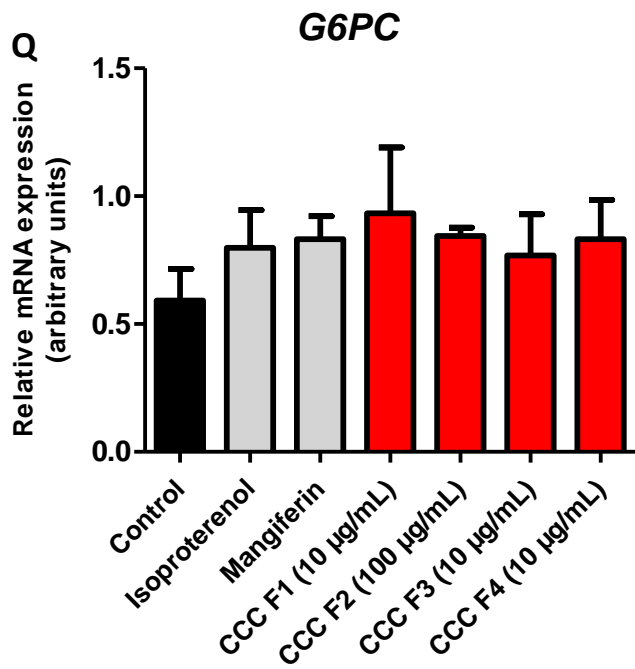
In terms of glucose metabolism and insulin signaling, no significant difference in the mRNA expression of *GLUT4*, *GPC6* and *ADIPOQ* was observed in adipocytes treated with isoproterenol, mangiferin or the CCC fractions, compared to control adipocytes (**Figs. 4.12P - R**), whereas CCC F3 increased *IRS1* mRNA expression (1.37 fold, $P < 0.05$) compared to control adipocytes (**Fig. 4.12O**). The mRNA expression of *CEBP α* , *CREB1*, *SREBF1*, and *GATA2* remained unaffected in response to treatment with isoproterenol, mangiferin, or the CCC fractions compared to control adipocytes (**Figs. 4.12S - V**). Similarly, treatment did not alter the mRNA expression of *FGF2*, *CPT1 α* and *Cs* (**Figs. 4.12W - Y**). The results for the mRNA expression of genes involved in lipid or fatty acid, glucose and energy metabolism in mature adipocytes are summarized in **Table 4.4**.

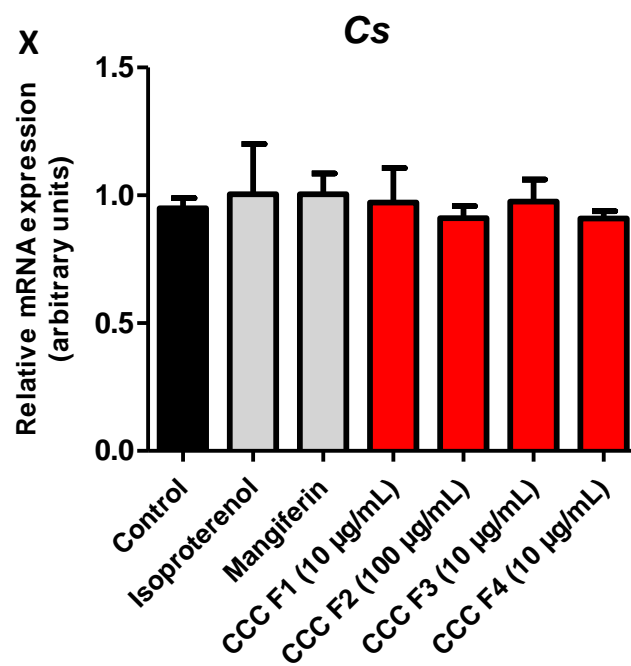
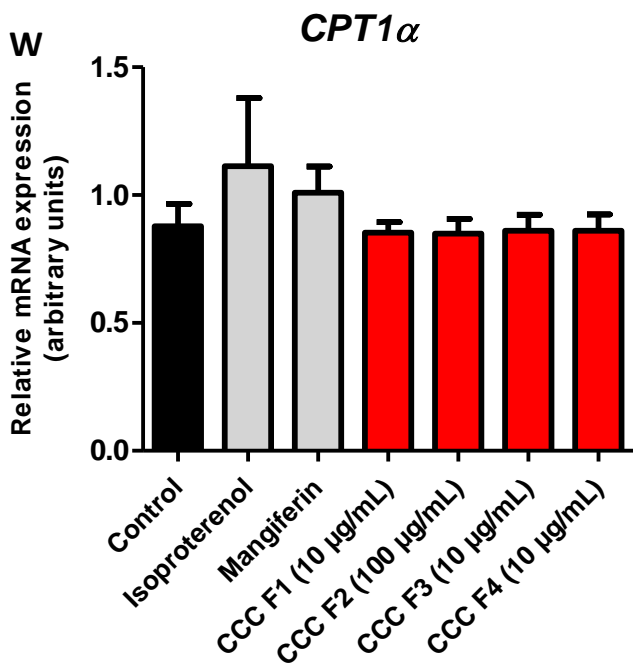
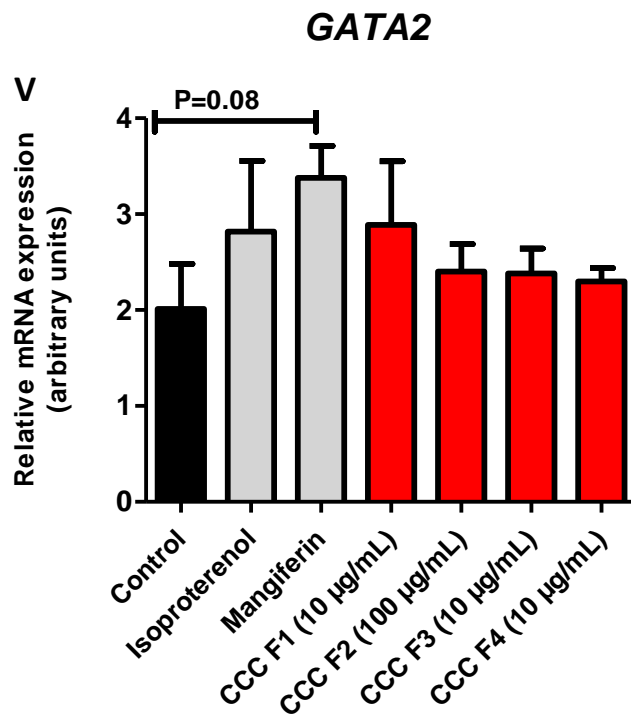
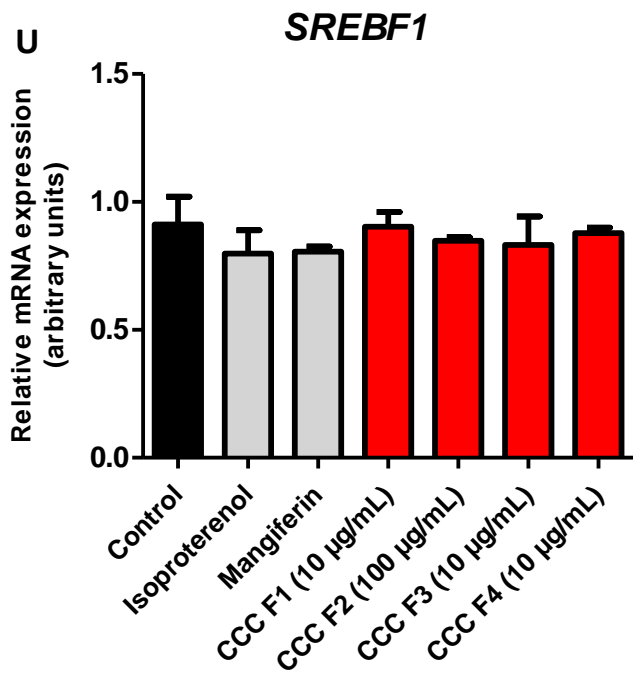












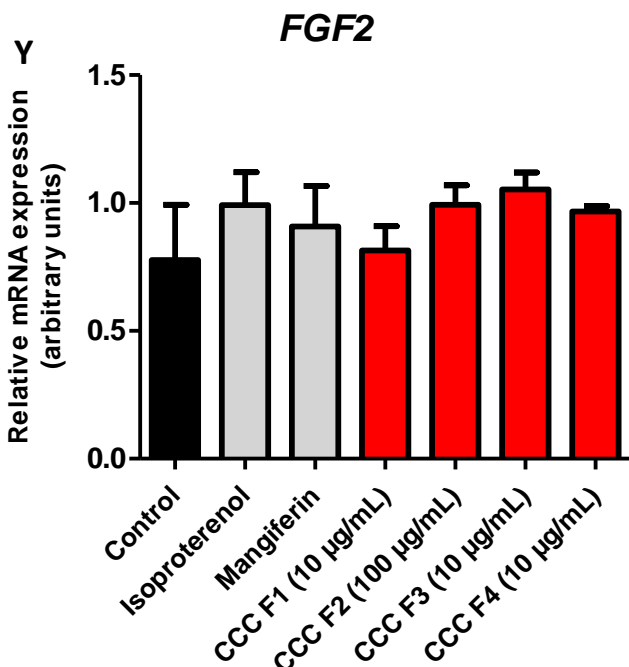


Figure 4.12 The effect of the CCC fractions on mRNA expression of genes involved in lipid, fatty acid, energy and glucose metabolism. Differentiated 3T3-L1 adipocytes were treated with the vehicle control, CCC F1 (10 µg/mL), CCC F2 (100 µg/mL), CCC F3 (10 µg/mL), CCC F4 (10 µg/mL), isoproterenol (10 µM) or mangiferin (0.001 µM) for 24 hours. Total RNA was extracted and gene expression was analyzed by qRT-PCR using *B2M* and *RPL13A* as endogenous controls. Genes measured for mRNA expression include *PPAR γ* (A), *PPAR α* (B), *LPL* (C), *HSL* (D), *FABP4* (E), *ACACA* (F), *FASN* (G), *SCD1* (H), *AMPK* (I), *SIRT1* (J), *SIRT3* (K), *PGC1 α* (L), *UCP2* (M), *UCP3* (N), *IRS1* (O), *GLUT4* (P), *G6PC* (Q), *ADIPOQ* (R), *C/EBP α* (S), *CREB1* (T), *SREBF1* (U), *GATA2* (V), *CPT1 α* (W), *Cs* (X) and *FGF2* (Y). Results are represented as mRNA expression relative to the mRNA expression of endogenous controls (*ACT β* and *RPL13A*), and expressed as mean \pm SEM for three independent experiments. Statistical significance is depicted as * $P < 0.05$ and ** $P < 0.01$ vs. vehicle control.

4.5 Effect of the CCC fractions on protein expression in mature 3T3-L1 adipocytes

As described in chapter 3, images for western blot were cut from the original blot (Fig. S8 A and B, supplementary data) to only represent samples used in this chapter. CCC F4 increased PPAR α protein expression (1.55-fold, $P < 0.05$), whereas treatment with CCC F1, CCC F2 or CCC F3, nor the controls, isoproterenol and mangiferin, significantly

affected PPAR α protein expression (**Fig. 4.13A**). The expression of PPAR γ was not affected by treatment with the CCC fractions, nor isoproterenol and mangiferin (**Fig. 4.13B**). The results for PPAR γ and PPAR α protein expression in mature adipocytes are summarized in **Table 4.5**.

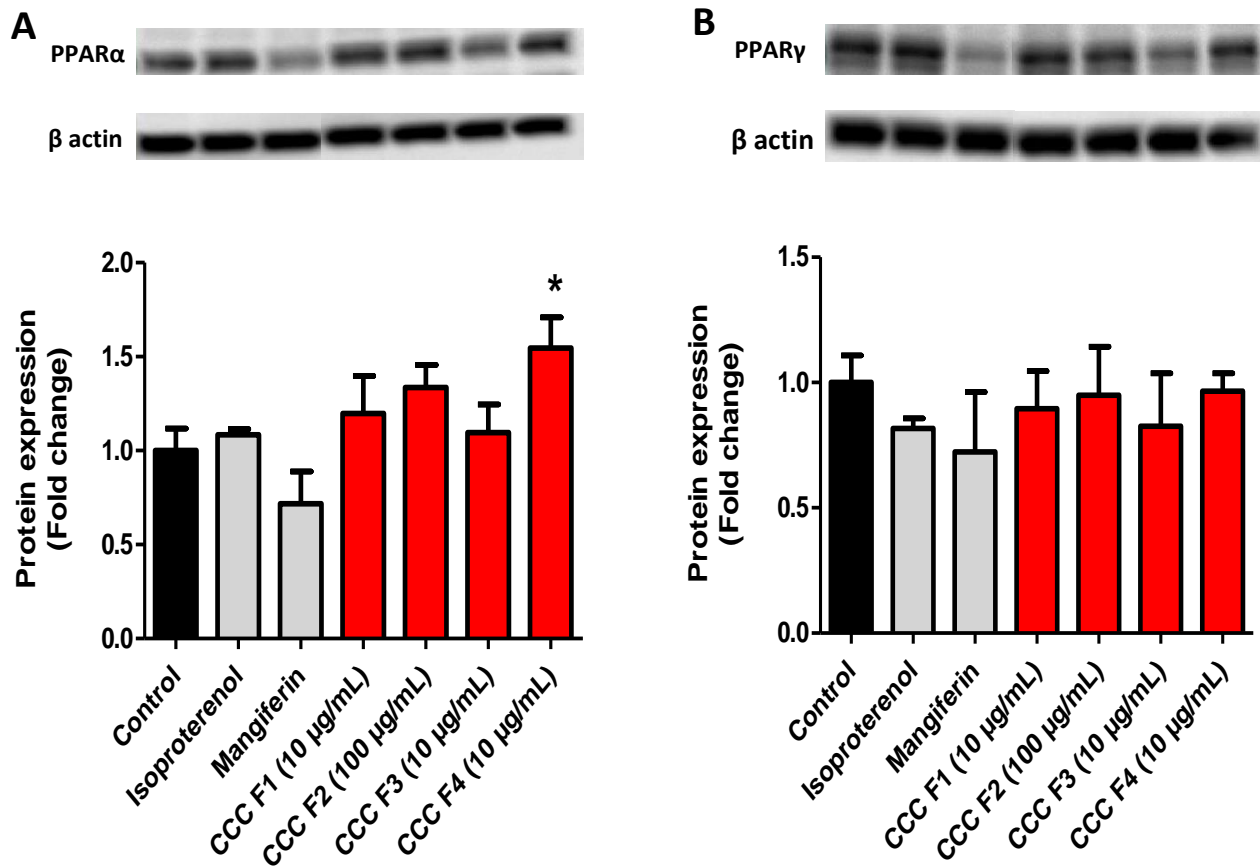


Figure 4.13 The effect of CCC fractions on PPAR α and PPAR γ protein expression. Differentiated 3T3-L1 adipocytes were treated with the vehicle control, CCC F1 (10 μ g/mL), CCC F2 (100 μ g/mL), CCC F3 (10 μ g/mL), CCC F4 (10 μ g/mL), isoproterenol (10 μ M) or mangiferin (0.001 μ M) for 24 hours. Proteins were extracted and protein expression of PPAR α (A) and PPAR γ (B) was assessed by western blot analysis using β actin as a reference protein. Results are reported as a fold change relative to the vehicle control and represent mean \pm SEM for three independent experiments.

4.6 Summary of results

The results described in this chapter are summarized in the tables below. In differentiating 3T3-L1 pre-adipocytes CCC F1, CCC F3 and CCC F4 decreased lipid accumulation at different concentrations, whereas treatment with CCC F2 showed no effect on lipid accumulation (**Table 4.2**). No effect was observed in TG content in differentiating pre-adipocytes treated with CCC F1, CCC F2, CCC F3 and CCC F4. Assessment of cell viability using the ATP assay showed that CCC F1 and CCC F3 decreased cell viability at the highest concentrations, whereas treatment with CCC F2 and CCC F4 did not affect cell viability (**Table 4.2**). In differentiated adipocytes, CCC F1, CCC F2 and CCC F4 decreased lipid content at various concentrations, whereas CCC F3 did not show any significant effect on decreasing lipid content (**Table 4.3**). Lipolytic activity was observed in mature adipocytes treated with CCC F1, CCC F2 and CCC F3, while no effect were seen in cells treated with CCC F4 (**Table 4.3**). No significant effect was observed in ATP content in adipocytes treated with the CCC fractions, while CCC F4 increased ATP content at the highest concentration (**Table 4.3**).

The mRNA expression of *PPAR γ* was increased by all CCC fractions, whereas the mRNA expression of *HSL* was increased by CCC F1 and CCC F2, and *UCP3* mRNA expression was increased in adipocytes treated with CCC F1 and CCC F4 (**Table 4.4**). Increased mRNA expression of *PGC1 α* and *IRS1* was observed in adipocytes treated with CCC F3 and *SIRT1* mRNA expression was increased in CCC F4 treated adipocytes (**Table 4.4**). Furthermore, the protein expression of *PPAR α* was increased in adipocytes treated with CCC F4 (**Table 4.5**).

Table 4.2 Summary of results for CCC fraction screening in differentiating 3T3-L1 pre adipocytes.

Experimental Assays	1 µg/mL	10 µg/mL	50 µg/mL	100 µg/mL
CCC F1				
Oil Red O	↓ 33.5***	↓ 19.2**	↓ 10.5	↓ 10.2
ATP	↓ 4.5	↓ 7	↓ 12.9	↓ 24.4***
CCC F2				
Oil Red O	↓ 7.4	↓ 4.7	↓ 11.7	↓ 16.3
ATP	↓ 9.3	↓ 13.9	↓ 11.5	↓ 14.9
CCC F3				
Oil Red O	↓ 24.1**	↓ 22.9**	↓ 20.6*	↓ 23.9**
ATP	↑ 4.5	↓ 8.4	↓ 17.2	↓ 21.5*
CCC F4				
Oil Red O	↓ 27.4***	↓ 15.3*	↓ 15*	↓ 12.6
ATP	↓ 10.5	↓ 4.3	↓ 6	↓ 9.5

↓: Decrease in percentage (%) vs. control

↑: Increase in percentage (%) vs. control

Significance depicted as: *P < 0.05, **P < 0.01 and ***P < 0.001 vs. vehicle control

Table 4.3 Summary of results for CCC fraction screening in differentiated 3T3-L1 adipocytes.

Experimental Assays	1 µg/mL	10 µg/mL	50 µg/mL	100 µg/mL
CCC F1				
Oil Red O	↓ 14.8	↓ 18.1	↓ 14.7	↓ 27.1**
Glycerol release	↑ 38.9*	↑ 21.6	↑ 39.1*	↑ 32.6
ATP	↓ 2	↓ 3.8	↓ 10.7	↓ 10.4
CCC F2				
Oil Red O	↓ 7.3	↓ 14.4	↓ 15.3	↓ 23**
Glycerol release	↑ 24.5	↑ 11.7	↑ 46.3*	↑ 45.1
ATP	↓ 6.9	↓ 12.5	↓ 8.7	↓ 6.4
CCC F3				
Oil Red O	↓ 11.8	↓ 16.7	↓ 14.8	↓ 7.7
Glycerol release	↑ 24.6*	↔	↓ 11.2	↓ 9.4
ATP	↔	↑ 4.3	↓ 2.8	↓ 6.9
CCC F4				
Oil Red O	↓ 13.3	↓ 23.4*	↓ 19.7	↓ 22.5*
Glycerol release	↑ 33	↑ 14.4	↓ 3.5	↑ 6.5
ATP	↓ 3.7	↔	↑ 9.3	↑ 14.9*

↓: Decrease in percentage (%) vs. control

↑: Increase in percentage (%) vs. control

Significance depicted as: *P < 0.05, **P < 0.01 and ***P < 0.001 vs. vehicle control

Table 4.4 Summary results for the effect of CCC fractions on mRNA expression in differentiated 3T3-L1 adipocytes.

Genes	Isoproterenol	Mangiferin	CCC F1	CCC F2	CCC F3	CCC F4
<i>ACACA</i>	↓ 0.67	↓ 0.67	↓ 0.73	↓ 0.74	↓ 0.88	↓ 0.73
<i>ADIPOQ</i>	↓ 0.88	↔	↔	↔	↑ 1.16	↔
<i>CREB1</i>	↑ 1.43	↑ 1.26	↑ 1.23	↑ 1.29	↑ 1.39	↑ 1.48
<i>CPT1α</i>	↑ 1.27	↑ 1.15	↔	↔	↔	↔
<i>CEBPα</i>	↔	↓ 0.77	↓ 0.8	↓ 0.84	↓ 0.75	↓ 0.79
<i>Cs</i>	↔	↔	↔	↔	↔	↔
<i>FABP4</i>	↓ 0.63	↓ 0.68	↓ 0.69	↓ 0.67	↓ 0.79	↓ 0.7
<i>FASN</i>	↓ 0.86	↓ 0.79	↓ 0.89	↓ 0.82	↔	↔
<i>FGF2</i>	↑ 1.28	↑ 1.17	↔	↑ 1.28	↑ 1.36	↑ 1.24
<i>GATA2</i>	↑ 1.4	↑ 1.68	↑ 1.44	↑ 1.19	↑ 1.18	↑ 1.14
<i>GLUT4</i>	↔	↓ 0.88	↔	↔	↑ 1.11	↔
<i>G6PC</i>	↑ 1.35	↑ 1.4	↑ 1.58	↑ 1.43	↑ 1.29	↑ 1.4
<i>HSL</i>	↑ 1.18	↑ 1.65*	↑ 1.6*	↑ 1.6*	↑ 1.4	↑ 1.35
<i>IRS1</i>	↑ 1.11	↑ 1.3	↑ 1.1	↑ 1.17	↑ 1.37*	↑ 1.3
<i>LPL</i>	↔	↓ 0.77	↓ 0.81	↓ 0.76	↓ 0.87	↓ 0.8
<i>PPARα</i>	↑ 1.22	↑ 1.12	↓ 0.89	↔	↔	↔
<i>PPARγ</i>	↔	↑ 1.16	↑ 1.19*	↑ 1.24*	↑ 1.39**	↑ 1.29*
<i>PGC1α</i>	↑ 1.19	↑ 1.33	↑ 1.28	↑ 1.25	↑ 1.32*	↑ 1.15
<i>AMPK</i>	↑ 1.16	↑ 1.17	↑ 1.26	↑ 1.25	↑ 1.41	↑ 1.32
<i>SIRT1</i>	↑ 1.38	↑ 1.39	↑ 1.28	↑ 1.53	↑ 1.56	↑ 1.64*
<i>SIRT3</i>	↔	↓ 0.8	↓ 0.75	↓ 0.84	↓ 0.81	↓ 0.74
<i>SCD1</i>	↓ 0.79	↓ 0.89	↔	↔	↔	↓ 0.89
<i>SREBF1</i>	↓ 0.87	↓ 0.88	↔	↔	↔	↔
<i>UCP2</i>	↑ 1.56	↑ 1.25	↑ 1.19	↑ 1.21	↑ 1.27	↑ 1.1
<i>UCP3</i>	↑ 1.3	↑ 1.47*	↑ 1.45*	↑ 1.37	↑ 1.49	↑ 1.52*

↓: Decrease in fold change vs. control

↑: Increase in fold change vs. control

↔: No significant fold change vs. control

Significance depicted as: *P < 0.05 and **P < 0.01 vs. vehicle control

Table 4.5 Summary results for the effect of CCC fractions on protein expression in differentiated 3T3-L1 adipocytes.

Protein	Isoproterenol	Mangiferin	CCC F1	CCC F2	CCC F3	CCC F4
PPAR α	↔	↓ 0.72	↑ 1.2	↑ 1.34	↔	↑ 1.55*
PPAR γ	↓ 0.81	↓ 0.72	↓ 0.89	↔	↓ 0.83	↔

↓: Decrease in fold change vs. control

↑: Increase in fold change vs. control

↔: No significant fold change vs. control

Significance depicted as: *P < 0.05 vs. vehicle control

CHAPTER 5

DISCUSSION

Obesity has reached epidemic proportions worldwide, and is often regarded as the greatest public health challenge of the 21st century (Rössner, 2002). Lifestyle modifications such as diet and exercise are the most effective anti-obesity interventions, however, failure to adhere to such therapies, significantly decreases their effectiveness (Hunter et al., 2008; Lagerros and Rössner, 2013). Moreover, the heavy reliance on pharmacotherapy to combat obesity is plagued by the serious adverse effects of many of these drugs (Adan, 2013). Phytotherapy is gaining increased attention globally, as an attractive alternative or adjunct to conventional obesity treatment. The use of phytochemicals to prevent or treat obesity are considered to be safer and more cost-effective than conventional medicine (Meydani and Hasan, 2010; Rayalam et al., 2008).

In the present study, we explored the anti-obesity potential of polyphenol-enriched extracts of *C. subternata*, *C. intermedia* and *C. maculata*. Using aqueous and organic fractions of these polyphenol enriched extracts, the anti-obesity potential of the most bioactive *in vitro* *Cyclopia* fraction (organic fraction of *C. intermedia*) was further investigated in the obese Lepr^{db/db} mouse model. The organic fraction of *C. intermedia* was further separated into subfractions, using HPLC, and retested *in vitro* in order to facilitate the identification of phenolic compounds associated with its anti-obesity properties.

5.1 Bioactivity varies according to *Cyclopia* species and phenolic content

The effect of the aqueous and organic fractions of *C. subternata*, *C. maculata* and *C. intermedia* on lipid content was assessed in 3T3-L1 adipocytes, the most commonly used *in vitro* model for obesity studies (Zeng et al., 2012). Our results confirmed that 3T3-L1 pre-adipocytes, cultured in differentiating media containing IBMX, Dexamethasone (Dex) and insulin, accumulated significantly more lipids than pre-adipocytes cultured without these chemicals. IBMX, Dex and insulin regulate several pathways involved in the activation of genes that regulate adipocyte differentiation. IBMX, a phosphodiesterase inhibitor, increases the concentration of intracellular cAMP and protein kinase A (PKA), required for the transcriptional activation of PPAR γ and consequently increases the expression of genes involved in adipogenesis (Kim et al., 2010). Dex binds and activates the glucocorticoid receptor, and subsequently activates

C/EBP δ and KLF15 (Asada et al., 2011), whereas insulin binds to the insulin receptor activating insulin signaling and transcription factors facilitating pre-adipocyte differentiation into mature adipocytes (Klemm et al., 2001). Furthermore, our results confirmed that 0.01% DMSO, used as a diluent in our assays, had no effect on lipid accumulation, thus validating the cell model, and the use of DMSO as a diluent in our experiments. This concentration of DMSO similarly had no effect on cytotoxicity, consistent with Sengupta et al. (2011) who reported that 0.1% DMSO had no cytotoxic effects in 3T3-L1 adipocytes. Isoproterenol, a β -adrenergic receptor agonist, responsible for stimulating lipolysis (Ranjit et al., 2011) also significantly reduced lipid content in differentiated 3T3-L1 adipocytes.

Fractions from aqueous methanol extracts of all three *Cyclopia* spp. decreased lipid content in 3T3-L1 adipocytes, although efficacy varied between species and their aqueous or organic fractions. For example, the aqueous fraction of *C. subternata* decreased lipid content at the higher doses only (50 $\mu\text{g/mL}$ and 100 $\mu\text{g/mL}$), whereas the organic fraction from *C. intermedia* decreased lipid content at 10 $\mu\text{g/mL}$, 50 $\mu\text{g/mL}$ and 100 $\mu\text{g/mL}$, while the aqueous fraction of *C. maculata* decreased lipid content at all concentrations tested (1 $\mu\text{g/mL}$ to 100 $\mu\text{g/mL}$). Differences in the anti-obesity potential of *Cyclopia* species have been previously reported. Dudhia et al. (2013) compared the activity of extracts of unfermented *C. subternata* and *C. maculata*, and fermented *C. maculata* in differentiating 3T3-L1 pre-adipocytes, and reported that although all extracts were able to inhibit intracellular lipid accumulation at higher doses (400 $\mu\text{g/mL}$ to 1600 $\mu\text{g/mL}$), differences in their activities were demonstrated for the concentration range investigated in the current study. Comparing the lipolytic activity of these three extracts in mature 3T3-L1 adipocytes, Pfeiffer et al. (2013) showed that only the fermented *C. maculata* extract was able to stimulate lipolysis at a concentration range of 60 $\mu\text{g/mL}$ to 100 $\mu\text{g/mL}$. These results show the variation in bioactivity between extracts of *Cyclopia* species and adds to the growing body of evidence of the importance of considering species variation in the development of health promoting nutraceuticals.

The importance of phenolic content in bioactivity has been widely reported (Bahadoran et al., 2013; Pandey and Rizvi, 2009; Trigueros et al., 2013). In this study, the ability of extracts of unfermented *Cyclopia* species to decrease lipid content varied according

to their aqueous and organic fractions. Aqueous and organic fractions were prepared by liquid-liquid fractionation using water as an aqueous solvent and butanol as an organic solvent, furthermore butanol was used to enrich the phenolic content of the organic fractions. Quantitative HPLC-DAD confirmed increased phenolic content in the organic fractions compared to their aqueous counterparts as previously reported by Mortimer et al. (2015). The organic fraction of the 40% aqueous methanol extract of *C. intermedia* decreased lipid content, with its aqueous fraction showing no effect. These results are consistent with those published by Mortimer et al. (2015), who showed that liquid-liquid fractionation of *C. subternata* (SM6Met) into an aqueous and organic fraction, resulted in enhanced phenolic content and bioactivity in the organic fraction. However, polyphenolic enrichment did not translate to increased bioactivity for the fractions obtained from 40% aqueous methanol extracts of *C. subternata* and *C. maculata*. For example, the aqueous fractions of *C. subternata* and *C. maculata*, despite having lower phenolic content, decreased lipid content, while their organic fractions showed no effect. Previously, Pfeiffer et al. (2013) reported increased anti-obesity effects for a fermented extract of *C. maculata* extract, compared to the unfermented extract, which had increased phenolic content. Fermentation is a process of oxidation of plant material, usually at high temperatures, to develop certain characteristics in tea infusions such as taste, smell or color and is associated with decreased phenolic content. These results suggest that phenolic quality, rather than quantity of polyphenols is important for determining bioactivity of plant extracts. Furthermore, Xu et al. (2014) demonstrated that luteolin was active at low concentrations supporting the hypothesis that polyphenols, even at low abundance, can mediate biological effects. Synergism between individual compounds in plant extracts and the loss of these synergistic links during fractionation (Herranz-López et al., 2012), could also explain the failure of the organic fractions to mediate anti-obesity effects.

The concentration of anti-obesity phenolic compounds previously implicated in anti-obesity, varied between extracts and fractions, and did not correlate with bioactivity. For example, the xanthone glucoside, mangiferin, present in high quantities in *Cyclopia* (Joubert et al., 2011), has been shown to inhibit differentiation of human mesenchymal stem cells into matured adipocytes (Subash-babu and Alshatwi, 2015). However, in this study, the aqueous fractions of *C. maculata* and *C. subternata*, containing

relatively low contents of mangiferin compared to their organic counterparts, showed bioactivity. Similar results were observed for other previously described anti-obesity compounds. The benzophenone iriflophenone-3-C- β -D-glucoside, also present in relatively high levels in honeybush infusions (Schulze et al., 2015) inhibits TG synthesis and the expression of associated genes in 3T3-L1 adipocytes (Zhang et al., 2011). The flavanone hesperidin, another major phenolic compound present in *Cyclopia* (Joubert et al., 2011), improved hypercholesterolemia and fatty liver by inhibiting the synthesis and absorption of cholesterol in Wistar rats fed a high cholesterol diet (Wang et al. 2011). Other compounds, not abundant in *Cyclopia* have also previously demonstrated anti-obesity activity. Luteolin decreased TG accumulation in 3T3-L1 pre-adipocytes by decreasing PPAR γ and C/EBP α mRNA and protein expression levels (Park et al., 2009), and ameliorated diet-induced obesity and insulin resistance in C57BL/6 mice (Xu et al., 2014). Eriocitrin improved diet-induced hepatic steatosis in zebra fish by inducing mitochondrial biogenesis (Hiramitsu et al., 2014). Our results suggest that compounds other than these are responsible for the anti-obesity effects observed after treatment with extracts of *C. subternata* and *C. maculata*. Interestingly, the flavanones neoponcirin and eriodictyol-O-deoxyhexoside-O-hexoside (a compound similar to eriocitrin), not previously identified in *Cyclopia* spp., were detected in the aqueous methanol extract of *C. intermedia* and its organic fraction, suggesting that novel compounds in *Cyclopia* may be mediating the anti-obesity effects. The anti-obesity effects of eriocitrin has been previously reported (Hiramitsu et al., 2014) and it is likely that eriodictyol-O-deoxyhexoside-O-hexoside has similar effects. No literature is available detailing investigations of neoponcirin for anti-obesity properties.

In this study, higher concentrations of mangiferin, isomangiferin and hesperidin were detected in the aqueous methanol extract of *C. subternata* compared to the aqueous hot water extract of *C. subternata* used by Dudhia et al. (2013). In contrast, the concentrations of mangiferin, isomangiferin and iriflophenone-3-C- β -D-glucoside were substantially lower in the aqueous methanol extract of *C. maculata* used in this study, compared to the aqueous hot water extract of *C. maculata* extract used by Dudhia et al. (2013), confirming variation within species as previously discussed. However, these conflicting results can also be attributed to factors such as seasonal variation, geographical location and processing of plant material (Joubert et al., 2008b). The *C.*

maculata used in this study was harvested from a commercial and experimental plantation in Beriaville during 2013, while the plant material used for Dudhia et al. (2013) was harvested in the wild from various locations in Riviersonderend in 2010, suggesting that these factors should be considered for the development of health promoting nutraceuticals.

To determine whether the anti-obesity effects observed for the fractions of *Cyclopia* extracts in this study was due to a decrease in metabolic activity (Kim et al., 2015), cell viability was assessed using the MTT and ATP assays. Similar to their effects on lipid content, the effect of *Cyclopia* spp. on cell viability varied according to species and between their aqueous and organic fractions. None of the fractions decreased mitochondrial dehydrogenase activity, with the aqueous and organic fractions of *C. subternata* and *C. intermedia* increasing mitochondrial dehydrogenase activity at all concentrations tested for *C. subternata*, and at 50 µg/mL and 100 µg/mL for *C. intermedia*. The ATP assay, considered to be more sensitive (Wang et al., 2010), showed decreased ATP content in adipocytes treated with the aqueous fraction of *C. intermedia* at 50 µg/mL and 100 µg/mL, and the organic fraction of *C. maculata* at all concentrations tested (1 µg/mL to 100 µg/mL). Recent concerns that polyphenols could interfere with the MTT assay (Han et al., 2010; Wang et al., 2010; Wisman et al., 2008) could account for the differences observed between the assays. Wang et al. (2010) showed that when LNCaP prostate and MCF-7 breast cancer cells were treated with (-)-epigallocatechin-3-gallate (EGCG), the MTT and 3-(4,5-dimethylthiazol-2-yl)-5-(3-carboxymethoxyphenyl)-2-(4-sulfophenyl)-2H-tetrazolium (MTS) assays overestimated cell viability compared to other methods such as ATP, DNA or trypan blue determinations.

Wang et al. (2015) also reported discrepancies between the results obtained with the MTT assay and the cell counting kit 8 (CCK-8) cell viability assays in EA.hy926 endothelial cells, and they suggested that the phenylethanoid glycosides isolated from *Cistanche tubulosa* could interfere with the MTT assay, thus increasing perceived cell viability due to interference by phenolic compounds. Several more studies have reported that plant extracts, phytoestrogens or anti-oxidants directly interact with MTT tetrazolium reduction in the absence of cells (Bruggisser et al. 2002). Rottlerin, a natural compound isolated from *Mallotus philippinensis* increased the mitochondrial

uncoupling activity rather than increasing the number of viable cells (Maioli et al., 2009). Likewise, in our study, the MTT content in adipocytes treated with the aqueous and organic fractions of *C. subternata* and *C. intermedia* was increased whereas the ATP was decreased or remained unaffected. This could suggest that these *Cyclopia* fractions increase the mitochondrial uncoupling activity in 3T3-L1 adipocytes, suggested by the increased expression of UCPs in adipocytes treated with these fractions, without necessarily affecting cell viability.

Neither the aqueous fraction of *C. maculata*, nor the organic fraction of *C. intermedia* affected MTT activity and ATP content significantly, suggesting that these extracts mediated their inhibitory effects on lipid content without affecting cell viability. Since both the aqueous fraction of *C. maculata* and the organic fraction of *C. intermedia* displayed anti-obesity effects and were possible candidates for further exploration, their effect on cell death, was assessed using propidium iodide. No significant effects were observed in cells treated with both fractions (**Addendum 3**), confirming that they exert their anti-obesity effects without being cytotoxic.

5.2 Evaluation of the anti-obesity effects of *C. intermedia*

Of the six fractions assessed for their anti-obesity effects in 3T3-L1 adipocytes (**Section 5.1**), the aqueous fraction of *C. maculata* and the organic fraction of *C. intermedia* showed the highest anti-obesity activity. Neoponcirin, a flavanone not previously detected in *Cyclopia* spp., was identified in the organic fraction of *C. intermedia* but not in the extract or fractions of *C. maculata*. Due to the reason mentioned above, and because aqueous extracts may contain monosaccharides and methanol soluble polysaccharides, which would add to calorie intake and may be detrimental to individuals with T2DM, the organic fraction of *C. intermedia* was selected for further exploration.

The organic fraction from the aqueous methanol extract of *C. intermedia* mediated its anti-obesity effects in 3T3-L1 adipocytes by modulation of lipid, FA and energy metabolism genes. Increased mRNA expression of *HSL* was observed in 3T3-L1 adipocytes treated with the organic fraction of *C. intermedia*, whereas the increased expression of *SIRT1* was not significantly regulated. Sirtuin 1 (SIRT1) is a nuclear

NAD⁺ dependent protein deacetylase of the seven sirtuins encoded by the mammalian genome (Li, 2013). SIRT1 regulates cellular metabolic processes such as energy and lipid metabolism by coupling cellular metabolic status and gene regulation through deacetylation of histones, transcription factors, and transcription co-factors (Li, 2013). In adipose tissue, SIRT1 induces fat breakdown and promotes remodeling of white adipose tissue towards brown adipose tissue. SIRT1 is activated by exercise, fasting, caloric restriction or natural compounds such as resveratrol, whereas high fat diet decreases SIRT1 expression (Li, 2013). SIRT1 deficiency in diet-induced obese and insulin resistant mice was associated with increased adiposity, reduced thermogenesis and degeneration of brown adipose tissue (Xu et al., 2016). Activation of SIRT1 by resveratrol inhibited adipogenic differentiation and improved myogenic differentiation in C3H10T1/2 mesenchymal stem cells by activating the Wnt/ β -catenin signalling pathway (Zhou et al., 2015), whereas in mice fed a standard laboratory diet, resveratrol decreased fat accumulation by increasing markers of brown fat tissues, including increased oxygen consumption (Andrade et al., 2014).

HSL is an essential enzyme for lipolysis (Schweiger et al., 2006), involving the sequential breakdown of TGs to three molecules of FFAs and one glycerol molecule (Duncan et al., 2007). HSL catalyzes the hydrolysis of several substrates including TGs, diacylglycerols, cholesteryl and retinyl esters (Holm, 2003). The role of HSL in lipolysis has been previously demonstrated using HSL-null mouse models (Ahmadian et al., 2007; Duncan, 2007). These knockout mice show decreased levels of FFAs and TGs, and low hepatic TG storage, suggesting that lipolysis in the absence of HSL is unable of maintaining a sufficient FA output (Haemmerle et al., 2002). Our findings of increased *HSL*, and non-significantly increased *SIRT1* mRNA expression could be consistent with reports suggesting that SIRT1 regulates HSL function in adipocytes. Shan et al. (2010) showed that inhibition of SIRT1 gene expression decreased the expression of HSL in porcine adipocytes. In contrast, Chakrabarti et al. (2011) showed that knockdown of SIRT1 in 3T3-L1 adipocytes, decreased lipolysis by decreasing the expression of ATGL via deacetylation of FOXO1 by SIRT1. The expression of HSL was not affected by SIRT1 knockdown, suggesting that in addition to HSL, SIRT1 regulates the expression of other lipolytic genes including ATGL (Chakrabarti et al., 2011). Lasa et al. (2012) assessed the effect of resveratrol on lipolysis and the specific roles of ATGL and HSL on lipolysis in 3T3-L1 adipocytes, SGBS human adipocytes,

and adipocytes derived from wild-type, ATGL knockout and HSL knockout mice. These authors showed that resveratrol stimulates lipolysis particularly by increasing ATGL expression (Lasa et al., 2012). Possible future work could investigate the effects of the organic fraction from the aqueous methanol extract of *C. intermedia* on both HSL and ATGL at protein level.

In adipocytes, *in vitro*, the mRNA expression of *UCP3* was increased after treatment with the organic fraction of *C. intermedia*, whereas no significant effect was observed in *UCP2* mRNA expression. Uncoupling proteins (UCPs) are inner mitochondrial proteins that are important regulators of mitochondrial metabolism and uncoupling of oxidative metabolism (Brand and Esteves, 2005; Rousset et al., 2004). *UCP2* mRNA is expressed in various tissues including white adipocytes whereas, *UCP3* is mainly expressed in muscles, heart and to a lesser extent in adipocytes (Thompson and Kim, 2004). Activation of *UCP2* and *UCP3* has been associated with increased antioxidant capacity and fatty acid oxidation (Brand and Esteves, 2005). *UCP3* protects against lipotoxicity by preventing the accumulation of FA anions or lipid peroxides in the mitochondrial matrix and in doing so, protects the mitochondria against the harmful effects induced by high levels of fatty acids (Schrauwen and Hesselink, 2004). The peroxisome proliferator-activated receptor (PPARs) transcription factor family have been shown to regulate or activate *UCP2* and *UCP3* (Bugge et al., 2010; Teruel et al., 2000). Rosiglitazone and Wy14643, agonists of PPAR γ and PPAR α respectively, increased *UCP3* expression in cultured fetal rat brown adipocytes. The expression of *UCP3* was more significant when cells were treated with the combination of rosiglitazone and Wy14643 (Teruel et al., 2000). In this study the increased expression of *UCP3* could also be associated with fatty acid oxidation, however this was not investigated in this study. Contrary to expectation, the mRNA expression of other energy metabolism genes including *PPAR α* , *SIRT3*, *PGC-1 α* , *UCP2* and *AMPK* was not significantly affected by treatment with the organic fraction of *C. intermedia*.

Furthermore, no statistical significance was observed in the mRNA expression of lipid and glucose regulating genes including *C/EBP α* , *SREBF1*, *CREB1*, *GATA2*, *FGF2*, *CPT1 α* , *Cs*, *IRS1*, *G6PC*, *GLUT4* and *ADIPOQ*, and the mRNA expression of lipogenic genes including *LPL*, *FABP4*, *ACACA*, *FASN* and *SCD1*, although the decreased mRNA expression of *LPL* was borderline significant ($P = 0.09$). *LPL* is synthesized by

several tissues including adipocytes and its main function in adipose tissue is to hydrolyze TG-rich lipoproteins such as chylomicrons and very low-density lipoproteins (VLDLs), releasing fatty acids which are taken up by adipocytes for storage in lipid droplets or used for oxidation (Wang and Eckel et al., 2009). Increased expression of *GLUT4*, *IRS1* and adiponectin is associated with insulin sensitivity and glucose uptake (Bruce et al., 2005), whereas increased expression of *CPT1 α* and *Cs* is associated with fatty acid and carbohydrate oxidation (Glatz et al., 2010). Furthermore, increased *LPL*, *FABP4*, *ACACA*, *FASN* and *SCD1* is associated with fatty acid uptake, transport and synthesis whereas increased *CE/BP α* , *SREBF1* and *FGF2* expression induces adipogenesis, and increased *GATA2* inhibits adipogenesis (Moreno-Navarrete and Fernández-Real, 2012). Increased *CREB1* expression induces insulin resistance (Qi et al., 2009).

PPAR γ is an important transcriptional regulator of adipocyte differentiation (Rosen et al., 1999). However, in mature adipocytes PPAR γ plays an important role in insulin signaling (Leonardini et al., 2009), and inducing browning of white adipose tissues (Petrovic et al., 2010). Increased mRNA expression of PPAR γ was observed after *C. intermedia* treatment, however no difference in PPAR γ expression was observed at the protein level. One possible reason for the differences in mRNA and protein expression of PPAR γ could be due to posttranscriptional and posttranslational modifications that are involved in converting mRNA into protein (Greenbaum et al., 2003). MicroRNAs, small non-coding RNA molecules that regulate gene expression by translational repression or mRNA degradation (Huntzinger and Izaurralde, 2011), could also contribute to the difference in mRNA and protein expression. Other possible reasons for the lack of correlation between mRNA and protein expression could be factors such as protein half-life, experimental error or experimental noise (Maier et al., 2009).

The anti-obesity effects of the organic fraction of the aqueous methanol extract of *C. intermedia* was confirmed in *Lepr^{db/db}* mice. Mice were treated with an up-scaled preparation of the organic fraction of *C. intermedia* and the effect on body weight assessed. LC-MS/MS analysis, quantitative HPLC-DAD and *in vitro* testing in 3T3-L1 adipocytes confirmed that the phenolic content and bioactivity of the extract prepared on large-scale was similar to the original extract, and that any biological effects

observed in mice would not be due to batch variation. Compared to their heterozygous lean $Lepr^{db/+}$ controls, obese $Lepr^{db/db}$ mice demonstrated increased body weight, increased food and water consumption, high levels of fasting plasma glucose and serum insulin, and glucose intolerance during the oral glucose tolerance test (OGTT), illustrating that $Lepr^{db/db}$ mice simulates the clinical characteristics of obesity and T2DM, and is an acceptable model to use in this study.

Treatment with 351.5 mg/kg of the organic fraction of *C. intermedia*, equivalent to five cups of honeybush tea, decreased body weight gain in obese $Lepr^{db/db}$ mice, whereas treatment with the lower dose (70.5 mg/kg), equivalent to one cup of honeybush tea, had no effect on body weight in obese $Lepr^{db/db}$ mice. The decrease in body weight gain was not associated with changes in food intake or water consumption. Our findings suggest that the decreased body weight after *C. intermedia* treatment is not due to appetite suppression, although this is debatable since the obese $Lepr^{db/db}$ mouse model has a leptin receptor deficiency, resulting in them being hyperphagic (Wang et al., 2014) and thus not useful for studies assessing appetite regulation. However, our findings are in agreement with others who have also reported anti-obesity effects of plant extracts or compounds without modulation of food or water intake. For example, Patel (2012) demonstrated that daily consumption of a hot water extract of *C. maculata* at 300 mg/kg for 12 weeks inhibited weight gain by 12.7% in non-obese Wistar rats fed a high fat, high sugar cafeteria diet without changes in food consumption. Zhao et al. (2015) showed that gamma-tocotrienol ($\gamma T3$), a natural derivative of vitamin E with antioxidant activity (Newaz and Nawal, 1999), decreased body weight gain in high-fat diet induced obese mice without affecting food intake. Ethanol extract of *Prunus mume* fruits also decreased body weight without reducing food intake in high-fat diet induced obese mice (Shin et al., 2013).

Compared to the lean $Lepr^{db/+}$ mice, the relative liver weight was significantly increased in the obese $Lepr^{db/db}$ control mice. The increase in liver weight could be associated with hepatosteatosis, although this was not assessed in this study. Hepatosteatosis, or fatty liver is a condition of fat accumulation in the liver usually induced by obesity, due to a high calorie diet (Jung and Choi, 2014). Treatment with the organic fraction of *C. intermedia* at 351.5 mg/kg increased the relative liver weight of $Lepr^{db/db}$ mice whereas no significant effect was observed in $Lepr^{db/db}$ mice treated with the lower dose

(70.5 mg/kg). Similar to our study, a hot water extract of *C. maculata* increased liver weight in obese and non-obese Wistar rats fed a high fat, high sugar cafeteria diet (Patel, 2012). Several studies have shown that plant extracts or polyphenols ameliorate hepatosteatosis by decreasing liver weight and the expression of genes or proteins associated with lipid and fatty acid metabolism in the liver (Aguirre et al., 2014; Park et al., 2013). Therefore, investigating the molecular mechanism of lipid metabolism in the liver could shed light on how the organic fraction of *C. intermedia* increases liver weight in $Lepr^{db/db}$ mice. Furthermore, the increased liver weight in $Lepr^{db/db}$ mice treated with the organic fraction of *C. intermedia* could be associated with increased glycogen synthesis in the liver as suggested by Islam (2011).

Although previous studies have demonstrated the anti-diabetic potential of *Cyclopia* spp. *in vivo*, our study showed that treatment with the organic fraction of *C. intermedia* did not have any effect on plasma glucose levels, serum insulin levels and OGTT in the $Lepr^{db/db}$ control mice compared to the $Lepr^{db/db}$ treated mice. Muller et al. (2011) reported that a hot water extract of *C. intermedia* decreased blood glucose concentrations in STZ-induced diabetic rats, and blood glucose and cholesterol concentrations in diet-induced obese insulin resistant rats. More recently, Chellan et al. (2014) demonstrated that an aqueous extract of *C. maculata* ameliorated STZ-induced diabetes in male Wistar rats, by improving glucose tolerance, decreasing fasting plasma glucose and decreasing pancreatic β -cell cytotoxicity. Further, Schulze et al. (2016) reported that a hot water extract of *C. subternata* improved glucose tolerance in STZ-induced diabetic rats. All these studies demonstrate the potential of *Cyclopia* extracts using Wistar rats, whereas in our study we used the obese $Lepr^{db/db}$ mouse model and therefore it is possible that the different anti-diabetic effects are due to the animal models used. The inability of the organic fraction of *C. intermedia* to demonstrate glucose lowering properties, as previously reported by Muller et al. (2011) could also be due to extract variation and treatment duration. In the lean $Lepr^{db/+}$ mice, treatment with the organic fraction of *C. intermedia* at both concentrations did not affect body weight, plasma glucose levels, serum insulin levels, OGTT and the liver weight compared to $Lepr^{db/+}$ control mice. This suggests that the organic fraction of *C. intermedia* could be a good therapeutic agent for obesity as it is selective for obese mice.

The mRNA expression of selected genes in adipose tissue of $Lepr^{db/db}$ mice and $Lepr^{db/+}$ control mice was measured using qRT-PCR. Adipose tissue consists of two major types of tissue, namely WAT whose main function is to store excess energy as fat and release it during energy demand, and BAT, whose function is to generate heat and increase energy expenditure (Cannon and Nedergaard, 2004; Gaidhu and Ceddia, 2011). Within WAT, different fat depots have different roles, for example the subcutaneous WAT (sWAT) is distributed throughout the body and is less metabolically active compared to visceral WAT. Visceral WAT (mesenteric, retroperitoneal or gonadal) is distributed in the abdominal area, surrounding the internal organs and is associated with the metabolic syndrome (Jensen, 2008). The gonadal WAT (gWAT) represents one of the largest adipose depots in rodents and is attached to the female uterus and ovaries, or male epididymis and testis (Bjørndal et al., 2011). The majority of BAT is found abundant in the interscapular region of rodents (iBAT) (Bjørndal et al., 2011).

Differences in gene expression were observed between $Lepr^{db/+}$ and $Lepr^{db/db}$ mice, and between different fat depots (sWAT, gWAT and iBAT) within these mice. The mRNA expression of *UCP1* and *UCP3* was decreased in $Lepr^{db/db}$ mice compared to their lean counterparts, whereas the mRNA expression of *UCP2* was increased in $Lepr^{db/db}$ mice compared to their lean counterparts. Obese mice were generally observed to be less active than their lean counterparts, thus decreased expression of *UCP1* is expected. Rong et al. (2007) showed that the transcriptional expression of *UCP1* and *UCP3* was decreased by 1.5 and 2.7 fold respectively, in the inguinal subcutaneous adipose tissue of $Lepr^{db/db}$ mice vs. $Lepr^{db/+}$ mice, whereas the expression of these proteins was decreased by 81.1 and 2.0 fold, respectively in the inguinal subcutaneous adipose tissue of high fat diet fed C57BL/6J mice vs. standard fat diet fed C57BL/6J mice. Furthermore, the expression of *UCP2* remained unchanged in these animals (Rong et al., 2007). *UCP2* is ubiquitously expressed in various tissues and its increased expression is associated with obesity and hyperinsulinemia (Gimeno et al., 1997). Increased *UCP2* mRNA expression in iBAT was accompanied by increased *CPT1 α* , a protein responsible for the transport of fatty acids across the mitochondrial matrix and facilitating fatty acid oxidation (Glatz et al., 2010).

When comparing the expression of the uncoupling proteins between the different adipose tissue depots, the mRNA expression of *UCP1*, *UCP2* and *UCP3* was increased by 2, 1.5 and 7.5 fold respectively in the gWAT of the *Lepr^{db/db}* mice compared to the expression of these genes in the sWAT of the *Lepr^{db/db}* mice. In iBAT of *Lepr^{db/db}* mice, the mRNA expression of *UCP1*, *UCP2* and *UCP3* was increased by 6 095, 2.4, and 19 fold, respectively compared to the expression of these genes in of the sWAT of *Lepr^{db/db}* mice. These results are consistent with reports of increased *UCP1* expression in BAT where its primary function is to increase energy expenditure via adaptive thermogenesis (Wu et al., 2013).

In the gWAT of *Lepr^{db/db}* mice, the mRNA expression of *SIRT1*, *SIRT3*, *AMPK*, *PGC1 α* , *PPAR γ* and *PPAR α* was increased by 4.5, 11.9, 19.5, 3.3, 5.6 and 9.9 fold, respectively compared to the mRNA expression of these genes in the sWAT of *Lepr^{db/db}* mice. Furthermore, the mRNA expression of *SIRT1*, *SIRT3*, *AMPK*, *PGC1 α* , *PPAR γ* and *PPAR α* was increased by 3.6, 7.7, 1.6, 111.2, 6.6 and 31.3 fold, respectively in the iBAT of *Lepr^{db/db}* mice compared to the expression of these genes in the gWAT. These results support studies suggesting that brown adipocytes are associated with increased energy metabolism and uncoupling activity (uncoupling respiration from oxidative phosphorylation to minimize ROS production) compared to white adipocytes (Wu et al., 2013). For example, *SIRT3* mRNA expression was decreased in the iBAT of *Lepr^{db/db}* mice compared to lean control mice, whereas no effect was observed in the sWAT and gWAT. *SIRT3* is highly expressed in brown adipose tissues and its expression is increased during fasting, caloric restriction or cold exposure (Shi et al., 2005). Compared to the lean control mice, the mRNA expression of *PGC1 α* was increased in the sWAT of *Lepr^{db/db}* mice, whereas the expression of *AMPK* was decreased in the iBAT of *Lepr^{db/db}* mice.

The mRNA expression of *ACACA*, *CREB1*, *FABP4*, *FASN*, *HSL*, *SCD1* and *SREBF1* was increased by 10, 11.8, 7.2, 11.4, 2.5, 5 and 11.5 fold, respectively in the gWAT of *Lepr^{db/db}* mice compared to the mRNA expression of these genes in the sWAT. This shows that the expression of lipogenic genes is more abundant in gWAT than it is in sWAT, thus the sWAT are less metabolically active compared to the gWAT, further confirming that visceral fat is more detrimental than subcutaneous fat and is associated with the metabolic syndrome (Hamdy et al., 2006). In OLETF rats, an animal model of

T2DM, ageing significantly increased the mRNA expression of lipogenic genes such as fatty acid binding protein (aP2), lipin1, and diacylglycerol acyltransferase 1 (DGAT1), and the expression of these genes was more prominent in the visceral fat than in subcutaneous fat (Park et al., 2016). The mRNA expression of *CREB1*, *SREBF1*, *ACACA*, *FASN*, *SCD1* and *HSL* was decreased in *Lepr^{db/db}* mice (in the sWAT and gWAT) compared to the lean control mice. These genes are important regulators of lipid, fatty acid and glucose metabolism. During obesity, *CREB1* is activated and induces insulin resistance, and gluconeogenic gene expression in adipose tissue and liver (Qi et al., 2009). SREBP1 gene encodes for the transcription factor SREBP-1c and thus induces fatty acid and TG synthesis by regulating the expression of lipogenic genes including ATP-citrate lyase (ACL), acetyl-CoA Carboxylase (ACC), fatty acid synthase (FASN), stearoyl-CoA desaturase (SCD), and glyceraldehyde-3-phosphate acyltransferase (GPAT) (Strable and Ntambi, 2010). The decrease in mRNA expression of lipogenic genes in the *Lepr^{db/db}* mice could be due to reduced lipogenic capacity in adipocytes of obese adipose tissues (Lan et al., 2003). In human obesity, decreased expression of lipogenic genes in adipose tissue was coupled with increased hepatic lipogenesis (Diraison et al., 2002). Therefore, decreased expression of lipogenic genes in sWAT and gWAT of *Lepr^{db/db}* mice could be associated with increased hepatic lipogenesis, possibly contributing to increased body weight and liver weight. Decreased mRNA expression of lipogenic genes was accompanied by increased *FABP4* mRNA expression in sWAT.

Treatment with the organic fraction of the aqueous methanol extract of *C. intermedia* increased the mRNA expression of *FGF2* in the gWAT of *Lepr^{db/db}* mice. Fibroblast growth factors (FGFs) have been implicated in several biological processes including adipogenesis, and particularly *FGF2* induces adipogenic differentiation of human adipose-derived stem cells (Kakudo et al., 2007). To the contrary, another *in vitro* cell culture study showed that increased expression of *FGF2* suppresses adipogenesis (Kim et al., 2015). Several studies have demonstrated that medicinal plant extracts or polyphenols decrease body weight without modulation of gene expression, particularly in adipose tissues (Zhao et al. 2015). As cited previously, γ T3 also decreased body weight gain in high-fat diet induced obese mice without inducing significant changes in adipogenic genes in the epididymal adipose tissues, although γ T3 significantly altered hepatic energy regulating genes (Zhao et al. 2015). Our results suggest that the

organic fraction of *C. intermedia* decreases body weight gain in *Lepr^{db/db}* mice without affecting food consumption, nor displaying major effects on the expression of lipogenic, fatty acid, glucose and energy metabolism genes in various adipose tissue depots, hinting that its anti-obesity effects are mediated by other mechanisms, such as inhibition of pancreatic lipase and other intestinal metabolic enzymes (Lunagariya et al., 2014).

5.3 HPLC fractionation of *Cyclopia intermedia* into four fractions with different bioactivity

To facilitate the identification of anti-obesity compounds, the organic extract of *C. intermedia*, which displayed anti-obesity properties *in vitro* and *in vivo*, was fractionated into four sub-fractions using HPLC. These fractions exhibited different effects on adipogenesis, lipogenesis and lipolysis in 3T3-L1 adipocytes. In differentiating 3T3-L1 pre-adipocytes, CCC F1 inhibited lipid accumulation at 1 and 10 µg/mL, CCC F2 had no effect, CCC F3 decreased lipid accumulation at all treatment concentrations, and CCC F4 decreased lipid accumulation at 1, 10 and 50 µg/mL only. In mature 3T3-L1 adipocytes, CCC F1 and 2 decreased lipid content at 100 µg/mL only, CCC fraction 3 had no effect, and CCC F4 decreased lipid content at 10 and 100 µg/mL. Furthermore, in mature adipocytes, CCC F1 stimulated lipolysis at 1 and 50 µg/mL, CCC F2 at 50 µg/mL, CCC F3 had no effect on lipolysis and CCC F4 increased lipolysis at 1 µg/mL only. The differences in ORO quantification and glycerol release assay results suggests that mechanisms other than lipolysis are responsible for decreasing lipid content.

The different bioactivities described above was due to the variation in phenolic compounds between the fractions. CCC F1 contained the benzophenone, iriflophenone-3-C-β-D-glucoside-4-O-β-D-glucoside and the flavone, vicenin-2, CCC F2 contained the benzophenone, iriflophenone-3-C-β-D-glucoside and the flavanones, hesperidin and eriodictyol-O-deoxyhexoside-O-hexoside, CCC F3 contained the xanthenes, mangiferin and isomangiferin, and CCC F4 contained neoponcirin. All fractions, at different concentrations, with the exception of CCC F2 in differentiating adipocytes, and CCC F3 in mature adipocytes, decreased lipid content. Similarly, all fractions, at different concentrations, stimulated lipolysis, except for CCC F3. These

results suggest that the organic extract of *C. intermedia* contained a number of different anti-obesity compounds that were retained in the different fractions.

As cited previously, Dudhia et al. (2013) showed that the hot water extracts of *C. subternata* and *C. maculata*, at concentrations ranging from 20 - 1600 µg/mL inhibit adipogenesis by decreasing lipid accumulation and triglyceride content in differentiating 3T3-L1 pre-adipocytes. However, in this study we did not observe any significant effects on TG content in differentiating 3T3-L1 pre-adipocytes treated with the CCC fractions, although significant effects were observed using the ORO assay. Differences observed between the two assays could be due to experimental or technical errors. Using different leaf solvent extracts (*n*-hexane, dichloro methane (DCM), ethyl acetate (EtOAc) and methanol (MeOH)) of *Aegle marmelos*, Karmase et al. (2013a) evaluated the anti-adipogenic potential of these extracts at concentrations varying from 25, 50, 75 and 100 µg/mL. The DCM extract showed the highest anti-obesity activity and was further separated into 14 compounds, of which after screening, 9 compounds demonstrated anti-adipogenic activity and 2 of these compounds, halfordinol and ethyl ether aegeline showed the highest activity for lipid reduction (Karmase et al., 2013a). In addition to the anti-adipogenic activity of the DCM extract of *Aegle marmelos* leaves, Karmase et al. (2013b) assessed the effects of 14 compounds isolated from this extract on lipogenesis and lipolysis. Of the 14 compounds tested, 12 compounds decreased lipid content and induced lipolysis in differentiated 3T3-L1 adipocytes and the two compounds showing highest activity were umbelliferone and esculetin (Karmase et al., 2013b). Interestingly, ethyl ether aegeline, a compound that showed highest anti-adipogenic activity (Karmase et al., 2013a) was not effective in decreasing lipid content and inducing lipolysis in these cells (Karmase et al., 2013b). This demonstrates that different phenolic compounds within extracts regulate different anti-obesity mechanisms.

Similarly, we found that mangiferin and isomangiferin, the major phenolic contents of CCC F3, were able to inhibit lipid accumulation in 3T3-L1 pre-adipocytes, but had no effect on lipid content nor lipolysis in adipocytes. These results suggest that the effect of mangiferin against lipid accumulation is more evident in differentiating pre-adipocytes compared to matured adipocytes as previously reported (Shimada et al., 2011; Subash-babu and Alshatwi, 2015). Subash-babu and Alshatwi (2015) showed

that mangiferin inhibited differentiation of human mesenchymal stem cells into mature adipocytes, while Shimada et al. (2011) reported that mangiferin did not suppress fat accumulation in mature 3T3-L1 adipocytes. No literature has been reported about the anti-obesity effects isomangiferin. In addition to its anti-obesity potential, several studies have demonstrated the anti-diabetic potential of mangiferin (Fang et al., 2011; Girón et al., 2009; Kumar et al., 2013).

Interestingly, CCC F4 demonstrated anti-adipogenic, anti-lipogenic and lipolytic effects in 3T3-L1 adipocytes. CCC F4 was enriched in neoponcirin, a compound identified for the first time in *Cyclopia* in this study. These results suggest that this compound has several anti-obesity properties which require further exploration. Similarly, CCC F1 inhibited adipogenesis, decreased lipogenesis and induced lipolysis in 3T3-L1 adipocytes and this fraction contained high iriflophenone-3-C- β -D-glucoside-4-O- β -D-glucoside and vicenin-2 contents. The anti-obesity effect of these compounds has not been reported, although the α -Glucosidase inhibitory activity was reported for the benzophenone glucosides, including iriflophenone-3-C- β -D-glucoside-4-O- β -D-glucoside (Beelders et al., 2014), thus demonstrating its anti-diabetic potential and therefore iriflophenone-3-C- β -D-glucoside-4-O- β -D-glucoside could be further explored for its anti-obesity properties.

CCC F2 only showed anti-lipogenic and lipolytic effect in 3T3-L1 adipocytes. This fraction contained the benzophenone, iriflophenone-3-C- β -D-glucoside and the two flavanones, hesperidin and eriodictyol-O-deoxyhexoside-O-hexoside. Iriflophenone-3-C- β -D-glucoside and hesperidin have previously demonstrated anti-obesity potential whereas the anti-obesity potential of eriodictyol-O-deoxyhexoside-O-hexoside has not been reported. This could suggest that, Iriflophenone-3-C- β -D-glucoside and hesperidin exert their anti-obesity effect by inducing lipolysis and decreasing lipogenesis. Iriflophenone-3-C- β -glucoside inhibited TG synthesis and free fatty acid accumulation, and decreased the expression of associated genes in 3T3-L1 adipocytes (Zhang et al., 2011). In Wistar rats fed a high cholesterol diet, hesperidin improved hypercholesterolemia and fatty liver by inhibiting the synthesis and absorption of cholesterol (Wang et al. 2011). Furthermore, iriflophenone-3-C- β -D-glucoside increased glucose uptake in rat adipocytes, demonstrating its anti-diabetic effect (Pranakhon et al., 2015).

Given that the MTT assay has several limitations over the ATP assay, especially the interference of polyphenols with the MTT, and the ATP assay is more sensitive compared to the MTT assay, the ATP assay was used to assess the effects of the CCC fractions on cell viability during 3T3-L1 pre-adipocyte differentiation and in differentiated 3T3-L1 adipocytes. Results showed that chronic treatment of differentiating 3T3-L1 pre-adipocytes with CCC F1 and CCC F3 induced cytotoxicity by decreasing ATP content, which was significant at 100 µg/mL, and suggests that the decreased lipid accumulation observed with these fractions could possibly be associated with decreased cell viability. Several studies have demonstrated that medicinal plant extracts or polyphenols decrease lipid accumulation or TG content by inducing apoptosis or decreasing cell viability (Kim et al., 2015; Popovich et al., 2010). More recently Kim et al. (2015) showed that an aqueous methanol extract of *Porphyra yezoensis* inhibits adipogenesis by inducing apoptosis in 3T3-L1 pre-adipocytes and decreasing cell viability in differentiated 3T3-L1 adipocytes. Acute treatment with the CCC fractions in mature adipocytes did not decrease cell viability as estimated using the ATP assay, although CCC F4 increased the ATP at 100 µg/mL. The increase in ATP by CCC F4 could be associated with increased mitochondrial activity, although further studies including the assessment of mitochondrial biogenesis, are needed to confirm this.

Our results illustrate the usefulness of bioactivity guided fractionation to identify bioactive compounds in plant extracts as widely reported by others (Harbilas et al., 2013; Klein et al., 2007; Michel et al., 2013). Such techniques, including HPCCC allow the isolation of compounds of interest from complex organic mixtures (Wu and Liang, 2010). Despite the usefulness of fractionation, concerns about loss of activity after fractionation due to effects of synergism are warranted. Synergism is the combination of two or more compounds resulting in greater effect as compared to the effect as individual compounds (Lewandowska et al., 2014). In complex mixture or in a combination of two or more compounds, polyphenols demonstrate additive, antagonistic or synergistic effects. In addition to polyphenol-polyphenol interactions, the combined actions of polyphenols with food components or drug interactions also occur (de Kok et al., 2008).

In HeLa cells, treatment with mangiferin and hesperidin induced apoptotic effects with mangiferin showing high activity compared to hesperidin, furthermore treatment with a combination of mangiferin and hesperidin improved the apoptotic effects, initially induced by hesperidin alone (Bartoszewski et al., 2014). Mortimer et al. (2015) showed that fractionation of the organic fraction of SM6Met extract, a methanol extract of *C. subternata*, into three fractions using HPLCCC, resulted in the three fractions retaining different phytoestrogenic effects compared to the organic fraction. Several other studies have reported on the synergistic effects of polyphenols in improving bioactivity (Bruckbauer and Zemel, 2014; Dai et al., 2008). A mixture of green tea polyphenols with vitamin E and vitamin C, showed remarkable increase in anti-oxidative activity compared to the efficacy of these antioxidants used as individual compounds (Dai et al., 2008).

In addition to their different effects on lipid metabolism, CCC fractions similarly displayed varying effects on gene expression. Increased *HSL* mRNA expression was observed in mature adipocytes treated with CCC F1 and CCC F2. In addition to increased mRNA expression of *HSL*, CCC F1 and CCC F2 also stimulated glycerol release, a marker of lipolysis, and decreased lipid content in differentiated 3T3-L1 adipocytes, suggesting that the decrease in lipid content by these fractions could be mediated by increased lipolysis (increased glycerol release and *HSL* expression). Similar results were reported by Park et al. (2011) who demonstrated that fucoidan, isolated from *Fucus vesiculosus* (brown algae), inhibited lipid content and induced lipolysis in mature 3T3-L1 adipocytes. Using different lipolytic agents such as isoproterenol, forskolin, dibutyryl cyclic AMP or theophylline, Morimoto et al. (2001) showed that treatment with these agents increased lipolysis without stimulating *HSL* activity, however the translocation of *HSL* from the cytosol to lipid droplets was increased by these lipolytic agents. Our study also showed that treatment with isoproterenol increased lipolysis in differentiated 3T3-L1 adipocytes without significant effects on *HSL* mRNA expression. Therefore, investigating the effects of the CCC fractions on phosphorylation and translocation of *HSL* is recommended for future studies.

Once again, no statistical significance was observed in the mRNA expression of genes implicated in lipid and glucose metabolism including *CEBP α* , *SREBF1*, *CREB1*,

GATA2, *FGF2*, *CPT1 α* , *Cs*, *G6PC*, *GLUT4* and *ADIPOQ*, and the mRNA expression of lipogenic genes including *FABP4*, *ACACA*, *FASN* and *SCD1*. Furthermore, the mRNA expression of energy metabolism genes including *SIRT3* and *UCP2* was not significantly affected by treatment with the CCC fractions. However, the decreased mRNA expression of *LPL* was borderline significant in adipocytes treated with CCC F2 ($P = 0.06$), suggesting that CCC F2 decreases lipid content in adipocytes by preventing fatty acid uptake by adipocytes.

The mRNA expression of *SIRT1* was increased in CCC F4 treated adipocytes suggesting that neoponcirin mediates its lipid lowering effect by increasing *SIRT1* mRNA expression. Increased *SIRT1* mRNA expression in adipocytes treated with CCC F3 was borderline significant and this was accompanied by increased *PGC1 α* mRNA expression. *SIRT1* has been shown to regulate *PGC1 α* via deacetylation and thus increase its transcriptional activation (Li, 2013). *PGC1 α* is a master regulator of mitochondrial biogenesis, and also regulates adaptive thermogenesis and lipid oxidation (Canto and Auwerx, 2009). Ectopic expression of *PGC-1 α* in white adipocytes increased *UCP-1* expression and also increased the expression of mitochondrial respiratory chain genes and mitochondrial DNA cellular content (Puigserver et al., 1998). Resveratrol, a natural polyphenol that activates *SIRT1*, increases *PGC-1 α* expression thus improving mitochondrial activity (Lagouge et al., 2006).

AMPK, an important energy metabolic sensor that regulates several metabolic processes including glucose and lipid metabolism (Srivastava et al., 2012) was increased in CCC F4 treated adipocytes. Although the increased expression of *AMPK* was border line significant, our findings are consistent with others who have also reported increased expression of *AMPK* and *PGC-1 α* . Lone et al. (2016) demonstrated that curcumin induced a brown fat-like phenotype in white adipocytes by increasing the expression of *AMPK* and brown fat-specific genes including *PGC-1 α* , *UCP1* and *PRDM16*. Moreover, *AMPK* is a catabolic enzyme that decreases energy consuming processes such as lipogenesis and stimulates energy producing processes such as lipolysis and fatty acid oxidation (Lim et al., 2010). Furthermore, the increased expression of *SIRT1*, as observed in this study, could also be due to its interaction with *AMPK*, as suggested by Canto and others (Canto and Auwerx, 2009; Canto et al.,

2009). The mRNA expression of *UCP3* was also increased after treatment with CCC F1 and CCC F4, suggesting that these fractions decrease lipid content in differentiated adipocytes by increasing mitochondrial uncoupling activity. The increased mRNA expression of *UCP3* was borderline significant in adipocytes treated with CCC F3 ($P = 0.07$).

Similar to the increased mRNA expression of *PPAR γ* in adipocytes treated with the organic fraction of *C. intermedia*, the mRNA expression of *PPAR γ* was increased in adipocytes treated with CCC F1, CCC F2, CCC F3 and CCC F4. This suggests that more than one polyphenol in the organic fraction of *C. intermedia* regulate the increased *PPAR γ* mRNA expression, as further fractionation of this fraction resulted in the CCC fractions all increasing *PPAR γ* in a similar manner as the organic *C. intermedia* fraction. CCC F3 showed the highest activity for increasing *PPAR γ* mRNA expression although this fraction was not effective in reducing lipid content in 3T3-L1 adipocytes. The increased expression of *PPAR γ* by CCC F3 treatment could be associated with the increased mRNA expression of *IRS1* (Leonardini et al., 2009). Once again, the expression of *PPAR γ* at protein level was not significantly affected by treatment with the CCC fractions, although significant changes were observed at the transcriptional level. However, the protein expression of *PPAR α* was increased in adipocytes treated with CCC F4. *PPAR α* promotes pre-adipocyte differentiation, whereas in adipocytes the role of *PPAR α* has been associated with fatty acid oxidation (Goto et al., 2011).

5.4 Shortcomings of the study

The limitations of this study include:

- *In vitro* cell models do not reflect the complexity of interactions between various tissues involved in the pathogenesis of obesity. For example, excessive lipolysis in adipose tissues induces insulin resistance in muscle or liver due to increased fatty acids deposition. However, the anti-obesity effects of the *C. intermedia* extract demonstrated in 3T3-L1 adipocytes were confirmed in obese *Lepr^{db/db}* mice, supporting the *in vitro* findings.

- The mRNA changes observed were not confirmed at the protein level, limiting the conclusions which could be made about the mechanism of action of the organic fraction of *C. intermedia* and its subfractions. Moreover, different mRNA gene expression results for *in vitro* and *in vivo* experiments were obtained, providing further support for the measurement of protein expression levels.
- Due to time and financial constraints, only the organic fraction of *C. intermedia* was selected (based on bioactivity and novel polyphenolic content) for further analysis. It would have been interesting to confirm *in vivo* bioactivity and perform sub-fractionation of the aqueous fractions of *C. maculata* and *C. subternata*, which also demonstrated anti-obesity effects.
- The organic fraction of *C. intermedia* was separated into four HPLC fractions only. If more fractions were separated, it would be possible to detect bioactivity of individual compounds.
- Quantitative RT-PCR experiments using animal tissues showed large variation due to individual animal heterogeneity, thus limiting statistical significance between experimental groups. However, due to ethical considerations, animal groups were kept to the minimum to detect biological activity.

5.6 Future work

The following future studies are recommended and some of them are based on the limitations of the current study:

- Due to the increased mRNA expression of *UCP3*, the role of the organic fraction of *C. intermedia* on mitochondrial activity and markers of brown fat remodeling is warranted.
- Investigation of the anti-diabetic potential of the organic fraction of *C. intermedia* and the CCC fractions on *in vitro* models would be informative.
- Obesity is associated with inflammation, oxidative stress and mitochondrial dysfunction, therefore future work should investigate the role of the organic fraction of *C. intermedia* on *in vitro* models that more accurately reflect *in vivo* disease pathophysiology.

- Investigate the effect of the organic fraction of *C. intermedia* and its sub-fractions on protein expression, which reflect molecular activity better than mRNA expression.
- Further fractionation of CCC fractions and re-testing *in vitro* and *in vivo*, to detect the anti-obesity compounds of *Cyclopia*.
- Determining anti-obesity effects in hypertrophied 3T3-L1 adipocytes, which are more representative of obesity *in vivo*.

5.7 Conclusion

This study has demonstrated the anti-obesity potential of the three commercially relevant *Cyclopia* spp., *C. subternata*, *C. intermedia* and *C. maculata* *in vitro* and further confirmed the anti-obesity potential of *C. intermedia* *in vivo*, providing evidence for the first about the anti-obesity potential of *C. intermedia* in addition to the currently known anti-obesity potential of *C. subternata* and *C. intermedia*. Moreover, phenolic enriched extracts of *C. subternata*, *C. intermedia* and *C. maculata* separated into their aqueous and organic fractions, exert different biological and cytotoxic effects. Furthermore, the aqueous fractions of *C. maculata* and *C. subternata* containing lower phenolic content, demonstrated increased anti-obesity activity compared to their organic counterparts, whereas the organic fraction of *C. intermedia* containing higher phenolic content, showed increased anti-obesity activity compared to its aqueous fraction illustrating that quality of polyphenols, rather than quantity are important for mediating biological activity. This study, for the first time detected the flavanone, neoponcirin in *Cyclopia* species, and is the first report of the anti-obesity properties of this compound. This study further demonstrates that the organic fraction of *C. intermedia* likely exerts its anti-obesity effect by increasing lipolysis, energy metabolism, uncoupling activity or brown fat remodeling of 3T3-L1 adipocytes due to increased expression of *HSL*, *SIRT1*, *UCP3* and *PPAR γ* at the transcriptional level. *In vivo* studies showed that the organic fraction of *C. intermedia* has anti-obesity potential by decreasing body weight gain in obese *Lepr^{db/db}* mice. The anti-obesity effect of the organic fraction of *C. intermedia* was not due to modulation of mRNA gene expression in adipose tissue of *Lepr^{db/db}* mice.

Bioactivity guided fractionation of the organic fraction of *C. intermedia* resulted in four major fractions with different phenolic content, and anti-obesity effects at the cellular and molecular levels. It is therefore unlikely that the anti-obesity properties of *C. intermedia* may be attributable to a single phenolic compound; the presence of more than one compound, with different mechanisms of action, or the synergistic or cumulative effects of more than one compound, may contribute to the bioactivity of the organic fraction of *C. intermedia* observed in this study.

In conclusion, this study, for the first time, provides evidence of the anti-obesity properties of *C. intermedia* *in vitro* and *in vivo*. A novel anti-obesity flavanone, neoponcirin, was identified in *C. intermedia*, the first discovery of this compound in *Cyclopia* spp. These results add to the growing body of evidence of the medicinal properties of this indigenous South African plant, supporting its commercialization as a health promoting beverage or as source material for the production of nutraceutical extracts.

REFERENCES

- Abad-García B, Berrueta LA, Garmón-Lobato S, Gallo B, Vicente F. 2009. A general analytical strategy for the characterization of phenolic compounds in fruit juices by high-performance liquid chromatography with diode array detection coupled to electrospray ionization and triple quadrupole mass spectrometry. *J Chromatogr A* 1216(28):5398-415.
- Abate N, Garg A, Peshock RM, Stray-Gundersen J, Grundy SM. 1995. Relationships of generalized and regional adiposity to insulin sensitivity in men. *J Clin Invest* 96(1):88-98.
- Abdul-Ghani MA, DeFronzo RA. 2010. Pathogenesis of insulin resistance in skeletal muscle. *J Biomed Biotechnol* 2010:476279.
- Abu-Elheiga L, Brinkley WR, Zhong L, Chirala SS, Woldegiorgis G, Wakil SJ. 2000. The subcellular localization of acetyl-CoA carboxylase 2. *Proc Natl Acad Sci* 97(4):1444-9.
- Adan RA. 2013. Mechanisms underlying current and future anti-obesity drugs. *Trends Neurosci* 36(2):133-40.
- Aditya BS, Wilding JPH. 2011. *Obesity: An Atlas of Investigation and Management*. First Edition. Clinical Publishing. United Kingdom. Page: 1.
- Aguirre L, Portillo MP, Hijona E, Bujanda L. 2014. Effects of resveratrol and other polyphenols in hepatic steatosis. *World J Gastroenterol* 20(23):7366-80.
- Ahmadian M, Duncan RE, Jaworski K, Sarkadi-Nagy E, Sul HS. 2007. Triacylglycerol metabolism in adipose tissue. *Future Lipidol* 2(2):229-37.
- Ahmadian M, Wang Y, Sul HS. 2010. Lipolysis in adipocytes. *Int J Biochem Cell Biol* 42(5):555-9.
- Akasaka T, Balasas T, Russell LJ, Sugimoto KJ, Majid A, Walewska R, Karran EL, Brown DG, Cain K, Harder L, et al. 2007. Five members of the CEBP transcription factor family are targeted by recurrent IGH translocations in B-cell precursor acute lymphoblastic leukemia (BCP-ALL). *Blood* 109(8):3451-61.
- Akiyama S, Katsumata S, Suzuki K, Ishimi Y, Wu J, Uehara M. 2010. Dietary hesperidin exerts hypoglycemic and hypolipidemic effects in streptozotocin-induced marginal type 1 diabetic rats. *J Clin Biochem Nutr* 46(1):87-92.
- Akkaoui M, Cohen I, Esnous C, Lenoir V, Sournac M, Girard J, Prip-Buus C. 2009. Modulation of the hepatic malonyl-CoA-carnitine palmitoyltransferase 1A partnership creates a metabolic switch allowing oxidation of de novo fatty acids. *Biochem J* 420(3):429-38.
- Alberti KG, Zimmet P, Shaw J, IDF Epidemiology Task Force Consensus Group. 2005. The metabolic syndrome--a new worldwide definition. *Lancet* 366(9491):1059-62.

- Alberti KG, Zimmet P, Shaw J. 2006. Metabolic syndrome--a new world-wide definition. A consensus statement from the international diabetes federation. *Diabet Med* 23(5):469-80.
- Ameer F, Scandiuzzi L, Hasnain S, Kalbacher H, Zaidi N. 2014. De novo lipogenesis in health and disease. *Metabolism* 63(7):895-902.
- Andersen CL, Jensen JL, Orntoft TF. 2004. Normalization of real-time quantitative reverse transcription-PCR data: A model-based variance estimation approach to identify genes suited for normalization, applied to bladder and colon cancer data sets. *Cancer Res* 64(15):5245-50.
- Anderson JW, Luan J, Hoie LH. 2004. Structured weight-loss programs: Meta-analysis of weight loss at 24 weeks and assessment of effects of intervention intensity. *Adv Ther* 21(2):61-75.
- Andrade JM, Frade AC, Guimaraes JB, Freitas KM, Lopes MT, Guimaraes AL, de Paula AM, Coimbra CC, Santos SH. 2014. Resveratrol increases brown adipose tissue thermogenesis markers by increasing SIRT1 and energy expenditure and decreasing fat accumulation in adipose tissue of mice fed a standard diet. *Eur J Nutr* 53(7):1503-10.
- Arita Y, Kihara S, Ouchi N, Takahashi M, Maeda K, Miyagawa J, Hotta K, Shimomura I, Nakamura T, Miyaoka K, et al. 1999. Paradoxical decrease of an adipose-specific protein, adiponectin, in obesity. *Biochem Biophys Res Commun* 257(1):79-83.
- Aritomi M and Kawasaki T. 1969. A new xanthone C-glucoside, position isomer of mangiferin, from *Anemarrhena asphodeloides* bunge. *Tetrahedron Lett* 12(12):941-4.
- Arya M, Shergill IS, Williamson M, Gommersall L, Arya N, Patel HR. 2005. Basic principles of real-time quantitative PCR. *Expert Rev Mol Diagn* 5(2):209-19.
- Asada M, Rauch A, Shimizu H, Maruyama H, Miyaki S, Shibamori M, Kawasome H, Ishiyama H, Tuckermann J, Asahara H. 2011. DNA binding-dependent glucocorticoid receptor activity promotes adipogenesis via kruppel-like factor 15 gene expression. *Lab Invest* 91(2):203-15.
- Babu PV, Liu D, Gilbert ER. 2013. Recent advances in understanding the anti-diabetic actions of dietary flavonoids. *J Nutr Biochem* 24(11):1777-89.
- Bahadoran Z, Mirmiran P, Azizi F. 2013. Dietary polyphenols as potential nutraceuticals in management of diabetes: A review. *J Diabetes Metab Disord* 12(1):43, 6581-12-43.
- Banerji MA, Lebowitz J, Chaiken RL, Gordon D, Kral JG, Lebovitz HE. 1997. Relationship of visceral adipose tissue and glucose disposal is independent of sex in black NIDDM subjects. *Am J Physiol* 273(2 Pt 1):E425-32.

- Barreca D, Bellocco E, Caristi C, Leuzzi U, Gattuso G. 2011. Kumquat (*Fortunella japonica* Swingle) juice: Flavonoid distribution and antioxidant properties. *Food Res Int* 44(7):2190-7.
- Bartoszewski R, Hering A, Marszall M, Stefanowicz Hajduk J, Bartoszezowska S, Kapoor N, Kochan K, Ochocka R. 2014. Mangiferin has an additive effect on the apoptotic properties of hesperidin in *Cyclopia* sp. tea extracts. *PLoS One* 9(3):e92128.
- Basen-Engquist K and Chang M. 2011. Obesity and cancer risk: Recent review and evidence. *Curr Oncol Rep* 13(1):71-6.
- Bates SH, Jones RB, Bailey CJ. 2000. Insulin-like effect of pinitol. *Br J Pharmacol* 130(8):1944-8.
- Bechmann LP, Hannivoort RA, Gerken G, Hotamisligil GS, Trauner M, Canbay A. 2012. The interaction of hepatic lipid and glucose metabolism in liver diseases. *J Hepatol* 56(4):952-64.
- Beecher, C.W.W., Farnsworth, N.R., Gyllenhaal, C., 1989. Pharmacologically active secondary metabolites from wood. In: Rowe J.W. (Ed). *Natural Products of Woody Plants II, Chemicals Extraneous to the Lignocellular Cell Wall*. Berlin, Springer-Verlag. Page: 1059-1164.
- Beelders T, Brand DJ, de Beer D, Malherbe CJ, Mazibuko SE, Muller CJ, Joubert E. 2014. Benzophenone C- and O-glucosides from *Cyclopia genistoides* (honeybush) inhibit mammalian alpha-glucosidase. *J Nat Prod* 77(12):2694-9.
- Berger JP, Akiyama TE, Meinke PT. 2005. PPARs: Therapeutic targets for metabolic disease. *Trends Pharmacol Sci* 26(5):244-51.
- Bhagat K, Vallance P. 1997. Inflammatory cytokines impair endothelium-dependent dilatation in human veins *in vivo*. *Circulation* 96(9):3042-7.
- Birari RB, Bhutani KK. 2007. Pancreatic lipase inhibitors from natural sources: Unexplored potential. *Drug Discov Today* 12(19-20):879-89.
- Bjorndal B, Burri L, Staalesen V, Skorve J, Berge RK. 2011. Different adipose depots: Their role in the development of metabolic syndrome and mitochondrial response to hypolipidemic agents. *J Obes* 2011:490650.
- Blundell JE, Macdiarmid JI. 1997. Passive overconsumption. Fat intake and short-term energy balance. *Ann N Y Acad Sci* 827:392-407.
- Boden G. 2011. Obesity, insulin resistance and free fatty acids. *Curr Opin Endocrinol Diabetes Obes* 18(2):139-43.
- Bond P, Goldblatt P. 1984. *Plants of the Cape Flora: A Descriptive Catalogue*. CTP Book Printers, Cape Town. Page: 285-286.
- Bournat JC, Brown CW. 2010. Mitochondrial dysfunction in obesity. *Curr Opin Endocrinol Diabetes Obes* 17(5):446-52.
- Bowie J. 1830. Sketches of the botany of South African. *South African Quarterly Journal*, 27-36.

- Brand MD, Esteves TC. 2005. Physiological functions of the mitochondrial uncoupling proteins UCP2 and UCP3. *Cell Metab* 2(2):85-93.
- Bray GA, Nielsen SJ, Popkin BM. 2004. Consumption of high-fructose corn syrup in beverages may play a role in the epidemic of obesity. *Am J Clin Nutr*. 79(4):537-43.
- Bray MS. 2008. Implications of gene-behavior interactions: Prevention and intervention for obesity. *Obesity (Silver Spring)* 16 Suppl 3:S72-8.
- Bremer AA, Stanhope KL, Graham JL, Cummings BP, Wang W, Saville BR, Havel PJ. 2011. Fructose-fed rhesus monkeys: A nonhuman primate model of insulin resistance, metabolic syndrome, and type 2 diabetes. *Clin Transl Sci* 4(4):243-52.
- Brownlee M. 2005. The pathobiology of diabetic complications: A unifying mechanism. *Diabetes* 54(6):1615-25.
- Bruce CR, Mertz VA, Heigenhauser GJ, Dyck DJ. 2005. The stimulatory effect of globular adiponectin on insulin-stimulated glucose uptake and fatty acid oxidation is impaired in skeletal muscle from obese subjects. *Diabetes* 54(11):3154-60.
- Bruckbauer A, Zemel MB. 2014. Synergistic effects of polyphenols and methylxanthines with leucine on AMPK/Sirtuin-mediated metabolism in muscle cells and adipocytes. *PLoS One* 9(2):e89166.
- Bruggisser R, von Daeniken K, Jundt G, Schaffner W, Tullberg-Reinert H. 2002. Interference of plant extracts, phytoestrogens and antioxidants with the MTT tetrazolium assay. *Planta Med* 68(5):445-8.
- Brun RP, Tontonoz P, Forman BM, Ellis R, Chen J, Evans RM, Spiegelman BM. 1996. Differential activation of adipogenesis by multiple PPAR isoforms. *Genes Dev* 10(8):974-84.
- Bugge A, Siersbaek M, Madsen MS, Gondor A, Rougier C, Mandrup S. 2010. A novel intronic peroxisome proliferator-activated receptor gamma enhancer in the uncoupling protein (UCP) 3 gene as a regulator of both UCP2 and -3 expression in adipocytes. *J Biol Chem* 285(23):17310-7.
- Calle EE, Rodriguez C, Walker-Thurmond K, Thun MJ. 2003. Overweight, obesity, and mortality from cancer in a prospectively studied cohort of U.S. adults. *N Engl J Med* 348(17):1625-38.
- Cannon B, Nedergaard J. 2004. Brown adipose tissue: Function and physiological significance. *Physiol Rev* 84(1):277-359.
- Canto C, Auwerx J. 2009. PGC-1alpha, SIRT1 and AMPK, an energy sensing network that controls energy expenditure. *Curr Opin Lipidol* 20(2):98-105.
- Canto C, Gerhart-Hines Z, Feige JN, Lagouge M, Noriega L, Milne JC, Elliott PJ, Puigserver P, Auwerx J. 2009. AMPK regulates energy expenditure by modulating NAD+ metabolism and SIRT1 activity. *Nature* 458(7241):1056-60.

- Cao H. 2014. Adipocytokines in obesity and metabolic disease. *J Endocrinol* 220(2):T47-59.
- Cao Z, Umek RM, McKnight SL. 1991. Regulated expression of three C/EBP isoforms during adipose conversion of 3T3-L1 cells. *Genes Dev* 5(9):1538-52.
- Chae BS and Shin TY. 2012. Hesperidin Ameliorates TNF- α -Mediated insulin resistance in differentiated 3T3-L1 Cells. *Nat Prod Res* 18(4):254 - 260.
- Chakrabarti P, English T, Karki S, Qiang L, Tao R, Kim J, Luo Z, Farmer SR, Kandror KV. 2011. SIRT1 controls lipolysis in adipocytes via FOXO1-mediated expression of ATGL. *J Lipid Res* 52(9):1693-701.
- Chan CY, Wei L, Castro-Munozledo F, Koo WL. 2011. (-)-Epigallocatechin-3-gallate blocks 3T3-L1 adipose conversion by inhibition of cell proliferation and suppression of adipose phenotype expression. *Life Sci* 89(21-22):779-85.
- Chan RS, Woo J. 2010. Prevention of overweight and obesity: How effective is the current public health approach. *Int J Environ Res Public Health* 7(3):765-83.
- Chang CJ, Tzeng T, Liou S, Chang Y and Liu I. 2011. Kaempferol regulates the lipid-profile in high-fat diet-fed rats through an increase in hepatic PPAR α Levels. *Planta Med* 77:1876-1882.
- Chaput JP, St-Pierre S, Tremblay A. 2007. Currently available drugs for the treatment of obesity: Sibutramine and orlistat. *Mini Rev Med Chem* 7(1):3-10.
- Chauhan RS, Dutt P. 2013. *Swertia ciliata* - A new source of mangiferin, amaroswerin and amarogentin. *Journal of Biologically Active Products from Nature* 3(2):161-5.
- Chellan N, Joubert E, Strijdom H, Roux C, Louw J, Muller CJ. 2014. Aqueous extract of unfermented honeybush (*Cyclopia maculata*) attenuates STZ-induced diabetes and beta-cell cytotoxicity. *Planta Med* 80(8-9):622-9.
- Cho AS, Jeon SM, Kim MJ, Yeo J, Seo KI, Choi MS, Lee MK. 2010. Chlorogenic acid exhibits anti-obesity property and improves lipid metabolism in high-fat diet-induced-obese mice. *Food Chem Toxicol* 48(3):937-43.
- Choi K, Kim YB. 2010. Molecular mechanism of insulin resistance in obesity and type 2 diabetes. *Korean J Intern Med* 25(2):119-29.
- Chondronikola M, Volpi E, Borsheim E, Porter C, Annamalai P, Enerback S, Lidell ME, Saraf MK, Labbe SM, Hurren NM, et al. 2014. Brown adipose tissue improves whole-body glucose homeostasis and insulin sensitivity in humans. *Diabetes* 63(12):4089-99.
- Coelho M, Oliveira T, Fernandes R. 2013. Biochemistry of adipose tissue: An endocrine organ. *Arch Med Sci* 9(2):191-200.
- Coetzee G, Marx IJ, Pengilly M, Bushula VS, Joubert E, Bloom M. 2008. Effect of rooibos and honeybush tea extracts against *Botrytis cinerea*. *S. Afr. J. Enol. Vitic.* 29, 8-13.

- Cowherd RM, Lyle RE, McGehee Jr, RE. 1999. Molecular regulation of adipocyte differentiation. *Cell Dev Biology* 10:3-10.
- Dai F, Chen W, Zhou B. 2008. Antioxidant synergism of green tea polyphenols with α -tocopherol and l-ascorbic acid in SDS micelles. *Biochimie* 90(10):1499-505.
- Das L, Bhaumik E, Raychaudhuri U, Chakraborty R. 2012. Role of nutraceuticals in human health. *J Food Sci Technol* 49(2):173-83.
- de Beer D, Schulze AE, Joubert E, de Villiers A, Malherbe CJ, Stander MA. 2012. Food ingredient extracts of *Cyclopia subternata* (honeybush): Variation in phenolic composition and antioxidant capacity. *Molecules* 17(12):14602-24.
- de Kok TM, van Breda SG, Manson MM. 2008. Mechanisms of combined action of different chemopreventive dietary compounds: A review. *Eur J Nutr* 47 Suppl 2:51-9.
- De Nyscchen, A.M., van Wyk, B.-E., van Heerden, F.R., Schutte, A.L. 1996. The major phenolic compounds in the leaves of *Cyclopia* species (honeybush tea). *Biochemical Systematics and Ecology* 24:243-246.
- Derosa G and Maffioli P. 2012. Anti-obesity drugs: A review about their effects and their safety. *Expert Opin Drug Saf* 11(3):459-71.
- Desai M, Beall M, Ross MG. 2013. Developmental origins of obesity: Programmed adipogenesis. *Curr Diab Rep* 13(1):27-33.
- Dharmananda, S., 2004. Honeybush: Healthful beverage tea from South Africa. Institute for traditional medicine, Portland, Oregon, USA.
- Ding L, Jin D, Chen X. 2010. Luteolin enhances insulin sensitivity via activation of PPAR γ transcriptional activity in adipocytes. *J Nutr Biochem* 21(10):941-7.
- Diraison F, Dusserre E, Vidal H, Sothier M, Beylot M. 2002. Increased hepatic lipogenesis but decreased expression of lipogenic gene in adipose tissue in human obesity. *American Journal of Physiology - Endocrinology and Metabolism* 282(1):E46-51.
- Dresner A, Laurent D, Marcucci M, Griffin ME, Dufour S, Cline GW, Slezak LA, Andersen DK, Hundal RS, Rothman DL, et al. 1999. Effects of free fatty acids on glucose transport and IRS-1-associated phosphatidylinositol 3-kinase activity. *J Clin Invest* 103(2):253-9.
- Du Toit J, Joubert E, Britz TJ. 1998. Honeybush Tea - A rediscovered indigenous South African herbal tea. *Journal of Sustainable Agriculture* 12:67-84.
- Dudhia Z, Louw J, Muller C, Joubert E, de Beer D, Kinnear C, Pheiffer C. 2013. *Cyclopia maculata* and *Cyclopia subternata* (honeybush tea) inhibits adipogenesis in 3T3-L1 pre-adipocytes. *Phytomedicine* 20(5):401-8.
- Duncan RE, Ahmadian M, Jaworski K, Sarkadi-Nagy E, Sul HS. 2007. Regulation of lipolysis in adipocytes. *Annu Rev Nutr* 27:79-101.

- Ekor M. 2014. The growing use of herbal medicines: Issues relating to adverse reactions and challenges in monitoring safety. *Front Pharmacol* 4:177.
- Emanuela F, Grazia M, Marco de R, Maria Paola L, Giorgio F, Marco B. 2012. Inflammation as a link between obesity and metabolic syndrome. *J Nutr Metab* 2012:476380.
- Fabbrini E, Sullivan S, Klein S. 2010. Obesity and nonalcoholic fatty liver disease: Biochemical, metabolic, and clinical implications. *Hepatology* 51(2):679-89.
- Fabricatore AN, Wadden TA. 2003. Treatment of obesity: An overview. *Clinical Diabetes* 21(2):67-72.
- Fajas L, Schoonjans K, Gelman L, Kim JB, Najib J, Martin G, Fruchart JC, Briggs M, Spiegelman BM, Auwerx J. 1999. Regulation of peroxisome proliferator-activated receptor gamma expression by adipocyte differentiation and determination factor 1/sterol regulatory element binding protein 1: Implications for adipocyte differentiation and metabolism. *Mol Cell Biol* 19(8):5495-503.
- Fang XK, Gao J, Zhu DN. 2008. Kaempferol and quercetin isolated from *euonymus alatus* improve glucose uptake of 3T3-L1 cells without adipogenesis activity. *Life Sci* 82(11-12):615-22.
- Farag YM, Gaballa MR. 2011. Diabetes: An overview of a rising epidemic. *Nephrol Dial Transplant* 26(1):28-35.
- FDA, 2007. Guidance for industry developing products for weight management, <<http://www.fda.gov/downloads/Drugs/GuidanceComplianceRegulatoryInformation/Guidances/ucm071612.pdf>> (July 1, 2011).
- Feng J, Yang XW, Wang RF. 2011. Bio-assay guided isolation and identification of alpha-glucosidase inhibitors from the leaves of *Aquilaria sinensis*. *Phytochemistry* 72(2-3):242-7.
- Fernandez-Sanchez A, Madrigal-Santillan E, Bautista M, Esquivel-Soto J, Morales-Gonzalez A, Esquivel-Chirino C, Durante-Montiel I, Sanchez-Rivera G, Valadez-Vega C, Morales-Gonzalez JA. 2011. Inflammation, oxidative stress, and obesity. *Int J Mol Sci* 12(5):3117-32.
- Ferre P, Foufelle F. 2007. SREBP-1c transcription factor and lipid homeostasis: Clinical perspective. *Horm Res* 68(2):72-82.
- Ferre P. 2004. The biology of peroxisome proliferator-activated receptors: Relationship with lipid metabolism and insulin sensitivity. *Diabetes* 53 Suppl 1:S43-50.
- Ferreira D, Kamara BI, Brandt EV, Joubert E. 1998. Phenolic compounds from *Cyclopia intermedia* (honeybush tea). 1. *J Agric Food Chem* 46(9):3406-10.
- Finucane MM, Stevens GA, Cowan MJ, Danaei G, Lin JK, Paciorek CJ, Singh GM, Gutierrez HR, Lu Y, Bahalim AN, et al. 2011. National, regional, and global trends in body-mass index since 1980: Systematic analysis of health examination surveys and epidemiological studies with 960 country-years and 9.1 million participants. *Lancet* 377(9765):557-67.

- Fleige S, Pfaffl MW. 2006. RNA integrity and the effect on the real-time qRT-PCR performance. *Mol Aspects Med* 27(2-3):126-39.
- Frayn KN, Arner P, Yki-Jarvinen H. 2006. Fatty acid metabolism in adipose tissue, muscle and liver in health and disease. *Essays Biochem* 42:89-103.
- Freytag SO, Paielli DL, Gilbert JD. 1994. Ectopic expression of the CCAAT/enhancer-binding protein alpha promotes the adipogenic program in a variety of mouse fibroblastic cells. *Genes Dev* 8(14):1654-63.
- Furukawa S, Fujita T, Shimabukuro M, Iwaki M, Yamada Y, Nakajima Y, Nakayama O, Makishima M, Matsuda M. 2004. Increased oxidative stress in obesity and its impact on metabolic syndrome. *114(12):1752-61.*
- Gaidhu MP, Ceddia RB. 2011. The role of adenosine monophosphate kinase in remodeling white adipose tissue metabolism. *Exerc Sport Sci Rev* 39(2):102-8.
- Gao CL, Zhu C, Zhao YP, Chen XH, Ji CB, Zhang CM, Zhu JG, Xia ZK, Tong ML, Guo XR. 2010. Mitochondrial dysfunction is induced by high levels of glucose and free fatty acids in 3T3-L1 adipocytes. *Mol Cell Endocrinol* 320(1-2):25-33.
- German AJ, Ryan VH, German AC, Wood IS, Trayhurn P. 2010. Obesity, its associated disorders and the role of inflammatory adipokines in companion animals. *Vet J* 185(1):4-9.
- Gibson DM, Harris RA, 2002. *Metabolic regulation in mammals*. Taylor and Francis. London Pages: 156-162.
- Gilmartin AB, Ural SH, Repke JT. 2008. Gestational diabetes mellitus. *Rev Obstet Gynecol* 1(3):129-34.
- Gimeno RE, Dembski M, Weng X, Deng N, Shyjan AW, Gimeno CJ, Iris F, Ellis SJ, Woolf EA, Tartaglia LA. 1997. Cloning and characterization of an uncoupling protein homolog: A potential molecular mediator of human thermogenesis. *Diabetes* 46(5):900-6.
- Girón MD, et al. *Salacia oblonga* extract increases glucose transporter 4-mediated glucose uptake in L6 rat myotubes: Role of mangiferin. *Clinical Nutrition* 28(5):565-74.
- Glatz JF, Luiken JJ, Bonen A. 2010. Membrane fatty acid transporters as regulators of lipid metabolism: Implications for metabolic disease. *Physiol Rev* 90(1):367-417.
- Goldberg IJ, Eckel RH, Abumrad NA. 2009. Regulation of fatty acid uptake into tissues: Lipoprotein lipase- and CD36-mediated pathways. *J Lipid Res* 50 Suppl:S86-90.
- Goldwasser J, Cohen PY, Yang E, Balaguer P, Yarmush ML, Nahmias Y. 2010. Transcriptional regulation of human and rat hepatic lipid metabolism by the grapefruit flavonoid naringenin: Role of PPAR alpha, PPARgamma and LXR alpha. *PLoS One* 5(8):e12399.

- Gordon T, Castelli WP, Hjortland MC, Kannel WB, Dawber TR. 1977. High density lipoprotein as a protective factor against coronary heart disease. The Framingham study. *Am J Med* 62(5):707-14.
- Goto T, Lee JY, Teraminami A, Kim YI, Hirai S, Uemura T, Inoue H, Takahashi N, Kawada T. 2011. Activation of peroxisome proliferator-activated receptor- α stimulates both differentiation and fatty acid oxidation in adipocytes. *J Lipid Res* 52(5):873-84.
- Graja A, Schulz TJ. 2015. Mechanisms of aging-related impairment of brown adipocyte development and function. *Gerontology* 61(3):211-7.
- Green H, Kehinde O. 1976. Spontaneous heritable changes leading to increased adipose conversion in 3T3 cells. *Cell* 7(1):105-13.
- Greenbaum D, Colangelo C, Williams K, Gerstein M. 2003. Comparing protein abundance and mRNA expression levels on a genomic scale. *Genome Biol* 4(9):117.
- Greenish HG. 1881. Cape Tea. *The Pharmaceutical Journal and Transactions* 11, 549-551.
- Gregoire FM, Smas CM, Sul HS. 1998. Understanding adipocyte differentiation. *Physiol Rev* 78(3):783-809.
- Grundy SM, Cleeman JI, Daniels SR, Donato KA, Eckel RH, Franklin BA, Gordon DJ, Krauss RM, Savage PJ, Smith SC, et al. 2005. Diagnosis and management of the metabolic syndrome. *Circulation* 112(17):2735-52.
- Guariguata L, Whiting DR, Hambleton I, Beagley J, Linnenkamp U, Shaw JE. Global estimates of diabetes prevalence for 2013 and projections for 2035. *Diabetes Res Clin Pract* 103(2):137-49.
- Guo F, Huang C, Liao X, Wang Y, He Y, Feng R, Li Y, Sun C. 2011. Beneficial effects of mangiferin on hyperlipidemia in high-fat-fed hamsters. *Mol Nutr Food Res* 55(12):1809-18.
- Guo X, Li H, Xu H, Woo S, Dong H, Lu F, Lange AJ, Wu C. 2012. Glycolysis in the control of blood glucose homeostasis. *Acta Pharmaceutica Sinica B* 2(4):358-67.
- Haemmerle G, Zimmermann R, Hayn M, Theussl C, Waeg G, Wagner E, Sattler W, Magin TM, Wagner EF, Zechner R. 2002. Hormone-sensitive lipase deficiency in mice causes diglyceride accumulation in adipose tissue, muscle, and testis. *Journal of Biological Chemistry* 277(7):4806-15.
- Hagopian K, Ramsey JJ, Weindruch R. 2008. Enzymes of glycerol and glyceraldehyde metabolism in mouse liver: Effects of caloric restriction and age on activities. *Biosci Rep* 28(2):107-15.
- Halberg N, Wernstedt-Asterholm I, Scherer PE. 2008. The adipocyte as an endocrine cell. *Endocrinol Metab Clin North Am* 37(3):753,68, x-xi.

- Hamdy O, Porramatikul S, Al-Ozairi E. 2006. Metabolic obesity: The paradox between visceral and subcutaneous fat. *Curr Diabetes Rev* 2(4):367-73.
- Han M, Li J, Tan Q, Sun Y, Wang Y. 2010. Limitations of the use of MTT assay for screening in drug discovery. *J Chin Pharmaceu Sci* 19:195-200.
- Harbilas D, Vallerand D, Brault A, Saleem A, Arnason JT, Musallam L, Haddad PS. 2013. *Populus balsamifera* extract and its active component salicortin reduce obesity and attenuate insulin resistance in a diet-induced obese mouse model. *Evid Based Complement Alternat Med* 2013:172537.
- Haslam DW, James WP. 2005. Obesity. *Lancet* 366(9492):1197-209.
- Herranz-Lopez M, Fernandez-Arroyo S, Perez-Sanchez A, Barrajon-Catalan E, Beltran-Debon R, Menendez JA, Alonso-Villaverde C, Segura-Carretero A, Joven J, Micol V. 2012. Synergism of plant-derived polyphenols in adipogenesis: Perspectives and implications. *Phytomedicine* 19(3-4):253-61.
- Hiramitsu M, Shimada Y, Kuroyanagi J, Inoue T, Katagiri T, Zang L, Nishimura Y, Nishimura N, Tanaka T. 2014. Eriocitrin ameliorates diet-induced hepatic steatosis with activation of mitochondrial biogenesis. *Scientific Reports* 4:3708.
- Hoerger TJ, Zhang P, Segel JE, Kahn HS, Barker LE, Couper S. 2010. Cost-effectiveness of bariatric surgery for severely obese adults with diabetes. *Diabetes Care* 33(9):1933-9.
- Holm C. 2003. Molecular mechanisms regulating hormone-sensitive lipase and lipolysis. *Biochem Soc Trans* 31(Pt 6):1120-4.
- Hsu CL, Yen GC. 2008. Phenolic compounds: Evidence for inhibitory effects against obesity and their underlying molecular signaling mechanisms. *Mol Nutr Food Res* 52(1):53-61.
- Hunter CM, Peterson AL, Alvarez LM, Poston WC, Brundige AR, Haddock CK, Van Brunt DL, Foreyt JP. 2008. Weight management using the internet a randomized controlled trial. *Am J Prev Med* 34(2):119-26.
- Huntzinger E, Izaurralde E. 2011. Gene silencing by microRNAs: Contributions of translational repression and mRNA decay. *Nat Rev Genet* 12(2):99-110.
- Ibdah JA, Perlegas P, Zhao Y, Angdisen J, Borgerink H, Shadoan MK, Wagner JD, Matern D, Rinaldo P, Cline JM. 2005. Mice heterozygous for a defect in mitochondrial trifunctional protein develop hepatic steatosis and insulin resistance. *Gastroenterology* 128(5):1381-90.
- Islam MS. 2011. Effects of the aqueous extract of white tea (*camellia sinensis*) in a streptozotocin-induced diabetes model of rats. *Phytomedicine* 19(1):25-31.
- Jakicic JM. 2009. The effect of physical activity on body weight. *Obesity (Silver Spring)* 17 Suppl 3:S34-8.
- James WP. 2008. The epidemiology of obesity: The size of the problem. *J Intern Med* 263(4):336-52.

- Jensen MD. 2008. Role of body fat distribution and the metabolic complications of obesity. *J Clin Endocrinol Metab* 93(11 Suppl 1):S57-63.
- Jo J, Gavrilova O, Pack S, Jou W, Mullen S, Sumner AE, Cushman SW, Periwai V. 2009. Hypertrophy and/or hyperplasia: Dynamics of adipose tissue growth. *PLoS Comput Biol* 5(3):e1000324.
- Joubert E, Gelderblom WC, De Beer D. 2009. Phenolic contribution of South African herbal teas to a healthy diet. *Nat Prod Commun* 4(5):701-18.
- Joubert E, Gelderblom WC, Louw A, de Beer D. 2008a. South African herbal teas: *Aspalathus linearis*, *Cyclopia* spp. and *Athrixia phyllicoides*--a review. *J Ethnopharmacol* 119(3):376-412.
- Joubert E, Joubert ME, Bester C, de Beer D, De Lange JH. 2011. Honeybush (*Cyclopia* spp.): From local cottage industry to global markets — the catalytic and supporting role of research. *S Afr J Bot* 77(4):887-907.
- Joubert E, Richards ES, Merwe JD, De Beer D, Manley M, Gelderblom WC. 2008b. Effect of species variation and processing on phenolic composition and in vitro antioxidant activity of aqueous extracts of *Cyclopia* spp. (honeybush tea). *J Agric Food Chem* 56(3):954-63.
- Joubert J, Norman R, Bradshaw D, Goedecke JH, Steyn NP, Puoane T, South African Comparative Risk Assessment Collaborating Group. 2007. Estimating the burden of disease attributable to excess body weight in South Africa in 2000. *S Afr Med J* 97(8 Pt 2):683-90.
- Jung UJ, Choi MS. 2014. Obesity and its metabolic complications: The role of adipokines and the relationship between obesity, inflammation, insulin resistance, dyslipidemia and nonalcoholic fatty liver disease. *Int J Mol Sci* 15(4):6184-223.
- Jung UJ, Lee MK, Park YB, Kang MA, Choi MS. 2006. Effect of citrus flavonoids on lipid metabolism and glucose-regulating enzyme mRNA levels in type-2 diabetic mice. *Int J Biochem Cell Biol* 38(7):1134-45.
- Kadowaki T, Yamauchi T, Kubota N, Hara K, Ueki K, Tobe K. 2006. Adiponectin and adiponectin receptors in insulin resistance, diabetes, and the metabolic syndrome. *J Clin Invest* 116(7):1784-92.
- Kaila B, Raman M. 2008. Obesity: A review of pathogenesis and management strategies. *Can J Gastroenterol* 22(1):61-8.
- Kakudo N, Shimotsuma A, Kusumoto K. 2007. Fibroblast growth factor-2 stimulates adipogenic differentiation of human adipose-derived stem cells. *Biochem Biophys Res Commun* 359(2):239-44.
- Kamara BI, Brand DJ, Brandt EV, Joubert E. 2004. Phenolic metabolites from honeybush tea (*Cyclopia subternata*). *J Agric Food Chem* 52(17):5391-5.
- Kamara BI, Brandt EV, Ferreira D, Joubert E. 2003. Polyphenols from honeybush tea (*Cyclopia intermedia*). *J Agric Food Chem* 51(13):3874-9.

- Kang S, Bajnok L, Longo KA, Petersen RK, Hansen JB, Kristiansen K, MacDougald OA. 2005. Effects of Wnt signaling on brown adipocyte differentiation and metabolism mediated by PGC-1 α . *Mol Cell Biol* 25(4):1272-82.
- Kang SI, Shin HS, Kim HM, Hong YS, Yoon SA, Kang SW, Kim JH, Ko HC, Kim SJ. 2012. Anti-obesity properties of a *Sasa quepaertensis* extract in high-fat diet-induced obese mice. *Biosci Biotechnol Biochem* 76(4):755-61.
- Karmase A, Birari R, Bhutani KK. 2013b. Evaluation of anti-obesity effect of *Aegle marmelos* leaves. *Phytomedicine* 20(10):805-12.
- Karmase A, Jagtap S, Bhutani KK. 2013a. Anti-adipogenic activity of *Aegle marmelos* correa. *Phytomedicine* 20(14):1267-71.
- Kassi E, Pervanidou P, Kaltsas G, Chrousos G. 2011. Metabolic syndrome: Definitions and controversies. *BMC Med* 9:48,7015-9-48.
- Kasuga M. 2006. Insulin resistance and pancreatic beta cell failure. *J Clin Invest* 116(7):1756-60.
- Kawano A, Nakamura H, Hata S, Minakawa M, Miura Y, Yagasaki K. 2009. Hypoglycemic effect of aspalathin, a rooibos tea component from *Aspalathus linearis*, in type 2 diabetic model db/db mice. *Phytomedicine* 16(5):437-43.
- Kelly T, Yang W, Chen CS, Reynolds K, He J. 2008. Global burden of obesity in 2005 and projections to 2030. *Int J Obes (Lond)* 32(9):1431-7.
- Kerner J, Hoppel C. 2000. Fatty acid import into mitochondria. *Biochim Biophys Acta* 1486(1):1-17.
- Kersten S. 2001. Mechanisms of nutritional and hormonal regulation of lipogenesis. *EMBO Rep* 2(4):282-6.
- Kim GW, Lin JE, Blomain ES, Waldman SA. 2014. Antiobesity pharmacotherapy: New drugs and emerging targets. *Clin Pharmacol Ther* 95(1):53-66.
- Kim H, Ahn Y. 2004. Role of peroxisome proliferator-activated receptor- γ in the glucose-sensing apparatus of liver and β -cells. *Diabetes* 53(suppl 1):S60-5.
- Kim H, Lee Y, Han T, Choi EM. 2015. The micosporine-like amino acids-rich aqueous methanol extract of laver (*Porphyra yezoensis*) inhibits adipogenesis and induces apoptosis in 3T3-L1 adipocytes. *Nutr Res Pract* 9(6):592-8.
- Kim HK, Jeong TS, Lee MK, Park YB, Choi MS. 2003. Lipid-lowering efficacy of hesperetin metabolites in high-cholesterol fed rats. *Clin Chim Acta* 327(1-2):129-37.
- Kim JB, Spiegelman BM. 1996. ADD1/SREBP1 promotes adipocyte differentiation and gene expression linked to fatty acid metabolism. *Genes Dev* 10(9):1096-107.
- Kim JB, Wright HM, Wright M, Spiegelman BM. 1998. ADD1/SREBP1 activates PPAR γ through the production of endogenous ligand. *Proc Natl Acad Sci USA* 95(8):4333-7.

- Kim JY, van de Wall E, Laplante M, Azzara A, Trujillo ME, Hofmann SM, Schraw T, Durand JL, Li H, Li G, et al. 2007. Obesity-associated improvements in metabolic profile through expansion of adipose tissue. *J Clin Invest* 117(9):2621-37.
- Kim S, Ahn C, Bong N, Choe S, Lee DK. 2015. Biphasic effects of FGF2 on adipogenesis. *PLoS One* 10(3):e0120073.
- King AJ. 2012. The use of animal models in diabetes research. *Br J Pharmacol* 166(3):877-94.
- Klein G, Kim J, Himmeldirk K, Cao Y, Chen X. 2007. Antidiabetes and anti-obesity activity of *Lagerstroemia speciosa*. *Evid Based Complement Alternat Med* 4(4):401-7.
- Klemm DJ, Leitner JW, Watson P, Nesterova A, Reusch JE-, Goalstone ML, Draznin B. 2001. Insulin-induced adipocyte differentiation: Activation of CREB rescues adipogenesis from the arrest caused by inhibition of prenylation. *Journal of Biological Chemistry* 276(30):28430-5.
- Klop B, Elte JW, Cabezas MC. 2013. Dyslipidemia in obesity: Mechanisms and potential targets. *Nutrients* 5(4):1218-40.
- Koh EH, Park JY, Park HS, Jeon MJ, Ryu JW, Kim M, Kim SY, Kim MS, Kim SW, Park IS, et al. 2007. Essential role of mitochondrial function in adiponectin synthesis in adipocytes. *Diabetes* 56(12):2973-81.
- Kokotkiewicz A, Luczkiewicz M, Pawlowska J, Luczkiewicz P, Sowinski P, Witkowski J, Bryl E, Bucinski A. 2013. Isolation of xanthone and benzophenone derivatives from *Cyclopia genistoides* (L.) vent. (Honeybush) and their pro-apoptotic activity on synoviocytes from patients with rheumatoid arthritis. *Fitoterapia* 90:199-208.
- Kokotkiewicz A, Luczkiewicz M, Sowinski P, Glod D, Gorynski K, Bucinski A. 2012. Isolation and structure elucidation of phenolic compounds from *Cyclopia subternata* vogel (Honeybush) intact plant and *in vitro* cultures. *Food Chem* 133(4):1373-82.
- Kullu J, Dutta A, Constaes D, Chaudhuri S, Dutta D. 2014. Experimental and modeling studies on microwave-assisted extraction of mangiferin from curcuma amada. *3 Biotech* 4(2):107-20.
- Kumar BD, Krishnakumar K, Jaganathan SK, Mandal M. 2013. Effect of mangiferin and mahanimbine on glucose utilization in 3T3-L1 cells. *Pharmacogn Mag* 9(33):72-5.
- Kwon H, Pessin JE. 2013. Adipokines mediate inflammation and insulin resistance. *Front Endocrinol (Lausanne)* 4:71.
- Lagerros YT, Rossner S. 2013. Obesity management: What brings success? *Therap Adv Gastroenterol* 6(1):77-88.
- Lagouge M, Arghmann C, Gerhart-Hines Z, Meziane H, Lerin C, Daussin F, Messadeq N, Milne J, Lambert P, Elliott P, et al. 2006. Resveratrol improves mitochondrial

- function and protects against metabolic disease by activating SIRT1 and PGC-1alpha. *Cell* 127(6):1109-22.
- Lan H, Rabaglia ME, Stoehr JP, Nadler ST, Schueler KL, Zou F, Yandell BS, Attie AD. 2003. Gene expression profiles of nondiabetic and diabetic obese mice suggest a role of hepatic lipogenic capacity in diabetes susceptibility. *Diabetes* 52(3):688-700.
- Lasa A, Schweiger M, Kotzbeck P, Churrua I, Simón E, Zechner R, Portillo MdP. 2012. Resveratrol regulates lipolysis via adipose triglyceride lipase. *J Nutr Biochem* 23(4):379-84.
- Lee CH, Olson P, Hevener A, Mehl I, Chong LW, Olefsky JM, Gonzalez FJ, Ham J, Kang H, Peters JM, et al. 2006. PPAR delta regulates glucose metabolism and insulin sensitivity. *Proc Natl Acad Sci USA* 103(9):3444-9.
- Lee H, Bae S, Yoon Y. 2013. The anti-adipogenic effects of (-)-epigallocatechin gallate are dependent on the WNT/beta-catenin pathway. *J Nutr Biochem* 24(7):1232-40.
- Lee M, Pramyothin P, Karastergiou K, Fried SK. 2014. Deconstructing the roles of glucocorticoids in adipose tissue biology and the development of central obesity. *Biochimica Et Biophysica Acta (BBA) - Molecular Basis of Disease* 1842(3):473-81.
- Lee MJ, Wu Y, Fried SK. 2010. Adipose tissue remodeling in pathophysiology of obesity. *Curr Opin Clin Nutr Metab Care* 13(4):371-6.
- Leonardini A, Laviola L, Perrini S, Natalicchio A, Giorgino F. 2009. Cross-talk between PPARgamma and insulin signaling and modulation of insulin sensitivity. *PPAR Res* 2009:818945.
- Lewandowska U, Gorlach S, Owczarek K, Hrabec E, Szewczyk K. 2014. Synergistic interactions between anticancer chemotherapeutics and phenolic compounds and anticancer synergy between polyphenols. *Postepy Hig Med Dosw (Online)* 68:528-40.
- Li J, Tong YY. 1992. Determination of active constituents in shi-wei (*Folium pyrrrosiae*) by high performance liquid chromatography. *Yao Xue Xue Bao* 27(2):153-156.
- Li X. 2013. SIRT1 and energy metabolism. *Acta Biochimica Et Biophysica Sinica* 45(1):51-60.
- Lim CT, Kola B, Korbonits M. 2010. AMPK as a mediator of hormonal signalling. *J Mol Endocrinol* 44(2):87-97.
- Lim U, Ernst T, Buchthal SD, Latch M, Albright CL, Wilkens LR, Kolonel LN, Murphy SP, Chang L, Novotny R, et al. 2011. Asian women have greater abdominal and visceral adiposity than Caucasian women with similar body mass index. *Nutr Diabetes* 1:e6.
- Lim S, Honek J, Xue Y, Seki T, Cao Z, Andersson P, Yang X, Hosaka K, Cao Y. 2012. Cold-induced activation of brown adipose tissue and adipose angiogenesis in mice. *Nat Protoc* 7(3):606-615.

- Liu M, Liu F. 2009. Transcriptional and post-translational regulation of adiponectin. *Biochem J* 425(1):41-52.
- Lone J, Choi JH, Kim SW, Yun JW. 2016. Curcumin induces brown fat-like phenotype in 3T3-L1 and primary white adipocytes. *J Nutr Biochem* 27:193-202.
- Lunagariya NA, Patel NK, Jagtap SC, Bhutani KK. 2014. Inhibitors of pancreatic lipase: State of the art and clinical perspectives. *Excli j* 13:897-921.
- Lutz TA, Woods SC. 2001. Overview of animal models of obesity. In: *Current protocols in pharmacology*. John Wiley & Sons, Inc.
- Machado M, Marques-Vidal P, Cortez-Pinto H. 2006. Hepatic histology in obese patients undergoing bariatric surgery. *J Hepatol* 45(4):600-6.
- Maffeis C. 2000. Aetiology of overweight and obesity in children and adolescents. *Eur J Pediatr* 159 Suppl 1:S35-44.
- Mahomoodally MF. 2013. Traditional Medicines in Africa: An Appraisal of Ten Potent African Medicinal Plants. *Evidence-Based Complementary and Alternative Medicine* 2013:617459.
- Maier T, Güell M, Serrano L. 2009. Correlation of mRNA and protein in complex biological samples. *FEBS Lett* 583(24):3966-73.
- Maioli E, Torricelli C, Fortino V, Carlucci F, Tommassini V, Pacini A. 2009. Critical appraisal of the MTT assay in the presence of rottlerin and uncouplers. *Biol Proced Online* 11:227-40.
- Malherbe CJ, Willenburg E, de Beer D, Bonnet SL, van der Westhuizen JH, Joubert E. 2014. Iriflophenone-3-C-glucoside from *Cyclopia genistoides*: Isolation and quantitative comparison of antioxidant capacity with mangiferin and isomangiferin using on-line HPLC antioxidant assays. *Journal of Chromatography B* 951–952:164-71.
- Marnewick J, Joubert E, Joseph S, Swanevelder S, Swart P, Gelderblom W. 2005. Inhibition of tumour promotion in mouse skin by extracts of rooibos (*Aspalathus linearis*) and honeybush (*Cyclopia intermedia*), unique South African herbal teas. *Cancer Lett* 224(2):193-202.
- Marnewick JL, Batenburg W, Swart P, Joubert E, Swanevelder S, Gelderblom WC. 2004. *Ex vivo* modulation of chemical-induced mutagenesis by subcellular liver fractions of rats treated with rooibos (*Aspalathus linearis*) tea, honeybush (*Cyclopia intermedia*) tea, as well as green and black (*Camellia sinensis*) teas. *Mutat Res* 558(1-2):145-54.
- Marnewick JL, Gelderblom WC, Joubert E. 2000. An investigation on the antimutagenic properties of South African herbal teas. *Mutat Res* 471(1-2):157-66.
- Marnewick JL, Joubert E, Swart P, Van Der Westhuizen F, Gelderblom WC. 2003. Modulation of hepatic drug metabolizing enzymes and oxidative status by rooibos

- (*Aspalathus linearis*) and honeybush (*Cyclopia intermedia*), green and black (camellia sinensis) teas in rats. J Agric Food Chem 51(27):8113-9.
- Marnewick JL, van der Westhuizen FH, Joubert E, Swanevelder S, Swart P, Gelderblom WC. 2009. Chemoprotective properties of rooibos (*Aspalathus linearis*), honeybush (*Cyclopia intermedia*) herbal and green and black (*Camellia sinensis*) teas against cancer promotion induced by fumonisin B1 in rat liver. Food Chem Toxicol 47(1):220-9.
- Martinez-Botas J, Anderson JB, Tessier D, Lapillonne A, Chang BH, Quast MJ, Gorenstein D, Chen KH, Chan L. 2000. Absence of perilipin results in leanness and reverses obesity in lepr(db/db) mice. Nat Genet 26(4):474-9.
- Mashmoul M, Azlan A, Khaza'ai H, Yusof BN, Noor SM. 2013. Saffron: A natural potent antioxidant as a promising anti-obesity drug. Antioxidants (Basel) 2(4):293-308.
- Matsuda M, Shimomura I. 2013. Increased oxidative stress in obesity: Implications for metabolic syndrome, diabetes, hypertension, dyslipidemia, atherosclerosis, and cancer. Obesity Research & Clinical Practice 7(5):e330-41.
- McGarry JD, Brown NF. 1997. The mitochondrial carnitine palmitoyltransferase system. from concept to molecular analysis. Eur J Biochem 244(1):1-14.
- Meydani M and Hasan ST. 2010. Dietary polyphenols and obesity. Nutrients 2(7):737-51.
- Mfenyana C, DeBeer D, Joubert E, Louw A. 2008. Selective extraction of *Cyclopia* for enhanced *in vitro* phytoestrogenicity and benchmarking against commercial phytoestrogen extracts. J Steroid Biochem Mol Biol 112(1-3):74-86.
- Michel C, El-sherei M, Islam W, Sleem A, Ahmed S. 2013. Bioactivity-guided fractionation of the stem bark extract of pterocarpus dalbergioides roxb. ex dc growing in Egypt. Bulletin of Faculty of Pharmacy, Cairo University 51(1):1-5.
- Mirza RH, Chi N, Chi Y, 2013. Therapeutic Potential of the Natural Product Mangiferin in Metabolic Syndrome. Journal of Nutritional Therapeutics 2:74-79.
- Mitchell JE, Crosby R, de Zwaan M, Engel S, Roerig J, Steffen K, Gordon KH, Karr T, Lavender J, Wonderlich S. 2013. Possible risk factors for increased suicide following bariatric surgery. Obesity (Silver Spring) 21(4):665-72.
- Miura T, Ichiki H, Iwamoto N, Kato M, Kubo M, Sasaki H, Okada M, Ishida T, Seino Y, Tanigawa K. 2001. Antidiabetic activity of the rhizoma of *Anemarrhena asphodeloides* and active components, mangiferin and its glucoside. Biol Pharm Bull 24(9):1009-11.
- Miyake Y, Suzuki E, Ohya S, Fukumoto S, Hiramitsu M, Sakaida K, Osawa T, Furuichi Y. 2006. Lipid-lowering effect of eriocitrin, the main flavonoid in lemon fruit, in rats on a high-fat and high-cholesterol diet. Journal of Food Science 71, S633-S637.
- Monsalve FA, Pyarasani RD, Delgado-Lopez F, Moore-Carrasco R. 2013. Peroxisome proliferator-activated receptor targets for the treatment of metabolic diseases. Mediators Inflamm 2013:549627.

- Montgomery MK, Turner N. 2015. Mitochondrial dysfunction and insulin resistance: An update. *Endocrine Connections* 4(1):R1-R15.
- Moreno-Navarrete JM, Fernández-Real JM. 2012. Adipocyte Differentiation. In: Symonds, M.E., (Ed). *Adipose Tissue Biology*. Springer. Page:17-38.
- Morimoto C, Kameda K, Tsujita T, Okuda H. 2001. Relationships between lipolysis induced by various lipolytic agents and hormone-sensitive lipase in rat fat cells. *Journal of Lipid Research* 42(1):120-7.
- Mortimer M, Visser K, de Beer D, Joubert E, Louw A. 2015. Divide and conquer may not be the optimal approach to retain the desirable estrogenic attributes of the cyclopia nutraceutical extract, SM6Met. *PLoS One* 10(7):e0132950.
- Mosmann T. 1983. Rapid colorimetric assay for cellular growth and survival: Application to proliferation and cytotoxicity assays. *J Immunol Methods* 65(1-2):55-63.
- Muller CJF, Joubert E, Gabuza K, De Beer D, Fey SJ, Louw J. 2011. Assessment of the antidiabetic potential of an aqueous extract of honeybush (*Cyclopia intermedia*) in streptozotocin and obese insulin resistant Wistar rats, in: Rasooli, I. (Ed.), *Phytochemicals: Bioactives and Impact on Health*. Intech, Croatia, page:311-332.
- Narkiewicz K. 2006. Obesity and hypertension - the issue is more complex than we thought. *Nephrol. Dial. Transplant* 21:264-267.
- Nassir F and Ibdah JA. 2014. Role of Mitochondria in Nonalcoholic Fatty Liver Disease. *Int J Mol Sci* 15:8713–8742.
- Newaz MA, Yousefipour Z, Nawal N, Adeeb N. 2003. Nitric oxide synthase activity in blood vessels of spontaneously hypertensive rats: Antioxidant protection by gamma-tocotrienol. *J Physiol Pharmacol* 54(3):319-27.
- Ng M, Fleming T, Robinson M, Thomson B, Graetz N, Margono C, Mullany EC, Biryukov S, Abbafati C, Abera SF, et al. Global, regional, and national prevalence of overweight and obesity in children and adults during 1980–2013: A systematic analysis for the global burden of disease study 2013. *The Lancet* 384(9945):766-81.
- Nguyen DM, El-Serag HB. 2010. The epidemiology of obesity. *Gastroenterol Clin North Am* 39(1):1-7.
- NHLBI Obesity Education Initiative Expert Panel on the Identification, Evaluation, and Treatment of Obesity in Adults (US). *Clinical Guidelines on the Identification, Evaluation, and Treatment of Overweight and Obesity in Adults: The Evidence Report*. Bethesda (MD): National Heart, Lung, and Blood Institute; 1998 Sep. Available from: <http://www.ncbi.nlm.nih.gov/books/NBK2003/>
- Niu Y, Li S, Na L, Feng R, Liu L, Li Y, Sun C. 2012. Mangiferin decreases plasma free fatty acids through promoting its catabolism in liver by activation of AMPK. *PLoS One* 7(1):e30782.

- Ntambi JM, Young-Cheul K. 2000. Adipocyte differentiation and gene expression. *J Nutr* 130(12):3122S-6S.
- Nye C, Kim J, Kalhan SC, Hanson RW. 2008. Reassessing triglyceride synthesis in adipose tissue. *Trends Endocrinol Metab* 19(10):356-61.
- Okabe Y, Shimada T, Horikawa T, Kinoshita K, Koyama K, Ichinose K, Aburada M, Takahashi K. 2014. Suppression of adipocyte hypertrophy by polymethoxyflavonoids isolated from *Kaempferia parviflora*. *Phytomedicine* 21(6):800-6.
- Pandey KB, Rizvi SI. 2009. Plant polyphenols as dietary antioxidants in human health and disease. *Oxid Med Cell Longev* 2(5):270-8.
- Park A, Kim WK, Bae KH. 2014. Distinction of white, beige and brown adipocytes derived from mesenchymal stem cells. *World J Stem Cells* 6(1):33-42.
- Park H, Jung UJ, Cho S, Jung H, Shim S, Choi M. 2013. Citrus unshiu peel extract ameliorates hyperglycemia and hepatic steatosis by altering inflammation and hepatic glucose- and lipid-regulating enzymes in db/db mice. *J Nutr Biochem* 24(2):419-27.
- Park HS, Kim SH, Kim YS, Ryu SY, Hwang JT, Yang HJ, Kim GH, Kwon DY, Kim MS. 2009. Luteolin inhibits adipogenic differentiation by regulating PPAR γ activation. *Biofactors* 35(4):373-9.
- Park MK, Jung U, Roh C. 2011. Fucoidan from marine brown algae inhibits lipid accumulation. *Mar Drugs* 9(8):1359-67.
- Park SE, Park CY, Choi JM, Chang E, Rhee EJ, Lee WY, Oh KW, Park SW, Kang ES, Lee HC, et al. 2016. Depot-specific changes in fat metabolism with aging in a type 2 diabetic animal model. *PLoS One* 11(2):e0148141.
- Patel O. 2012. The effect of *Cyclopia maculata* on adipogenesis and adipolysis in Wistar rats. MSc Thesis, University of the Western Cape, Bellville, South Africa.
- Patel P, Abate N. 2013. Role of Subcutaneous Adipose Tissue in the Pathogenesis of Insulin Resistance. *Journal of Obesity* 2013:1-5.
- Pessin JE, Bell GI. 1992. Mammalian facilitative glucose transporter family: Structure and molecular regulation. *Annu Rev Physiol* 54:911-30.
- Petersen KF, Shulman GI. 2006. Etiology of insulin resistance. *Am J Med* 119(5 Suppl 1):S10-6.
- Petrova A, Davids LM, Rautenbach F, Marnewick JL. 2011. Photoprotection by honeybush extracts, hesperidin and mangiferin against UVB-induced skin damage in SKH-1 mice. *J Photochem Photobiol B* 103(2):126-39.
- Petrovic N, Walden TB, Shabalina IG, Timmons JA, Cannon B, Nedergaard J. 2010. Chronic peroxisome proliferator-activated receptor gamma (PPAR γ) activation of epididymally derived white adipocyte cultures reveals a population of

- thermogenically competent, UCP1-containing adipocytes molecularly distinct from classic brown adipocytes. *J Biol Chem* 285(10):7153-64.
- Pheiffer C, Dudhia Z, Louw J, Muller C, Joubert E. 2013. *Cyclopia maculata* (honeybush tea) stimulates lipolysis in 3T3-L1 adipocytes. *Phytomedicine* 20(13):1168-71.
- Pitt JJ. 2009. Principles and applications of liquid chromatography-mass spectrometry in clinical biochemistry. *Clin Biochem Rev* 30(1):19-34.
- Poirier P, Giles TD, Bray GA, Hong Y, Stern JS, Pi-Sunyer FX, Eckel RH. 2006. Obesity and cardiovascular disease: Pathophysiology, evaluation, and effect of weight loss. *Circulation* 113(6):898-918.
- Popkin BM. 2005. Using research on the obesity pandemic as a guide to a unified vision of nutrition. *Public Health Nutr* 8(6A):724-9.
- Popovich DG, Li L, Zhang W. 2010. Bitter melon (*Momordica charantia*) triterpenoid extract reduces preadipocyte viability, lipid accumulation and adiponectin expression in 3T3-L1 cells. *Food and Chemical Toxicology* 48(6):1619-26.
- Pranakhon R, Aromdee C, Pannangpetch P. 2015. Effects of iriflophenone 3-C-beta-glucoside on fasting blood glucose level and glucose uptake. *Pharmacogn Mag* 11(41):82-9.
- Puigserver P, Wu Z, Park CW, Graves R, Wright M, Spiegelman BM. 1998. A cold-inducible coactivator of nuclear receptors linked to adaptive thermogenesis. *Cell* 92(6):829-39.
- Qi L, Saberi M, Zmuda E, Wang Y, Altarejos J, Zhang X, Dentin R, Hedrick S, Bandyopadhyay G, Hai T, et al. 2009. Adipocyte CREB promotes insulin resistance in obesity. *Diabetes* 58(3):277-86.
- Randle PJ, Garland PB, Hales CN, Newsholme EA. 1963. The glucose fatty-acid cycle. its role in insulin sensitivity and the metabolic disturbances of diabetes mellitus. *Lancet* 1(7285):785-9.
- Ranjit S, Boutet E, Gandhi P, Prot M, Tamori Y, Chawla A, Greenberg AS, Puri V, Czech MP. 2011. Regulation of fat specific protein 27 by isoproterenol and TNF-alpha to control lipolysis in murine adipocytes. *J Lipid Res* 52(2):221-36.
- Rayalam S, Yang JY, Ambati S, Della-Fera MA, Baile CA. 2008. Resveratrol induces apoptosis and inhibits adipogenesis in 3T3-L1 adipocytes. *Phytother Res* 22(10):1367-71.
- Reagan-Shaw S, Nihal M, Ahmad N. 2008. Dose translation from animal to human studies revisited. *Faseb j* 22(3):659-61.
- Richard AJ, Amini-Vaughan J, Ribnicky DM and Stephens JM. 2013. Naringenin inhibits adipogenesis and reduces insulin sensitivity and adiponectin expression in adipocytes. *Evidence-Based Complementary and Alternative Medicine* 2013:1-10.

- Rispail N, Morris P, Webb JK, 2005. Phenolic compounds: extraction and analysis. A.J. Marquez (Ed.), Lotus Japonicas Handbook, Springer, Netherlands, pp. 349-355.
- Rong JX, Qiu Y, Hansen MK, Zhu L, Zhang V, Xie M, Okamoto Y, Mattie MD, Higashiyama H, Asano S, et al. 2007. Adipose mitochondrial biogenesis is suppressed in db/db and high-fat Diet–Fed mice and improved by rosiglitazone. *Diabetes* 56(7):1751-60.
- Rosen ED, Hsu CH, Wang X, Sakai S, Freeman MW, Gonzalez FJ, Spiegelman BM. 2002. C/EBP alpha induces adipogenesis through PPARgamma: A unified pathway. *Genes Dev* 16(1):22-6.
- Rosen ED, Sarraf P, Troy AE, Bradwin G, Moore K, Milstone DS, Spiegelman BM, Mortensen RM. 1999. PPAR gamma is required for the differentiation of adipose tissue in vivo and in vitro. *Mol Cell* 4(4):611-7.
- Rosen ED, Walkey CJ, Puigserver P, Spiegelman BM. 2000. Transcriptional regulation of adipogenesis. *Genes Dev* 14(11):1293-307.
- Ross SA, Dzida G, Vora J, Khunti K, Kaiser M, Ligthelm RJ. 2011. Impact of weight gain on outcomes in type 2 diabetes. *Curr Med Res Opin* 27(7):1431-8.
- Rossner S. 2002. Obesity: The disease of the twenty-first century. *Int J Obes Relat Metab Disord* 26 Suppl 4:S2-4.
- Rothman KJ. 2008. BMI-related errors in the measurement of obesity. *Int J Obes (Lond)* 32 Suppl 3:S56-9.
- Rousset S, Alves-Guerra MC, Mozo J, Miroux B, Cassard-Doulicier AM, Bouillaud F, Ricquier D. 2004. The biology of mitochondrial uncoupling proteins. *Diabetes* 53 Suppl 1:S130-5.
- Ruderman NB, Park H, Kaushik VK, Dean D, Constant S, Prentki M, Saha AK. 2003. AMPK as a metabolic switch in rat muscle, liver and adipose tissue after exercise. *Acta Physiol Scand* 178(4):435-42.
- Sanderson M, Mazibuko SE, Joubert E, de Beer D, Johnson R, Pheiffer C, Louw J, Muller CJ. 2014. Effects of fermented rooibos (*aspalathus linearis*) on adipocyte differentiation. *Phytomedicine* 21(2):109-17.
- Savage DB. 2005. PPAR gamma as a metabolic regulator: Insights from genomics and pharmacology. *Expert Rev Mol Med* 7(1):1-16.
- Sawaya RA, Jaffe J, Friedenber L, Friedenber FK. 2012. Vitamin, mineral, and drug absorption following bariatric surgery. *Curr Drug Metab* 13(9):1345-55.
- Schrauwen P, Hesselink MK. 2004. The role of uncoupling protein 3 in fatty acid metabolism: Protection against lipotoxicity? *Proc Nutr Soc* 63(2):287-92.
- Schuklenk U, Zhang EY. 2014. Public health ethics and obesity prevention: The trouble with data and ethics. *Monash Bioeth Rev* 32(1-2):121-40.

- Schulze AE, Beelders T, Koch IS, Erasmus LM, De Beer D, Joubert E. 2015. Honeybush herbal teas (*Cyclopia* spp.) contribute to high levels of dietary exposure to xanthenes, benzophenones, dihydrochalcones and other bioactive phenolics. *Journal of Food Composition and Analysis* 44:139-48.
- Schulze AE, de Beer D, de Villiers A, Manley M, Joubert E. 2014. Chemometric analysis of chromatographic fingerprints shows potential of *Cyclopia maculata* (andrews) kies for production of standardized extracts with high xanthone content. *J Agric Food Chem* 62(43):10542-51.
- Schulze AE, De Beer D, Mazibuko SE, Muller CJ, Roux C, Willenburg EL, Nyunai N, Louw J, Manley M, Joubert E. 2016. Assessing similarity analysis of chromatographic fingerprints of *Cyclopia subternata* extracts as potential screening tool for in vitro glucose utilisation. *Anal Bioanal Chem* 408(2):639-49.
- Schutte AL. 1997. Systematics of the genus *Cyclopia* vent. (Fabaceae, Podalyrieae). *Edinburgh Journal of Botany* 54(02):125-70.
- Schweiger M, Schreiber R, Haemmerle G, Lass A, Fledelius C, Jacobsen P, Tornqvist H, Zechner R, Zimmermann R. 2006. Adipose triglyceride lipase and hormone-sensitive lipase are the major enzymes in adipose tissue triacylglycerol catabolism. *J Biol Chem* 281(52):40236-41.
- Sengupta K, Golakoti T, Chirravuri V, Marasetti A. 2011. An Herbal Formula LI85008F Inhibits Lipogenesis in 3T3-L1 Adipocytes. *Food and Nutrition Sciences* 2(8): 809-817.
- Abad-Garcia B, Berrueta LA, Garmon-Lobato S, Gallo B, Vicente F. 2009. A general analytical strategy for the characterization of phenolic compounds in fruit juices by high-performance liquid chromatography with diode array detection coupled to electrospray ionization and triple quadrupole mass spectrometry. *J Chromatogr A* 1216(28):5398-415.
- Shan T, Ren Y, Liu Y, Zhu L, Wang Y. 2010. Breed difference and regulation of the porcine sirtuin 1 by insulin. *J Anim Sci* 88(12):3909-17.
- Shaw K, O'Rourke P, Del Mar C, Kenardy J. 2005. Psychological interventions for overweight or obesity. *Cochrane Database Syst Rev* (2)(2):CD003818.
- Shi T, Wang F, Stieren E, Tong Q. 2005. SIRT3, a mitochondrial sirtuin deacetylase, regulates mitochondrial function and thermogenesis in brown adipocytes. *J Biol Chem* 280(14):13560-7.
- Shimada T, Nagai E, Harasawa Y, Watanabe M, Negishi K, Akase T, Sai Y, Miyamoto K, Aburada M. 2011. *Salacia reticulata* inhibits differentiation of 3T3-L1 adipocytes. *J Ethnopharmacol* 136(1):67-74.
- Shin EJ, Hur HJ, Sung MJ, Park JH, Yang HJ, Kim MS, Kwon DY, Hwang J. 2013. Ethanol extract of the *Prunus mume* fruits stimulates glucose uptake by regulating PPAR- γ in C2C12 myotubes and ameliorates glucose intolerance and fat accumulation in mice fed a high-fat diet. *Food Chem* 141(4):4115-21.

- Siddiqui MR, AlOthman ZA, and Rahman N 2013. Analytical Techniques in Pharmaceutical Analysis: A Review. *Arabian Journal of Chemistry* (2013). In Press, Corrected Proof.
- Sies H. 1997. Oxidative stress: Oxidants and antioxidants. *Exp Physiol* 82(2):291-5.
- Sissing L, Marnewick J, de Kock M, Swanevelder S, Joubert E, Gelderblom W. 2011. Modulating effects of rooibos and honeybush herbal teas on the development of esophageal papillomas in rats. *Nutr Cancer* 63(4):600-10.
- Smith BR, Schauer P, Nguyen NT. 2008. Surgical approaches to the treatment of obesity: Bariatric surgery. *Endocrinol Metab Clin North Am* 37(4):943-64.
- Smith BR, Schauer P, Nguyen NT. 2011. Surgical approaches to the treatment of obesity: Bariatric surgery. *Med Clin North Am* 95(5):1009-30.
- Smith SC, Collins A, Ferrari R, Holmes DR, Logstrup S, McGhie DV, Ralston J, Sacco RL, Stam H, Taubert K, et al. 2012. Our time: A call to save preventable death from cardiovascular disease (heart disease and stroke). *Circulation* 126(23):2769-75.
- Spiegelman BM. 1998. PPAR-gamma: Adipogenic regulator and thiazolidinedione receptor. *Diabetes* 47(4):507-14.
- Srinivasan K, Ramarao P. 2007. Animal models in type 2 diabetes research: An overview. *Indian J Med Res* 125(3):451-72.
- Srivastava RA, Pinkosky SL, Filippov S, Hanselman JC, Cramer CT, Newton RS. 2012. AMP-activated protein kinase: An emerging drug target to regulate imbalances in lipid and carbohydrate metabolism to treat cardio-metabolic diseases. *J Lipid Res* 53(12):2490-514.
- Stemmer K, Perez-Tilve D, Ananthakrishnan G, Bort A, Seeley RJ, Tschop MH, Dietrich DR, Pfluger PT. 2012. High-fat-diet-induced obesity causes an inflammatory and tumor-promoting microenvironment in the rat kidney. *Dis Model Mech* 5(5):627-35.
- Stephens JM. 2012. The fat controller: Adipocyte development. *PLoS Biol* 10(11):e1001436.
- Strable MS, Ntambi JM. 2010. Genetic control of de novo lipogenesis: Role in diet-induced obesity. *Crit Rev Biochem Mol Biol* 45(3):199-214.
- Subash-Babu P, Alshatwi AA. 2015. Evaluation of antiobesity effect of mangiferin in adipogenesis-induced human mesenchymal stem cells by assessing adipogenic genes. *J Food Biochem* 39(1):28-38.
- Sutherland LN, Capozzi LC, Turchinsky NJ, Bell RC, Wright DC. 2008. Time course of high-fat diet-induced reductions in adipose tissue mitochondrial proteins: Potential mechanisms and the relationship to glucose intolerance. *Am J Physiol Endocrinol Metab* 295(5):E1076-83.

- Szkudelska K, Nogowski L, Szkudelski T. 2009. Resveratrol, a naturally occurring diphenolic compound, affects lipogenesis, lipolysis and the antilipolytic action of insulin in isolated rat adipocytes. *J Steroid Biochem Mol Biol* 113(1-2):17-24.
- Tansey JT, Sztalryd C, Hlavin EM, Kimmel AR, Londos C. 2004. The central role of perilipin a in lipid metabolism and adipocyte lipolysis. *IUBMB Life* 56(7):379-85.
- Terblanche SE. 1982. Report on Honeybush Tea. Department of Biochemistry. University of Port Elizabeth, Port Elizabeth, South Africa.
- Teruel T, Smith SA, Peterson J, Clapham JC. 2000. Synergistic activation of UCP-3 expression in cultured fetal rat brown adipocytes by PPAR alpha and PPARgamma ligands. *Biochem Biophys Res Commun* 273(2):560-4.
- Thompson MP, Kim D. 2004. Links between fatty acids and expression of UCP2 and UCP3 mRNAs. *FEBS Lett* 568(1-3):4-9.
- Tong L, Harwood HJ, Jr. 2006. Acetyl-coenzyme A carboxylases: Versatile targets for drug discovery. *J Cell Biochem* 99(6):1476-88.
- Trigueros L, Pena S, Ugidos AV, Sayas-Barbera E, Perez-Alvarez JA, Sendra E. 2013. Food ingredients as anti-obesity agents: A review. *Crit Rev Food Sci Nutr* 53(9):929-42.
- Vainio H, Bianchini F, 2002. IARC Handbooks of Cancer Prevent–Weight Control and Physical Activity. Lyon, France: IARC Press.
- Van der Merwe JD, Joubert E, Richards ES, Manley M, Snijman PW, Marnewick JL, Gelderblom WC. 2006. A comparative study on the antimutagenic properties of aqueous extracts of *Aspalathus linearis* (rooibos), different *Cyclopia* spp. (Honeybush) and camellia sinensis teas. *Mutat Res* 611(1-2):42-53.
- Van Wyk B-. 2011. The potential of South African plants in the development of new medicinal products. *S Afr J Bot* 77(4):812-29.
- Vazquez-Vela ME, Torres N, Tovar AR. 2008. White adipose tissue as endocrine organ and its role in obesity. *Arch Med Res* 39(8):715-28.
- Verhoog NJ, Joubert E, Louw A. 2007. Evaluation of the phytoestrogenic activity of *Cyclopia genistoides* (honeybush) methanol extracts and relevant polyphenols. *J Agric Food Chem* 55(11):4371-81.
- Verhoog NJD, Joubert E, Louw A. Screening of four *Cyclopia* (honeybush) species for putative phyto-oestrogenic activity by oestrogen receptor binding assays: Research article. *S.Afr.J.Sci.*
- Villena JA, Roy S, Sarkadi-Nagy E, Kim KH, Sul HS. 2004. Desnutrin, an adipocyte gene encoding a novel patatin domain-containing protein, is induced by fasting and glucocorticoids: Ectopic expression of desnutrin increases triglyceride hydrolysis. *J Biol Chem* 279(45):47066-75.
- Visagie A, et al. 2015. Commercial honeybush (*Cyclopia* spp.) tea extract inhibits osteoclast formation and bone resorption in RAW264.7 murine Macrophages—An

- in vitro* study. International Journal of Environmental Research and Public Health 12(11).
- Visser K, Mortimer M, Louw A. 2013. *Cyclopia* extracts act as ER alpha antagonists and ER beta agonists, *in vitro* and *in vivo*. PLoS One 8(11):e79223.
- Wakil SJ, Abu-Elheiga LA. 2009. Fatty acid metabolism: Target for metabolic syndrome. Journal of Lipid Research 50(Supplement):S138-43.
- Wang B, Trayhurn P. 2006. Acute and prolonged effects of TNF-alpha on the expression and secretion of inflammation-related adipokines by human adipocytes differentiated in culture. Pflugers Arch 452(4):418-27.
- Wang B, Chandrasekera PC, Pippin JJ. 2014. Leptin- and leptin receptor-deficient rodent models: Relevance for human type 2 diabetes. Curr Diabetes Rev 10(2):131-45.
- Wang H, Eckel RH. 2009. Lipoprotein lipase: From gene to obesity. American Journal of Physiology - Endocrinology and Metabolism 297(2):E271-88.
- Wang ND, Finegold MJ, Bradley A, Ou CN, Abdelsayed SV, Wilde MD, Taylor LR, Wilson DR, Darlington GJ. 1995. Impaired energy homeostasis in C/EBP alpha knockout mice. Science 269(5227):1108-12.
- Wang P, Henning SM, Heber D. 2010. Limitations of MTT and MTS-based assays for measurement of antiproliferative activity of green tea polyphenols. PLoS One 5(4):e10202.
- Wang X, Hasegawa J, Kitamura Y, Wang Z, Matsuda A, Shinoda W, Miura N, Kimura K. 2011. Effects of hesperidin on the progression of hypercholesterolemia and fatty liver induced by high-cholesterol diet in rats. J Pharmacol Sci 117(3):129-38.
- Wang YJ, Zhou SM, Xu G, Gao YQ. 2015. Interference of phenylethanoid glycosides from *cistanche tubulosa* with the MTT assay. Molecules 20(5):8060-71.
- Wang YW, Sun GD, Sun J, Liu SJ, Wang J, Xu XH, Miao LN. 2013. Spontaneous type 2 diabetic rodent models. J Diabetes Res 2013:401723.
- Wang YX, Lee CH, Tjep S, Yu RT, Ham J, Kang H, Evans RM. 2003. Peroxisome-proliferator-activated receptor delta activates fat metabolism to prevent obesity. Cell 113(2):159-70.
- Weyermann J, Lochmann D, Zimmer A. 2005. A practical note on the use of cytotoxicity assays. Int J Pharm 288(2):369-76.
- Wilcox LJ, Borradaile NM, de Dreu LE, Huff MW. 2001. Secretion of hepatocyte apoB is inhibited by the flavonoids, naringenin and hesperetin, via reduced activity and expression of ACAT2 and MTP. J Lipid Res 42(5):725-34.
- Williams L, Seki Y, Vuguin PM, Charron MJ. 2014. Animal models of in utero exposure to a high fat diet: A review. Biochimica Et Biophysica Acta (BBA) - Molecular Basis of Disease 1842(3):507-19.

- Wing RR, Venditti E, Jakicic JM, Polley BA, Lang W. 1998. Lifestyle intervention in overweight individuals with a family history of diabetes. *Diabetes Care* 21(3):350-9.
- Wisman KN, Perkins AA, Jeffers MD, Hagerman AE. 2008. Accurate assessment of the bioactivities of redox-active polyphenolics in cell culture. *J Agric Food Chem* 56(17):7831-7.
- World Health Organization, 2014. Facts and figures on childhood obesity. Commission on Ending Childhood Obesity. Available at: <http://www.who.int/end-childhood-obesity/facts/en/>. Accessed: 21 May 2016.
- World Obesity Federation, 2015. About obesity. Available at: <http://www.worldobesity.org/resources/aboutobesity/>. Accessed: 21 May 2016.
- Wu J, Cohen P, Spiegelman BM. 2013. Adaptive thermogenesis in adipocytes: Is beige the new brown? *Genes Dev* 27(3):234-50.
- Wu S, Liang J. 2010. Counter-current chromatography for high throughput analysis of natural products. *Comb Chem High Throughput Screen* 13(10):932-42.
- Wu Z, Wang S. 2013. Role of kruppel-like transcription factors in adipogenesis. *Dev Biol* 373(2):235-43.
- Wu Z, Xie Y, Bucher NL, Farmer SR. 1995. Conditional ectopic expression of C/EBP beta in NIH-3T3 cells induces PPAR gamma and stimulates adipogenesis. *Genes Dev* 9(19):2350-63.
- Xanthakos SA. 2009. Nutritional deficiencies in obesity and after bariatric surgery. *Pediatr Clin North Am* 56(5):1105-21.
- Xie JT, Zhou YP, Dey L, Attele AS, Wu JA, Gu M, Polonsky KS, Yuan CS. 2002. Ginseng berry reduces blood glucose and body weight in db/db mice. *Phytomedicine* 9(3):254-8.
- Xing X, Li D, Chen D, Zhou L, Chonan R, Yamahara J, Wang J, Li Y. 2014. Mangiferin treatment inhibits hepatic expression of acyl-coenzyme A:Diacylglycerol acyltransferase-2 in fructose-fed spontaneously hypertensive rats: A link to amelioration of fatty liver. *Toxicol Appl Pharmacol* 280(2):207-15.
- Xu F, Zheng X, Lin B, Liang H, Cai M, Cao H, Ye J, Weng J. 2016. Diet-induced obesity and insulin resistance are associated with brown fat degeneration in SIRT1-deficient mice. *Obesity (Silver Spring)* 24(3):634-42.
- Xu N, Zhang L, Dong J, Zhang X, Chen Y, Bao B, Liu J. 2014. Low-dose diet supplement of a natural flavonoid, luteolin, ameliorates diet-induced obesity and insulin resistance in mice. *Molecular Nutrition & Food Research* 58(6):1258-68.
- Yang ZH, Miyahara H, Takeo J, Katayama M. 2012. Diet high in fat and sucrose induces rapid onset of obesity-related metabolic syndrome partly through rapid response of genes involved in lipogenesis, insulin signalling and inflammation in mice. *Diabetol Metab Syndr* 4(1):32,5996-4-32.

- Yeh WC, Cao Z, Classon M, McKnight SL. 1995. Cascade regulation of terminal adipocyte differentiation by three members of the C/EBP family of leucine zipper proteins. *Genes Dev* 9(2):168-81.
- Yoon JW, Jun HS. 2005. Autoimmune destruction of pancreatic beta cells. *Am J Ther* 12(6):580-91.
- Yoon SA, Kang SI, Shin HS, Kang SW, Kim JH, Ko HC, Kim SJ. 2013. p-coumaric acid modulates glucose and lipid metabolism via AMP-activated protein kinase in L6 skeletal muscle cells. *Biochem Biophys Res Commun* 432(4):553-7.
- Yoshida H, Watanabe W, Oomagari H, Tsuruta E, Shida M, Kurokawa M. 2013. Citrus flavonoid naringenin inhibits TLR2 expression in adipocytes. *J Nutr Biochem* 24(7):1276-84.
- Yu C, Chen Y, Cline GW, Zhang D, Zong H, Wang Y, Bergeron R, Kim JK, Cushman SW, Cooney GJ, et al. 2002. Mechanism by which fatty acids inhibit insulin activation of insulin receptor substrate-1 (IRS-1)-associated phosphatidylinositol 3-kinase activity in muscle. *J Biol Chem* 277(52):50230-6.
- Yun JW. 2010. Possible anti-obesity therapeutics from nature--a review. *Phytochemistry* 71(14-15):1625-41.
- Zeng XY, Zhou X, Xu J, Chan SM, Xue CL, Molero JC, Ye JM. 2012. Screening for the efficacy on lipid accumulation in 3T3-L1 cells is an effective tool for the identification of new anti-diabetic compounds. *Biochem Pharmacol* 84(6):830-7.
- Zhang BB, Moller DE. 2000. New approaches in the treatment of type 2 diabetes. *Curr Opin Chem Biol* 4(4):461-7.
- Zhang HH, Halbleib M, Ahmad F, Manganiello VC, Greenberg AS. 2002. Tumor necrosis factor-alpha stimulates lipolysis in differentiated human adipocytes through activation of extracellular signal-related kinase and elevation of intracellular cAMP. *Diabetes* 51(10):2929-35.
- Zhang Y, Qian Q, Ge D, Li Y, Wang X, Chen Q, Gao X, Wang T. 2011. Identification of benzophenone C-glucosides from mango tree leaves and their inhibitory effect on triglyceride accumulation in 3T3-L1 adipocytes. *J Agric Food Chem* 59(21):11526-33.
- Zhao L, Kang I, Fang X, Wang W, Lee MA, Hollins RR, Marshall MR, Chung S. 2015. Gamma-tocotrienol attenuates high-fat diet-induced obesity and insulin resistance by inhibiting adipose inflammation and M1 macrophage recruitment. *Int J Obes (Lond)* 39(3):438-46.
- Zhou Y, Zhou Z, Zhang W, Hu X, Wei H, Peng J, Jiang S. 2015. SIRT1 inhibits adipogenesis and promotes myogenic differentiation in C3H10T1/2 pluripotent cells by regulating wnt signaling. *Cell Biosci* 5:61,015-0055-5. eCollection 2015.
- Zhu Y, Qi C, Korenberg JR, Chen XN, Noya D, Rao MS, Reddy JK. 1995. Structural organization of mouse peroxisome proliferator-activated receptor gamma

(mPPAR gamma) gene: Alternative promoter use and different splicing yield two mPPAR gamma isoforms. *Proc Natl Acad Sci USA* 92(17):7921-5.

Zych M, Folwarczna J, Trzeciak HI. 2009. Natural phenolic acids may increase serum estradiol level in ovariectomized rats. *Acta Biochim Pol* 56(3):503-7.

ADDENDUM 1 - Animal Ethics Approval



UNIVERSITEIT • STELLENBOSCH • UNIVERSITY
jou kennisvennoot • your knowledge partner

Protocol Approval

Date: 04-Dec-2013

PI Name: Jack, Babalwa BU

Protocol #: SU-ACUM13-00028

Title: An investigation into the anti-obesity properties of Cyclopia

Dear Babalwa Jack, the Response to Modifications, was reviewed on 04-Dec-2013 by the Research Ethics Committee: Animal Care and Use via committee review procedures and was approved. Please note that this clearance is only valid for a period of twelve months. Ethics clearance of protocols spanning more than one year must be renewed annually through submission of a progress report, up to a maximum of three years.

Applicants are reminded that they are expected to comply with accepted standards for the use of animals in research and teaching as reflected in the South African National Standards 10386: 2008. The SANS 10386: 2008 document is available on the Division for Research Developments website www.sun.ac.za/research.

Please remember to use your protocol number, SU-ACUM13-00028 on any documents or correspondence with the REC: ACU concerning your research protocol.

Please note that the REC: ACU has the prerogative and authority to ask further questions, seek additional information, require further modifications or monitor the conduct of your research.

We wish you the best as you conduct your research.

If you have any questions or need further help, please contact the REC: ACU secretariat at or .

Sincerely,

REC: ACU Secretariat

Research Ethics Committee: Animal Care and Use

SAMRC Animal Ethics Approval Certificate

Decision of the Animal Ethics Committee for the use of living vertebrates for research, diagnostic procedures and product development

APPROVAL PERIOD: September 2013 - November 2014

PROJECT NUMBER:	10/13			
PROJECT TITLE:	"An investigation into the anti-Obesity properties of Cyclopi".			
PROJECT LEADER:	Dr Carmen Pfeiffer			
DIVISION:	Diabetes Discovery Platform (DDP)			
CATEGORY:	Diabetes			
SPECIES OF ANIMAL:	Mouse	BKS.Cg-Dock 7 (m)	Lepr(db)/J	Male 30g 6 weeks old
NUMBER OF ANIMALS:	48			
NOT APPROVED:	n/a			
APPROVED:	2 September 2013			

PLEASE NOTE: Should the number or species of animal(s) required, or the experimental procedure(s) change, please submit a revised animal ethics clearance form to the animal ethics committee for approval before commencing with the experiment



PROF D DU TOIT

DATE: 2nd September 2013

CHAIRPERSON ANIMAL ETHICS COMMITTEE

ADDENDUM 2 - Reagents and Buffers solutions**List of Reagents**

Product name	Catalogue number	Supplier
3-(4,5-dimethylthiazol-2-yl)-2,5-diphenyltetrazolium bromide (MTT)	M2003	Sigma-Aldrich , St Louis, MO, USA
3-isobutyl -1-methyl-xanthine (IBMX)	I5879	Sigma-Aldrich , St Louis, MO, USA
3T3-L1 pre-adipocytes	CL-173	American Type Culture Collection (ATCC), Manassas, VA, USA
Albumin, Bovine Fraction V (fatty acid free)	A1302	Melford Laboratories, Ipswich Suffolk, U.K.
Anti-Rabbit IgG (Horseradish peroxidase labelled secondary antibody)	sc-2012	Santa Cruz Biotechnology, Santa Cruz, CA, USA
ATP assay kit	LT27-008	ViaLight, Lonza, Basel, Switzerland
Beta actin (Act β) antibody	Sc-47778	Santa Cruz Biotechnology, Santa Cruz, CA, USA
Bio-Rad Protein DC assay kit	500-0201	Biorad, Hercules, California, USA
Carbon dioxide (CO ₂)	K239C	Air Products, Centurion, SA
Cell counting chamber slides	C10228	Life Technologies Corporation, Carlsbad, CA, USA
Cell lysis Buffer	FNN0011	Life Technologies Corporation, Carlsbad, CA, USA
CELLBIND -24 well plates	3337	Corning, MA, USA
CELLBIND -6 well plates	3335	Corning, MA, USA
CELLBIND -96 well plates	3300	Corning, MA, USA
Centrifuge tubes (15mL; 50mL)	GEN-1860 5810R	Sigma-Aldrich , St Louis, MO, USA
Chloroform	136112-00-0	Sigma-Aldrich , St Louis, MO, USA
Coomassie blue stain	161-0437	Bio-Rad, Hercules, CA, USA
Cryotubes	430659	Corning, MA, USA
Crystal violet		
Dexamethasone	D4902	Sigma-Aldrich , St Louis, MO, USA
Dimethyl sulfoxide (DMSO)	276855	Sigma-Aldrich , St Louis, MO, USA
Dulbecco`s modified Eagle`s medium (DMEM without phenol red)	D5030	Sigma-Aldrich , St Louis, MO, USA
Dulbecco`s modified Eagle`s medium (DMEM)	12-604Q	Lonza, Walkersville, MD, USA
Dulbecco`s phosphate buffered saline (DPBS)	17-513F	Lonza, Walkersville, MD, USA
Eppendorf tubes	30123301	Sigma-Aldrich , St Louis, MO, USA
Ethanol	2875	Sigma-Aldrich , St Louis, MO, USA
Ethanol absolute, 200 proof for molecular	E7023-500	Sigma-Aldrich , St Louis, MO, USA
Fetal bovine serum	BC/S0615-HI	Lonza, Walkersville, MD, USA
Filter Pads	23385	Sigma-Aldrich , St Louis, MO, USA
Glucose powder	D5030	Sigma-Aldrich , St Louis, MO, USA
Glycerol assay kit	K630-100	Biovision, Milpitas, CA, USA

Insulin	I92785	Sigma-Aldrich , St Louis, MO, USA
Isopropanol	I9516	Sigma-Aldrich , St Louis, MO, USA
Linco rat insulin kit	EZRMI-13K	Millipore, Bellerica, MA, USA
Low fat free milk powder	2082054	Clover, JHB, SA
Methanol	67-56-1	Sigma-Aldrich , St Louis, MO, USA
<i>n</i> -Butanol	71-36-3	Sigma-Aldrich , St Louis, MO, USA
Newborn Calf Serum (NCS)	BC/S0125-HI	The Scientific Group, JHB, SA
Nuclease free water	Am9937	Ambion, Austian, USA
Oil O Red	1320-06-5	Sigma, St Louise, MO, USA
PCR plates	N8010560	Applied Biosystems, Foster City, CA, USA
Phenylmethanesulfonyl fluoride (PMSF)	11206893001	Roche, Basel, Switzerland
PolyvinylideneFluoridine Membrane (PVDF)	88585	Pierce, Rockford, IL, USA
Ponceau S Stain	p23295	Sigma-Aldrich , St Louis, MO, USA
PPAR α antibody	Ab8934	Abcam, Abcam, Cambridge, MA, USA
PPAR γ antibody	2430-S	Cell Signalling Technology, Danvers, MA, USA
Propidium iodide	P4170	Sigma-Aldrich , St Louis, MO, USA
Protease Inhibitors	11206893001	Roche, Basel, Switzerland
RNase free water	Am9937	Ambion, Austin, TX, USA
RNeasy mini kit	74106	Qiagen, Hilden, Germany
Running buffer SDS	161-0772	Bio-Rad, Hercules, CA, USA
SDS-PAGE gels	161-0993	Bio-Rad, Hercules, CA, USA
Sodium bicarbonate (NaHCO ₃)	M2645	Sigma-Aldrich , St Louis, MO, USA
Sodium hydroxide (NaOH)	109140	Merck, Whitehouse Station, NJ, USA
Stainless steel beads 5mm	69989	Qiagen, Hilden, Germany
Sterile TC water	59900C	Lonza, Walkersville, MD, USA
SYBR Green mix	4385612	Applied Biosystems, Foster City, CA, USA
T75 Flasks	658975	Greiner bio-one, Frickenhausen, Germany
Qiazol reagent	79306	Qiagen, Hilden, Germany
Triglyceride Kit	K622-100	Biovision, Milpitas, CA, USA
Tris	93352	Sigma-Aldrich , St Louis, MO, USA
Trypan blue	15050-065	Invitrogen, Carlsbad, CA, USA
Trypsin	17-161F	Lonza, Walkersville, MD, USA
Tween-20	58980C	Sigma-Aldrich , St Louis, MO, USA
Whatman 3MMChr sheets	3030-931	Sigma-Aldrich , St Louis, MO, USA

Buffers and media used in this study**1. DMEM without phenol red media**

Reagent	Final Conc.	MW	Amount/1L
DMEM	8.3 g/L	-	8.3 g
BSA (no fatty acids)	0.1%	-	1 g
NaHCO ₃	3.7 g/L	84.01	3.7 g
D-Glucose	4.5 g/L	180.16	4.5 g

2. Sorenson's buffer

Reagent	Final Conc.	Amount/1L
Glycine	0.1 M	0.751 g
NaCl	0.1 M	0.584 g

The pH of the buffer was adjusted to pH10.5 with 0.1 mM NaOH.

3. Destaining solution for Western blots

Reagents	Amount/1L
15% methanol	150 mL
20% acetic acid	200 mL

4. Transfer buffer for Western blot

Reagent	Final Conc.	MW	Amount/1L
Tris	25 mM	121.1	3.03 g
Glycine	192 mM	75.5	14.4 g
Distilled water	-	-	800 mL
Methanol	-	-	200 mL

5. 10 × Tris-buffered saline

Reagent	Final Conc.	MW	Amount/1L
Tris	200 mM	121.1	24.22 g
NaCl	1.37 M	58.44	80.06 g
Distilled water	-	-	1000 mL

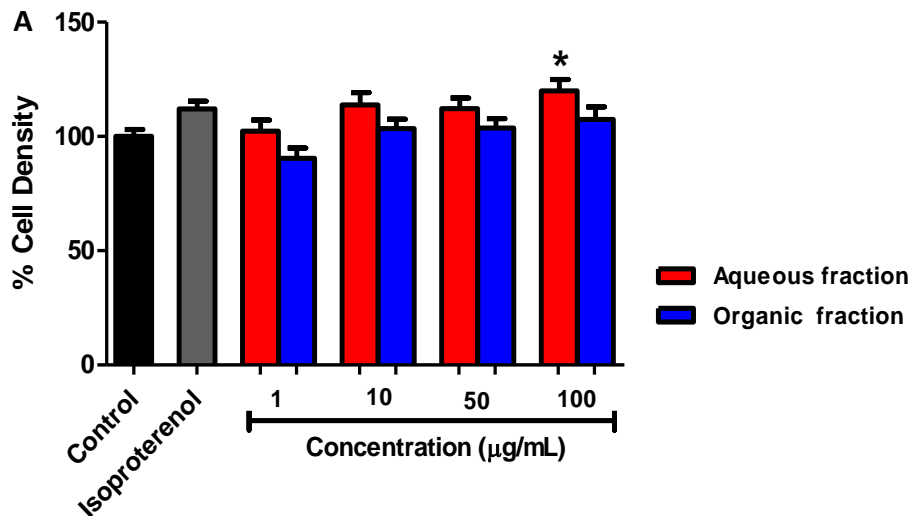
6. 1 × Tris-buffered saline and Tween 20 (1 × TBST)

1 × TBST was prepared by diluting 100 mL of 10 × TBST with 900 mL of distilled water (v/v), thereafter 1 mL Tween 20 was added. The buffer was kept at 4°C.

ADDENDUM 3 - Supplementary Data

1. Crystal violet staining

The effect of the aqueous and organic fractions of *C. maculata*, *C. intermedia* and *C. subternata* on cell density was quantified with crystal violet staining and used to normalize Oil Red O assay results. Compared to the MTT and the ATP cell viability measures, results showed that treatment with the aqueous and organic fractions of *C. maculata*, *C. intermedia* and *C. subternata* did not affect cell viability as the percentage cell density was not significantly reduced in response to treatment with these fractions. Furthermore treatment with the aqueous fraction of *C. maculata* increased cell density at 100 $\mu\text{g/mL}$ (Figs. S1 A - C). Further treatment of 3T3-L1 pre-adipocytes differentiated in the presence of the CCC fractions and differentiated 3T3-L1 adipocytes treated with the CCC fractions for 24 hours, showed that cell density did not vary between the treatment conditions (Figs. S2 A - D and Figs. S3 A - D).



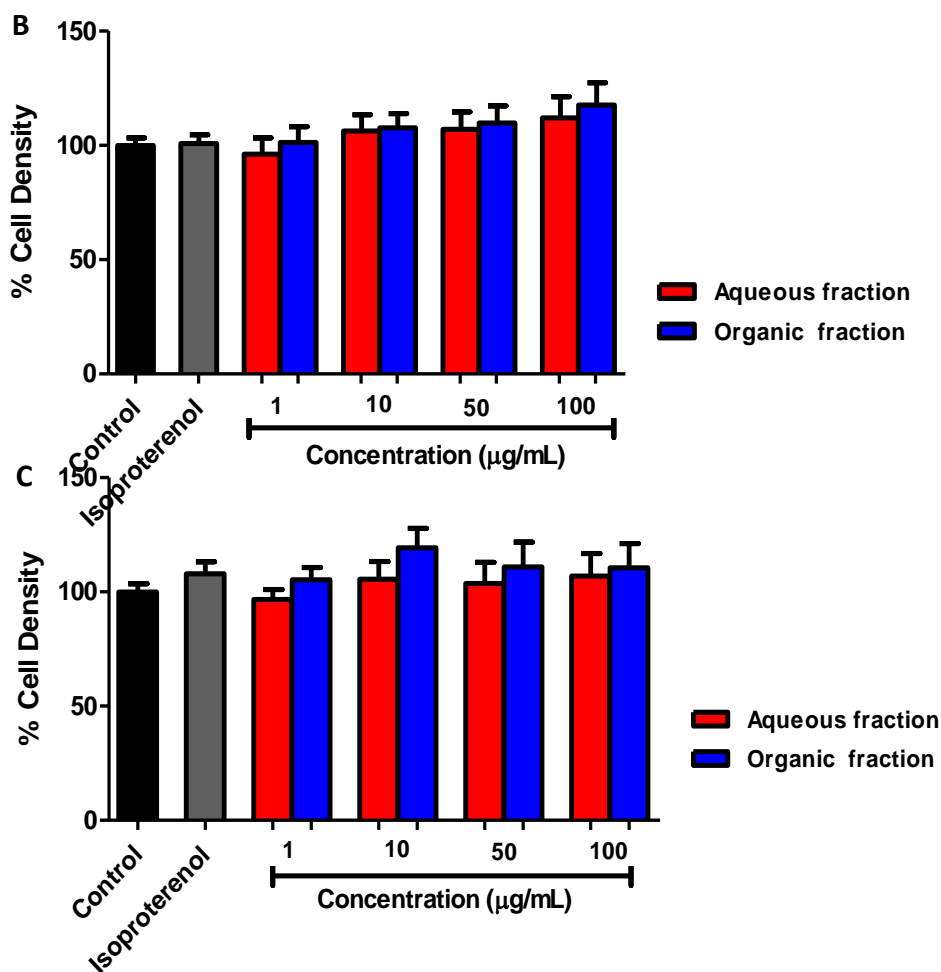


Figure S1 The effect of aqueous and organic fractions, prepared from 40% aqueous methanol extracts of *C. maculata*, *C. intermedia* and *C. subternata* on cell density in 3T3-L1 adipocytes. Differentiated 3T3-L1 adipocytes were exposed to aqueous and organic fractions of *C. maculata* (A), *C. intermedia* (B) and *C. subternata* (C) at various concentrations, vehicle control or isoproterenol for 24 hours. Cell density was quantified using crystal violet staining. Results are expressed as a percentage relative to the vehicle control (set at 100%), and are shown as the mean \pm SEM for three independent experiments, each performed in triplicate. Significance is depicted as * $P < 0.05$ vs. vehicle control.

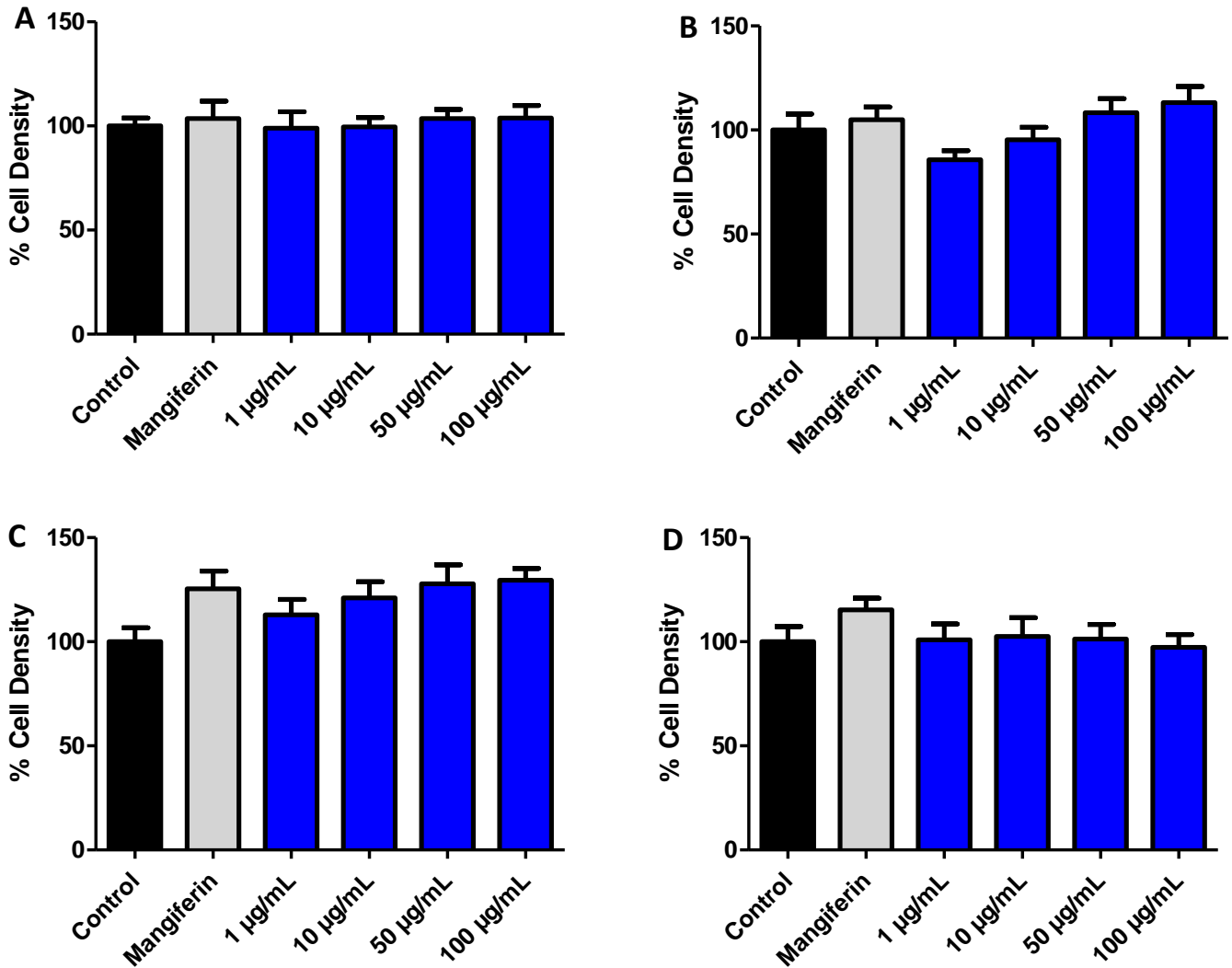


Figure S2 The effect of CCC F1, CCC F2, CCC F3 and CCC F4 on cell density in differentiating 3T3-L1 pre-adipocytes. Differentiating 3T3-L1 pre-adipocytes were exposed to the vehicle control, CCC F1 (A), CCC F2 (B), CCC F3 (C) or CCC F4 (D) (at various concentrations), or mangiferin daily for eight days. Cell density was quantified using crystal violet staining. Results are expressed as a percentage relative to the vehicle control (set at 100%), and are shown as mean \pm SEM for three independent experiments, each performed in triplicate.

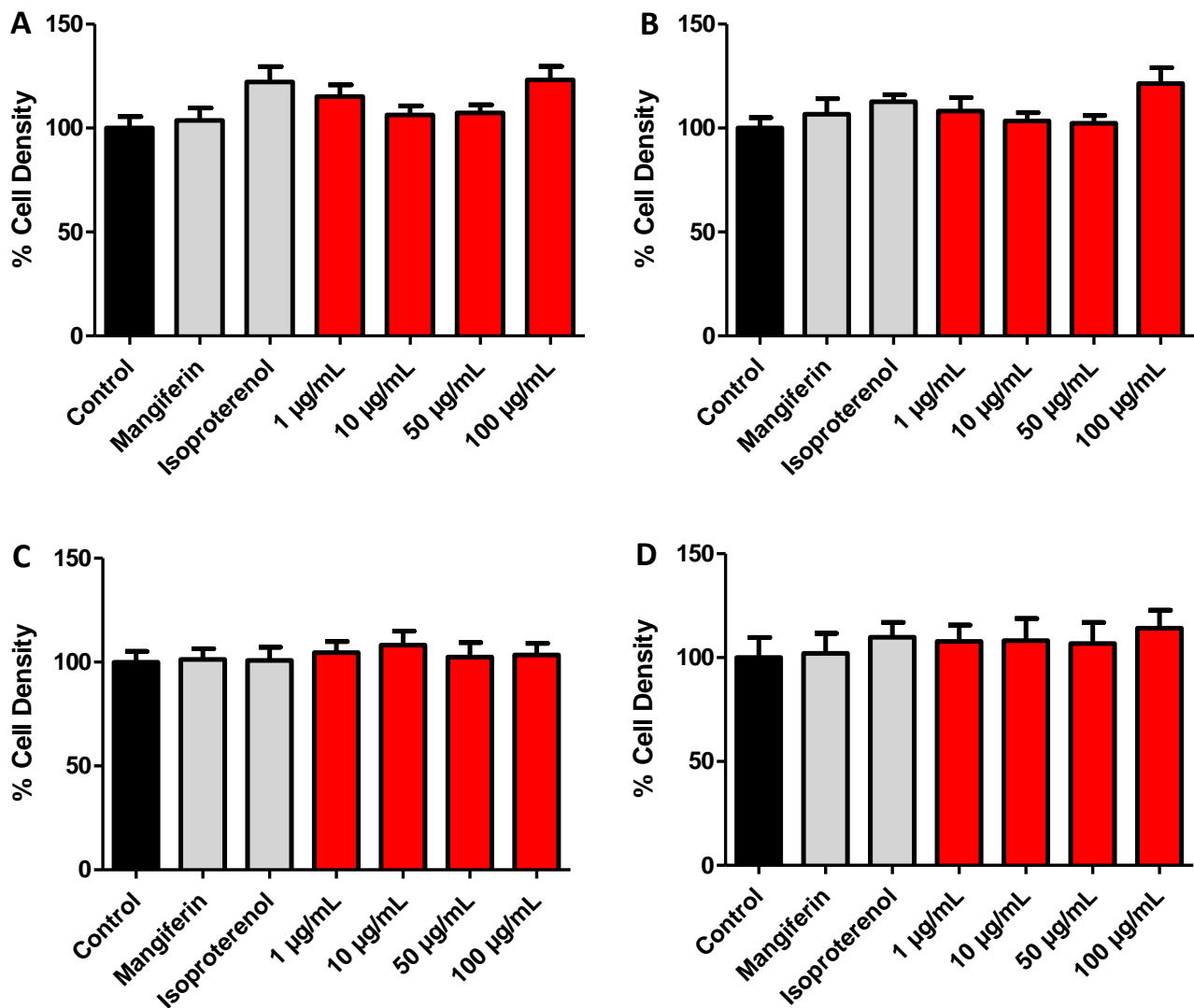


Figure S3 The effect of CCC F1, CCC F2, CCC F3 and CCC F4 on cell density in differentiated 3T3-L1 adipocytes. Differentiated 3T3-L1 adipocytes were exposed to the vehicle control, CCC F1 (A), CCC F2 (B), CCC F3 (C) or CCC F4 (D) (at various concentrations), or mangiferin for 24 hours. Cell density was quantified using crystal violet staining. Results are expressed as a percentage relative to the vehicle control (set at 100%), and are shown as mean \pm SEM for three independent experiments, each performed in triplicate.

2. Propidium iodide staining

The aqueous fraction of *C. maculata* and the organic fraction of *C. intermedia* showed the highest anti-obesity effect without any affecting cell viability. Therefore the cytotoxic effects of these fractions were further evaluated by measuring necrotic cell death using propidium iodide staining. Results indicate that there was no significant necrotic cell death in adipocytes treated with both fractions.

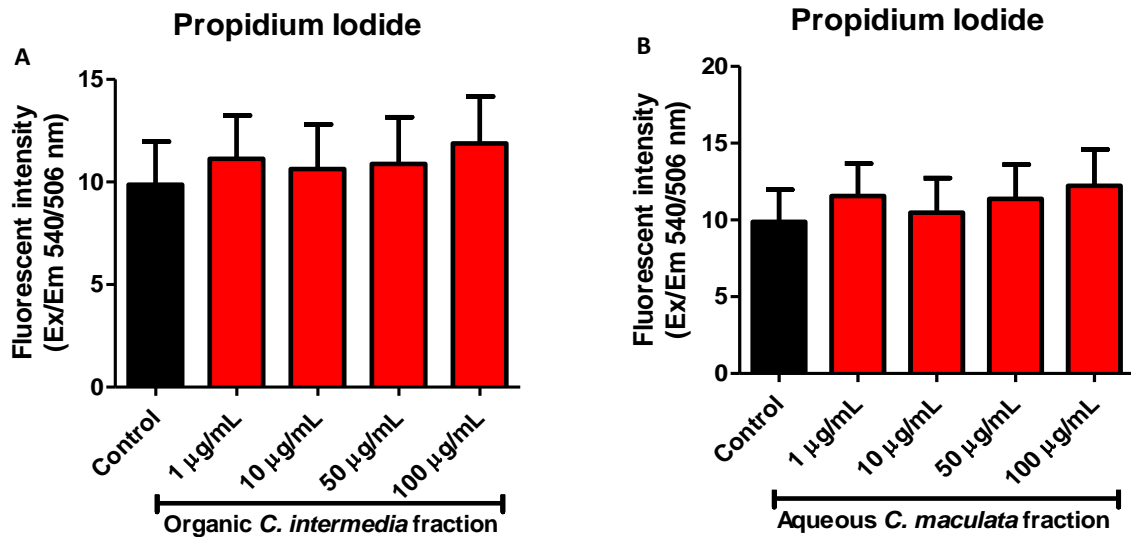


Figure S4 The effect of the organic fraction of *C. intermedia* and the aqueous fraction of *C. maculata* on propidium iodide staining. Differentiated adipocytes were treated with the organic *C. intermedia* (A) and the aqueous *C. maculata* (B) fractions for 24 hours and cell viability assessed with propidium iodide staining. Results are expressed as the percentage relative to the vehicle control (set at 100%), and are shown as the mean \pm SEM for three independent experiments, each performed in triplicate.

3. *In vitro* validation of the up-scaled organic fraction of *C. intermedia*

The organic fraction of *C. intermedia* was prepared on large scale for *in vivo* animal experiments and HPLCC fractionation. The upscaled fraction was validated for its bioactivity, by treating differentiated adipocytes with both the small (old) and large-scale (new) fractions of *C. intermedia* at various concentrations (1, 10, 50 and 100 µg/mL) and assessing their effects on lipid accumulation using the ORO assay, and cell viability using the MTT and ATP assays.

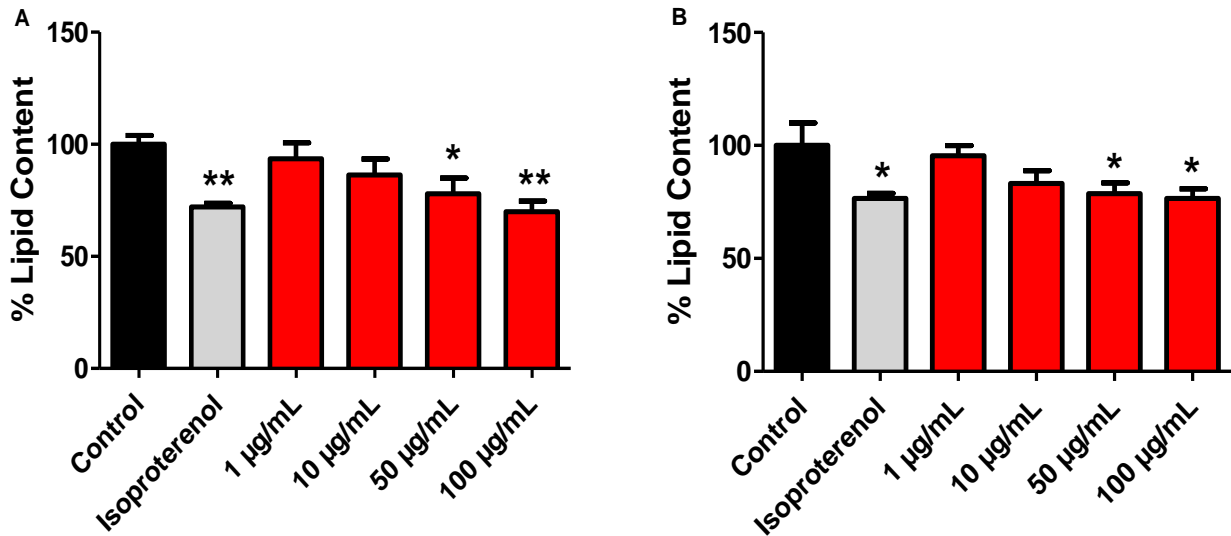


Figure S5 The effect of the old and new organic fraction of *C. intermedia* on lipid accumulation in 3T3-L1 adipocytes. Differentiated adipocytes were treated with the old (A) and new (B) organic fraction of *C. intermedia* for 24 hours at various concentrations (1, 10, 50 and 100 µg/mL) and lipid content was assessed using the Oil Red O assay. Results are expressed as the percentage relative to the vehicle control (set at 100%), and are shown as the mean ± SEM for two independent experiments, each performed in triplicate. Significance is depicted as *P < 0.05 and **P < 0.01 vs. vehicle control.

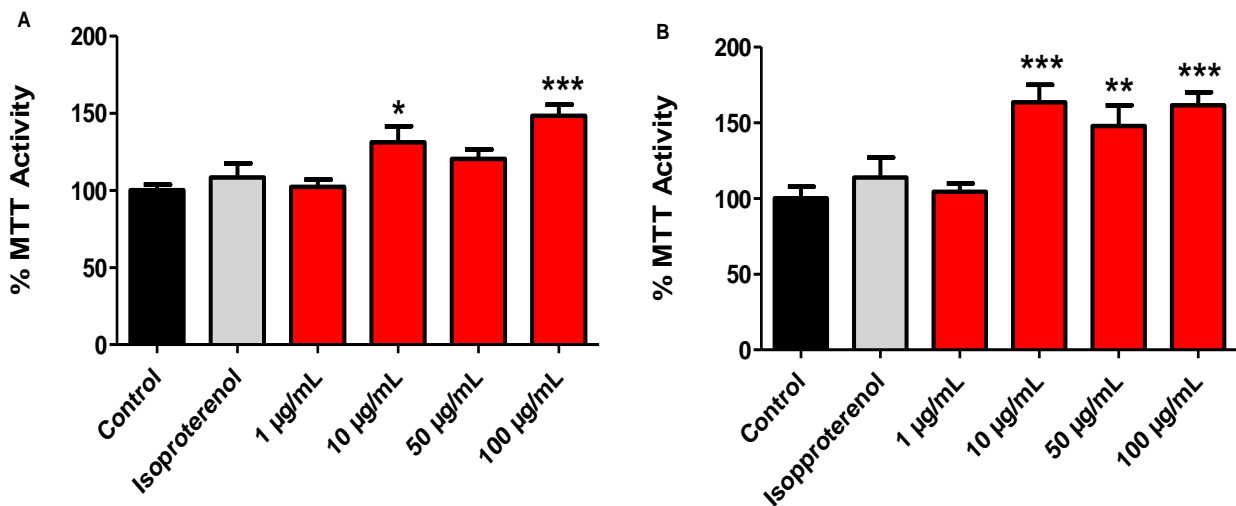


Figure S6 The effect of the old and new organic fraction of *C. intermedia* on the mitochondrial dehydrogenase activity in 3T3-L1 adipocytes. Differentiated adipocytes were treated with the old (A) and new (B) organic fraction of *C. intermedia* for 24 hours at various concentrations (1, 10, 50 and 100 µg/mL) and mitochondrial dehydrogenase activity was measured using the MTT assay. Results are expressed as the percentage relative to the vehicle control (set at 100%), and are shown as the mean ± SEM for two independent experiments, each performed in triplicate. Significance is depicted as *P < 0.05, **P < 0.01 and ***P < 0.001 vs. vehicle control.

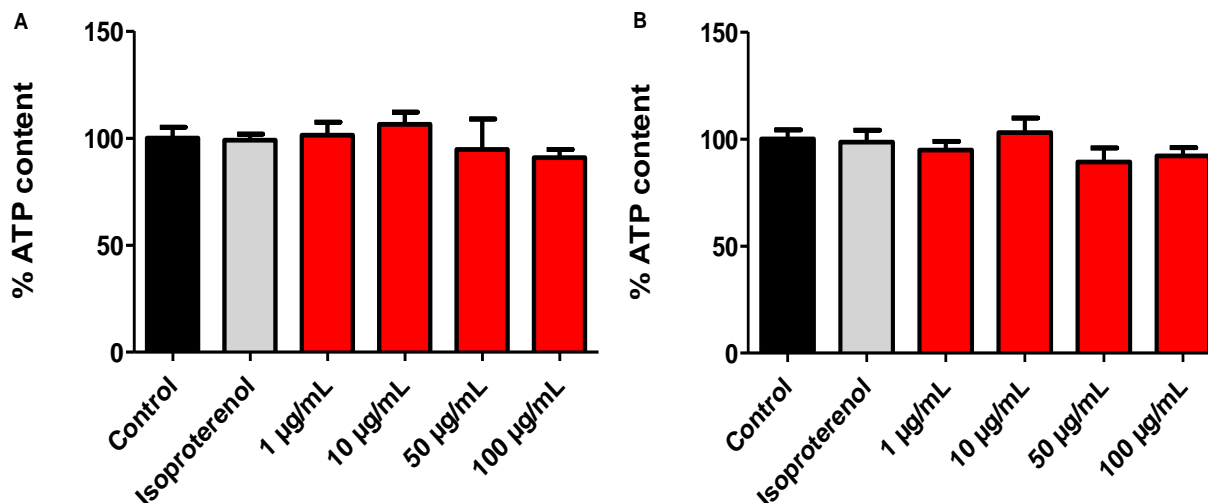


Figure S7 The effect of the old and new organic fraction of *C. intermedia* on the ATP content in 3T3-L1 adipocytes. Differentiated adipocytes were treated with the old (A) and new (B) organic fraction of *C. intermedia* for 24 hours at various concentrations (1, 10, 50 and 100 µg/mL) and ATP content was measured using the ATP assay kit. Results are expressed as the percentage relative to the vehicle control (set at 100%), and are shown as the mean \pm SEM for two independent experiments, each performed in triplicate.

4. Western Blot Analysis

Complete images of PPAR γ and PPAR α blots and their respective housekeeping gene (β actin) are presented in Figs. S8 A – B. this data is added to show that the blots were cut, as the samples in the blots were represented at different chapters of the results.

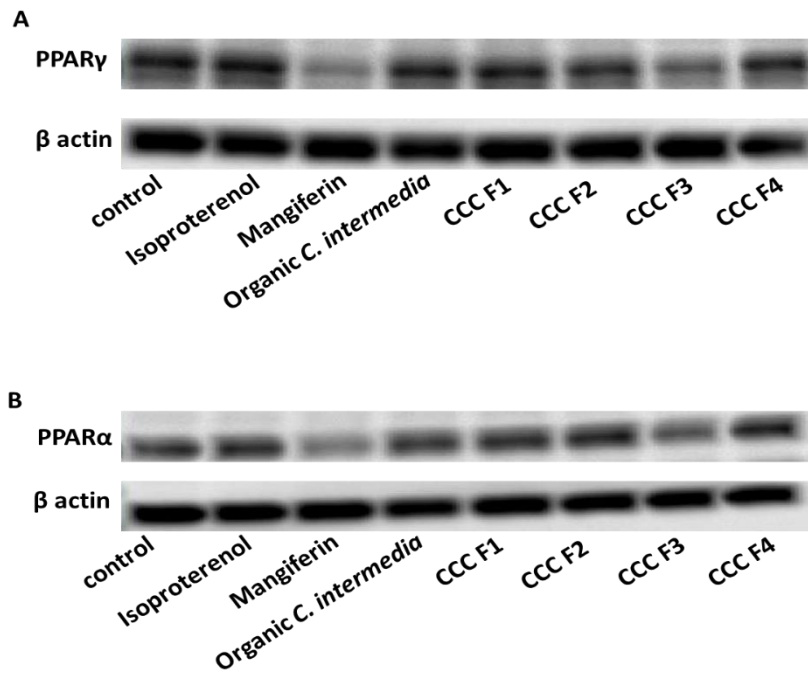


Figure S8 The effect of the organic fraction of *C. intermedia* and the CCC fractions on PPAR α and PPAR γ protein expression. Differentiated 3T3-L1 adipocytes were treated with the vehicle control, organic *C. intermedia* fraction (50 μ g/mL), CCC F1 (10 μ g/mL), CCC F2 (100 μ g/mL), CCC F3 (10 μ g/mL), CCC F4 (10 μ g/mL), isoproterenol (10 μ M) or mangiferin (0.001 μ M) for 24 hours. Proteins were extracted and protein expression of PPAR γ (A) and PPAR α (B) was assessed by western blot analysis using β actin as a reference protein. Results are reported as a fold change relative to the vehicle control and represent mean \pm SEM for three independent experiments.